Distribution Agreement

In presenting this thesis or dissertation as a partial fulfillment of the requirements for an advanced degree from Emory University, I hereby grant to Emory University and its agents the non-exclusive license to archive, make accessible, and display my thesis or dissertation in whole or in part in all forms of media, now or hereafter known, including display on the world wide web. I understand that I may select some access restrictions as part of the online submission of this thesis or dissertation. I retain all ownership rights to the copyright of the thesis or dissertation. I also retain the right to use in future works (such as articles or books) all or part of this thesis or dissertation.

_____ _____

Callie Preast Wigington Date

Characterization of Disease-relevant Targets of RNA Binding Proteins

By
Callie Preast Wigington
Doctor of Philosophy

Graduate Division of Biological and Biomedical Sciences
Biochemistry, Cell and Developmental Biology

_____
Anita H. Corbett
Advisor

_____
Gary J. Bassell
Committee Member

_____
Paul W. Doetsch
Committee Member

_____
Eric A. Ortlund
Committee Member

_____
Maureen A. Powers
Committee Member

_____
Paula M. Vertino
Committee Member

Accepted:

_____
Lisa A Tedesco, Ph.D.
Dean of James T. Laney School of Graduate Studies

_____
Date

Characterization of Disease-relevant Targets of RNA Binding Proteins

By

Callie Preast Wigington
B.S., Georgia Southern University, 2008

Advisor: Anita H. Corbett, Ph.D.

An abstract of
A dissertation submitted to the Faculty of the
James T. Laney School of Graduate Studies of Emory University
in partial fulfillment of the requirements for the degree of
Doctor of Philosophy in the
Graduate Division of Biological and Biomedical Sciences
Biochemistry, Cell and Developmental Biology
2015

ABSTRACT

Characterization of Disease-relevant Targets of RNA Binding Proteins

By Callie Preast Wigington

Messenger RNA (mRNA) serves as the intermediate molecule in the flow of genetic information from DNA to protein and is subject to extensive regulatory events, collectively referred to as post-transcriptional processing. These events include the capping, splicing, 3' end processing, export and eventual decay of an mRNA transcript. Each of these processing events is mediated by a host of post-transcriptional factors, including RNA binding proteins and noncoding RNAs. The critical nature of these steps in ensuring proper gene expression is supported by the observation that dysregulation of many RNA binding proteins is associated with a variety of human diseases, including intellectual disability and cancer. Therefore, the functional characterization of newly discovered RNA binding proteins as well as the identification of novel targets for canonical RNA binding proteins is an important objective to understand the underlying molecular pathogenesis of disease. In this work, we demonstrate that the novel polyadenosine RNA binding protein, ZC3H14, specifically interacts with and modulates the pre-mRNA processing of the *ATP5G1* transcript, which encodes a key ATP synthase subunit. Consistent with a loss of ATP synthase activity, we observe reduced cellular ATP levels and a striking mitochondrial fragmentation phenotype upon knockdown of ZC3H14. We hypothesize that these defects in cellular ATP levels and mitochondrial morphology may, at least in part, underlie the observed intellectual disability in patients with loss-of-function mutations in *ZC3H14*. In this work, we also present a novel mode of post-transcriptional regulation of the *PDCD4* transcript, which encodes a novel tumor suppressor that is downregulated in a number of cancer types, including breast. We demonstrate that the two well-characterized U-rich RNA binding proteins, HuR and TIA1, compete for interaction with overlapping binding sites on the *PDCD4* 3'UTR, resulting in positive regulation of *PDCD4* mRNA and protein levels in breast cancer cells. The findings presented here not only demonstrate the importance of post-transcriptional processing events in ensuring precise gene expression, but also provide evidence that the two transcripts analyzed in these studies play important roles in the molecular pathogenesis of disease.

Characterization of Disease-relevant Targets of RNA Binding Proteins

By

Callie Preast Wigington
B.S., Georgia Southern University, 2008

Advisor: Anita H. Corbett, Ph.D.

A dissertation submitted to the Faculty of the
James T. Laney School of Graduate Studies of Emory University
in partial fulfillment of the requirements for the degree of
Doctor of Philosophy in the
Graduate Division of Biological and Biomedical Sciences
Biochemistry, Cell and Developmental Biology
2015

ACKNOWLEDGEMENTS

Well, it's finally here. The end of graduate school. At times it felt as though this journey would never end and then again there were times when it seemed to fly by. There were tremendous highs (yay for positive controls!) and brutal lows; however, those points were likely the times when I grew the most. I'm so thankful for the experiences and friendships that I have gained along the way. There are a number of people that helped me get here and I would like to sincerely thank each and every one of them from the bottom of my heart.

To Anita: my mentor and friend. Your guidance and motivation throughout the last 6 years has been invaluable. You have shaped me into the scientist that I am today and I am forever grateful. I am confident that our relationship will continue throughout the years but I am so sad to leave the lab and the phase of life where I get to see you all the time. I'm truly going to miss your bright and tenacious spirit. You are one of a kind.

To the members of my committee, who were always there with a word of encouragement and a wealth of really great ideas. Thank you so much for the guidance – I couldn't have done it without you.

A special thanks to members of the Corbett lab past and present: Allison Lange, Alex Frere, Shana Kerr, Laura McLane, Seth Kelly, Changhui Pak, Brianne Kallam, Nick Bauer, Sharon Soucek, Katherine Mills-Lujan, Ayan Banerjee, Sara Leung, Milo Fasken, Jennifer Rha, Annie McPherson, Kevin Morris, and Stephanie Jones. Showing up to work with you people everyday was an absolute joy. I so appreciate your support, guidance and advice over the years. I will miss you all so much!

To my closest friends: Rebecca Shealy, Whitney Swanson, Anna McGrady, Amanda Jones, Michelle Sherman, Chase Swanson, Bret White, Scott Jones and David Sherman. The weekends that we spent brunching, exploring, drinking and enjoying each other made the long weeks in lab worth it. You all have been such a support to me over the years and I can't wait to see our relationships grow in the years to come.

To my family: Where would I be without all of you? I am the luckiest person in the world to have each and every one of you in my life. I feel empowered to be whoever I want to be and achieve whatever I set out to achieve because of you. Thanks for the love, support and laughs throughout my life. Here's to many more years of joy!

To my Stella bean: my sweetest girl, my fluffy baby. Your sweet kisses and wiggles at the beginning (and end!) of every day make me so happy. I love you!

Finally, to the love of my life, my truest friend, my heart. I most of all want to thank you, Robert Wigington, for the support, joy, and wisdom that you provide me daily. I absolutely could not have done this without you.

TABLE OF CONTENTS

FIGURES

TABLES

Chapter 1: Introduction

A portion of this chapter is adapted from the following published work:

Wigington, C.P., Williams, K.R., Meers, M.P., Bassell, G.J., and Corbett, A.H. (2014) *Wiley Interdisciplinary Reviews RNA* **5**, 601-622. "Poly(A) RNA Binding Proteins and Polyadenosine RNA: New Members and Novel Functions."

SECTION 1

Regulation of gene expression by eukaryotic post-transcriptional processing

Every cell in a multicellular, or metazoan, organism contains the same genetic material within its nucleus. The neurons and glia that are responsible for the function of the brain contain the same DNA sequence as the circulating lymphocytes that ensure the protection that is provided by the immune system. The primary difference between these diverse cell types (~200 in humans) found within the human body is the location and timing of the genes expressed in these cells, or what is commonly referred to as the "spatiotemporal control of gene expression." This spatiotemporal control is executed in many ways, including transcriptional (i.e. which genes are transcribed and how much) and post-transcriptional (i.e. how the transcribed mRNAs are processed to influence their expression) processing events that all work together to maintain the proper gene expression profile of a given cell.

The transcriptional control of gene expression determines not only which genes are transcribed in a given cell, but also how much RNA is produced and for how long. Transcription factors, which are DNA binding proteins that stimulate or repress the transcription of genes in diverse ways, are one of the primary modulators of transcription. Transcription factors are a diverse class of proteins that are activated in a number of different ways to stimulate or repress target genes, including ligand binding and phosphorylation (1,2). For instance, phosphorylation of the well-studied transcription factor, c-Myc, results in activation and through interactions with other transcriptional

factors, drives the transcription of many genes (3,4), including those involved in B-cell proliferation (5). Another mechanism of transcriptional control involves the bundling of DNA around octameric protein complexes termed histones, which modulates the activation or repression of genes based on the accessibility of the DNA. This accessibility is determined by modifications to the N-terminal tails of histone proteins as well as modifications made directly to the DNA molecule itself (6,7). These transcriptional mechanisms are absolutely critical to ensure precise gene expression; however, extensive study in the field of post-transcriptional processing, or events that occur to an mRNA coincident with or following transcription, also play an important part in maintaining proper gene expression and, in turn, cell function and fate.

A multitude of post-transcriptional processing events occur on an mRNA transcript throughout its lifecycle (8) and are schematized in Figure 1.1. RNA polymerase II (PolII) is the polymerase responsible for transcription of DNA to produce mRNA (9) and is stimulated by the binding of transcription factors to the upstream genomic region as well as the phosphorylation state of its C-terminal domain (CTD), which contains up to 52 copies of the heptapeptide sequence YSPTSPS (10). Upon activation of transcription, PolII traverses the length of the genomic loci that it is transcribing and generates an RNA copy of the encoded DNA. As the RNA transcript is produced, processing events take place to begin the maturation of the message via processing factors that are loaded onto the CTD of RNA PolII (11). The loading of these factors onto the CTD ensures their presence at necessary locations and couples transcription to processing of pre-mRNAs (11). These events are often referred to as co-transcriptional and we include them within our definition of post-transcriptional processing.

As PolII generates a pre-mRNA transcript, the 5' end of the message emerges from the transcription complex. To protect the message from degradation machinery within the nucleus (and eventually in the cytoplasm), a 7-methylguanosine molecule is added to the 5' end of the message and is referred to as the 5' cap (12). The 5' cap is rapidly bound by the cap-binding complex, CBC20/80, in order to further protect the transcript from degradation (13). The 5' cap structure (along with other post-transcriptional processing events) also serves as a signal for downstream processing events and ultimately to the export machinery to indicate that proper processing has taken place and that this mRNA is competent for export to the cytoplasm (13-16).

Another early step in post-transcriptional processing is the splicing of intronic regions out of a pre-mRNA transcript. Introns in humans are typically large stretches of RNA sequence that lie between RNA exons, or those regions present in a mature mRNA. Splicing of many transcripts is constitutive and occurs on these mRNAs in virtually all cases and cell types (17); however, many genes (~50% in humans (18)) are subject to alternative splicing, meaning the differential inclusion and exclusion of various exons throughout the body of a pre-mRNA transcript. At a given genomic locus, RNA PolII transcribes the whole region and splicing factors (proteins and small RNAs that mediate and/or direct/repress splicing) dictate which version of the message will be expressed in a given cell type at a given time (19). Splicing events result in the joining of the 3' end and 5' start of two exons and, in higher eukaryotes, a multiprotein complex, referred to as the exon junction complex (EJC), is deposited 20-24 nucleotides upstream of the splice site and serves as a signal and platform for downstream processing events such as export and 3' end processing (20,21).

During the course of transcription, factors that stimulate and execute the cleavage at the 3' end of a pre-mRNA transcript are loaded onto the C-terminal tail of RNA PolII (22,23) and upon reaching the proper signal, cleavage occurs and 3' end processing commences. Upon cleavage, a series of adenosine residues are added to the 3' end of the transcript (~200-250 adenosines in human cells (24)) and comprise what is referred to as the poly(A) tail. With the exception of the histone mRNAs, which undergo a distinct 3' end processing mechanism (25), all mRNAs are polyadenylated (26); however, recent studies suggest there may be diversity in poly(A) tail length between classes of mRNA transcripts (27,28). Much like the cap structure that protects the 5' end of an mRNA from 5'-3' degradation machinery (13), the poly(A) tail is bound by poly(A) binding proteins (Pabs, which will be discussed extensively in the next section) (29) and is subsequently protected from 3'-5' degradation machinery (30). The poly(A) tail also serves as a signal for export-competent mRNPs within the nucleus and eventually aids in translation in the cytoplasm (29).

Upon proper processing of an mRNA that is ready to be exported, the mRNA (and bound proteins) interacts with multiple proteins coating the nuclear pore to be exported (31,32). Because export of a translationally incompetent or misspliced mRNA could be detrimental to the cell, this step of post-transcriptional processing is tightly regulated and receives multiple signals (33,34). Upon transport of mRNAs to the cytoplasm, a molecular transition occurs wherein many nuclear RNA binding proteins are exchanged for cytoplasmic versions upon or shortly after export (31). For instance, the nuclear cap-binding complex CBC20/80 is exchanged for the eukaryotic translation initiation factor 4E (eIF4E) upon translocation to the cytoplasm (35). Upon undergoing

the molecular wardrobe change, there are a number of different fates for mRNAs within the cytoplasm. Most mRNAs are rapidly engaged by the translational machinery and subject to translation to produce protein products. However, there are many examples of mRNAs that are trafficked to different locations within the cell to provide a pool of transcript close to the site where it is needed (36,37). For instance, many neuronal-specific mRNAs that encode factors necessary for proper axonal function are packaged into granules and transported along the length of an axon for delivery to the axon terminal (38). Upon reaching the axon terminal, they are locally translated and the resulting protein products are put to use on site (39). Some mRNAs that are exported are not immediately necessary and may need to be stored for later. These mRNAs can be stored in distinct cytoplasmic foci referred to as processing bodies, or P bodies (40), and be re-engaged with the translational machinery upon specific cellular signals (41,42). These translationally repressed, stored mRNAs provide the cells with a mechanism for rapid response to cellular stimuli that necessitate the production of certain proteins.

The eventual fate of every mRNA transcript is decay by various degradation factors (43). The length of time that an mRNA exists in the cell differs greatly between transcripts. For instance, the *c-Fos* mRNA, which encodes a proto-oncogene, has a half-life of 10-15 minutes in mammalian cells while the *β-globin* mRNA, which encodes the most common form of hemoglobin, has a half-life of more than 24 hours in the same cells (44). The diversity in half-life between transcripts depends on cis-elements within the mRNA, typically within the 3' untranslated region (3'UTR), which are bound by a broad class of RNA binding proteins and microRNAs (miRNAs) that regulate mRNA stability in myriad ways. In mammals, the initiating event in mRNA degradation is the removal of

adenosines from the poly(A) tail, or deadenylation (45). The shortening of the poly(A) tail is carried out in two phases by multiple complexes and upon reaching a critically short length, stimulates removal, or decapping, of the 5' cap (45). Removal of the two primary protective features present on an mRNA (the 5' cap and poly(A) tail) renders the transcript vulnerable to degradation from both the 5' and 3' end (45).

These post-transcriptional processing events, from the initial transcriptional event in the nucleus all the way to the decay of the message in the cytoplasm, are critical to ensure proper gene expression. Any misstep in processing can result in either degradation by nuclear surveillance machinery or the release of improperly processed transcripts into the cytoplasm where they can generate potentially harmful protein products (33,34). To ensure the proper processing of mRNAs, many of these events are coupled to one another via transcription. As discussed earlier, post-transcriptional processing factors interact with the CTD of RNA PolII to ensure their presence at the respective step in RNA processing (11). There is evidence that the phosphorylation state of the CTD (which changes across the length of the transcribed region (46)) influences the binding of post-transcriptional factors and directs the timing of their presence on the CTD (47-50), and therefore ensures the proper processing of each transcript. Each of the nuclear processing events described here leave a "mark" on mRNAs in the form of RNA binding protein complexes that serve as signals that proper processing has taken place and ensures the selective transport of export-competent mRNAs to the cytoplasm.

Factors that mediate post-transcriptional processing

As outlined here, post-transcriptional processing is a complicated series of events that function together with the ultimate goal of producing properly processed mRNA transcripts that are capable of being translated into functional protein products. Every step of post-transcriptional processing is regulated by a host of factors, including noncoding RNAs (ncRNAs) and RNA binding proteins. RNA binding proteins are a diverse class of proteins. Current studies predict that the human genome encodes approximately 1,900 RNA binding proteins (51) with significant diversity in their RNA binding domains. The most prevalent and best-characterized RNA binding domain is the RNA recognition motif, or RRM (52). RRM-containing RNA binding proteins comprise a group of more than 200 proteins (51). Other common RNA binding motifs include Arginine Glycine Glycine (RGG) domains, K Homology (KH) motifs as well as Cysteine Cysteine Histidine Cysteine (CCHC) and CCCH zinc fingers. These motifs along with more than 30 others (51) demonstrate the diversity in RNA binding proteins. Many RNA binding proteins contain more than one RNA binding domain, many with multiple types of domains. There is also considerable diversity in the classes of RNAs that are bound by different RNA binding proteins. There are RNA binding proteins that recognize single stranded RNA with considerable degeneracy in sequence specificity, as well as RNA binding proteins that recognize certain sequences, such as AU- or U-rich element binding proteins (discussed in Chapter 4) or the poly(A) binding proteins, which are discussed extensively in the next section. The observed combinatorial composition of RNA binding domains in many proteins as well as diversity within the RNA binding surfaces

themselves provides a wide array of sequence specificity that can be achieved with this family of proteins.

In addition to RNA binding proteins, there is a growing understanding of the role that noncoding RNAs (ncRNAs) play in regulating gene expression. The best-characterized type of ncRNA that has a role in post-transcriptional processing is the microRNA (miRNA), which base pairs with sequences found most often in the 3'UTR of target mRNAs (53). The binding of these 21-25 nucleotide RNAs, in cooperation with a miRNA binding complex, results in the translational repression and/or degradation of the message (53,54). Predicted miRNA binding sites are found in all mRNA transcripts and certain miRNA binding sites are represented in certain classes of transcripts such that one miRNA can regulate a set of related mRNAs (53). For instance, the *let-7* miRNA coordinates many of the mRNAs that contribute to cellular development and differentiation (55). miRNAs are therefore considered to be coordinators of gene expression. Other classes of ncRNAs that influence post-transcriptional events include (but are not limited to) the small nuclear RNAs (snRNAs), which are involved in mRNA splicing (56,57) as well as small nucleolar RNAs (snoRNAs), which are responsible for adding chemical modifications to ribosomal and transfer RNAs (58,59). Of note, ncRNAs do not function alone. They are bound by a number of different proteins that allow their function(s) to take place. For instance, miRNAs are bound by the RISC complex and are loaded onto transcripts to mediate repression or degradation (53,54). Also, snRNAs are complexed with RNA binding proteins to form snRNPs, or the complexes that mediate RNA splicing (56,57). Therefore the interfacing of these factors is critical to ensure proper gene expression. Because our understanding of ncRNAs is still in early stages, we

are at the tip of the iceberg in understanding how all of these factors work together to influence gene expression.

RNA binding proteins in human disease

As discussed extensively throughout this dissertation, post-transcriptional processing events are critical to ensure the proper gene expression profile of a cell or tissue. Therefore, the proper expression and function of RNA binding proteins (and ncRNAs), which mediate and direct the vast majority of post-transcriptional events, is imperative for maintenance of cell health. There are many examples of diseases that occur upon dysregulation of RNA binding proteins. For instance, the cytoplasmic mRNA cap binding protein, eIF4E, is overexpressed in many cancer types (60) and can drive oncogenic transformation in nontransformed cell lines (61). eIF4E overexpression is a widespread feature in breast cancer and patients with high levels of eIF4E experience higher rates of recurrence and death (62). As another example, autosomal recessive loss-of-function mutations in the gene encoding the Survival of Motor Neuron protein 1, or *SMN1*, result in spinal muscular atrophy (SMA), the most common genetic form of infant mortality (63,64). SMN1 is involved in the biogenesis of snRNPs, which are crucial for proper mRNA splicing, as well as regulation of axonal mRNP granules (64,65). Sadly, patients with SMA experience severe muscle atrophy and weakness in proximal limb muscles that often results in premature death (63). These are just two examples from a long list of RNA binding proteins that are implicated in human disease. Shown in Table 1.1 is a partial list of disease-associated RNA binding proteins. This table will surely

grow as our understanding of RNA binding proteins and their diverse role in post-transcriptional processing increases.

SECTION 2

The poly(A) tail: discovery and addition

As described in Section 1, the addition of a poly(A) tail to the cleaved 3' end of a growing pre-mRNA is a key post-transcriptional processing event. The poly(A) tail was discovered in the 1970s upon digestion of polysome-associated mRNAs with RNases that cut after C, G and U residues (66). These studies revealed an RNase-resistant fraction that was ultimately determined to be a polyadenosine stretch at the 3' end of transcripts that was not encoded by the DNA sequence (67-71). With the exception of the histone mRNAs (25), all eukaryotic mRNAs contain a poly(A) tail. Following the discovery of the poly(A) tail, the advent of DNA sequencing technologies revealed an evolutionarily conserved AAUAAA sequence upstream of the poly(A) tail (72). Further sequencing analyses revealed that this sequence, termed the poly(A) signal (PAS), which is slightly degenerate (70% AAUAAA and 15% AUUAAA present in human mRNAs (73)), is necessary for 3' end formation (74-76). These studies demonstrated that the PAS determines the 3' end of an mRNA and not the stop codon, as previously thought (77).

As mentioned previously, cleavage at the 3' end of an mRNA is the initiating event in 3' end processing and is mediated by multiple large protein complexes, including cleavage and polyadenylation specificity factor (CPSF) and the cleavage stimulatory factor (CStF) (78). CPSF is comprised of five subunits: CPSF-30, -73, -100, -160 and hFip1, all of which are necessary for cleavage and polyadenylation of an mRNA (78). The largest subunit, CPSF-160, is responsible for binding to the AAUAAA/AUUAAA

PAS (79), while CPSF-73 harbors the endonucleolytic activity required to cleave the transcript (80). CStF binds to an evolutionarily conserved U- or GU-rich sequence located downstream of the PAS, termed the downstream element (DSE), and in doing so ensures efficient 3' end formation (81,82). The actual cleavage event occurs at a location between the PAS and DSE and typically occurs 3' to an adenosine residue within the context of a CA dinucleotide (80). Other sequence elements, such as auxiliary upstream and downstream elements play roles in further enhancing efficient 3' end processing, but are not necessary for 3' end formation (78,83). The importance of these signals and subsequent 3' end formation is supported by single point mutations in the PAS of the *α2*- and *β-globin* genes that lead to two rare forms of thalassemia (84,85).

With the exception of the histone mRNAs, which undergo a cleavage-only 3' end processing reaction (86), all eukaryotic mRNAs are cleaved and polyadenylated. These events occur co-transcriptionally (87) via the loading of 3' end processing factors onto the CTD of PolII (88,89). As mentioned earlier, the PAS (and subsequent cleavage) determines the end of an mRNA (77); however, recent deep sequencing analyses reveal that more than half of human mRNAs possess alternative polyadenylation sites, thus expanding the possible lengths and sequences of 3'UTRs (73,90,91). Interestingly, shifts in PAS selection are observed during neuronal activation (92) and oncogenic transformation (93). The sequences encoded in the 3'UTR and the factors that are bound to it greatly influence many aspects of post-transcriptional regulation (8), including mRNA localization (36), translation (94), and stability (43). Therefore, shifts in 3'UTR length alter the composition of post-transcriptional regulatory sequences on an mRNA and can have a profound influence on gene expression, underscoring the importance of

elucidating the factors associated with and events surrounding alternative polyadenylation.

Immediately following cleavage at the 3' end, the second phase of 3'end processing commences with the addition of a poly(A) tail to the 3' cleavage product. Poly(A) tails are bound by a specific family of RNA binding proteins termed poly(A) RNA binding proteins, or Pabs, which are multifunctional players in gene expression (95). The events surrounding polyadenylation and an extensive introduction to the Pab family is presented in the following section.

Canonical poly(A) binding proteins

Conventional Pab proteins are typically defined by the presence of an RNA recognition motif (RRM) combined with biochemical evidence to demonstrate specific, high affinity binding to polyadenosine RNA. A single nuclear Pab, termed PABPN1, and multiple cytoplasmic Pabs, termed PABPC1, 3-5 and L1, have been identified in multiple organisms. PABPC1 is ubiquitously expressed while the remaining PABPC homologs differ in their spatial and temporal expression pattern. PABPN1 and PABPC1 are the best studied Pab proteins and are hence referred to here as the canonical Pabs. The terms PABPN1 and PABPC will be used throughout this chapter to refer to any ortholog of PABPN1 or PABPC1.

Nuclear poly(A) binding protein 1: PABPN1

PABPN1 is the primary nuclear Pab and is highly conserved among eukaryotes (96). PABPN1 is expressed ubiquitously in metazoans and PABPN1 orthologs have been analyzed in *D. melanogaster* and *C. elegans*, as well as *S. pombe*. However, to date there is no comparable PAPBN1 counterpart in *S. cerevisiae* (97). The PABPN1 protein consists of a number of functional domains, which are diagramed in Figure 1.2. The best characterized domain of PABPN1 is the RRM found toward the C-terminus of the protein, which mediates high affinity polyadenosine RNA binding (98). PABPN1 recognizes 10 to 11 nucleotides (99,100) and detailed binding studies suggest that most of these adenosines, if not all, are bound by PABPN1 in a base-specific manner (100). The arginine-rich region located C-terminal to the RRM also contributes to adenosine RNA recognition (101). This domain is asymmetrically methylated; however, the methylation has no apparent effect on the affinity, specificity, or cooperativity of RNA binding (98,101), and instead modulates interactions with the PABPN1 nuclear import receptor, transportin (102,103). The helical domain N-terminal to the RRM is required for stimulation of poly(A) polymerase (PAP). Of note, the stretch of ten alanines located immediately adjacent to the initiating methionine is expanded to anywhere from 12-17 alanines in the late-onset human disease, oculopharyngeal muscular dystrophy (OPMD), which is characterized by a progressive weakening of a specific group of muscles in the head as well as limb muscles in some instances of the disease (96). How this modest alanine expansion leads to this tissue-specific disease is unknown.

The role of PABPN1 in polyadenylation has been extensively studied largely through elegant biochemical studies (24,104,105). These conventional functions of

PABPN1 are schematized in Figure 1.2. As stated previously, 3' end processing of pre-mRNA transcripts occurs via a two-part process consisting of cleavage and subsequent polyadenylation. These processing events are mediated by a large, heterooligomeric protein complex that is comprised in part of PAP and CPSF (106). Upon cleavage of the pre-mRNA by CPSF-73, PAP begins to add adenosine residues to the upstream cleavage product in a slow, or distributive, manner. Binding of PABPN1 to the first 11 adenosines stimulates PAP activity and triggers processive polyadenylation (104,105). Evidence that PABPN1 increases the affinity of PAP for RNA, thus leading to processive polyadenylation by a tethering mechanism is provided through analysis of RNA binding mutants of PABPN1 that are unable to stimulate processive polyadenylation (24). In addition, amino acid changes in the helical domain of PABPN1, which do not affect the affinity of PABPN1 for RNA, but do abrogate binding to PAP, also eliminate PABPN1-mediated stimulation of processive polyadenylation (105).

In the "molecular ruler" model, PABPN1 binds the initial 11-14 adenosines, and then coats the growing poly(A) tail to form 21 nm spherical particles that enable the RNA to fold back and maintain an interaction between CPSF and PAP (24,107). When a length of 200-300 adenosines is reached, this complex is disrupted and the phase of processive polyadenylation is complete (Figure 1.2) (24). This model is supported by experiments using electron and scanning force microscopy with oligo(A) RNA and purified PABPN1 protein (107). These studies using primarily purified proteins have provided the field with significant insight into the role of PABPN1 in regulating polyadenylation; however, further studies to assess the role of PABPN1 in the context of other RNA binding

proteins as well as other functions that have emerged for this protein are required to build a complete model of polyadenylation.

Proper 3’ end processing and polyadenylation of transcripts is required for efficient mRNA export from the nucleus to the cytoplasm (106). The finding that PABPN1 can shuttle between the nucleus and the cytoplasm has led to the suggestion that PABPN1 could contribute to poly(A) RNA export from the nucleus (108) (Figure 1.2). Consistent with this suggestion, nuclear accumulation of poly(A) RNA is observed in cells expressing the Influenza A virus NS1 protein (NS1A), which binds to and inhibits the nuclear-cytoplasmic shuttling of PABPN1 (109). Furthermore, primary muscle cells depleted of PABPN1 also display nuclear accumulation of bulk poly(A) RNA (110). Altered steps in the polyadenylation process could cause this nuclear poly(A) RNA retention, as proper polyadenylation is required for efficient mRNA export from the nucleus (106,111,112). However, two independent studies using templated poly(A) tracts present at the 3’ ends of reporter transcripts show that these artificial substrates are exported (113,114), suggesting that the presence of a tail alone may be sufficient for RNA export and therefore raising the question of how the steps of polyadenylation are coordinated with the generation of an export-competent mRNP complex. These studies suggest that PABPN1 could regulate mRNA export from the nucleus, but further analyses are required to understand whether PABPN1 plays a direct role in modulating this critical step in gene expression or whether effects on upstream events such as polyadenylation impair subsequent mRNA export.

Cytoplasmic poly(A) binding protein: PABPC

The major cytoplasmic poly(A) binding protein, PABPC, is ubiquitously expressed and found in all eukaryotes. As shown in Figure 1.2, PABPC contains four tandem RNA recognition motifs (RRMs), an unstructured linker region and a C-terminal helical domain with five α-helices (97,115). PABPC contacts polyadenosine RNA through the RRMs and requires a minimum of 12 nucleotides for high affinity binding (116). Together RRMs 1 and 2 mediate oligo(A) binding while other pairwise combinations or single RRMs are not sufficient for binding (117). However, binding of all four RRMs is required to account for the ~25 nucleotide footprint of PABPC (116,118). In addition, the N-terminal RRMs and the C-terminal α-helical domain serve as protein-protein interaction domains to mediate the various functions of PABPC. The RRMs facilitate binding to eukaryotic initiation factor 4G (eIF4G) (119), the α-helices facilitate binding to eukaryotic release factor 3 (eRF3) (120) and promote PABPC dimerization (121). Both of these domains are involved in binding Poly(A) binding protein Interacting Proteins (PAIPs) (122,123) and GW182, an RNA induced silencing complex (RISC) protein (124). Thus, PABPC serves as a platform to coordinate multiple players that modulate gene expression.

The role of PABPC in regulating mRNA translation has been extensively studied (97,115) (Figure 1.2). Studies with *S. cerevisiae* reveal that cytoplasmic mRNAs form a closed loop structure to promote 40S ribosomal subunit recruitment (125). PABPC is required to assume this structure, which facilitates efficient translation (119,126,127). The cap-binding complex, eIF4F, enables formation of the closed loop structure with the eIF4G subunit linking the 5’ cap-bound eIF4E subunit to poly(A) tail-bound PABPC

(Figure 1.2) (127,128). Further evidence suggests that PABPC could play a role in 60S ribosomal subunit joining (129-131) and promote ribosome recycling by interacting with eukaryotic release factor 3 (eRF3) (132). In summary, PABPC mediates a number of interactions between the translationally poised mRNA and ribosome that underlie the role in ensuring efficient translation.

Similar to the role in translation, the function of PABPC in modulating mRNA decay is well established (97,115) (Figure 1.2). mRNA decay is a multi-step process that is typically initiated by poly(A) tail shortening to a length of 10-15 nucleotides (45). Deadenylation is followed by decapping with the Dcp1-Dcp2 complex and digestion by the 5'- to 3'-exoribonuclease Xrn1 (45). PABPC inhibits the deadenylase, which blocks the initial step of mRNA decay (30,133). PABPC also interacts with other RNA binding proteins, including the novel Pab hnRNP-Q1, to inhibit the decay of specific mRNA transcripts by blocking deadenylase or endonuclease activity (134-136). Therefore, PABPC affects both global and transcript-specific mRNA decay.

Novel roles for canonical Pabs

The well-studied roles of the canonical Pabs, PABPN1 and PABPC, in modulating polyadenylation, translation, and mRNA decay demonstrate the importance of these proteins in post-transcriptional processing. However, recent studies reveal diverse, novel functions of these canonical Pabs (29,95), expanding our understanding of how these key proteins regulate gene expression and pointing toward a new model that integrates the novel and canonical functions of PABPN1 and PABPC. These studies have unveiled roles for PABPN1 as a key factor in influencing poly(A) site selection

(137,138), regulating lncRNA expression (139), coordinating a novel nuclear RNA decay pathway (140), and the pioneer round of translation (141). Additionally, recent work has revealed roles for PABPC in miRNA-mediated repression and decay (95,124), nonsense-mediated decay (95,142), LINE retrotransposition (143,144), mRNA localization (145), and poly(A) independent roles in translation (144,146,147). Together, these studies greatly expand our understanding of the function of PABPN1 and PABPC in mRNA processing events (29). Future studies of interest include analyzing how the multiple functions of PABPN1 and PABPC are coordinated to influence gene expression, as well as how novel Pabs such as ZC3H14, hnRNP-Q1 and LARP4 fit into the picture of post-transcriptional processing via binding to polyadenosine RNA (Figure 1.3).

ZC3H14 is a novel poly(A) RNA binding protein

Zinc finger CCCH-type containing protein #14 (ZC3H14) is the evolutionarily conserved human counterpart of a novel class of zinc finger Pabs (148). The canonical Pabs, PABPN1 and PABPC, bind polyadenosine RNA via RRM motifs (29); however, biochemical studies provide evidence that the zinc fingers in ZC3H14 confer specific binding to polyadenosine RNA (148), thus establishing a novel mode of polyadenosine RNA recognition. Putative orthologs of ZC3H14, which share a common domain structure, have been studied in a variety of model organisms, including *S. cerevisiae* (149) (Nab2), *D. melanogaster* (150) (dNab2), *C. elegans* (151) (SUT-2), and *M. musculus* (152) (ZC3H14/MSUT-2) and will be discussed later in this section.

A linearized schematic of ZC3H14 is shown in Figure 1.3. The N-terminus of ZC3H14 adopts a proline tryptophan isoleucine (PWI)-like fold, which, in yeast, mediates interactions with nuclear pore-associated proteins and facilitates proper mRNA export from the nucleus (153). A classical nuclear localization signal (cNLS) is predicted to be responsible for targeting ZC3H14 to the nucleus (154). The tandem CCCH zinc fingers located at the C-terminus of ZC3H14 are responsible for high affinity polyadenosine RNA recognition (148,149). *ZC3H14* is alternatively spliced to encode at least four distinct isoforms, all of which include the C-terminal zinc fingers and therefore are all predicted to interact with polyadenosine RNA (154).

As schematized in Figure 2.1A, isoforms 1-3 of ZC3H14 are very similar to one another, with the only differences arising from the alternative inclusion and/or exclusion of a few, small internal exons (154). Isoform 4, however, is very different from the others as it is transcribed from a different start site and lacks the N-terminal PWI-like fold and putative cNLS (Figure 2.1) (154). Expressed sequence tag (EST) data along with qRT-PCR analyses suggest that variant 4 is expressed at much lower levels than the other three variants in many tissues (Figure 3.1), but is enriched in mouse brain and testes (154). As expected from the predicted cNLS, isoforms 1-3 of ZC3H14 localize to the nucleus at steady-state, specifically in nuclear speckles (160), which are sites that house RNA processing factors (155). Localization of a GFP-tagged construct of isoform 4 supports the predicted cytoplasmic localization of this isoform based on the lack of a cNLS (154). Treatment with the transcriptional inhibitor, Actinomycin D (ActD) (156), leads to alteration in the number and size of nuclear speckles (157). Consistent with typical dynamics for nuclear speckle proteins, we observe a concomitant change in the

localization of ZC3H14 at these sites upon treatment with ActD (154). Interestingly, we also observe an increase in nuclear isoforms 1-3 of ZC3H14 in the cytoplasm upon treatment with ActD (data not shown), consistent with other RNA binding proteins that relocalize in response to stress (158). These data suggest that ZC3H14 isoforms localize to specific compartments at steady-state, but their localization is dynamic in response to cellular stressors, such as ActD.

ZC3H14: Insight from model organisms

Although little is known about the molecular function of human ZC3H14, studies in model organisms provide insight into potential roles in post-transcriptional processing. The majority of these studies have been carried out in *S. cerevisiae* analyzing Nab2. The Nab2 protein localizes to the nucleus at steady-state, but shuttles between the nucleus and cytoplasm (159). Nab2 associates with poly(A) mRNA transcripts prior to export (149), likely modulating polyadenylation and facilitating the generation of export-competent mRNPs (160,161). *S. cerevisiae* cells expressing N-terminal deletion mutants of Nab2 display nuclear accumulation of poly(A) RNA as well as extended poly(A) tails (159,162). However, the existence of Nab2 RNA binding mutants that confer defects in poly(A) tail length with no nuclear accumulation of poly(A) RNA highlights the critical role of the zinc finger domain in poly(A) tail length regulation (163).

Recent structural analyses of both *S. cerevisiae* and *C. thermophilum* ZC3H14 reveal that three zinc fingers interact to form an RNA binding module (164,165). The crystal structure of zinc fingers 3-5 of *C. thermophilum* Nab2 in complex with an A_8

RNA oligo revealed that these zinc fingers form the binding unit that interacts with polyadenosine RNA with base-specific interactions on multiple adenosine residues (165). These three zinc fingers share the greatest homology with hZC3H14 zinc fingers 1-3 and *S. cerevisiae* Nab2 zinc fingers 5-7, which is consistent with previous studies implicating the final three zinc fingers of Nab2 in high affinity polyadenosine RNA binding (148) as well as poly(A) tail length control (166,167). Further analysis of the crystal structure revealed that although multiple adenosine-specific interactions are present, the spacing of the individual zinc fingers within the binding unit could result in Nab2 also binding to degenerate, or A-rich sequences instead of solely to poly(A) tracts. This information opens the possibility that this family of proteins could bind to poly(A) tails as well as A-rich sequences, and presents a model in which ZC3H14 could interact with a diverse spectrum of RNA transcripts.

Additional insight into a potential function for ZC3H14 has been obtained from a *D. melanogaster* loss-of-function model of *ZC3H14*, *dNab2* null flies (150). Studies in this model demonstrate that dNab2 has specificity for polyadenosine RNA *in vitro* and that RNA isolated from *dNab2* null flies displays extended poly(A) tails. However, no defect in bulk poly(A) mRNA export has been detected (150), lending support to a primary role for ZC3H14 in control of poly(A) tail length. Consistent with this model, siRNA-mediated depletion of ZC3H14 from cultured murine cells causes extended poly(A) tails with no apparent impact on poly(A) RNA localization (168). Together, these data suggest a role for ZC3H14 in modulating post-transcriptional processing via an interaction with the poly(A) tail. Due to the presence of multiple Pabs in human cells, an

important objective moving forward will be integrating the function of these distinct proteins that all interact with a common element, the poly(A) tail.

ZC3H14 in critical for proper neuronal function

Interest in this novel class of zinc finger Pabs has been sparked by recent studies showing that a mutation of *ZC3H14* that results in a premature stop codon and subsequent loss of this ubiquitously expressed protein leads to an autosomal recessive form of nonsyndromic intellectual disability (150). The brain-specific phenotype in these patients suggests that the function of ZC3H14 is particularly critical in the highly specialized cells found in the brain. With respect to the role of zinc finger Pabs in the brain suggested by the phenotype of *ZC3H14* patients, behavioral defects observed in *dNab2* null flies can be rescued by transgenic expression of either *Drosophila* Nab2 or human ZC3H14 specifically in neurons (168). This result demonstrates the critical role of Nab2/ZC3H14 in ensuring proper neuronal function and also provides experimental evidence for the functional conservation of this protein family through evolution. Rescue of neuronal phenotypes is accompanied by rescue of the molecular phenotype of extended poly(A) tails also observed in *dNab2* mutant flies (150,168). Together, these data suggest that the role of ZC3H14 in poly(A) tail length control may underlie its function in development and disease.

An independent line of experimentation provides a further link between ZC3H14 and neuronal function. A screen for suppressors of the neurotoxicity of aggregated tau protein in *C. elegans* identified mutations in the Suppressor of Tauopathy 2 (*SUT-2*)

gene, which encodes the nematode ortholog of ZC3H14 (151). Loss of function mutations in *SUT-2* suppressed the uncoordinated phenotype, tau aggregation, and the observed neurodegenerative changes in this worm model, suggesting that SUT-2, when present, enhances tau-induced neurotoxicity (151). Further analysis of the human protein ZC3H14/mammalian SUT-2 (MSUT-2) demonstrate reduced MSUT-2 staining in the hippocampus, a region of the brain affected by tau pathology (169), in patients with Alzheimer's disease (152). The authors suggest that decreased MSUT2 staining in patient neurons may reflect a population of neurons that are spared from tau pathology and subsequent neurodegeneration (152).

The existence of multiple loss-of-function models of ZC3H14 with neuronal phenotypes strongly suggests a critical role for ZC3H14 in neurons. However, ZC3H14 is ubiquitously expressed, so understanding the tissue-specific phenotype upon loss of this protein is a primary objective moving forward.

Defining a role for ZC3H14 in mRNA processing

As discussed throughout this section, there are two primary objectives of this study, the first of which focuses on understanding the role of ZC3H14 in post-transcriptional processing events in human cells. Orthologs of ZC3H14 have been studied in a variety of model organisms, including *D. melanogaster* (150) and *S. cerevisiae* (149); however, the roles of Nab2 and dNab2 are not completely conserved. For instance, loss of dNab2 in flies does not result in a defect in poly(A) mRNA export (150), which is a well-established phenotype of yeast cells expressing mutant versions of Nab2 (159,162).

Determining the role of ZC3H14 in mRNA processing events will likely include addressing which (if any) of the roles discovered in model organisms are conserved in human cells. Another important point to take into account is the presence of at least one other nuclear Pab in human cells, PABPN1. Whether ZC3H14 and PABPN1 have overlapping or divergent roles in mRNA processing via the poly(A) tail is yet to be determined and proves to be an important objective in future studies. A recent study of ZC3H14 and PABPN1 orthologs in fission yeast has begun to address this issue (170), yielding promising insight into this question of redundancy of nuclear Pabs.

Whether ZC3H14 plays a role in mRNA processing itself is also unclear. Recent work in *S. cerevisiae* presents a model where Nab2 is involved in mRNA quality control and the generation of export-competent mRNPs (160,161). mRNA processing events are tightly coupled to one another, making the study of individual steps or processing events difficult to elucidate. However, these studies suggest that Nab2 may serve as a signal to indicate that proper mRNA processing has occurred and/or a coordinator of these events, ultimately resulting in the selective export of properly processed mRNAs. Finally, studies performed in yeast and flies focus on a single isoform of Nab2/dNab2; however, human cells express at least four distinct isoforms of ZC3H14 (154). The longer, nuclear isoforms of ZC3H14 are the most similar to Nab2 and dNab2 based on sequence and domain analysis. The presence of a distinct cytoplasmic isoform of ZC3H14 that can likely bind polyadenosine RNA suggests that ZC3H14 has a role in modulating mRNA in the cytoplasm. Integrating the function of multiple isoforms of ZC3H14 in human cells will yield a more comprehensive understanding of this novel Pab family.

The second objective of our studies focuses on tissue specificity: how does the loss of a ubiquitously expressed protein, which presumably has functions in many cell types, result in a tissue-specific phenotype? One leading hypothesis centers on the idea of specificity in the spectrum of mRNA targets that are bound and regulated by ZC3H14. Perhaps the transcripts that are specifically bound by ZC3H14 are either expressed exclusively in neurons or are simply expressed at higher levels in neuronal tissue and therefore loss of regulation of these transcripts renders these cells more susceptible to loss of ZC3H14. However, achievement of specificity by a polyadenosine RNA binding protein that could, in theory, bind to every mRNA transcript (with a poly(A) tail) is another challenging issue in itself. Current work in our lab is focused on elucidating binding partners of ZC3H14 that may aid in achieving transcript and/or functional specificity. Finally, many RNA processing factors are highly expressed in neuronal tissue and there is a higher level of RNA processing in the brain than many other tissues (51,171), so the brain could simply be more susceptible to loss of ZC3H14 than other tissues. Whether the critical post-transcriptional role of ZC3H14 exists only in neurons is yet to be determined but remains an active area of research.

Many of the questions raised here are addressed in Chapter 2 of this dissertation, which focuses on a specific and robustly affected mRNA target of ZC3H14, which may have underlying implications for the intellectual disability that occurs in patients with loss of ZC3H14.

SECTION 3

The 3' untranslated region

As described previously, the 3' end of a pre-mRNA is not determined by the end of the mRNA coding sequence, but instead by a poly(A) signal and subsequent 3' end processing at a defined site downstream of the coding sequence. This region between the end of the coding sequence and the poly(A) tail is referred to as the 3' untranslated region, or the 3'UTR, and represents an active site for post-transcriptional processing events. There is significant diversity in the lengths of 3'UTRs in human transcripts, ranging anywhere from <100 nucleotides all the way up to more than 10 kilobases in some instances (172,173). Although the 3'UTR (as a non-coding region of an mRNA) is under less evolutionary constraint than the coding region, early sequence analyses revealed that there is considerable conservation within regions of 3'UTRs (174), which were later determined to represent functional elements within the 3'UTR that are bound by a variety of post-transcriptional factors. These post-transcriptional factors include many different types of RNA binding proteins as well as miRNAs, both of which play critical roles in influencing gene expression via the 3'UTR.

The sequences present in the 3'UTR and the factors that are bound to it greatly influence many aspects of post-transcriptional regulation (8), including mRNA localization (36), translation (94), and stability (43). For instance, the presence of a conserved 54 nucleotide element in the 3'UTR of the *β-Actin* mRNA mediates binding by zipcode-binding protein 1 (ZBP1), resulting in the specific localization of this mRNA in the dendrites of rat hippocampal neurons (175,176). In addition, the translation of many

mRNAs is modulated by interaction between the cytoplasmic polyadenylation element binding protein (CPEB) and cytoplasmic polyadenylation elements found within the 3'UTR of target mRNAs (177). Binding of CPEB to CPE-containing mRNAs results in binding of other CPEB binding partners, shortening of the poly(A) tail, and (in most cases), temporary translational repression (94,177). Finally, the presence of AU- or U-rich sequences within the 3'UTR of transcripts can lead to increased or decreased mRNA half-life, depending on the factor bound to the particular element (43,178). These AU- and U-rich elements and their role in mRNA stability will be discussed more extensively later in this section.

An additional layer of complexity in 3'UTR-mediated regulation is represented by microRNAs (miRNAs), which are small noncoding RNAs (ncRNAs) that repress target expression by base pairing to sequences within the 3'UTRs of mRNA transcripts (53,179). One miRNA can bind to many mRNAs, often times within a certain class of transcripts, and in doing so can regulate an entire cellular program, such as the role of the *let-7* miRNA in regulating development and differentiation (55). Recent work has shown that miRNAs and RNA binding proteins participate in intense cross-talk and regulation on 3'UTRs, deepening the complexity of how post-transcriptional factors influence gene expression via the 3'UTR (180). Regardless of the complexity of these events, clearly the presence of multiple, sometimes competitive and/or cooperative binding events allow cells to fine-tune the timing, location and levels of expressed mRNAs.

Transcriptome profiling studies performed in recent years have revealed that more than half of mRNAs contain 3'UTRs with variable lengths, a phenomenon caused by the alternative 3' end processing events that result in 3'UTRs of different lengths (90,91).

This process is referred to as alternative polyadenylation (APA) and extensive study in this area has revealed that altering the length of a 3'UTR can have a tremendous effect on gene expression (181,182). For instance, the 3'UTR of the myogenic transcription factor, *Pax7*, which is required for survival and proliferation of muscle stem cells (183), is targeted by *miR-206*, which promotes muscle differentiation (184). In muscle stem cells, *Pax7* evades targeting (and subsequent repression) by *miR-206* through the use of an upstream PAS that results in a shorter 3'UTR (181). This shorter 3'UTR is expressed specifically in muscle stem cells and allows for continued expression of elevated *Pax7* levels to maintain a sufficient population of muscle stem cells (181). This study is just one (of many) example of how alteration of the 3'UTR length can have significant effects on gene expression.

Sequencing analyses performed on 3'UTR sequences across various tissues reveal interesting trends in tissue specificity with respect to 3'UTR length. For instance, analysis of the 3'UTRs from mRNAs isolated from brains, specifically hippocampal tissue, reveals significantly longer 3'UTRs compared to many other tissues (172). Additionally, mRNAs isolated from various tumor samples typically have shorter 3'UTRs than mRNAs isolated from normal control tissue (92,93,182,185). These shorter 3'UTRs contain fewer regulatory elements and correlate with enhanced proliferation, thus making the investigation of 3'UTR-dependent regulation of mRNAs an important area of research. In the remainder of this section and throughout Chapter 4, we will discuss one specific class of RNA binding proteins and the importance of their interaction with the 3'UTRs of cancer-relevant mRNAs.

AU-rich elements and the factors that bind them

As mentioned in the previous section, conserved sequence elements located within the 3'UTRs of mRNA transcripts typically serve as sites of functional conservation. One of the well-studied roles of cis-elements in the 3'UTR is the regulation of mRNA stability. AU-rich elements, or AREs, are the best characterized cis-element involved in mRNA degradation (43). These elements were first identified as highly conserved sequences in the 3'UTR of highly labile mRNAs that encode transcripts such as *Tumor Necrosis Factor α* (*TNF α*), *fibronectin*, and many of the interferons (186). Shortly thereafter, the 3'UTR of *c-Fos*, which encodes a proto-oncogenic transcription factor (187) and contains an ARE, was fused to a *β-globin* reporter transcript, resulting in significantly reduced mRNA stability (188). This experiment provided the first evidence that ARE-containing 3'UTRs might confer reduced or altered mRNA stability. Finally, the first definitive evidence that the ARE is in fact the destabilizing element within the 3'UTR came from the addition of the 51 nucleotide ARE from the *GM-CSF* 3'UTR into a *β-globin* 3'UTR reporter construct, which specifically resulted in destabilization of this transcript (189). The importance of these ARE elements for maintaining precise control of gene expression and, in turn, cell health is highlighted by many studies, one of which demonstrates that deletion of the ARE in the *c-Fos* 3'UTR results in oncogenic transformation due to the robustly increased stability of this otherwise tightly regulated transcript (190). These foundational studies, which characterized the identity and importance of AU-rich elements, led to an era of intense focus on identifying the factor(s) that bind to AREs and execute their role in post-transcriptional processing.

AU-rich element binding proteins, or ARE-BPs, are a well-studied class of ~20 RNA binding proteins that are involved in mRNA stability and, as more recently defined, translational regulation (178). Extensive studies have identified many different ARE-BPs that mediate the observed destabilization of ARE-containing mRNAs. These factors include the well-studied RNA binding proteins ARE/poly(U)-binding/degradation Factor 1 (AUF1), the KH-type Splicing Regulatory Protein (KSRP), Tristetraprolin (TTP) and Butyrate Response Factor 1 (BRF1) (43). These proteins are diverse in their RNA binding modules, however, each of them have specificity for AREs and in binding to these elements, nucleate the binding of other mRNA stability factors, including ribonucleases, resulting in rapid mRNA degradation (43). Another well-characterized ARE-BP is T-cell Intracellular Antigen 1, or TIA1, which represses the translation of target mRNAs, such as *TNFα*, by binding to the ARE in its 3'UTR (191). TIA1 also plays an important role in splicing by binding to U-rich intronic regions of target mRNAs (192). Finally, the best-studied family of ARE-BPs is the Hu family of RNA binding proteins, which include Human Antigen A (HuA)/HuR, HuB, HuC and HuD (43). The members of this family have well-studied roles in positively regulating the stability of target mRNAs (178) and are also implicated in a number of types of cancer (193), thus making them an important class of RNA binding proteins to study.

The onset of the sequencing era has greatly expanded our understanding of the prevalence of AREs found within mRNA sequences. An estimated 5-8% of the transcriptome contains AREs, including many proto-oncogenes, cell cycle regulators and apoptotic factors, demonstrating that ARE-containing mRNAs encode proteins with diverse functions (194). These studies were performed using algorithms to identify

classical ARE motifs as well as CLIP-seq analyses with ARE-BPs demonstrating binding to these AU- and U-rich elements. Despite this onslaught of information, our understanding of how these sequences influence stability and translation is still limited. For instance, do all of the AREs identified by sequence analysis have functional relevance? Also, there are many different types of ARE-BPs. What dictates which proteins bind to certain AREs at a given time/location? Finally, recent work has demonstrated that many ARE-BPs interact with their own mRNAs (as well as other ARE-BP mRNAs) and influence their expression (195), suggesting complex regulatory networks for this protein family. Understanding the spectrum of targets bound by specific ARE-BPs as well as the functional consequence of binding by individual or competitive/coordinate ARE-BPs will certainly broaden our understanding of 3'UTR-mediated regulation by AU-rich binding proteins.

HuR and TIA1, two U-rich element-binding proteins

The mRNA stabilizing factor, HuR

As mentioned earlier, the Hu family is a well-studied class of RNA binding proteins that bind to AU-rich elements, typically within the 3'UTR of target mRNAs and positively regulate mRNA stability (178). The Hu family members were first identified as neuronal antigens recognized by sera from patients with paraneoplastic encephalomyelitis (196). Cloning of the sequences encoding these antigens revealed their significant conservation to the Embryonic Lethal Abnormal Vision (ELAV) family of RRM-containing proteins in *Drosophila* (196), which are involved in mRNA processing,

specifically in neuronal tissues (197). Consistent with the expression pattern of ELAV in *Drosophila*, HuB, HuC and HuD are expressed primarily in terminally differentiated neurons (198) and many studies have focused on their importance in binding to AREs within the 3'UTRs of many neuron-specific mRNAs (198-202).

HuR is the ubiquitously expressed member of this family of proteins and was discovered in an attempt to identify any other Hu family members that are expressed in non-neuronal cell types (203). In this study, HuR was purified from HeLa cells and functionally characterized through binding studies with the *c-Fos* 3'UTR (203), a well-characterized ARE-containing mRNA (44). Nearly 20 years of study into the role of this ubiquitously expressed protein in mRNA stability as well as its association with various types of cancer has led to HuR being the best-characterized member of this family.

A linearized domain map of HuR is shown in Figure 1.4A. HuR contains three RRMs; however, only RRMs 1 and 2 are involved in ARE recognition (204,205). A recent co-crystal structure of HuR RRMs 1 and 2 in complex with an AUUUUUUAUUUU RNA oligomer demonstrated that while RRM1 is the primary ARE recognition domain within HuR, the conformational change that takes place upon RNA binding leads to additional interactions between RRM2 and the target mRNA, ultimately increasing RNA binding affinity (206). The third RRM of HuR is less understood. Preliminary biochemical studies performed in the late nineties demonstrated that RRM3 has affinity for long stretches of polyadenosine and may therefore interact with the poly(A) tail (204,205). Finally, the HuR nucleocytoplasmic shuttling domain, or HNS, which is located in the hinge region between RRMs 2 and 3, mediates the nucleocytoplasmic shuttling of HuR (207). There is significant sequence conservation

between the four members of the Hu family, specifically within the sequences that encode the RRMs (198), supporting their critical importance for the function of this protein family.

HuR is localized primarily to the nucleus at steady-state; however, multiple studies have demonstrated that HuR shuttles and can shift in localization toward the cytoplasm upon cellular stress, including transcriptional inhibition (207) and oxidative stress (208). The well-studied role of HuR takes place in the cytoplasm where it positively regulates the stability (209) and translation (193) of target mRNAs. A few well-characterized mRNA targets of HuR include *c-Fos* (210-212), *Cyclin D1* (213), *GM-CSF* (211), *TNFα* (214) and *Cox-2* (215), highlighting the diversity in mRNA targets that are regulated by HuR.

The mechanism of mRNA stabilization by HuR is unclear, although multiple models exist (Figure 1.4B). One model suggests a physical block to prevent destabilizing ARE-BPs and ribonucleases from accessing and degrading the mRNA, perhaps through oligomerization of HuR on target mRNAs. Studies have also demonstrated interplay between HuR and miRNA machinery on specific transcripts that results in modulation of the stability and/or translation of the target mRNA (216,217). Multiple recent studies have demonstrated a role for HuR in promoting the translation of mRNA targets (Figure 1.4B) (218-220); however, a unifying mechanism for translational regulation has not emerged. In addition, recent work has begun to unveil nuclear functions of HuR, including playing a role Alternative Polyadenylation (APA) (221,222) and pre-mRNA splicing (223-225). Together, these studies expand our understanding of how HuR

regulates gene expression and suggest that the complex role of HuR in modulating gene expression must be defined on a target-by-target basis.

The translational regulator, TIA1

As mentioned earlier in this section, the ARE-BP, TIA1, is involved both splicing and translational regulation of target mRNAs (226). TIA1 was initially identified as a granule-associated protein in cytolytic T lymphocytes (CTLs, or "killer cells"), which are the immune cells responsible for the recognition and elimination of infected and transformed cells (227,228). TIA1 was characterized as an apoptosis-promoting factor due to its ability to induce DNA fragmentation in targeted cells (226); however, the role of TIA1 in apoptosis was unexpected due to sequence analyses that revealed its identity as an RNA binding protein (227). Although a specific role for TIA1 in the promotion of apoptosis is still unclear, many studies have revealed that it is involved in the translational repression and splicing of many mRNAs that are involved in the apoptotic program (226), thus making TIA1 an important protein to study within the context of cancer.

As shown in Figure 1.4, TIA1 contains three tandem RRMs (227,229). RRM2 of TIA1 has specificity for U-rich RNA and mediates high affinity binding to intronic and 3′UTR regions of target mRNAs in cooperation with RRM3 (230,231). The C-terminus of TIA1 contains a glutamine-rich (Q-rich) domain (227,229), which is characteristic of prion proteins and is, in fact, required for TIA1-mediated stress granule assembly, which will be discussed later in this section (232-234). The RRM1 and Q-rich domains are both involved in recruitment of the splicing factor, U1 snRNP, to U-rich intronic regions, resulting in exon inclusion (235). Like HuR, TIA1 has a steady-state nuclear localization

but can shuttle between the nucleus and cytoplasm (232). The shuttling function of TIA1 is mediated by specific sequence elements present within RRMs 2 and 3 (236). In response to cellular stressors such as transcriptional inhibition and oxidative stress, TIA1 can shift in localization toward the cytoplasm, where it binds to the 3′UTR of target transcripts and promotes the formation and sorting of translationally incompetent preinitiation complexes into stress granules, resulting in translational repression (236-238). A few well-studied targets of TIA1 include *TNFα* (191), *Cox-2* (239), *MMP13* (240), and the *β_2-adrenergic receptor* (241) mRNAs, demonstrating a rich diversity in targets of TIA1.

The role of TIA1 in translational repression is well-studied (Figure 1.4B) (237). TIA1 is a critical component of mammalian stress granules (233), which are distinct cytoplasmic foci that form in cells exposed to various stresses including heat, UV irradiation, oxidative conditions and hyperosmolarity (237). Analysis of the components of stress granules reveals the presence of many translation initiation factors, suggesting that the mRNPs present there are stalled at the initiation of translation (237,242). Binding of TIA1 to AREs located within the 3'UTRs of target mRNAs promotes the formation of a noncanonical preinitiation complex, which is a stress granule core component and leads to translational repression of the bound mRNA (Figure 1.4B) (233). Interestingly, the formation and dissipation of stress granules upon treatment (and removal) with certain stress granule-inducing drugs, such as arsenite, suggests that these are dynamic domains that are specifically involved in translational repression during times of stress (232,233,237). Interestingly, analysis of transcripts present in stress granules revealed that certain abundantly expressed transcripts, such as those that encode housekeeping

proteins, are repressed and stored within stress granules, while transcripts encoding stress-responsive proteins are actively translated (237,242), suggesting elegant specificity in translational regulation during times of stress. Together, these studies underscore the importance of TIA1 in translational regulation, specifically within the context of stressed cells.

TIA1 also has a well-studied role in splicing (Figure 1.4B) (192). TIA1 interacts with U-rich regions located downstream of weak 5' splice sites in target mRNAs (243). Binding of TIA1 to these intronic U-rich stretches results in the recruitment of the U1 snRNP (235), which is one of the initial factors present at 5' splice sites and assists in the commitment to pre-mRNA splicing at that location (244,245). The interaction between TIA1 and the U1 snRNP promotes of the inclusion of downstream exons (192,226,243), including those in *FGFR2* (192), *Msl-2* (243), *NF1* (246) and *Fas* (243) pre-mRNAs. The proteins produced from these TIA1-promoted, exon-enhanced transcripts often have very different roles than those produced from the exon-excluded version, such as the case with the Fas receptor (247), which will be discussed later. Much like HuR, these studies suggest that the role of TIA1 in modulating target mRNAs is diverse and should be characterized on an individual transcript basis.

HuR and TIA1 binding studies: targets and recognition

As discussed throughout this section, the identification and characterization of HuR and TIA1 target mRNAs is an important area of research. The advent of various RIP (RNA immunoprecipitation), CLIP (cross-linking IP), iCLIP (individual nucleotide

resolution CLIP) and Par-CLIP (photoactivatable-ribonucleoside-enhanced CLIP) - sequencing approaches has expanded our ability to identify the spectrum of RNA targets bound by select RNA binding proteins.

Multiple independent transcriptome-wide CLIP-Seq studies on HuR have been performed in recent years yielding very interesting results. These studies were performed in HeLa and HEK293 cells each using at least one of the CLIP-seq approaches described above (224,225,248,249). The primary and most consistent finding from these sequencing studies is the observation that HuR has preference for U-rich RNA sequences (as opposed to the previously described AU-rich target sequence) located primarily within the 3'UTRs and introns of target mRNAs (224,225,248,249). Many transcripts contained HuR binding sites in either an intron or the 3'UTR; however, the largest population of HuR target mRNAs contained HuR binding sites in both regions (225). Transient knockdown of HuR followed by sequencing analyses confirmed the functional importance of HuR binding and even demonstrated that transcripts containing multiple HuR binding sites (in intronic and 3'UTR sequences) are more stable than transcripts with one binding site. Identification of HuR binding sites within intronic regions suggests a role for HuR in pre-mRNA processing. In fact, these studies observed HuR-dependent changes in splicing of many transcripts (224,225).

A handful of these CLIP-seq studies also performed RNA secondary structure prediction analyses on their target motifs, revealing a putative secondary structural motif for HuR binding (224,249). An over-representation of U-rich motifs predicted to be located within variably sized hairpin loops was detected in one study (249). Another study reported a U-rich preference for HuR binding within 3′UTRs; however,

computational folding predictions suggested single-stranded U-rich motifs with no indication of hairpins (224). Further structure-function studies are required to determine whether HuR does in fact have a structural preference for target sequences.

Finally, analysis of HuR binding sites and their location relative to predicted miRNA binding sites also yielded interesting results. A number of HuR binding sites were identified in close proximity to predicted or validated miRNA binding sites (224,225,249). These results are consistent with a recent study demonstrating that HuR interacts with the 3'UTR of *CAT-1* mRNA after stress, and in doing so, relieves the *miR-122*-mediated repression (41). Together, these studies suggest that at least one of the roles for HuR in cancer may be mediated via interplay with miRNA machinery.

A recent iCLIP study was performed in HeLa cells to determine the spectrum of TIA1 mRNA targets (231). Much like HuR, TIA1 binding sites were also U-rich, single-stranded elements located within introns and 3'UTR sequences. TIA1 binding sites were observed primarily within 3'UTRs and further analysis revealed that they were distributed throughout the 3'UTR (231). Alternatively, the vast majority of intronic TIA1 binding sites were restricted to regions directly downstream of 5' splice sites, as expected from previous studies (231). These transcriptome-wide studies not only provide us with rich information about the characteristics and geography of HuR and TIA1 binding sites, they also provide us with novel candidate targets to study in mechanistic detail. Moving forward, the functional characterization of novel HuR and TIA1 targets and the post-transcriptional consequence of binding will be an important area of research, specifically for cancer-relevant mRNAs.

HuR and TIA1 are coordinate regulators of gene expression

As described earlier, there are multiple post-transcriptional factors that modulate various aspects of gene expression via an interaction with the 3'UTR. Many of these factors, including HuR and TIA1, have been shown to coordinate and/or compete with other factors to fine-tune gene expression. For instance, there are a number of studies that demonstrate competition between HuR and TIA1 for binding to 5′ splice sites in numerous cell types (223,250,251). Additionally, HuR and TIA1 bind to non-overlapping sites within the 3'UTR of the *cytochrome c* (*CYCS*) transcript, which encodes a key regulator of apoptosis (252). This observed cooperative interaction on the *CYCS* 3'UTR results in coordination of *CYCS* translation (220). Finally, recent work demonstrates that the 3'UTR of the *β-actin* mRNA is bound by HuR and TIA1, potentially via a competitive interaction that influences the translation of *β-actin* (253,254). Adding another layer of complexity to the system is the observation that HuR and TIA1 bind to their own as well as one another's 3′UTRs, suggesting a complicated feedback loop (195,220). Together, these results support a role for HuR and TIA1 in coordinately regulating the expression of target transcripts; however, the complexity in regulation observed between these studies suggests that these processing events should be individually defined for each transcript.

HuR and TIA1 in cancer

The role of HuR in cancer has been studied extensively. Analysis of HuR target mRNAs reveals a diverse group of transcripts that encode cell cycle regulators, apoptotic factors as well as many other proteins involved in carcinogenesis (255). A recent review revealed that HuR target mRNAs are significantly represented within four major cancer traits (256): self-sufficiency in growth signals; evasion of apoptosis; sustained angiogenesis; and invasion and metastasis (255). Many of these transcripts are highly labile and therefore have short half-lives. A leading hypothesis for the role of HuR in cancer involves the overexpression or altered localization of HuR that results in an over stabilization of these transcripts that are otherwise rapidly turned over. As described earlier, the steady-state localization of HuR is primarily nuclear; however, HuR shuttles and the well-studied role of HuR in modulating the stability of target mRNAs occurs in the cytoplasm. Comparison of tumor samples to normal tissue in a number of different studies reveals elevated cytoplasmic levels of HuR in breast, colon, ovarian, prostate, pancreatic and oral cancers (255). In many of these studies, the abundance and cytoplasmic localization of HuR correlates with higher grade and reduced survival (257-259). For example, increased cytoplasmic localization of HuR in breast tumor samples correlates with poor prognosis and reduced survival (259).

As discussed earlier, TIA1 is an apoptosis-promoting factor (226). TIA1 binds to many transcripts that have roles in apoptosis, including the *Fas* mRNA (243), which encodes a key death receptor involved in the induction of apoptosis (247,260). Promotion

of exon inclusion by TIA1 on the *Fas* pre-mRNA results in the production of a Fas isoform that is membrane-bound and upon binding to the Fas ligand, transduces apoptotic signaling (247). In the absence of TIA1, exon skipping results in the production of a soluble Fas isoform that interacts with the Fas ligand in the extracellular space and inhibits apoptotic signaling (261,262). This is one example of how TIA1 is implicated in apoptosis. TIA1 also regulates the translation of a number of apoptotic mRNAs including *TNF-α* (191,226). Recently, a number of apoptotic factors whose transcripts are bound by HuR have also been identified including *Prothymosin α* (263), *Cytochrome C* (220), *Bcl-2* and *Mcl-1* (226,264). These studies point toward a potential role for HuR and TIA1 in coordinating the apoptotic program (264). Understanding the interplay between HuR and TIA1 is critical to further understanding the post-transcriptional mechanisms that regulate HuR and TIA1 target mRNAs, including the cancer-relevant programmed cell death 4 (*PDCD4*) transcript, which is the focus of Chapter 4.

Scope and significance of this dissertation

Eukaryotic post-transcriptional processing is comprised of a complex and highly regulated series of events that ultimately serve to generate fully processed, translatable mRNA transcripts that eventually code for proteins. The proper expression and regulation of RNA binding proteins that carry out each of these post-transcriptional events are critical to maintain cell health and identity, as evidenced by the observation that many human diseases are caused by or associated with the dysregulation of RNA binding proteins (see Table 1.1). Some RNA binding protein-associated diseases are caused by global changes in RNA processing as a result of the dysregulation of a single RNA binding protein. However, the molecular pathogenesis of many diseases is the result of a set of mRNA transcripts, or targets, that are specifically dysregulated by loss, mutation, or overexpression of an RNA binding protein. These mRNAs are described as disease-relevant mRNAs because the improper processing of these transcripts leads to alterations in the level and/or function of the encoded protein, therefore contributing to a disease phenotype. The overarching goal of my dissertation is to identify disease-relevant mRNA targets of RNA binding proteins and understand the role of the RNA binding proteins in regulating those targets.

In Chapter 2, I characterize the ATP synthase subunit mRNA, *ATP5G1,* as a target of the novel poly(A) RNA binding protein, ZC3H14. Patients with loss-of-function mutations in *ZC3H14* are intellectually disabled and display severe cognitive defects (150). Upon knockdown of ZC3H14 in human cells, we observe a significant reduction in the steady-state level of *ATP5G1* mRNA, which encodes an ATP synthase subunit C

protein that is considered to be a linchpin for ATP synthesis (265,266). Subsequently, we observe a concomitant drop in cellular ATP levels as well as a distinct mitochondrial fragmentation phenotype in these cells, consistent with defects observed in other neurological diseases (267). We hypothesize that the significant impact on *ATP5G1* and cellular ATP levels upon knockdown of ZC3H14 may underlie the observed intellectual disability and aberrant neuronal function in patients (150,268).

Chapter 3 focuses on various modes of regulation of *ZC3H14* in human cells. I demonstrate that ZC3H14 steady-state protein levels correlate with the estrogen receptor status of a panel of breast cancer cell lines; however, estrogen stimulation experiments reveal that *ZC3H14* is not an estrogen-responsive gene, suggesting an alternative mode of regulation on ZC3H14 levels that results in this intriguing correlation. I go on to demonstrate that ZC3H14, much like many other RNA binding proteins (195), binds to its own transcript, resulting in interesting cross-regulation between *ZC3H14* splice variants. I hypothesize that ZC3H14 interacts with its own transcript via a polyadenosine stretch within the 3'UTR, consistent with a study performed on the *S. cerevisiae* ortholog of ZC3H14, Nab2 (269). Finally, I summarize the findings of a transcriptome-wide sequencing analysis that we performed to identify the prevalence and distribution of internal, or encoded, polyadenosine stretches within the human transcriptome.

The work presented in Chapter 4 focuses on the post-transcriptional regulation of a novel target of HuR and TIA1, Programmed Cell Death 4 mRNA, or *PDCD4*, which encodes a novel tumor suppressor that is downregulated in many types of cancer (270). The *PDCD4* 3'UTR is a well-studied target of the onco*miR-21* (271,272) and is being explored as a potential target for antineoplastic therapies (273). In this study, we

demonstrate competitive binding of the two U-rich RNA binding proteins, HuR and TIA1, to overlapping regions on the *PDCD4* 3'UTR. We observe a decrease in *PDCD4* steady-state mRNA and protein levels upon knockdown of HuR and/or TIA1, supporting a role for these proteins in positively regulating *PDCD4* mRNA levels. Intriguingly, nucleocytoplasmic fractionation experiments reveal that the regulation of *PDCD4* mRNA stability is distinct from other HuR-bound mRNAs and likely represents a critical target of HuR and TIA1 in breast cancer cells.

The two mRNAs that we selected for extensive analysis in Chapters 2 and 4 not only provided us with disease-relevant mRNA targets that may provide insight into the molecular pathogenesis of disease, but also provide novel mechanistic data for the function of these RNA binding proteins in post-transcriptional processing. As we begin to understand the complex interactions and myriad functions of RNA binding proteins, we can integrate all of this knowledge into a systems-based approach to biology, thus leading us to a better understanding of how the cell works and, more importantly, how the cell can go bad.

Table 1.1. A selection of mRNA binding proteins implicated in human disease.

RNA binding protein	Disease	Post-transcriptional Function
ZC3H14	Intellectual Disability	Poly(A) tail length (268) mRNA quality control (161)
PABPN1	Oculopharyngeal Muscular Dystrophy	Polyadenylation, 3'end Processing (96)
SMN	Spinal Muscular Atrophy	snRNP Biogenesis (65)
eIF4E	Cancer	Cap-dependent Translation (60,61)
HuR (HuA)	Cancer	mRNA Stability, Translation (255)
Hu Family (HuA, B, C, D)	Paraneoplastic Neurologic Syndromes	mRNA Stability, Translation (198)
FMRP	Fragile X Syndrome	Translation (274)
MBNL1	Myotonic Dystrophy	Splicing (275)
SF2/ASF	Cancer	Splicing (276)
SAM68	Cancer	Splicing, mRNA Export, Translation (277)
QKI	Cancer	Splicing (278)
TPR	Cancer	mRNA Export (279)
ATXN1/2	Spinocerebellar Ataxia	RNA Processing (280)
TIA1	Distal Myopathy	Splicing, Translation (281)

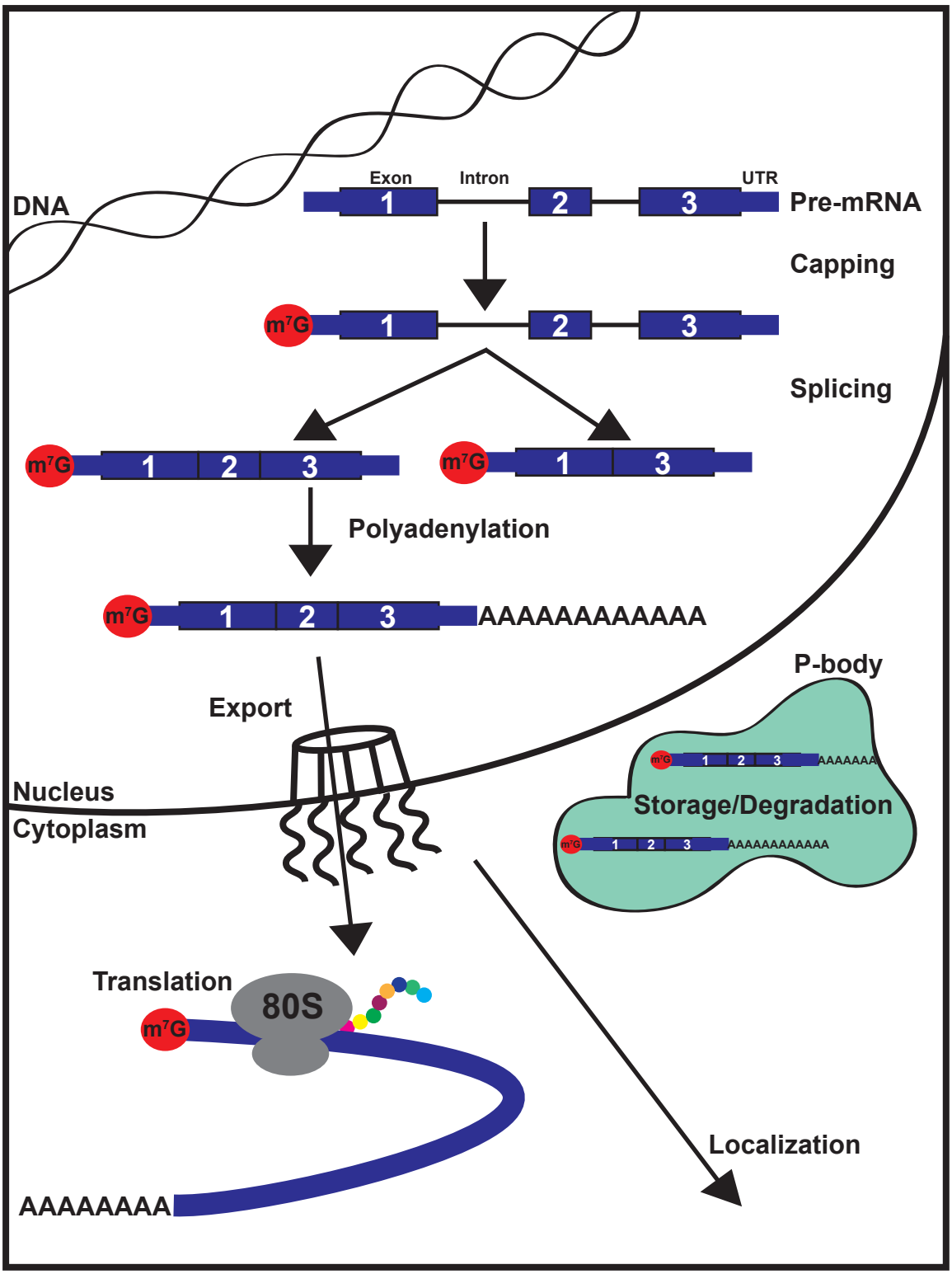
DNA
Exon
Intron
UTR
1
2
3
Pre-mRNA
Capping
m7G
Splicing
Polyadenylation
AAAAAAAAAAAA
P-body
Export
Nucleus
Cytoplasm
Storage/Degradation
AAAAAAA
AAAAAAAAAAAA
Translation
80S
AAAAAAAA
Localization

FIGURE 1.1. An overview of eukaryotic post-transcriptional processing. DNA is transcribed by RNA PolII to produce a premature mRNA transcript, or pre-mRNA. Pre-mRNAs undergo extensive processing in the nucleus to produce an export-competent mature mRNA transcript. These processing events include the addition of a 7-methylguanosine cap structure to the 5' end of the message, the removal, or splicing, out of intronic regions, as well as the addition of a 3' poly(A) tail. Fully processed mRNAs are exported through the nuclear pore complex where they can interact with translation machinery to produce proteins, be transported to specific cellular locations such as axonal synapses, or stored/degraded in distinct cytoplasmic foci such as p-bodies.

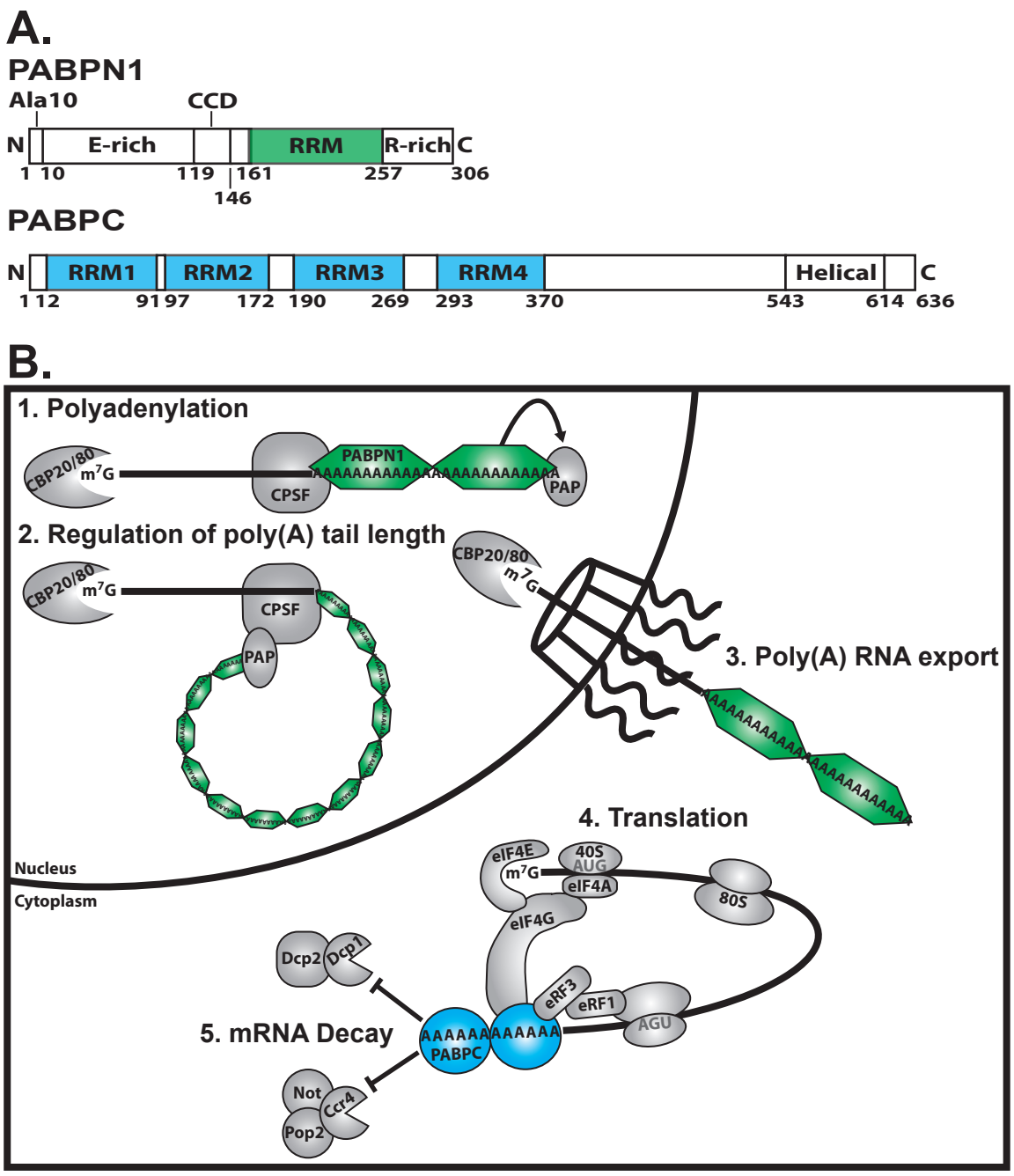

FIGURE 1.2. The canonical poly(A) binding proteins, PABPN1 and PABPC, play multiple roles in post-transcriptional processing. *A*) The domain structures for the canonical Pabs PABPN1 and PABPC are schematized here. PABPN1 is a nuclear Pab that contains a stretch of 10 alanines (Ala10) that are expanded in OPMD, a glutamic acid-rich domain (E-rich), a coiled-coil domain (CCD), an RNA recognition motif (RRM) that is responsible for high affinity polyadenosine RNA binding, as well as an arginine-rich (R-rich) domain at the C-terminus. PABPC is a cytoplasmic Pab that interacts with polyadenosine RNA via RRMs (RRM1-4) and contains a C-terminal Helical domain. *B*) The role of PABPN1 (green hexagon) in modulating 3'end processing of mRNA transcripts is well established and consists of the following molecular functions:

1. Polyadenylation: PABPN1 interacts with poly(A) polymerase to stimulate processive polyadenylation; 2. Regulation of poly(A) tail length: PABPN1 interacts with the cleavage and polyadenylation specificity factor (CPSF) to modulate and ensure proper poly(A) tail length; and 3. Poly(A) RNA export: Although whether the role is direct or indirect is unknown, defects in PABPN1 function can lead to nuclear accumulation of poly(A) RNA. This observation together with the fact that PABPN1 shuttles between the nucleus and the cytoplasm have led to the suggestion that PABPN1 function is required for efficient poly(A) RNA export from the nucleus. PABPC (blue circle) plays a well-defined role in modulating gene expression including: 4. Translation: PABPC binds to eukaryotic translation initiation factor 4G (eIF4G), which bridges interactions between the 5'- and 3'-ends of the mRNA and facilitates efficient translation initiation and 5. mRNA decay: PABPC binds to eukaryotic release factor 3 (eRF3), which facilitates ribosome recycling and thus inhibits mRNA decay by protecting the poly(A) tail from decapping enzymes (Dcp1 and Dcp2) as well as exonucleases such as the Ccr4-Pop2-Not complex. The following factors are also incorporated into the model shown: Cap binding proteins 20 and 80 (CBP20/80); 7 methylguanosine cap (m7G); eukaryotic translation initiation factor 4E (eIF4E); eukaryotic small ribosome (40S); eukaryotic translation initiation factor 4A (eIF4A); eukaryotic ribosome (80S); and eukaryotic release factor 1 (eRF1).

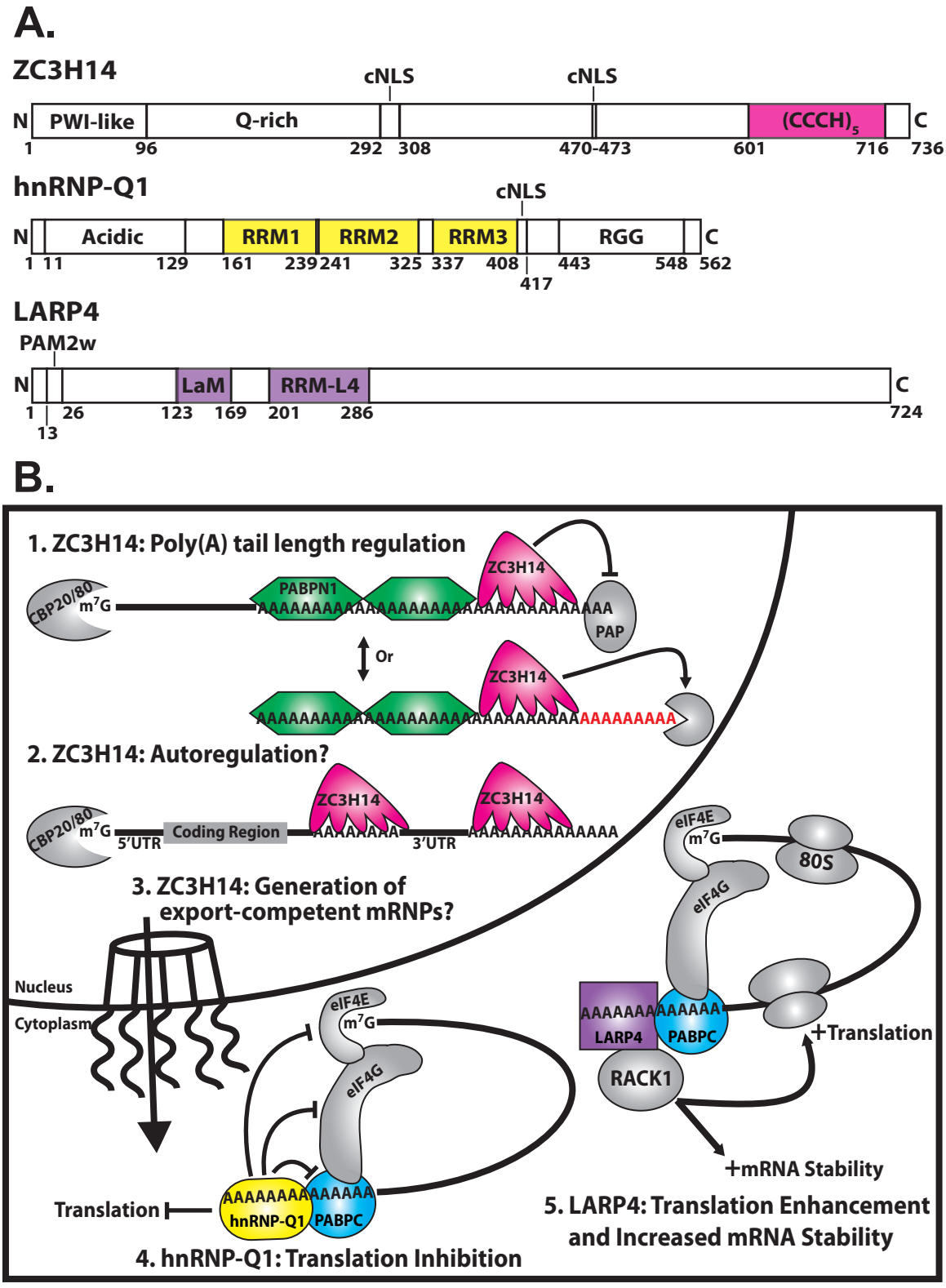
A.
ZC3H14
cNLS
cNLS
N
PWI-like
Q-rich
(CCCH)5
C
1
96
292
308
470-473
601
716
736
hnRNP-Q1
cNLS
N
Acidic
RRM1
RRM2
RRM3
RGG
C
1
11
129
161
239
241
325
337
408
417
443
548
562
LARP4
PAM2w
N
LaM
RRM-L4
C
1
13
26
123
169
201
286
724
B.
1. ZC3H14: Poly(A) tail length regulation
CBP20/80
m7G
PABPN1
ZC3H14
PAP
Or
ZC3H14
2. ZC3H14: Autoregulation?
CBP20/80
m7G
5'UTR
Coding Region
3'UTR
ZC3H14
ZC3H14
3. ZC3H14: Generation of
export-competent mRNPs?
Nucleus
Cytoplasm
eIF4E
m7G
eIF4G
eIF4E
m7G
eIF4G
80S
LARP4
PABPC
RACK1
+Translation
+mRNA Stability
Translation
hnRNP-Q1
PABPC
4. hnRNP-Q1: Translation Inhibition
5. LARP4: Translation Enhancement
and Increased mRNA Stability

FIGURE 1.3. Novel Pab family members. *A*) The domain structures for three novel Pab family members (ZC3H14, hnRNP-Q1, and LARP4) are schematized here. ZC3H14 is a novel nuclear Pab that interacts with polyadenosine RNA via tandem CysCysCysHis (CCCH) zinc fingers and also contains an N-terminal Proline Tryptophan Isoleucine-like (PWI-like) fold that mediates interactions with the nuclear pore, a glutamine-rich (Q-rich) domain of unknown function, and two putative classical nuclear localization signals (cNLS). hnRNP-Q1 is a novel cytoplasmic Pab that is presumed to bind polyadenosine RNA via RRMs (RRM1-3) and contains an Acidic N-terminal domain as well as an Arginine Glycine Glycine (RGG) domain, both of which mediate protein-protein interactions. A putative weak cNLS is also present in hnRNP-Q1. LARP4 is a novel cytoplasmic Pab that interacts with polyadenosine RNA via a La Motif (LaM) in conjunction with an RRM-like 4 domain (RRM-L4). LARP4 interacts with PABPC via a poly(A) binding protein interacting motif (PAM2) domain that contains an atypical tryptophan in the consensus sequence (PAM2w). *B*) The functions proposed for the new members of the Pab family described here (ZC3H14, hnRNP-Q1, and LARP4) are illustrated. The novel nuclear zinc finger Pab, ZC3H14 (pink five-fingered shape) plays a role in 1. poly(A) tail length regulation: ZC3H14 could limit poly(A) tail length either by inhibiting Poly(A) Polymerase (PAP) or by recruiting a 3'-5' exonuclease (grey Pac-man); 2. Autoregulation: Like its S. cerevisiae counterpart, Nab2, ZC3H14 may bind to and autoregulate its own mRNA transcript via an A15 stretch present in the 3'UTR; and 3. Generation of export-competent mRNPs: ZC3H14 could play a direct role in the generation of properly packaged mRNPs that are poised for export but most data to support this function comes from studies of S. cerevisiae Nab2. Alternatively, proper polyadenylation could be required to assemble export-competent mRNPs and the role for Nab2/ZC3H14 could be indirect. The novel cytoplasmic Pab, hnRNP-Q1 (yellow ellipse), plays a role in 4. Translation inhibition: hnRNP-Q1 competes with PABPC for binding to poly(A) tails and consequently preventing the formation of the translation initiation complex. The other novel cytoplasmic Pab, LARP4 (purple rectangle), is implicated in 5. Translation enhancement and increased mRNA stability: LARP4 interacts with PABPC as well as the ribosome-associated protein, RACK1, to positively modulate mRNA translation and decay. The following factors are also incorporated into the model shown: Cap binding proteins 20 and 80 (CBP20/80); 7 methylguanosine cap (m7G); eukaryotic translation initiation factor 4E (eIF4E); eukaryotic translation initiation factor 4G (eIF4G); and eukaryotic ribosome (80S).

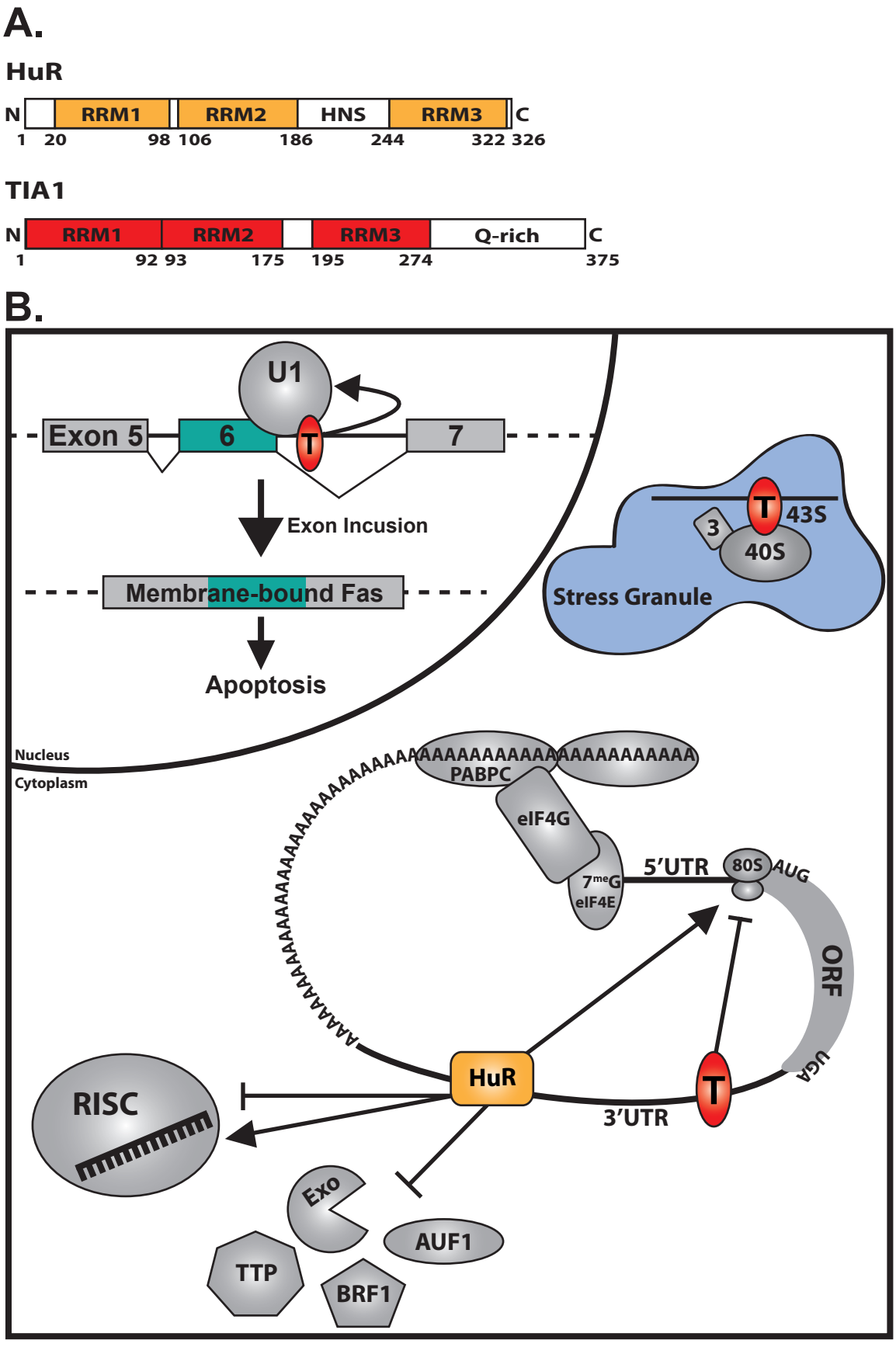
A.
HuR
N
RRM1
RRM2
HNS
RRM3
C
1 20 98 106 186 244 322 326
TIA1
N
RRM1
RRM2
RRM3
Q-rich
C
1 92 93 175 195 274 375
B.
U1
Exon 5
6
T
7
Exon Incusion
Membrane-bound Fas
Apoptosis
Nucleus
Cytoplasm
T
43S
3
40S
Stress Granule
AAAAAAAAAAAAAAAAAAAAAAAAAAAAAAAAAAAAAAAA
PABPC
eIF4G
7meG
eIF4E
5'UTR
80S
AUG
ORF
UGA
HuR
T
3'UTR
RISC
Exo
AUF1
TTP
BRF1

FIGURE 1.4. HuR and TIA1, two U-rich RNA binding proteins, play multifunctional roles in post-transcriptional processing. *A*) The domain structures for HuR and TIA1 are schematized here. HuR is a U-rich element RNA binding protein that binds primarily to the 3'UTRs of target transcripts via two N-terminal RNA Recognition Motifs (RRMs). A third C-terminal RRM has affinity for polyadenosine RNA and is thought to interact with the poly(A) tail. HuR localizes to the nucleus at steady-state but has been shown to shuttle between the nucleus and cytoplasm in response to various stimuli. The shuttling of HuR is mediated by the HuR Nucleocytoplasmic Shuttling sequence (HNS). TIA1 is another RNA binding protein with affinity for U-rich sequences. TIA1 contains three tandem RRMs followed by a prion-related Glutamine-rich (Q-rich) domain. Extensive binding studies have established that RRM 2 is responsible for binding to U-rich RNA while RRM3 enhances this binding event. RRM1 and the Q-rich domain mediate interactions with the U1 snRNP, which influences splice site selection. TIA1 also shuttles between the nucleus and cytoplasm, but displays a steady-state nuclear localization. The nucleocytoplasmic shuttling of TIA1 is mediated by sequence elements in RRMs 2 and 3. *B*) The well-studied functions of HuR and TIA1 are schematized here. HuR and TIA1 are represented as an orange rectangle and red oval, respectively. All other proteins are in grey. TIA1 has a well-studied role in splicing. In the nucleus, TIA1 interacts with U-rich intronic sequences located downstream of 5' weak splice sites (shown here binding downstream of exon 6 of the *Fas* pre-mRNA). Binding of TIA1 to these intronic sequences results in recruitment of the U1 snRNP (U1), which is one of the initial factors present at 5' splice sites and assists in the commitment to pre-mRNA splicing at that location. Therefore, TIA1 promotes the inclusion of otherwise "cryptic" exons. The *Fas* pre-mRNA is alternatively spliced to form two divergent protein products. The exon-included variant (shown here) encodes a membrane-bound Fas protein that transduces apoptotic signaling. TIA1 also has a well-studied role in translational repression in the cytoplasm. TIA1 interacts with U-rich elements in the 3'UTR of target mRNAs and promotes the formation of a noncanonical preinitiation complex (composed of the 40S ribosomal subunit (40S), eIF3 (3) and other components, resulting an a 43S complex), which is a stress granule core component, thus resulting in stress granule recruitment and translational repression. HuR also binds to U-rich elements primarily within the 3'UTRs of target transcripts and in doing so, increases mRNA stability. The observed increase in stability is thought to be the result of HuR blocking the access of other destabilizing U-rich binding proteins, such as TTP, AUF1 and BRF1, as well as exoribonucleases (Exo). HuR has also been shown to positively regulate the translation of target mRNAs via interactions with the 3'UTR. Finally, recent work has described a complex relationship between HuR and the miRNA machinery (RISC). These independent studies have observed both coordinate and competitive relationsips between HuR and miRNAs, suggesting that the role of HuR in interfacing with miRNAs is context- and transcript-dependent. The following factors are also incorporated into the model shown: poly(A) binding protein C1 (PABPC); open reading frame (ORF); 7 methylguanosine cap (m7G); eukaryotic translation initiation factor 4E (eIF4E); eukaryotic translation initiation factor 4G (eIF4G); and eukaryotic ribosome

Chapter 2: ZC3H14 ensures proper processing of *ATP5G1* pre-mRNA

A portion of this chapter is adapted from the following paper:

Wigington, C.P., Newman, L.E., Morris, K.J. and Corbett, A.H. (2015) *In resubmission*. "The Polyadenosine RNA Binding Protein, Zinc Finger Cys_3His Protein #14 (ZC3H14), Regulates the pre-mRNA Processing of a Key ATP Synthase Subunit mRNA."

INTRODUCTION

The fate and function of a cell are determined not only by the spectrum of genes that are expressed but also the spatial and temporal regulation of expressed mRNAs (282). The processing of mRNAs is referred to as post-transcriptional processing and is critical to ensure proper cell health and function (8,283). A myriad of post-transcriptional regulatory RNA binding proteins execute the post-transcriptional program, which includes events such as the capping, splicing, 3' end processing, export and localization of mRNAs (8). Precise expression and function of RNA binding proteins is critical to ensure the proper gene expression profile of a cell (283). The importance of RNA binding proteins is illustrated by the number of human diseases that result from mutation or dysregulation of these RNA binding proteins including links to cancer (284-286) and neuronal diseases (287-290). Understanding the role of newly discovered, or previously uncharacterized, RNA binding proteins in the post-transcriptional processing of target mRNAs is key in delineating the regulation of gene expression as well as molecular mechanisms underlying human disease.

One newly characterized RNA binding protein is the zinc finger polyadenosine RNA binding protein, Zinc finger CCCH protein #14, or ZC3H14 (148,154). Extensive biochemical studies show that ZC3H14 employs five evolutionarily conserved tandem $Cysteine_3Histidine$ (CCCH) zinc fingers to recognize polyadenosine RNA with high affinity and specificity (148). In contrast, the well-studied Poly(A) binding proteins (Pabs), Poly(A) Binding Protein Cytoplasmic 1 (PABPC1) and Poly(A) Binding Protein

Nuclear 1 (PABPN1), recognize polyadenosine RNA via globular RNA Recognition Motifs (98,116-118). Thus ZC3H14 presents a novel mode of polyadenosine RNA recognition and expands the Pab family of RNA binding proteins.

As illustrated in Figure 2.1A, ZC3H14 is alternatively spliced to form at least four splice variants that encode four distinct protein isoforms (154). Isoforms 1-3 each contain an N-terminal Proline Tryptophan Isoleucine (PWI)-like domain (154), which mediates interactions with the nuclear pore (153), as well as a predicted classical Nuclear Localization Signal (cNLS) (154). The three longer isoforms of ZC3H14 are localized to the nucleus at steady-state (154); however, isoform 4, which lacks the exon containing the predicted cNLS, exhibits a steady-state cytoplasmic localization (154). All four described isoforms contain the five tandem C-terminal CCCH zinc fingers, and are therefore expected to interact with polyadenosine RNA with similar affinity (148,154). Interestingly, a recent study demonstrated that multiple patients from separate families in rural Iran possess loss-of-function mutations in the *ZC3H14* genomic locus and have a severe form of autosomal recessive intellectual disability (150), suggesting a critical role for ZC3H14 in mRNA processing events that are necessary for proper neuronal function (290).

The RRM-containing Pabs PABPC1 and PABPN1 have well-studied and ubiquitous roles in post-transcriptional processing (29); however, the role of ZC3H14 in post-transcriptional mRNA processing is unclear. Extensive work on the *S. cerevisiae* ortholog of ZC3H14, Nab2, reveals that this essential protein plays roles in poly(A) tail

length control (163), poly(A) mRNA export (159), target transcript stability (291) and RNA quality control in the nucleus (160,161). Genetic analyses performed in *D. melanogaster* reveal a conserved function of *Drosophila* Nab2 (dNab2) in post-transcriptional processing, specifically in neurons (268), consistent with the brain dysfunction observed in patients. Understanding the role of ZC3H14 in human cells is not only critical to determine the molecular basis for the observed neuronal phenotype in patients, but also to integrate the function of ZC3H14 into our current understanding of the Pab family of proteins.

To understand the role of ZC3H14 in human cells, we employed a genome-wide analysis to assess the consequence of ZC3H14 knockdown. Identifying transcripts that are modulated by the loss of ZC3H14 will not only provide useful candidate targets for the analysis of post-transcriptional processing defects, but also may provide insight into molecular mechanisms that could contribute to brain dysfunction in patients lacking *ZC3H14*. In this study, we provide evidence from our genome-wide study that ZC3H14 has specific targets in human cells, as evidenced by the much smaller percentage of transcripts affected by knockdown of ZC3H14 than with another nuclear Pab, PABPN1. We selected and identified the *ATP5G1* transcript as a specific target of ZC3H14. *ATP5G1* encodes one of the proteins that comprise the C subunit of ATP synthase (292), which is responsible for the majority of ATP production in eukaryotic cells (293). We demonstrate that knockdown of ZC3H14 in human cells results in a decrease in *ATP5G1* steady-state mRNA levels and a corresponding reduction in cellular ATP levels. ZC3H14 binds to the *ATP5G1* transcript and positively regulates the pre-mRNA processing of

ATP5G1. Finally, we show that loss of ZC3H14 or ATP5G1 by siRNA-mediated knockdown leads to a severe mitochondrial fragmentation phenotype. Together, these results support a role for ZC3H14 in modulating the quality control of target mRNA transcripts.

RESULTS

Knockdown of ZC3H14 decreases *ATP5G1* mRNA levels

Previous studies of ZC3H14 orthologs in model organisms suggest a spectrum of post-transcriptional functions (159,163,291) that may influence the fate of bound target transcripts (161). To examine the function of ZC3H14 in human cells, we sought to identify candidate target mRNA transcripts via an unbiased, genome-wide approach. To accomplish this goal, we performed a microarray analysis on MCF-7 cells, a commonly used human breast cancer cell line (ATCC HTB-22), transfected with either control scramble siRNA or siRNA targeting ZC3H14. To compare ZC3H14 to a more conventional Pab, we also performed knockdown of the well-studied nuclear Pab, PABPN1 (29,97,115). PABPN1 is predicted to bind to and regulate the 3'-end processing of numerous polyadenylated mRNAs (24,104,105) and has the potential to regulate the steady-state level of many cellular mRNAs. A recent study demonstrated that knockdown of PABPN1 in HeLa cells resulted in a ≥1.5-fold change of ~13.5% of expressed transcripts in those cells (3% and 10.5% increased and decreased, respectively) (139). If ZC3H14, as another nuclear Pab, also binds and regulates a large number of

polyadenylated transcripts, we would expect to see similar effects on the number of mRNA transcripts affected upon knockdown of each nuclear Pab.

As shown in Figure 2.1B, we achieve robust knockdown of both ZC3H14 and PABPN1 protein upon transfection with each specific siRNA. To identify differentially expressed transcripts between control cells or cells depleted of ZC3H14 or PABPN1, total RNA was used for cDNA generation and hybridized to the Illumina HumanHT-12 v4 Expression BeadChip microarray platform. Significance Analysis of Microarrays (SAM) analysis was employed to determine statistically significant differentially expressed genes (≥1.5-fold change) between treatment groups. As shown in Figure 2.1C, knockdown of PABPN1 affected the steady-state level of 2,375 or ~17% of transcripts expressed in these cells, as calculated from our analyses (1,285 increased and 1,090 decreased transcripts out of 13,722 total). However, knockdown of ZC3H14 resulted in a change in steady-state level of only 171 or ~1% of expressed transcripts (101 increased and 70 decreased transcripts out of 13,918 total). To validate the results of the microarray, we performed qRT-PCR analyses with primers to a selection of the ZC3H14-affected transcripts (Figure 2.1D). As shown in Figure 2.1D, the fold-changes calculated by qRT-PCR analysis correlate strongly with the results of the microarray, supporting the validity of the genome-wide study. The observation that PABPN1 knockdown affects a significant percentage of expressed transcripts supports the well-studied role of PABPN1 in 3' end processing and polyadenylation of numerous mRNA transcripts (24,104,105) and is consistent with the previous study performed in HeLa cells (139). We hypothesize that the significantly smaller number of transcripts that show altered steady-state level

upon ZC3H14 knockdown represents a pool of transcripts that are regulated by ZC3H14 in a specific manner.

To determine how ZC3H14 alters target transcripts, we selected one robustly affected target for further analysis. The ATP Synthase Subunit C1, or *ATP5G1*, transcript is robustly decreased (3-fold) upon knockdown of ZC3H14 (Figure 2.1E). However, *ATP5G1* mRNA levels are not affected by knockdown of PABPN1 (Figure 2.1F), suggesting that it is not a general target of regulation by nuclear Pabs and that *ATP5G1* may in fact be specifically regulated by ZC3H14.

To confirm that the effect of ZC3H14 on *ATP5G1* steady-state levels is not limited to MCF-7 cells, we extended our analysis to a number of different human cells lines. As shown in Figure 2.1G, we achieved robust knockdown of ZC3H14 in HeLa (cervical adenocarcinoma, ATCC CCL-2), HEK293 (embryonic kidney, ATCC CRL-1573), MB-231 (breast adenocarcinoma, ATCC HTB-26), and D556 (medulloblastoma, (294)) cells. Total RNA isolated from these cells was used for qRT-PCR analysis with *ATP5G1* and the control ribosomal protein, large, P0 (*RPLP0*) primers. Results of this analysis revealed a consistent reduction of *ATP5G1* steady-state mRNA levels across all cell lines tested (Figure 2.1G). Together these data demonstrate a robust and specific effect of ZC3H14 knockdown on the *ATP5G1* transcript that is consistent across multiple human cell lines.

A previous study demonstrated that MCF-7 cells produce 80% of their ATP by oxidative phosphorylation (the remaining 20% coming from glycolysis) (295), whereas HeLa cells and many other cancer cell lines primarily use glycolysis for ATP production (296). Because we eventually wanted to investigate whether knockdown of ZC3H14 had an impact on cellular ATP levels and energy metabolism via regulation of *ATP5G1*, we used the MCF-7 cell line for our analyses throughout this study. Furthermore, we observe the largest impact on *ATP5G1* steady-state levels upon ZC3H14 knockdown in MCF-7 cells as compared to the other cell lines examined.

Re-expression of ZC3H14 isoform 1 partially rescues the decrease in *ATP5G1* transcript

To confirm that the effect on *ATP5G1* is due specifically to depletion of ZC3H14, we performed a rescue experiment with siRNA-resistant Myc-tagged constructs of ZC3H14. To delineate the role of nuclear and cytoplasmic isoforms of ZC3H14 within this rescue experiment, we co-transfected plasmids expressing Myc-ZC3H14 Iso1 (nuclear; see Figure 2.1A) or Myc-ZC3H14 Iso4 (cytoplasmic; see Figure 2.1A) with ZC3H14 siRNA into MCF-7 cells. As shown in Figure 2.2A, we achieve robust expression of both Myc-ZC3H14 isoform 1 and isoform 4. RNA isolated from these cells was used for cDNA generation and subsequent qRT-PCR analysis with primers to detect *ATP5G1* and a control transcript, *18s rRNA*. As shown in Figure 2.2B, expression of the Myc-tagged ZC3H14 isoform 1 resulted in a significant rescue of steady-state *ATP5G1* mRNA levels, compared to knockdown alone. In contrast, Myc-ZC3H14 isoform 4 does

not rescue the effect of knockdown on *ATP5G1* levels, suggesting that the nuclear isoform of ZC3H14 is required to regulate *ATP5G1* mRNA. Although the rescue achieved with Myc-ZC3H14 isoform 1 is significant, levels of *ATP5G1* mRNA are not fully restored. This partial rescue could be due to expression of a single isoform of ZC3H14 (Iso1) when the endogenous gene encodes multiple isoforms of the protein (see Figure 2.1A). Together, these results demonstrate that the decrease of *ATP5G1* mRNA levels is due to depletion of nuclear ZC3H14.

ZC3H14 modulates cellular ATP levels

The *ATP5G1* transcript encodes one of the 15 subunits of ATP synthase (293); specifically subunit C. Subunit C is one of the transmembrane components of the F_o portion of ATP synthase, which is responsible for proton translocation across the inner mitochondrial membrane (293). The proton-driven rotation of subunit C and subsequent rotation of the F_1 stalk provides energy for ATP synthesis by subunit α and β in the mitochondrial matrix. Interestingly, the C subunit is comprised of multiple copies (eight in humans (297)) of the C protein, which are derived from multiple genomic loci (292,298,299). As schematized in Figure 2.3A, the *ATP5G1*, *ATP5G2*, and *ATP5G3* genes are nuclear-encoded genes that are transcribed from three separate genomic loci and give rise to unique mature mRNAs. These unique mRNAs encode precursor proteins with identical C-termini and unique N-terminal peptides that are cleaved upon mitochondrial import (292,298,299). Upon cleavage of the mitochondrial targeting

peptides, the identical protein products are integrated into the C subunit ring at an undetermined stoichiometry.

Recent work suggests that although the three subunit C proteins are identical in sequence, they cannot functionally substitute for one another and are all required to constitute a fully functional C subunit (300,301). Previous studies suggest that the *ATP5G1* transcript is expressed at the lowest levels among the three transcripts and is regulated distinctly from *ATP5G2* or *ATP5G3* (302,303). To determine the relative levels of *ATP5G1*, *-2*, and *-3* in MCF-7 cells, we isolated RNA from untreated cells and performed qRT-PCR analysis with transcript-specific primers. As shown in Figure 2.3B, we found that the steady-state level of *ATP5G1* mRNA is significantly lower than the level *ATP5G2* or *ATP5G3* in these cells, consistent with previous observations (302,303). To determine whether the effect of ZC3H14 knockdown is specific to *ATP5G1*, we performed knockdown of ZC3H14 and analyzed the steady-state level of each *ATP5G* mRNA in these samples. Consistent with the results of the microarray, *ATP5G1* mRNA was the only subunit C mRNA affected by ZC3H14 knockdown, suggesting that ZC3H14 specifically regulates expression of *ATP5G1* (Figure 2.3C).

As schematized in Figure 2.3A, the mature protein products of the C subunit are completely identical, preventing us from determining whether knockdown of ZC3H14 results in a specific decrease in the level of ATP5G1 protein. However, previous studies demonstrated that ATP5G1 is rate-limiting for ATP synthase assembly and function and therefore is critical for overall function of the complex and determining cellular ATP

levels (265,266). We hypothesized that if the ZC3H14-dependent reduction of *ATP5G1* mRNA results in a decrease in steady-state protein levels, then we should observe a decrease in total cellular ATP levels. To determine whether knockdown of ZC3H14 modulates cellular ATP levels, we performed a cellular ATP extraction followed by a luciferase-based ATP quantification assay (Figure 2.3D). As expected, treatment of cells with the electron transport chain inhibitor, rotenone (304), resulted in a significant decrease in cellular ATP levels (Figure 2.3D). Cells treated with siRNA targeting *ATP5G1* directly or *ZC3H14* also displayed significantly decreased cellular ATP levels, suggesting that ZC3H14 impacts the function of ATP5G1 (Figure 2.3D).

To extend our analysis to other electron transport chain, or oxidative phosphorylation (OXPHOS), machinery mRNAs, we compared control cells treated with scramble siRNA to cells depleted for ZC3H14 and then performed qRT-PCR with primers specific to a set of transcripts that represent nuclear-encoded mitochondrial proteins from each of the five OXPHOS complexes (I: *NDUFA4*, II: *SDHB*, III: *UQCRFS1*, IV: *CoxIV*, and V: *ATP5B*) (305). As shown in Figure 2.3E, no change in steady-state mRNA levels of the OXPHOS subunit mRNAs examined was detected, supporting the idea that ZC3H14 does not play a general role in regulating OXPHOS or mitochondrial mRNAs and suggests that the observed impact on cellular ATP levels is not due to a general impact on mitochondrial health and/or function. Together these data demonstrate that ZC3H14 specifically regulates the steady-state level of *ATP5G1* mRNA and suggest that ZC3H14 could play a role in regulating cellular ATP levels.

ZC3H14 binds to specific mRNAs

Extensive *in vitro* binding studies demonstrate that ZC3H14 recognizes polyadenosine RNA via five evolutionarily conserved CCCH zinc fingers (148), suggesting that ZC3H14 could bind to any and all polyadenylated mRNAs. However, in our microarray analysis we observed a small number of transcripts that showed significant changes in steady-state levels upon ZC3H14 knockdown. We hypothesized that this relatively small number of affected transcripts represents a set of target transcripts that are both bound and regulated at the steady-state RNA level by ZC3H14. To test whether ZC3H14 binds to ATP synthase subunit C mRNAs, we subjected MCF-7 cells to RNA-IP analyses using ZC3H14 antibody-conjugated protein G beads. As shown in Figure 2.4A, we achieve robust purification of ZC3H14 in the ZC3H14 bound fraction with no purification in the pre-immune control bound fraction. To identify RNA transcripts that co-purify with ZC3H14, qRT-PCR analysis was performed (Figure 2.4B). We observe a significant enrichment of *ATP5G1* mRNA upon purification of ZC3H14. We also observe enrichment of *ATP5G3* mRNA, suggesting that while ZC3H14 can bind to both transcripts, it specifically modulates the steady-state level of only *ATP5G1*.

A previous study in *S. cerevisiae* demonstrated that the ZC3H14 ortholog, Nab2, binds and autoregulates the levels of its own mRNA transcript via an internal encoded stretch of 26 adenosines within the 3'UTR (269). Like Nab2, the human *ZC3H14* 3'UTR contains an internal stretch of 15 adenosines that could confer binding by ZC3H14. Consistent with many other RNA binding proteins that bind their own transcripts (195),

we observe robust enrichment of *ZC3H14* mRNA upon purification of ZC3H14 (Figure 2.4B), suggesting that this mode of autoregulation is conserved in human cells. We did not, however, observe enrichment for the *GAPDH*, *RPLP0* or *ATP5G2* transcripts upon ZC3H14 purification (Figure 2.4B). Together, these results suggest that ZC3H14 does in fact bind to specific transcripts, such as *ATP5G1*, in MCF-7 cells.

ZC3H14 interacts with *ATP5G1* mRNA in the nucleus

As described earlier, isoforms 1-3 of ZC3H14 (which are recognized by the N-terminal ZC3H14 antibody; Figure 2.1A) localize to the nucleus at steady-state (154). Although the ZC3H14 siRNAs used throughout this study target all known variants of *ZC3H14*, we observe rescue of *ATP5G1* mRNA levels upon re-introduction of a nuclear isoform of ZC3H14 (Figure 2.2B). These results suggest that the effect of ZC3H14 on *ATP5G1* mRNA a nuclear event. However, the *S. cerevisiae* ortholog of ZC3H14, Nab2, which also displays a steady-state nuclear localization, shuttles between the two compartments (159), suggesting that Nab2/ZC3H14 may have some role in the cytoplasm.

To examine the effect of ZC3H14 knockdown in the nuclear and cytoplasmic compartments, we transfected cells with scramble or ZC3H14 siRNA and collected cells 48 hours later. Whole cell, nuclear and cytoplasmic lysates were collected by nucleocytoplasmic fraction, as described in Experimental Procedures. To confirm robust knockdown in these samples as well as efficient fractionation, we subjected the samples

to immunoblot analysis with ZC3H14, Tubulin and HuR antibodies (Figure 2.5A). As expected, we observe primarily cytoplasmic and nuclear localization of Tubulin and HuR, respectively, confirming efficient fractionation of these cells. The lower exposure blot of ZC3H14 demonstrates robust knockdown of ZC3H14 as well as clear steady-state nuclear localization of ZC3H14. The higher exposure blot reveals a small pool of ZC3H14 present in the cytoplasm that is also reduced upon ZC3H14 knockdown (Figure 2.5A).

To determine whether the steady-state level of ATP5G1 mRNA is decreased in a specific compartment upon ZC3H14 knockdown, we collected RNA from the nuclear and cytoplasmic samples in Figure 2.5A and performed qRT-PCR analyses with *GAPDH*, *ZC3H14* and *ATP5G1* primers. As shown in Figure 2.5B, we observe a robust decrease in steady-state *ATP5G1* mRNA levels in the nuclear and cytoplasmic samples, suggesting that the effect of ZC3H14 knockdown of *ATP5G1* mRNA levels is, at least in large part, a nuclear event. As expected, we observe significant reduction in *ZC3H14* steady-state mRNA levels upon knockdown with no change in the steady-state levels of the control, *GAPDH* transcript (Figure 2.5B).

We hypothesize that the observation of a nuclear effect on *ATP5G1* mRNA levels could be due to a binding event between ZC3H14 and *ATP5G1* specifically in the nucleus. To determine whether ZC3H14 binds to the *ATP5G1* transcript in the nucleus and/or cytoplasm of MCF-7 cells, we performed ZC3H14 RNA-IP analyses on nuclear and cytoplasmic samples. As shown in Figure 2.5C, we achieve efficient fractionation of

these cells, as evidenced by the primarily cytoplasmic and nuclear localization of Tubulin and HuR, respectively. We also observe significantly more ZC3H14 in the nuclear samples, as expected. Despite the difference in ZC3H14 levels between the two compartments, we observe robust enrichment of ZC3H14 in the bound fractions from each compartment, with no enrichment in the pre-immune control samples (Figure 2.5C).

RNA isolated from input and bound fractions within each compartment were subjected to qRT-PCR analyses with *GAPDH*, *ATP5G1* and *ZC3H14* primers. As shown in Figure 2.5D, we observe significant enrichment of *ATP5G1* mRNA upon purification of ZC3H14 in the nucleus, but not in the cytoplasm. We also observe modest, but significant enrichment for *GAPDH* mRNA in the nuclear fraction only. Interestingly, we observe robust enrichment for *ZC3H14* mRNA in the nuclear and cytoplasmic fractions, suggesting that the mode of ZC3H14 binding to its cognate mRNA is different than other mRNAs examined, potentially via interactions with the conserved, internal polyadenosine sequence in the 3'UTR. Together, these data suggest that ZC3H14 interacts with the *ATP5G1* transcript specifically within the nucleus and that ZC3H14 may play a role in modulating nuclear processing events that are involved in the maturation of *ATP5G1* mRNA.

ZC3H14 is involved in the pre-mRNA processing of *ATP5G1*

The observation that ZC3H14 has a specific effect on the nuclear pool of *ATP5G1* mRNA suggests that ZC3H14 may be involved in nuclear processing events surrounding

the maturation of the *ATP5G1* transcript. Previous studies performed in yeast suggest that Nab2 is involved in the generation of export-competent mRNPs (160,161). To determine whether *ATP5G1* pre-mRNA levels are affected upon knockdown of ZC3H14, we performed qRT-PCR analysis with *ATP5G1* and *RPLP0* pre-mRNA primers with RNA collected from the whole and fractionated cell samples in Figures 2.5A and B. As shown in Figure 2.6A, knockdown of ZC3H14 did not have a significant effect on the whole cell or nuclear population of *ATP5G1* pre-mRNA levels, supporting preliminary data (not shown) that ZC3H14 does not have an effect on transcription. However, we do observe an increase in *ATP5G1* pre-mRNA levels in the cytoplasm upon ZC3H14 knockdown, resulting in a significantly decreased nuclear:cytoplasmic ratio of ATP5G1 pre-mRNA. As expected, we did not observe any significant changes in the levels or distribution of the control *RPLP0* pre-mRNA (Figure 2.6A, right).

The observation that reduction of ZC3H14 results in a shift in the distribution of *ATP5G1* pre-mRNA in these cells suggests that ZC3H14 may interact with pre-mRNAs to coordinate pre-mRNA processing/maturation events. To address this hypothesis, we performed qRT-PCR analyses with *RPLP0*, *RPLP0* pre-mRNA, *ATP5G1*, *ATP5G1* pre-mRNA and *ZC3H14* primers on RNA isolated from the input and bound fractions of ZC3H14 RNA-IPs (Figure 2.4A). Consistent with previous analyses, we achieve robust enrichment of *ATP5G1* and *ZC3H14* mRNA upon purification of ZC3H14 (Figure 2.6B); however, we do not observe significant enrichment of *RPLP0* mRNA. Intriguingly, we observe robust enrichment of *ATP5G1* and *RPLP0* pre-mRNAs upon ZC3H14 pulldown, in fact, at significantly higher levels that their respective mature mRNAs (Figure 2.6B).

Together, these data support a model (Figure 2.6C, left panel) where ZC3H14 interacts with pre-mRNAs in the nucleus, likely via interactions with the poly(A) tail, and coordinates post-transcriptional processing events on specific pre-mRNAs (such as *ATP5G1*). The coupling of these processing events leads to the generation of export-competent mRNPs and prevents aberrantly/incompletely-processed mRNAs from exiting the nucleus. In cells with reduced levels of ZC3H14 (Figure 2.6C, right panel), ZC3H14 is unable to recruit and/or coordinate nuclear post-transcriptional processing events on target transcripts, resulting in decreased production of mature target mRNAs (such as *ATP5G1*) and an increase in improperly/incompletely-processed mRNAs in the cytoplasm.

Knockdown of ZC3H14 causes mitochondrial fragmentation phenocopying loss of ATP5G1

A previous study demonstrated that decreasing the steady-state level of *ATP5G1* mRNA results in altered mitochondrial morphology (306), consistent with the idea that proper mitochondrial health and function are critical for normal mitochondrial morphology (307,308). These data, along with our observation that knockdown of ZC3H14 results in a significant decrease in steady-state *ATP5G1* levels and subsequently cellular ATP levels, suggest that the loss of ZC3H14 might affect mitochondrial morphology. To assess any changes in mitochondrial morphology, we transfected cells with siScramble, siATP5G1, or siZC3H14. After 48 hours, we fixed cells and stained for

either cytochrome C (a mitochondrial intermembrane space protein (309)) or HSP60 (a mitochondrial matrix protein (310)). Control cells either treated with no siRNA (not shown) or treated with scrambled siRNA (Figure 2.6A, left panel) exhibited normal mitochondria with a tubular, threadlike morphology. In contrast, cells transfected with ZC3H14 siRNA display mitochondria that are spherical and smaller than those imaged in unaffected cells (Figure 2.6A, middle panel). In agreement with previous work (301), we observed a fragmented mitochondrial phenotype in cells transfected with ATP5G1 siRNA (Figure 2.6A, middle panel). Consistent with the observation that ZC3H14 decreases the steady-state level of *ATP5G1*, we also observed a similar degree of mitochondrial fragmentation in cells treated with siZC3H14 (Figure 2.6A, right panel). For quantification, cells were scored on the basis of normal mitochondria (predominantly tubular) or fragmented mitochondria (predominantly spherical). As quantified in Figure 2.6B, samples transfected with either ZC3H14 siRNA or ATP5G1 siRNA had three times as many cells with fragmented mitochondria as control cells, representing 30% of the cell population. We estimate a ~60% transfection efficiency in the MCF7 cells, so this 30% represents roughly half of transfected cells that show altered mitochondrial morphology. Therefore, we conclude that loss of ZC3H14 causes mitochondrial fragmentation and also phenocopies the loss of ATP5G1.

Mitochondrial fragmentation is commonly observed in cells undergoing apoptosis (311). To determine whether knockdown of *ATP5G1* or *ZC3H14* induces apoptosis, causing the observed mitochondrial fragmentation phenotype, we analyzed levels of cleaved Poly (ADP-ribose) Polymerase (PARP). PARP is cleaved during programmed

cell death (312) and is therefore a marker for apoptosis. As shown in Figure 2.6C, treatment of cells with Staurosporine, a protein kinase C inhibitor and potent inducer of apoptosis (313), resulted in PARP cleavage. However, treatment of cells with mock transfection, siScramble, siZC3H14 or siATP5G1 resulted in no detectable PARP cleavage product, suggesting that cells treated with siRNA are not undergoing apoptosis. Furthermore, no evidence of cytochrome C release (another marker of cells undergoing apoptosis (314)) was observed in the mitochondrial staining images of siRNA-treated cells (data not shown), providing additional support that knockdown of ZC3H14 or ATP5G1 does not trigger apoptosis.

DISCUSSION

In this study, we performed a genome-wide analysis to assess the impact of ZC3H14 depletion on the steady-state levels of mRNA transcripts. Compared to cells treated with PABPN1 siRNA which displayed a modulation (≥1.5-fold increase or decrease) in the steady-state level of ~17% of all expressed transcripts, knockdown of ZC3H14 lead to a significant change in the steady-state level of only ~1% of all expressed transcripts. These results have several implications. First, ZC3H14 could target a very specific subset of RNAs. Alternatively, ZC3H14 could impact gene expression in a manner that does not alter steady-state poly(A) RNA levels. For instance, ZC3H14 could modulate the localization and/or translation of target transcripts. The microarray employed also would not detect changes in mRNA export from the nucleus or even splicing within the nucleus. Although our microarray platform can detect many common

splice variants of certain genes, we are limited in the splicing events that we can observe upon depletion of ZC3H14. Finally, depletion of ZC3H14 could impact RNA transcripts not present on the microarray platform such as long noncoding RNAs or miRNAs. However, there are a number of candidate targets identified from the microarray analysis that do demonstrate a change in the steady-state level upon knockdown of ZC3H14, suggesting that ZC3H14 may function in regulating the transcription, processing and/or stability of this subset of mRNAs.

To understand the precise manner in which ZC3H14 regulates target transcripts that are affected at steady-state levels, we selected the robustly affected transcript, *ATP5G1*, which encodes a key ATP synthase subunit C protein (292). The results from the microarray analysis revealed that knockdown of ZC3H14 and not PABPN1 resulted in a nearly three-fold decrease in the steady-state level of *ATP5G1* mRNA in MCF-7 cells, suggesting that this transcript is specifically regulated by ZC3H14 and is not a general target of nuclear Pabs. We validated and extended the results of the microarray analysis not only to other human cell lines, but also to the other ATP synthase subunit C mRNAs, *ATP5G2* and *-3*. ZC3H14 knockdown leads to a specific reduction in *ATP5G1* mRNA in all cell types tested but not the other two *ATP5G* transcripts. Finally, we achieve partial rescue of *ATP5G1* mRNA levels upon re-introduction of a tagged nuclear isoform of ZC3H14 (isoform 1), but not the cytoplasmic isoform 4, suggesting that the nuclear isoforms of ZC3H14 are important for maintaining control of *ATP5G1* mRNA levels.

Nucleocytoplasmic fractionation reveals that the effect of ZC3H14 knockdown on *ATP5G1* levels is, at least in large part, a nuclear event. Interestingly, RNA-IP analyses performed on fractionated cells reveal a clear enrichment for *ATP5G1* mRNA only in the nuclear compartment. Further support for a role for ZC3H14 in nuclear processing of *ATP5G1* mRNA is evidenced by the significantly decreased nuclear:cytoplasmic ratio of *ATP5G1* pre-mRNA caused by an increase in *ATP5G1* pre-mRNA in the cytoplasm. Finally, RNA-IP analyses reveal that upon purification of ZC3H14, we observe significantly higher enrichment for *ATP5G1* pre-mRNA than the mature ATP5G1 mRNA, suggesting preferential association with transcripts still undergoing nuclear processing. These findings are consistent with a recent study in *S. pombe* that demonstrate a role for Nab2 in acting at the level of the unspliced pre-mRNA and playing a role in promoting mRNAs that are competent for export to the cytoplasm (170). We hypothesize that the inability to properly coordinate the nuclear processing of the *ATP5G1* pre-mRNA results in a significant decrease in the production of mature *ATP5G1* mRNA.

The observed decrease in *ATP5G1* steady-state mRNA levels correlates with decreased cellular ATP levels and a striking mitochondrial fragmentation phenotype, phenocopying loss of ATP5G1. Importantly, knockdown of ZC3H14 does not trigger PARP cleavage, suggesting that the effect on mitochondrial health and function is not indicative of initiation of the apoptotic program. Together these data support a model where ZC3H14 positively regulates the steady-state levels of a specific target transcript that plays a critical role in cellular respiration.

The protein product of ATP5G1 is critical for maintaining cellular energy levels, as evidenced by the fact that ATP synthase levels are determined by ATP5G1 levels in certain tissues (266). *ATP5G1* is the most evolutionarily divergent of the three C subunit genes (302) and is regulated differently at the transcriptional level (302) as well as in response to various stimuli (315). Aside from our current study, the only other work examining the post-transcriptional processing of the *ATP5G1* transcript is from studies performed in rat neuronal cells, which demonstrate that the *ATP5G1* transcript is localized to and locally translated in axonal tips (306) and is a functional target of *miR-338* (316). Loss of *ATP5G1* expression specifically in axons resulted in decreased ATP levels, increased reactive oxygen species (ROS), and an attenuation of axonal growth rates (306), suggesting that ATP5G1 plays a key role in maintaining proper energy metabolism in neurons. These data provide evidence for an additional mechanism that cells employ to ensure tight regulation of *ATP5G1* and, in turn, proper ATP production. Furthermore, this study reveals another example of how *ATP5G1* is specifically and differentially regulated as compared to the other *ATP5G* mRNAs and their respective protein products.

The *ATP5G1* transcript not only serves as a good target for delineating the role of ZC3H14 in post-transcriptional processing, but also provides possible insight into the molecular mechanisms that underlie the observed intellectual disability in patients with mutation of *ZC3H14* (150). The observed general effect on *ATP5G1* observed upon ZC3H14 knockdown in multiple, diverse cell lines (including a human neuronal cell line)

supports the model that ZC3H14 plays a conserved and important role in neurons. Recent work on *D. melanogaster* Nab2 (dNab2) demonstrates that re-expression of dNab2 (150) ZC3H14 isoform 1 (268) specifically in the neurons of dNab2 null flies rescues developmental and locomotor defects observed in these flies (150,268). These studies underscore the importance of ZC3H14 in the brain and demonstrate that re-expression in neurons is sufficient to restore function.

Properly functioning mitochondria are clearly important in all cell types, but particularly in the cells of the brain, which are responsible for the consumption of 25% and 20% of our daily glucose and oxygen consumption, respectively (317,318). Neurons rely almost exclusively on ATP production via oxidative phosphorylation (319) and are unable to switch to glycolysis when oxidative phosphorylation becomes limited (320). In this study, we found a ~30% drop in cellular ATP levels with knockdown of either ZC3H14 or ATP5G1. In particular, knockdown of either protein caused a similar loss of ATP as compared to rotenone, an electron transport chain inhibitor (304). From these data, we conclude that energy production is compromised in cells where ZC3H14 is lost, suggesting a possible respiration defect. In addition, loss of either ZC3H14 or ATP5G1 severely altered mitochondrial morphology, resulting in smaller, round mitochondria. The mitochondrial fragmentation phenotype is frequently observed with loss of electron transport chain function (321-323). Though it is appreciated that fragmentation results from an imbalance of mitochondrial fission and fusion and that these are coupled to energy metabolism, regulation of these processes remains an active area of research (324,325). Of note, disruption of normal fission/fusion is observed in many neurological

disease, including dominant optic atrophy, Charcot-Marie-Tooth type 2A, Parkinson's disease, Alzheimer's disease, and Huntington's disease (267). Therefore, we conclude that regulation of *ATP5G1* by ZC3H14 is likely to have effects on mitochondria that could be detrimental to neurons.

A major research question is how ubiquitously expressed RNA binding proteins with general roles in mRNA processing are implicated in tissue-specific disease. For instance, a mutation in the gene encoding the ubiquitously expressed nuclear Pab, PABPN1, results in a very specific form of muscular dystrophy that affects the ocular and pharyngeal muscles (96). How these specific craniofacial muscles are selectively impacted when all cell types have a requirement for mRNA 3' end processing and polyadenylation events is yet to be determined. Similarly, the patients that possess loss-of-function mutations in *ZC3H14* have a non-syndromic form of intellectual disability (150). Why a loss of ZC3H14 in all tissues would result in a brain-specific phenotype is an intriguing question. In fact, many RNA binding proteins are implicated in neuronal disease (171). Perhaps there are critical binding partners for ZC3H14 found only in neurons. Alternatively, the high energy requirements found in this highly specialized cell type make them more vulnerable to a loss or reduction of this critically important protein. We hypothesize that ZC3H14, by ensuring the proper pre-mRNA processing of the *ATP5G1* transcript, plays a critical role in maintaining proper cellular energy levels and, in turn, mitochondrial health and signaling at neuronal synapses.

Table 2.1. Primer sequences used in this study.

Gene Name	Forward	Reverse
18s rRNA	GAGACTCTGGCATGCTAACTAG	GGACATCTAAGGGCATCACAG
RPLP0	GGGCGACCTGGAAGTCCAACT	CCCATCAGCACCACAGCCTTC
GAPDH	AAGGTCGGAGTCAACGGATTTGG	GATGACAAGCTTCCCGTTCTC
ZC3H14	CTACCATCACCCCATCTCAC	AGGGACAATCTGGTTTAGTACAC
ATP5G1	CCTCCTTCTTGAATAGCCCAG	CCCCAGCACCAATAAACTTG
Pre-*ATP5G1*	GAGTCAGCCACCTGTCCTTATGCC	CTGGTCTGGAACTCCCGTCTGG
Pre-*RPLP0*	GTGGCCATGGATCTGCTGGTTGTC	CCCACTTTGTCTCCAGTCTTGATCAG CTG

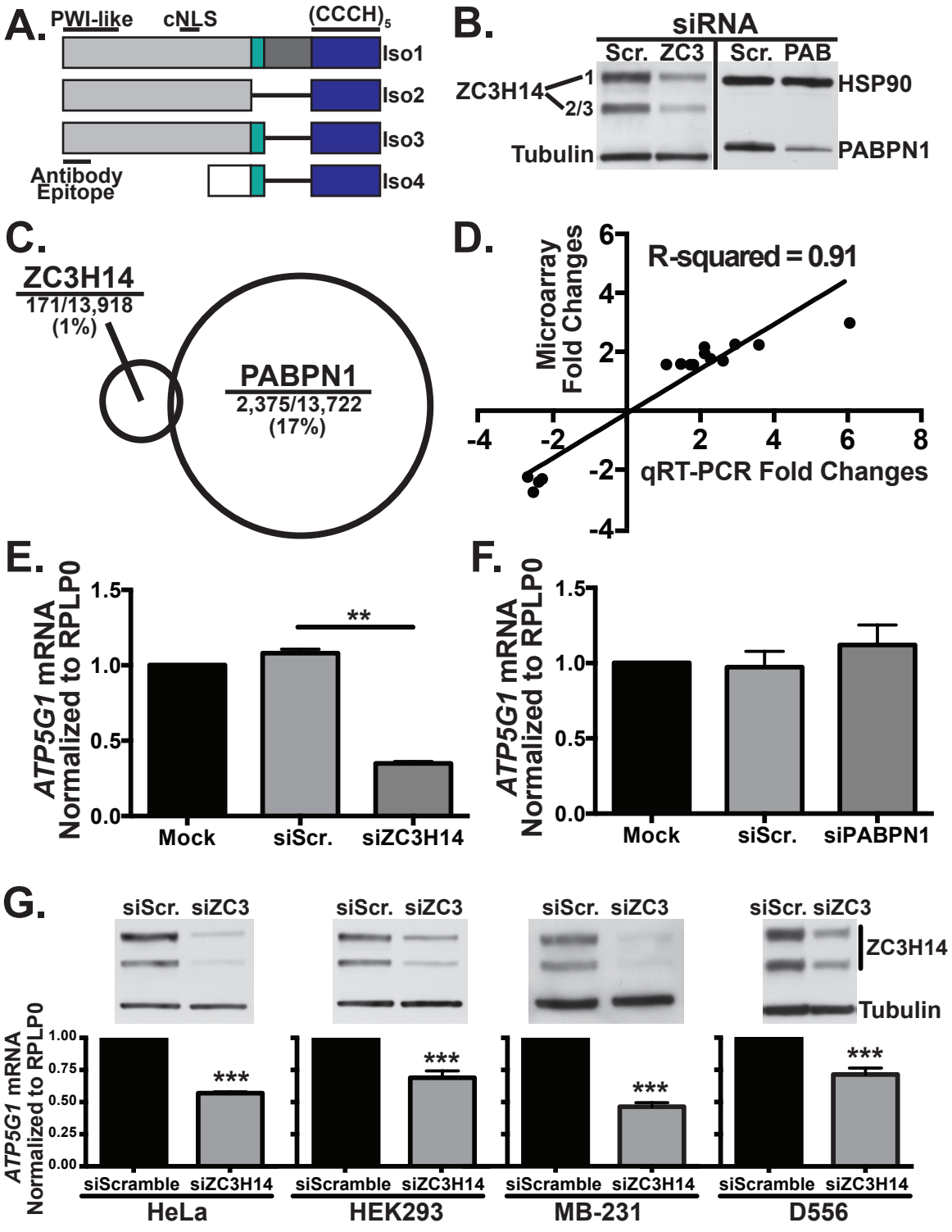
A.
PWI-like
cNLS
(CCCH)5
Iso1
Iso2
Iso3
Iso4
Antibody Epitope
B.
siRNA
Scr. ZC3
Scr. PAB
ZC3H14
1
2/3
HSP90
Tubulin
PABPN1
C.
ZC3H14
171/13,918
(1%)
PABPN1
2,375/13,722
(17%)
D.
R-squared = 0.91
Microarray Fold Changes
qRT-PCR Fold Changes
E.
ATP5G1 mRNA Normalized to RPLP0
**
Mock
siScr.
siZC3H14
F.
ATP5G1 mRNA Normalized to RPLP0
Mock
siScr.
siPABPN1
G.
siScr. siZC3
ZC3H14
Tubulin
ATP5G1 mRNA Normalized to RPLP0
***
siScramble siZC3H14
HeLa
HEK293
MB-231
D556

Figure 2.1: Knockdown of ZC3H14 decreases *ATP5G1* mRNA levels in all cell types examined. *A*) ZC3H14 is alternatively spliced to form at least four distinct protein isoforms (Iso1-4); three longer isoforms (Iso1-3) and a shorter isoform (Iso4). All isoforms contain the C-terminal CCCH5 zinc finger domain (blue) that confers RNA binding. Isoforms 1-3 differ from one another only in selective inclusion of exons 10-12 (teal and dark grey). These isoforms all contain an N-terminal Proline Tryptophan Isoleucine-like (PWI-like) fold as well as a predicted classical NLS (cNLS). Consistent with the presence of a cNLS, Iso1-3 are all localized to the nucleus at steady-state. ZC3H14 isoform 4 contains a distinct N-terminal exon (white). As the cNLS is absent from this isoform, Iso4 localizes to the cytoplasm at steady-state. The ZC3H14 antibody used in this study recognizes the N-terminal domain of isoforms 1-3 (Antibody Epitope). *B*) To assess knockdown, MCF-7 cells transfected with scramble (Scr.), ZC3H14 (ZC3), or PABPN1 (PAB) siRNA were subjected to immunoblot analysis with ZC3H14 or PABPN1 antibody and control antibodies to detect Tubulin and Heat Shock Protein 90 (HSP90). Robust knockdown of ZC3H14 and PABPN1 was observed with no effect on tubulin or HSP90 (controls). *C*) Total RNA isolated from MCF-7 cells transfected as in (*B*) was used for cDNA generation and hybridization to the Illumina BeadChip microarray platform. A schematic is shown indicating the relative number of transcripts that show a change (>1.5-fold) in steady-state level for each knockdown with size of circle representing fraction of transcripts impacted. Significance Analysis of Microarrays (SAM) analysis revealed that 171 out of 13,918 (~1%) of expressed transcripts in the transfected cells were affected (increased or decreased) by knockdown of ZC3H14 (101 increased and 70 decreased), whereas PABPN1 knockdown modulated 2,375 out of 13,722 (~17%) expressed transcripts (1,285 increased and 1,090 decreased). *D*) Fold-change values of select affected transcripts identified by the microarray analysis were plotted against fold-changes of the same select transcripts obtained by qRT-PCR analyses. Linear regression was used to determine the R2 value of 0.91, which represents a significant correlation between the results of both analyses and validates the effect on the transcripts analyzed. *E*) and *F*) Total RNA isolated from MCF-7 cells treated with mock transfection (Mock), scramble siRNA (siScr.), ZC3H14 (siZC3H14, Panel E) or PABPN1 (siPABPN1, Panel *F*) siRNA was used for cDNA generation and qRT-PCR analysis with transcript-specific primers to detect *ATP5G1* and the control *RPLP0* mRNA. Knockdown of ZC3H14 (Panel *E*), but not PABPN1 (Panel *F*), results in a significant decrease in *ATP5G1* steady- state mRNA levels. *G*) HeLa, HEK293, MB-231 and D556 cells (left to right) were transfected with scramble or ZC3H14 siRNA. Transfected cells were subjected to immunoblot analysis to confirm knockdown (top) with ZC3H14 and Tubulin (control) antibodies as well as qRT-PCR analysis (bottom) with *ATP5G1* and *RPLP0* (control) primers. Robust knockdown of ZC3H14 in each cell type resulted in a significant decrease in *ATP5G1* steady-state mRNA levels. Values represent the mean ± SEM for n=3 independent experiments. ** and *** represent $p \leq 0.01$ and $p \leq 0.001$, respectively.

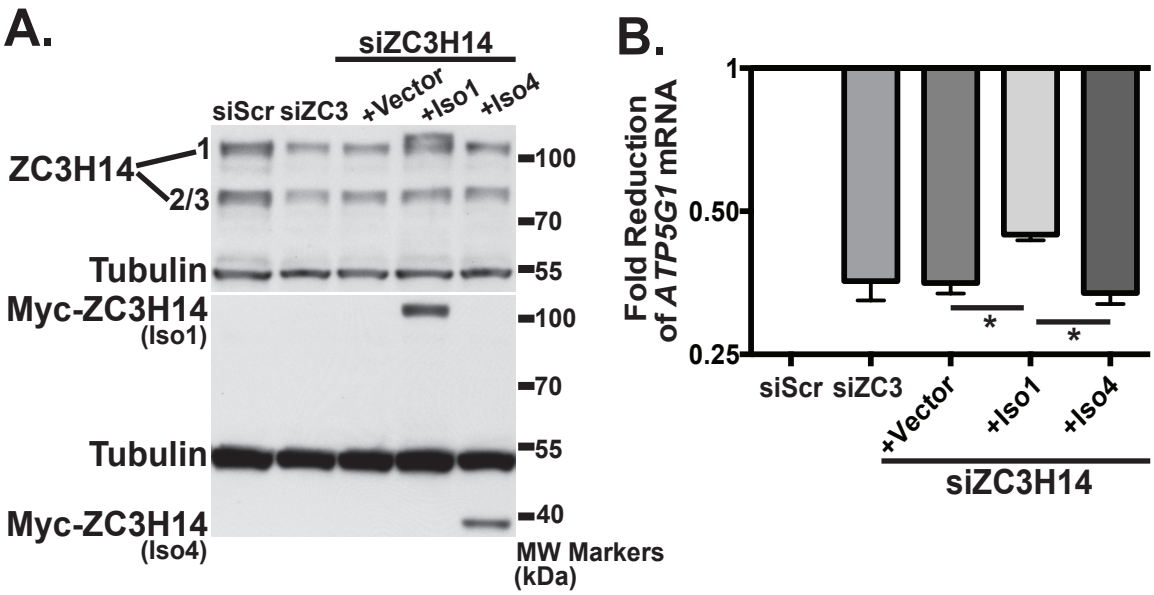

Figure 2.2: Re-expression of ZC3H14 isoform 1 restores *ATP5G1* transcript levels. To rescue the effect of ZC3H14 knockdown on *ATP5G1* mRNA levels, MCF-7 cells were transfected with either scramble (siScr.) or ZC3H14 (siZC3) siRNA alone or co-transfected with ZC3H14 siRNA and pcDNA3 (Vector), Myc-tagged ZC3H14 Isoform 1 (Iso1), or Myc-tagged ZC3H14 Isoform 4 (Iso4) for 48 hours. The Myc-tagged ZC3H14 constructs harbor silent mutations in the ZC3H14 siRNA-targeting regions and are therefore refractory to siRNA knockdown. Transfected cells were subjected to immunoblot analysis (*A*) with ZC3H14, Tubulin (control) or Myc antibody and qRT-PCR analysis (*B*) with primers specific to *ATP5G1* and control *18s rRNA*. Scramble control values are set to 1.0 and fold-reduction of ATP5G1 mRNA is represented on a log2 axis. A significant rescue of *ATP5G1* mRNA upon re-expression of Myc-Iso1 but not –Iso4 is indicated by *, which represents $p \leq 0.05$. Values represent the mean ± SEM for n=3.

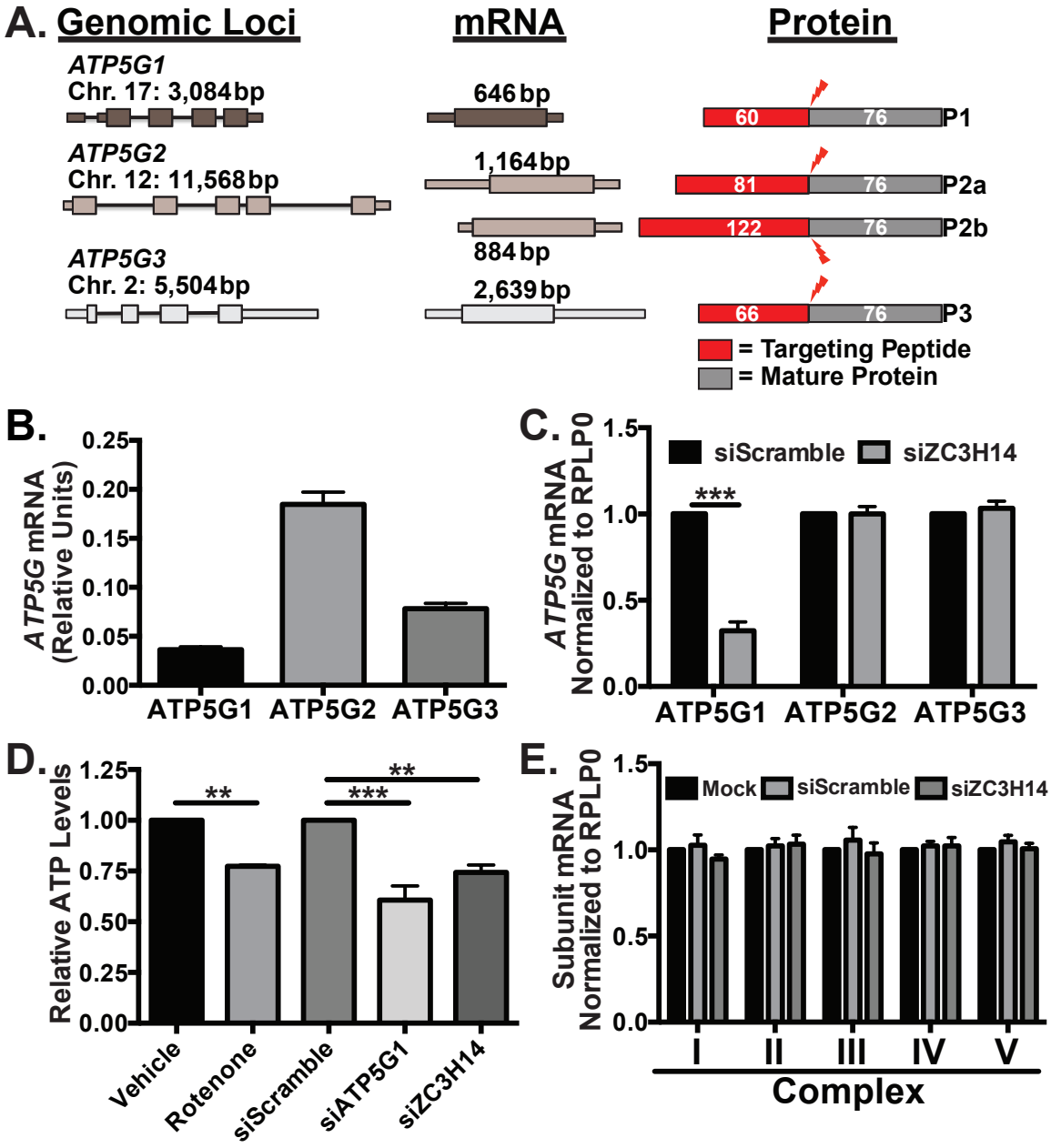

Figure 2.3: ZC3H14 modulates cellular ATP levels. *A*) The *ATP5G1*, *ATP5G2* and *ATP5G3* transcripts are transcribed from three separate genomic loci on chromosomes (Chr.) 17, 12 and 2, respectively. The *ATP5G1*, *-2*, and *-3* genes and their corresponding mRNAs have varying lengths (reported in base pairs, bp; thin bars=introns, thicker bands=UTRs, boxes=coding regions) and encode distinct protein products (P1, P2, and P3). *ATP5G2* is alternatively spliced to form two distinct mRNAs and subsequent protein products, P2a and P2b. The encoded protein products contain identical C-termini with variable N-terminal mitochondrial targeting peptides (red, with the number of amino acids indicated) that are cleaved (red lightning bolt) upon import into the mitochondria. The resulting mature protein products (dark grey) are completely identical in amino acid sequence (76 amino acids). *B*) Total RNA isolated from MCF-7 cells was used for qRT-PCR analysis with primers specific to each of the *ATP5G* mRNAs. The relative value of

each *ATP5G* mRNA was calculated by 2^-Ct and is reported as relative units. *C*) MCF-7 cells transfected with scramble control or ZC3H14 siRNA were subjected to RNA isolation and qRT-PCR analysis with primers specific to all three *ATP5G* mRNAs as well as the control transcript, *RPLP0*. Values are set to 1.0 for siScramble and normalized to RPLP0. Knockdown of ZC3H14 results in a specific and robust decrease in *ATP5G1* steady-state mRNA levels. *D*) To assess cellular ATP levels, cells treated with vehicle control, the electron transport chain inhibitor, rotenone, scramble siRNA, or siRNA targeting *ATP5G1* or *ZC3H14* were subjected to boiling water extraction and ATP level quantification using a luciferase-based assay. Cellular ATP levels are normalized to vehicle control or siScramble which are both set to 1.0 and plotted as relative ATP levels. ZC3H14 knockdown results in decreased cellular ATP levels similar to that observed with rotenone treatment or knockdown of ATP5G1. *E*) Cells treated with a mock transfection, scramble siRNA, or ZC3H14 siRNA were harvested and total RNA was used for qRT-PCR analyses. Primers specific to one representative nuclear-encoded mitochondrial mRNA from each OXPHOS complex as well as the control transcript, *RPLP0*, were used to assess any overall impacts of ZC3H14 on steady-state levels of transcripts encoding OXPHOS components I: *NDUFA4*, II: *SDHB*, III: *UQCRFS1*, IV: *CoxIV*, and V: *ATP5B*. Relative mRNA values for each OXPHOS mRNA from mock transfection are set to 1.0. Values represent the mean ± SEM for n=3 independent experiments. ** and *** represent $p \leq 0.01$ and $p \leq 0.001$, respectively.

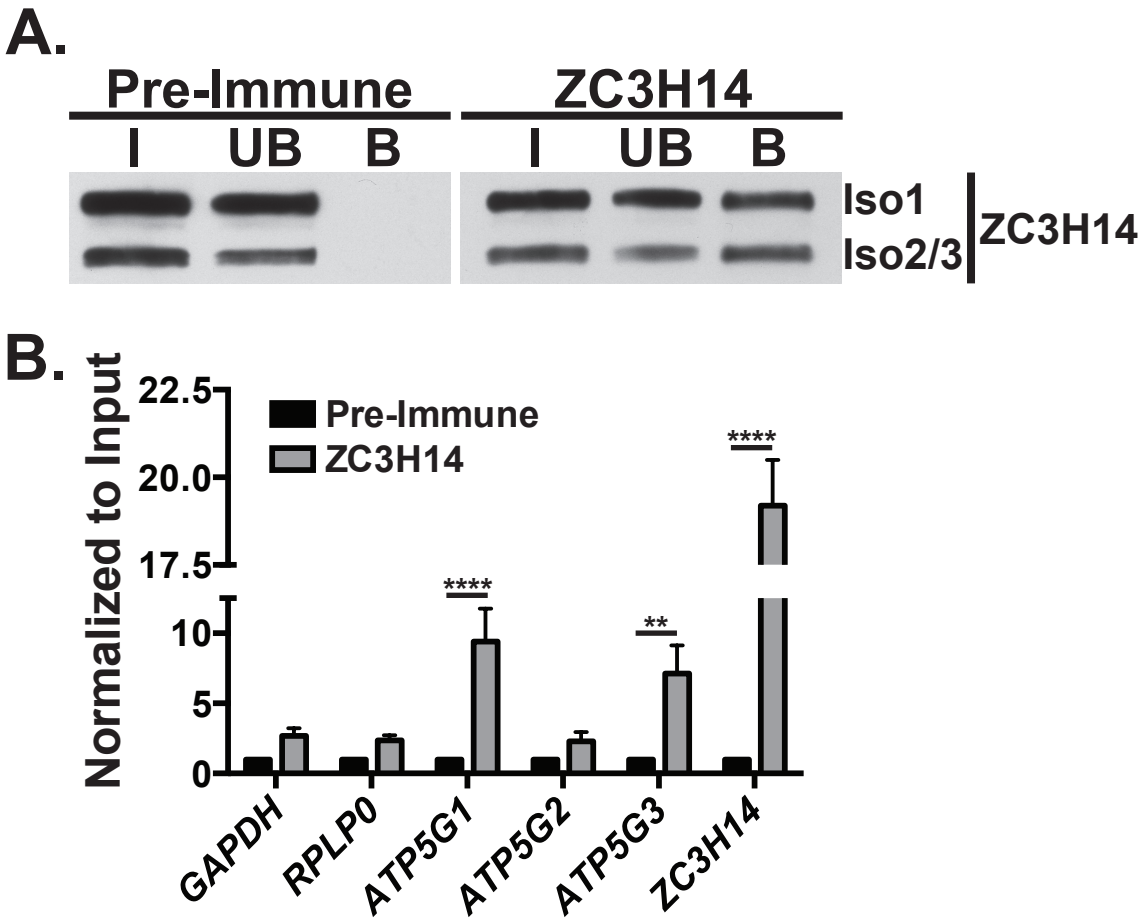

Figure 2.4: ZC3H14 binds to select mRNAs. Endogenous nuclear isoforms of ZC3H14 were immunoprecipitated from MCF-7 cells using either ZC3H14 antibody-bound protein A/G beads or rabbit pre-immune serum-coated beads. *A*) Proteins from the Input (I), unbound (UB) and bound (B) fractions were resolved on an SDS-PAGE gel and subjected to immunoblotting with ZC3H14 antibody. The nuclear ZC3H14 isoforms were detected in the ZC3H14-bound fraction but not the pre-immune bound fraction. *B*) RNA isolated from the ZC3H14 RNA-IP was subjected to qRT-PCR analyses with *GAPDH*, *RPLP0*, *ATP5G1*, *ATP5G2*, *ATP5G3* and *ZC3H14* primers. mRNA levels in the ZC3H14 bound fractions were normalized to input levels and then compared by fold-enrichment over pre-immune control. Significant enrichment of *ATP5G1*, *ATP5G3* and *ZC3H14* transcripts was observed with ZC3H14 IP. Values represent the mean ± SEM for n=3. ** and **** represent $p \leq 0.01$ and $p \leq 0.0001$, respectively.

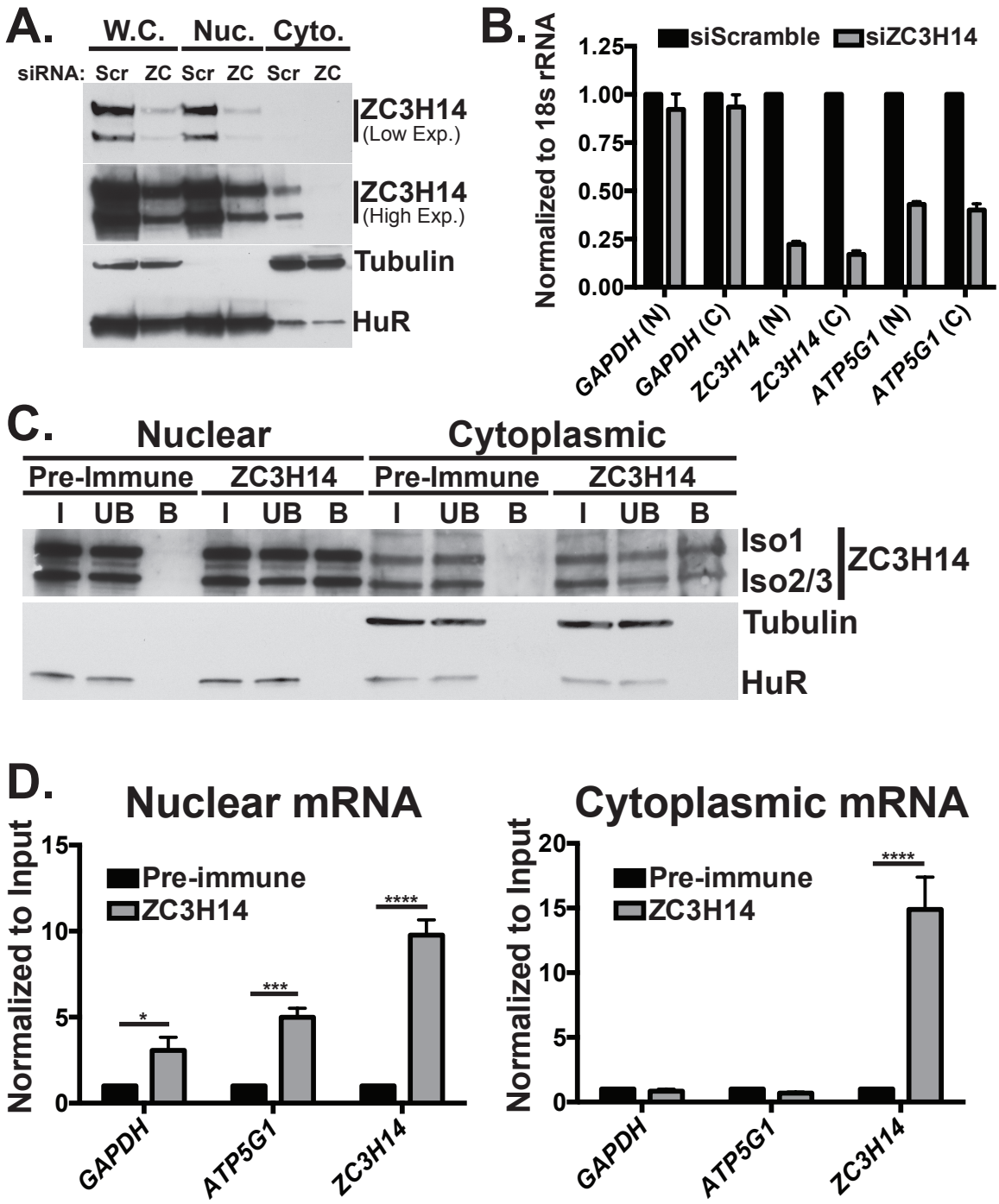

Figure 2.5: ZC3H14 binds to *ATP5G1* mRNA specifically in the nucleus. To determine if the effect on *ATP5G1* mRNA levels upon ZC3H14 knockdown is specific to a particular compartment, MCF-7 cells were transiently transfected with either Scramble (Scr.) or ZC3H14 (ZC) siRNA. Transfected cells were collected 48 hours later and subjected to nucleocytoplasmic fractionation. *A*) Protein from Whole Cell (W.C.), Nuclear (Nuc.) and Cytoplasmic (Cyto.) samples were subjected to immunoblot analysis with ZC3H14, Tubulin and HuR antibodies. As expected and consistent with clean fractionation, HuR and Tubulin display primarily nuclear and cytoplasmic localizations, respectively. Con

sistent with a previous study demonstrating steady-state nuclear localization of ZC3H14 in HeLa cells, we detect ZC3H14 primarily in the nucleus of MCF-7 cells. Robust knockdown of ZC3H14 in the whole cell and nuclear fractions is shown in the lower exposure blot (Low Exp.). A higher exposure (High Exp.) of the same blot demonstrates robust ZC3H14 knockdown in the cytoplasmic fraction as well. *B*) Total RNA isolated from samples in (*A*) was used for cDNA generation and qRT-PCR analysis with *GAPDH*, *ZC3H14* and *ATP5G1* primers. Knockdown of ZC3H14 resulted in a robust decrease of *ZC3H14* and *ATP5G1* steady-state mRNA levels in the nucleus and cytoplasm. To determine whether ZC3H14 interacts with *ATP5G1* mRNA in the nucleus and/or cytoplasm, MCF-7 cells were subjected to nucleocytoplasmic fractionation followed by RNA-IP, as in Figure 4. *C*) Proteins from the Input (I), unbound (UB) and bound (B) fractions were subjected to immunoblot analysis with ZC3H14, HuR and Tubulin antibodies. We achieve robust enrichment of ZC3H14 in each compartment. As expected, HuR and Tubulin are present primarily in the nuclear and cytoplasmic fractions, respectively. *D*) Total RNA isolated from the ZC3H14 RNA-IP in each compartment was subjected to qRT-PCR analysis with *GAPDH*, *ATP5G1* and *ZC3H14* primers. mRNA levels in the ZC3H14 bound fraction of each compartment were normalized to input levels and then compared by fold-enrichment over pre-immune control. Significant enrichment of *GAPDH*, *ATP5G1* and *ZC3H14* mRNAs was observed in the nucleus; however, *ZC3H14* was the only transcript enriched in the cytoplasmic samples. Data points represent the mean ± SEM for n=3 independent experiments. *, *** and **** represent $p \leq 0.05$, $p \leq 0.001$ and $p \leq 0.0001$, respectively.

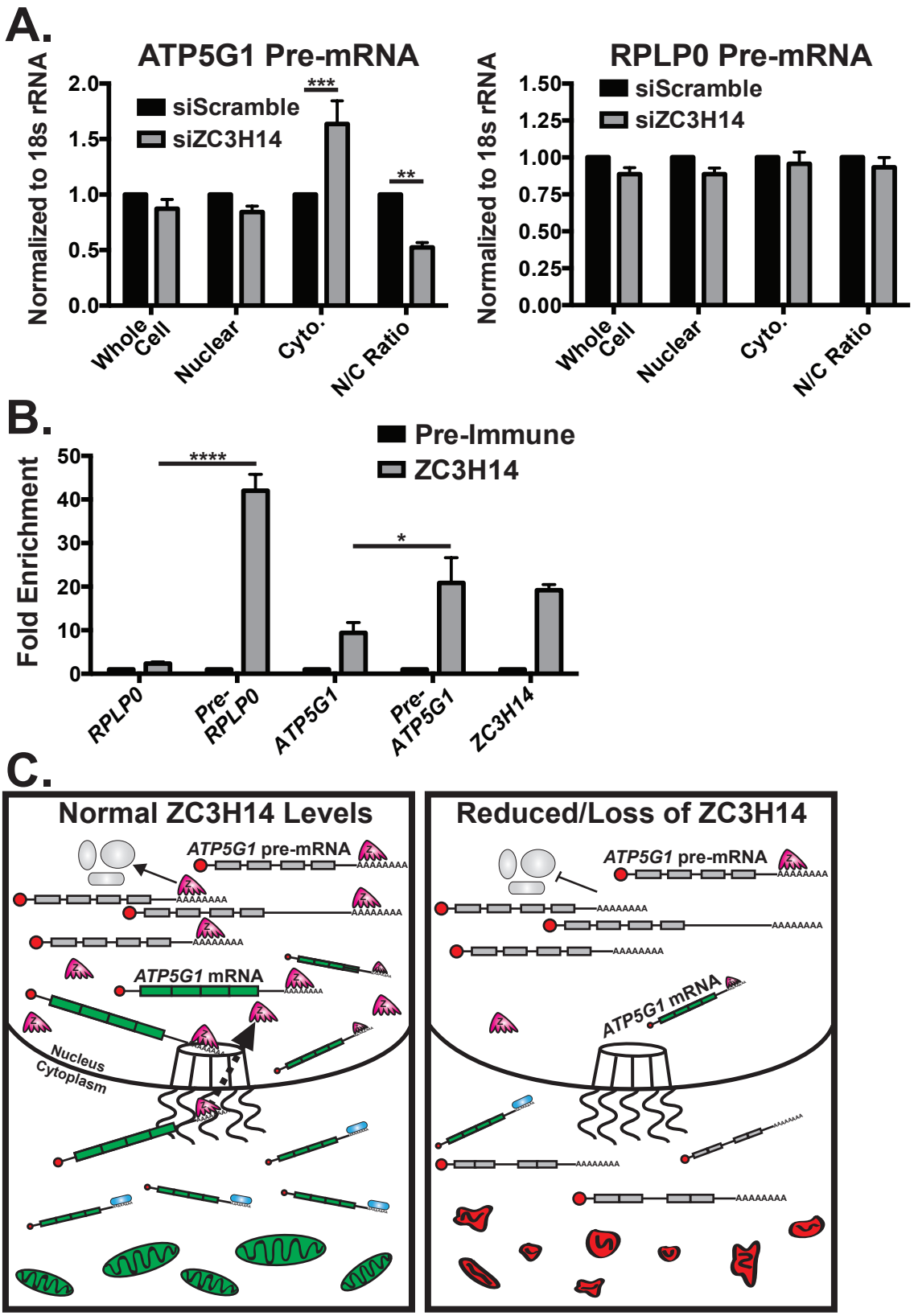
A.
ATP5G1 Pre-mRNA
Normalized to 18s rRNA
siScramble
siZC3H14
***
**
2.0
1.5
1.0
0.5
0.0
Whole Cell
Nuclear
Cyto.
N/C Ratio
RPLP0 Pre-mRNA
Normalized to 18s rRNA
siScramble
siZC3H14
1.50
1.25
1.00
0.75
0.50
0.25
0.00
Whole Cell
Nuclear
Cyto.
N/C Ratio
B.
Fold Enrichment
Pre-Immune
ZC3H14
****
*
50
40
30
20
10
0
RPLP0
Pre-RPLP0
ATP5G1
Pre-ATP5G1
ZC3H14
C.
Normal ZC3H14 Levels
ATP5G1 pre-mRNA
ATP5G1 mRNA
Nucleus
Cytoplasm
Reduced/Loss of ZC3H14
ATP5G1 pre-mRNA
ATP5G1 mRNA

Figure 2.6: ZC3H14 is involved in the pre-mRNA processing of *ATP5G1*. *A*) Total RNA isolated from cells in Figure 5A were subjected to qRT-PCR analysis with primers to detect *ATP5G1* (left) and *RPLP0* (right) pre-mRNA. Knockdown of ZC3H14 did not affect the nuclear steady-state levels of *ATP5G1* or *RPLP0* pre-mRNA; however, cytoplasmic *ATP5G1* pre-mRNA levels increased in the ZC3H14 knockdown samples. Cytoplasmic *RPLP0* pre-mRNA levels were unchanged in the same samples. The Nuclear:Cytoplasmic (N/C) ratio of *ATP5G1* pre-mRNA is significantly decreased upon ZC3H14 knockdown, likely due to the increased cytoplasmic levels of *ATP5G1* pre-mRNA. The N/C ratio of *RPLP0* pre-mRNA is unchanged upon ZC3H14 knockdown. *B*) RNA isolated from samples in Figure 4 were subjected to qRT-PCR analysis with *RPLP0*, *RPLP0* pre-mRNA (*Pre-RPLP0*), *ATP5G1*, *ATP5G1* pre-mRNA (*Pre-ATP5G1*) and *ZC3H14* primers. Consistent with the results from Figure 4B, we observe significant enrichment of *ATP5G1* and *ZC3H14* mRNAs in the ZC3H14 bound fraction. Interestingly, we observe significantly higher enrichment of *RPLP0* and *ATP5G1* pre-mRNA levels compared to their respective mature transcripts. *C*) Left: In cells with normal levels of ZC3H14 (Z; pink, five-fingered shape), ZC3H14 interacts with poly(A) tails throughout nuclear processing events to ensure the coordination of proper pre-mRNA (represented with grey exons and including introns) processing events as well as and to couple these events to export, resulting in the selective export of export-competent mRNPs (represented with green, spliced exons). ZC3H14 is likely removed during the process of export (black dotted arrow). The proper production and export of *ATP5G1* mRNA maintains a healthy pool of mitochondria (green ovals at bottom of image). Right: In cells with reduced ZC3H14 levels, post-transcriptional processing events are not properly coordinated, resulting in a decrease in the production of mature mRNA and an increase in improperly and/or incompletely processed pre-mRNAs in the cytoplasm and a disruption in normal mitochondrial morphology (red shapes at bottom of image). Data points represent the mean ± SEM for n=3 independent experiments. *, **, *** and **** represent $p \leq 0.05$, $p \leq 0.01$, $p \leq 0.001$ and $p \leq 0.0001$, respectively.

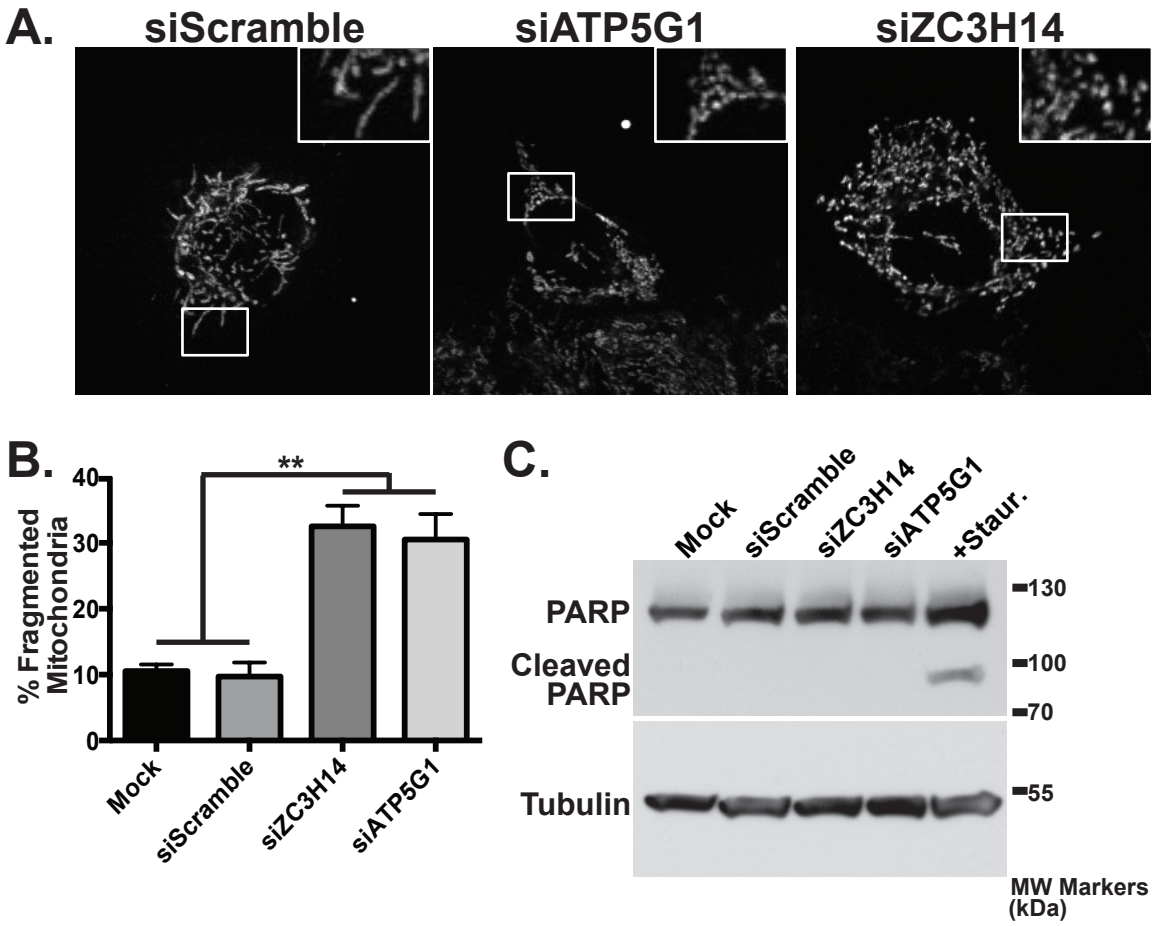

Figure 2.7: Knockdown of ZC3H14 results in fragmented mitochondria. *A*) MCF-7 cells transfected with either scramble (left), ATP5G1 siRNA (middle), or ZC3H14 (right) were fixed, permeabilized, and subjected to immunofluorescence with cytochrome C antibody. Insets are enlarged from the boxed regions of cells to better highlight mitochondrial morphology. Mitochondrial morphology in cells transfected with scrambled siRNA was indistinguishable from cells transfected with no siRNA (data not shown). *B*) Cells were scored for the presence of normal or fragmented mitochondria. Data is represented as a mean averaged from three independent experiments (N=304 for mock transfected cells, 311 for scrambled siRNA, 307 for ZC3H14 siRNA, 307 for ATP5G1 siRNA). The difference between control cells and either ZC3H14 or ATP5G1 cells was statistically significant. *C*) MCF-7 cells treated with mock transfection, scramble, ZC3H14, or ATP5G1 siRNA or the apoptotic inducer Staurosporine (Staur.) were subjected to immunoblot analysis with PARP or tubulin antibody. The presence of Cleaved PARP product only in the Staurosporine-treated samples suggests that the other cell populations are not undergoing apoptosis. Values represent the mean ± SEM for n=3 independent experiments. ** represents $p \leq 0.01$. Images are representative of n=3 independent experiments with 100 cells per experiment in each treatment group.

EXPERIMENTAL PROCEDURES

Cell culture

MCF-7 cells (ATCC HTB-22; Estrogen Receptor positive [ER+] breast cancer cell line (326)) were obtained from ATCC and maintained in Dulbecco's modified Eagle's medium (DMEM) supplemented with 10% FBS and antibiotics. DNA plasmids and siRNA (Invitrogen) were transfected into cultured cells using Lipofectamine2000 (Invitrogen) according to manufacturer's protocol.

Plasmids and chemicals

FLAG fusion constructs were generated using PCR primers that include the FLAG sequence to create N- or C-terminally FLAG-tagged protein isoforms. PCR products were then purified and subcloned into the pcDNA3.1 vector (Invitrogen). To generate the Myc-tagged ZC3H14 constructs, the N-terminal FLAG tag present in the ZC3H14 constructs was removed and replaced (subcloned) with a digested oligonucleotide encoding an N-terminal Myc tag. siRNA-resistant constructs were generated by site-directed mutagenesis (Stratagene) using primers that create silent mutations within the regions targeted by siRNA. For PARP cleavage assays, cells were treated with 1 μM Staurosporine (Enzo Life Sciences) for 3 hours. The siRNA targeting sequences for ZC3H14 are 5'-CACATTCTACCATCCCACCATTAAT-3' and 5'-

TGTTTGTTTGTTCACCCAAATTGTA-3'. The siRNA targeting sequence for ATP5G1 is 5'-TCTCCAGCTCTGATCCGCTGTTGTA-3'.

Immunoblotting

MCF-7 cells were harvested and washed in 1X PBS and then lysed on ice in RIPA-2 buffer (150 mM NaCl, 1% NP40, 0.5% deoxycholate, 0.1% SDS, 50 mM Tris pH 8.0) containing protease inhibitors (PLAC: 3 μg/ml of pepstatin, leupeptin, aprotinin, and chymostatin and 0.5 mM PMSF). Immunoblotting was performed using standard methods (327). Briefly, 30 μg of total protein lysate per sample was resolved by SDS-PAGE and transferred onto a nitrocellulose membrane. For immunoblotting, a 1:5,000 dilution of rabbit polyclonal ZC3H14 (154), rabbit polyclonal PABPN1 (110), or Tubulin (Sigma; Clone DM1A) antibody, a 1:2,000 dilution of HSP90 (Santa Cruz; Clone F-8) antibody, or a 1:1,000 dilution of PARP (Pharmingen; Clone 4C10-5), HuR (Santa Cruz; Clone 3A2), or Myc (Cell Signaling; Clone 9B11) antibody was used followed by 1:3,000 dilutions of HRP-conjugated goat anti-mouse IgG or HRP-conjugated goat anti-rabbit IgG secondary antibodies (Jackson ImmunoResearch).

Microarray analyses

MCF-7 cells were transfected with siScramble, siZC3H14, or siPABPN1 and collected 48 hours later. Transfected MCF-7 cells were lysed using QIAshredder columns (Qiagen) and total RNA was isolated using the RNeasy Mini Kit (Qiagen). RNA integrity

from triplicate samples was assessed on an Agilent Bioanalyzer 2100 and cDNA samples were generated and hybridized to the Illumina HumanHT-12 v4 Expression BeadChip microarray platform by the Emory Integrated Genomics Core. To discover differentially expressed transcripts between treatment groups, a two-class unpaired Significance Analysis of Microarrays (SAM) analysis was employed with a false discovery rate of 0%. An additional cut-off of 1.5-fold was used to identify significantly affected (increased or decreased) transcripts. This dataset is accessible at www.ncbi.nlm.nih.gov/geo/query/acc.cgi?acc=GSE62067.

RNA isolation and quantitative RT-PCR

Total RNA was isolated from MCF-7 cells using TRIzol reagent (Invitrogen) in accordance with the manufacturer's instructions. Reverse transcriptase reactions with M-MLV RT (Invitrogen) used 1 μg of RNA for a final concentration of 50 ng/μL cDNA per sample that was used for quantitative RT-PCR.

For qRT-PCR analyses, 1 μg of total RNA was transcribed to cDNA as described above. Relative mRNA levels were measured by quantitative PCR analysis of triplicate samples of 5 ng cDNA with QuantiTect SYBR Green Master Mix using an Applied Biosystems real time machine (ABI). Results were analyzed using the ΔΔCT method (328) and normalized to *18s rRNA* or *RPLP0* transcript. Statistical significance was determined using either a Student's T-test or a one- or two-way ANOVA. Primer sequences used for qRT-PCR analyses are shown in Table 2.1. Pre-validated qRT-PCR

primers for *ATP5G2*, *ATP5G3* and the OXPHOS subunit mRNAs *NDUFA4*, *SDHB*, *UQCRFS1*, *COXIV* and *ATP5B* were ordered from SABiosciences.

Cellular ATP assays

Cells were plated in 6-well dishes and treated for 48 hours with siScramble, siZC3H14, or siATP5G1 siRNA (Invitrogen) according to manufacturer's protocol. Separate sets of cells were treated with vehicle control (DMSO; Sigma) or 1 μM rotenone (Enzo Life Sciences) for three hours. All cells were harvested and counted side-by-side and then lysed using a one-step boiling water cellular ATP extraction as previously described (329). Total cellular ATP levels were assayed with the Enliten ATP Assay System (Promega) and normalized to siScramble or vehicle control.

RNA immunoprecipitation

To probe interactions between ZC3H14 and target mRNAs in whole cell lysates, RNA-IP anslyses were performed on MCF-7 cells grown to near confluency in 150-mm plates. Cells were rinsed twice with ice cold PBS, collected on ice, and resuspended in RNA-IP buffer (50 mM Tris-HCl, pH 7.4, 100 mM NaCl, 32 mM NaF, 0.5% NP-40 in DEPC-treated water) supplemented with 1 mM DTT, 100 U/mL RNase OUT (Invitrogen) and 1 cOmplete mini protease inhibitor tablet (Roche; 1 tablet/10 mL of buffer). Cells were sonicated on ice 5 times (program: 9 seconds at 0.5 output) and then passed through a 27 gauge syringe 5 times and placed back on ice for 20 minutes with

occasional vortexing. Lysates were spun at 13,000 RPM for 10 minutes at 4°C and protein concentration was determined with a standard BCA assay. Protein G magnetic beads (DYNA beads; Invitrogen) were rinsed and resuspended in RNA-IP buffer and incubated with pre-immune rabbit serum or an equal volume of N-terminal ZC3H14 antibody (154) for 1 hour at room temperature. Bead/antibody and bead/pre-immune samples were rinsed in RNA-IP buffer and added to clarified cell lysates, followed by incubation at 4°C overnight while tumbling end over end (10% removed prior to overnight incubation for input samples). After incubation, beads were magnetized, unbound samples were collected (10% of input), and washed 5 times with ice cold RNA-IP buffer. ZC3H14/RNA complexes were eluted and isolated with TRIzol reagent (Invitrogen) and purified according to manufacturer's instructions.

To determine interactions between ZC3H14 and target RNAs in separate cellular compartments, RNA-IP assays were carried out as described above, with the following alterations: Confluent MCF-7 cells were rinsed twice with ice cold PBS, collected on ice, and subjected to nucleocytoplasmic fractionation (described in the following section). Upon isolation and separation of the cytoplasmic lysates, the nuclear fraction was rinsed once with ice cold TSE buffer (10 mM Tris, 300 mM sucrose, 1 mM EDTA, 0.1%NP-40, pH 7.5), sonicated and passed through a syringe as described above. Nuclear samples were incubated on ice for 20 minutes with occasional vortexing, followed by a 10 minute spin at 13,000 RPM at 4°C. The protein concentration from each compartment was determined by a standard BCA assay. Lysates from each compartment were subjected to immunoprecipitation as described in the previous section.

RNA isolated from input and bound fractions for pre-immune and ZC3H14 samples were subjected to RNA isolation and qRT-PCR as described above. mRNA levels in the ZC3H14 bound fractions (for whole cell and within each compartment) were normalized to input levels and then compared by fold-enrichment over pre-immune control.

Nucleocytoplasmic Fractionation

To isolate distinct pools of RNA and protein from nuclear and cytoplasmic fractions, cells were collected on ice, spun down, and resuspended in ice-cold fractionation buffer (10 mM Tris-HCl, pH 7.4, 10 mM NaCl, 3 mM $MgCl_2$, 0.5% (v/v) NP-40) supplemented with 1 mM DTT, 100 U/mL RNase OUT (Invitrogen), and 1 mini cOmplete protease inhibitor tablet (Roche; 1 tablet/10 mL of buffer) for 10 minutes on ice. Cell lysates were spun down and the supernatant, or cytoplasmic fraction was separated from the nuclear pellet. RNA was isolated from each fraction with TRIzol reagent (Invitrogen) and protein samples were prepared with RIPA-2 buffer (as described above).

Immunofluorescence and imaging

MCF-7 cells were plated and transfected with scramble or ZC3H14 siRNA (Invitrogen) using Lipofectamine2000 (Invitrogen) according to manufacturer's protocol.

Following a 48-hour transfection, cells were re-plated at a 1:2 dilution onto matrigel (BD Biosciences) coated coverslips and allowed to attach overnight. The following day, cells were fixed in 4% PFA in PBS (15 minutes at RT) and then permeabilized in Triton X-100 (0.1% in PBS, 10 minutes), blocked (1% BSA in PBS, 1 hour), and stained overnight with a 1:1,000 dilution of cytochrome C (BD Biosciences; Clone 6H2.B4) or a 1:5,000 dilution of HSP60 (Enzo Life Sciences; Clone LK-2) antibodies diluted in blocking buffer. The coverslips were then washed 4 times with PBS (5 minutes) and stained with a 1:500 dilution of anti-mouse 546 secondary antibody (Alexa fluorophores, Invitrogen). Coverslips were washed 4 times, stained with Hoescht 33342, and mounted using Prolong Antifade (Invitrogen). Representative cells were imaged using an Olympus FluoView 1000 confocal microscope using a 100× objective (NA 1.45) with laser excitation at 543 nm.

For quantitative analyses, a cell was scored as “normal” if its mitochondria appeared predominantly tubular, and “fragmented” if mitochondria appeared predominantly small and spherical. For each experiment at least 100 cells were scored. Values are represented as mean ± SEM from three independent experiments. Statistical analysis was performed using a one-way ANOVA and a value of $p<0.05$ was considered significant.

Chapter 3: Investigating Multiple Aspects of *ZC3H14* Regulation

A portion of this chapter is adapted from the following published work:

Wigington, C.P., Williams, K.R., Meers, M.P., Bassell, G.J., and Corbett, A.H. (2014) *Wiley Interdisciplinary Reviews RNA* **5**, 601-622. "Poly(A) RNA Binding Proteins and Polyadenosine RNA: New Members and Novel Functions."

INTRODUCTION

The identity and fate of a cell is determined by the spatial and temporal regulation of its gene expression profile. The transcriptional control of gene expression, mediated by epigenetic modifications to the DNA as well as binding and subsequent regulation by a host of transcription factors, is a critical and well-studied event. However, post-transcriptional processing events, which include the capping, splicing, 3' end processing, export, translation, transport and eventual decay of an mRNA transcript (8), are also critical to ensure the proper gene expression profile of a cell or tissue. Post-transcriptional processing events are mediated by a host of factors, including non-coding RNAs (ncRNAs) and RNA binding proteins (330,331). The importance of RNA binding proteins in maintaining tight control of gene expression is highlighted by the observation that many RNA binding proteins are mutated or dysregulated in various types of human disease (286), which underscores the importance of understanding the regulation and expression of newly-characterized RNA binding proteins with links to disease.

The Zinc Finger Cys_3His protein #14 is a ubiquitously expressed, nuclear poly(A) binding protein (Pab) that binds to polyadenosine RNA with high affinity (148,154). A recent study identified a small group of patients from rural Iran, born out of consanguineous relationships between first cousins, who possess loss-of-function mutations in *ZC3H14* that cause an autosomal recessive form of non-syndromic intellectual disability (150). The role of ZC3H14 in human cells is not clear; however, studies of ZC3H14 orthologs in various model systems suggest that ZC3H14 likely plays

a diverse role in RNA processing (150,167), potentially as an mRNA surveillance factor to coordinate mRNA quality control (161).

The patients that lack ZC3H14 clearly highlight the importance of ZC3H14 in the brain. In fact, many RNA processing factors are enriched in the brain (51) and extensive alternative splicing, mRNA transport, and local translation are observed at higher levels in the brain than other tissues (reviewed in (171)). However, ZC3H14 is ubiquitously expressed (154) and, therefore, likely has critical roles in other cell types underscoring the importance of identifying regulatory mechanisms that govern the expression and regulation of *ZC3H14* mRNA and protein.

In this chapter, we characterize multiple aspects of *ZC3H14* expression in order to gain insight into cellular pathways that control the expression of *ZC3H14*. We observe an intriguing correlation between ZC3H14 steady-state protein levels and the Estrogen Receptor (ER) status of various breast cancer cell lines; however, analysis of *ZC3H14* steady-state mRNA levels (total and individual splice variants) reveals consistent mRNA levels across all cell types tested. Investigation of the *ZC3H14* locus and various ENCODE datasets via the UCSC genome browser provides evidence for multiple transcription factors that regulate *ZC3H14* in MCF-7 cells. Consistent with previous study on the *S. cervisiae* ortholog of ZC3H14, Nab2 (269), we demonstrate that ZC3H14 binds specifically to its own mRNA transcript, potentially via a conserved stretch of 15 adenosines located within the *ZC3H14* 3'UTR. Finally, we share the results of our transcriptome-wide analysis of templated polyadenosine stretches located within mRNA

transcripts, providing an additional point of regulation for Pabs such as ZC3H14 outside the confines of the poly(A) tail.

RESULTS

ZC3H14 steady-state protein levels correlate with the Estrogen Receptor status of select breast cancer cell lines

As described in the Introduction and throughout Chapter 2, precise regulation of ZC3H14 levels is critical for proper neuronal function, as evidenced by patients that lack ZC3H14 and display severe cognitive deficits (150). The intellectual disability observed in these patients certainly underscores the critical role of ZC3H14 in the brain; however, *ZC3H14* is ubiquitously expressed (154) and likely serves important roles in other cell types. We took advantage of a number of open access databases that contain a wealth of expression data from human cells and tissues to investigate *ZC3H14* expression patterns and correlative disease studies.

Preliminary analysis of genome-wide studies deposited in the Oncomine database (332) suggest that the steady-state level of *ZC3H14* varies across breast tumor samples, specifically correlating with Estrogen Receptor (ER) status, a commonly used prognostic tool in breast cancers (333,334). These genome-wide studies were performed in primary tumor samples and analyzed steady-state mRNA levels of thousands of genes. To confirm and extend these preliminary analyses in a simplified and readily available

system, we grew and maintained five different breast cancer cell lines and subjected them to protein analysis. We selected three commonly used ER(-) breast cancer cell lines (HS578, MB231 and MB468) and two ER(+) breast cancer cell lines (MCF-7 and T47D) for these studies.

To determine whether the steady-state ZC3H14 protein levels correlate with ER status across the selected cell lines, we collected cells of each type, isolated protein, and performed immunoblot analysis of biological triplicate samples with an N-terminal ZC3H14 antibody that recognizes the three nuclear forms of ZC3H14 (154). Immunoblot analysis of the same samples with an ER alpha antibody confirms the ER status of these cells (Figure 3.1A). As shown in Figure 3.1A, analysis of steady-state ZC3H14 Isoform 1 (Iso1) levels normalized to Tubulin (loading control) across triplicate samples from each cell type reveals a consistently lower amount of ZC3H14 protein in the ER(-) cell lines compared to the ER(+) samples (quantification of these data in Figure 3.1B). These results suggest that steady-state ZC3H14 protein levels correlate with the Estrogen Receptor status of the cell lines tested.

ZC3H14 **is not an estrogen responsive gene**

Estrogen Receptor α (ERα or ER) is a well-studied nuclear hormone receptor that is activated upon binding the hormone, estrogen. Upon binding to estrogen, ERα dimerizes and translocates to the nucleus, where it binds to Estrogen Response Elements (EREs) in the DNA or other transcription factors and up- or down-regulates the

expression of many genes, including many genes important for reproductive and mammary tissue function (335-337). The observation that ZC3H14 steady-state protein levels are higher in the ER(+) cell types examined in Figure 3.1A than the ER(-) cell types suggests a simple model wherein *ZC3H14* is a target of ERα-induced transcription.

Investigation of the *ZC3H14* locus in the UCSC genome browser reveals a number of potential mechanisms for transcriptional regulation of *ZC3H14*. The *ZC3H14* locus occupies a 50 kilobase region on the long arm of chromosome 14 (partially schematized at the top of Figure 3.2A). As schematized in Figure 2.1A, *ZC3H14* is alternatively spliced to generate at least four distinct splice variants (154). These splice variants are depicted in ascending order in Figure 3.2A, with *Variant 4* utilizing an alternate transcriptional start site between coding exons 9 and 10 of *Variants 1-3*. Displayed below the *ZC3H14* gene schematic is an overlay of Histone 3 Lysine 27 Acetylation (H3K27Ac) across the *ZC3H14* locus from seven different cell lines. H3K27Ac is a mark for active enhancer regions and is often enriched near promoter regions (338). As shown in Figure 3.2A, a clear peak in H3K27Ac is located at the transcriptional start site of the first three splice variants of *ZC3H14*, suggesting active and ongoing transcription at this site.

Overlay of DNase sensitivity clusters across this region of the *ZC3H14* locus reveals a striking increase in DNase sensitivity surrounding the *ZC3H14* transcriptional start site. Regions of DNA that are sensitive to cleavage by DNase represent regions of the genome that lack a condensed chromatin structure and are therefore accessible to

interacting proteins such as transcription factors (339). Finally, Chromatin ImmunoPrecipitation and sequencing (ChIP-seq) studies reveal a strong enrichment for various transcription factors at the *ZC3H14* start site (Figure 3.2A). Of note, one study performed ChIP-Seq with c-Myc, CTCF and PolII antibodies on serum-stimulated MCF-7 cells and revealed a significant enrichment of all three factors at the *ZC3H14* start site upon serum stimulation, suggesting a spike in transcription. ChIP-seq studies performed with ERα antibodies did not reveal binding of ERα at or near *ZC3H14* promoter regions. In addition, analysis of sequence data from studies that mapped ERE sites across the genome (335,337) did not reveal any consensus EREs at or near the *ZC3H14* locus. Together, these data suggest that *ZC3H14* is actively transcribed across a variety of cell types and is likely regulated by multiple transcription factors, including c-Myc and CTCF in MCF-7 cells.

In silico analysis of the *ZC3H14* locus suggests that *ZC3H14* is regulated by a number of different transcription factors, including c-Myc, as identified in multiple ChIP-Seq studies in MCF-7 cells (340). c-Myc stimulates the transcription of many different genes, including cyclins and E2F transcription factors (341-343). In fact, *c-Myc* is an ERα target gene and estrogen stimulation leads to activation of *c-Myc* (344). The observation that *ZC3H14* steady-state levels correlate with the ER status in the panel of breast cancer cell lines tested led us to hypothesize that *ZC3H14* might be an estrogen-responsive gene, potentially via c-Myc. To determine whether *ZC3H14* steady-state transcript levels increase upon estrogen treatment, we hormone depleted MCF-7 cells (an ER[+] breast cancer cell line (326)) for 72 hours and then treated cells with DMSO

(vehicle control) or Estrogen. Total RNA was isolated from cells collected at increasing time points after drug addition and used to generate cDNA for subsequent qRT-PCR analyses with primers to detect *ZC3H14 Variants 1-3* or *4* as well as the control estrogen responsive gene, *pS2* (345). As expected, treatment with control vehicle, DMSO, did not result in stimulation of any of the transcripts tested (Figure 3.2A). As shown in Figure 3.2B, treatment with estrogen resulted in a striking increase in *pS2* steady-state mRNA levels, as expected for an estrogen-responsive gene. In contrast, none of the *ZC3H14* transcripts tested demonstrated a response to treatment with estrogen, suggesting that *ZC3H14* is not an estrogen-responsive gene. However, the wealth of ENCODE transcription factor ChIP-Seq data (340) suggests that there are many other pathways and mechanisms that have the potential to modulate the transcriptional output of *ZC3H14* in different cell types.

To analyze the steady-state level of *ZC3H14* mRNA across the breast cancer cell lines tested in Figure 3.1, we isolated and purified total cellular RNA from each cell type and generated cDNA for use in qRT-PCR analyses. We designed one set of PCR primers that span two exons in the C-terminal zinc finger region of *ZC3H14*, which is common to all described variants and is termed *Pan ZC3H14*. To detect individual splice variants, we designed primers that span exon-exon boundaries unique to each splice variant (*Variants 1-4*). As shown in Figure 3.2D, qRT-PCR analysis with each primer set revealed a consistent and unique pattern of *ZC3H14* expression across this panel of cell lines. Total steady-state *ZC3H14* (*Pan ZC3H14*) levels were consistent between all five cell lines and did not correlate with the ER status, consistent with our observation that *ZC3H14* is not

an estrogen responsive gene. *ZC3H14 Variant 1* steady-state levels were also consistent between cell types tested; however *Variant 1* levels differed from the other three variants tested in each cell type. For instance, *Variants 2 and 3* were consistently expressed at higher levels than *1* or *4* and *Variant 4* levels were significantly lower than all other variants tested. This trend in relative levels of *ZC3H14 Variants* between cell lines suggests that different cell types likely share unique mechanisms to fine-tune the level and ratio of *ZC3H14* mRNA.

Overexpression of ZC3H14 isoforms reveals cross regulation of splice variants

While the transcriptional regulation of *ZC3H14* is a critically important step in maintaining tight control of *ZC3H14* levels in cells, there are also key post-transcriptional regulatory events that could regulate the steady-state levels of *ZC3H14*. ZC3H14 is a zinc finger-containing RNA binding protein that has affinity for polyadenosine RNA (148,150). Many RNA binding proteins bind to their own mRNA transcripts and autoregulate the abundance of cognate mRNA and protein products (195). To determine whether ZC3H14 may autoregulate the levels of its individual splice variants, we transfected MCF-7 cells with plasmids encoding FLAG-tagged Isoforms 1 and 4 of ZC3H14 (Iso1 and Iso4, respectively) or a pcDNA3 vector (control). To confirm the expression of each of the FLAG-tagged proteins, we isolated protein from the transfected cells and performed immunoblot analysis for ZC3H14 as well as a control protein, Human Antigen R (HuR). As shown in Figure 3.3A, both of the FLAG-tagged ZC3H14

isoforms are robustly overexpressed in these cells. As expected, expression of the control protein, HuR, was unaffected by ZC3H14 overexpression.

Total cellular RNA collected from transfected cells was subjected to cDNA generation and qRT-PCR analyses with primers to detect total *ZC3H14* mRNA (*Pan ZC3H14*) and the individual *ZC3H14* splice variants (*Variants 1-4*) as well as the control transcript, *GAPDH* (Figure 3.3B). As expected, overexpression of FLAG-ZC3H14 Isos 1 and 4 both resulted in a robust increase in *Pan ZC3H14* steady-state mRNA levels. We also observed a significant increase in *Variant 1* and *4* steady-state levels upon overexpression of the cognate FLAG-tagged ZC3H14 isoform. Interestingly, we observe a unique pattern of crosstalk between the two isoforms examined here. For instance, overexpression of FLAG-ZC3H14 Iso1 resulted in a robust increase in the steady-state level of *Variants 2* and *3* while only moderately affecting *Variant 4* levels. Likewise, overexpression of FLAG-ZC3H14 Iso4 also induced a significant increase in *Variants 2* and *3* steady-state levels; however, we do not observe any effect on *ZC3H14 Variant 1* mRNA levels upon Isoform 4 overexpression. These results suggest that cross regulation likely occurs between ZC3H14 proteins and transcripts, potentially via RNA binding protein/RNA physical interactions.

Two nuclear Pabs, ZC3H14 and PABPN1, bind to their own transcripts

We observe an interesting expression pattern of *ZC3H14* splice variants upon overexpression of FLAG-ZC3H14 Isos 1 and 4 (Figure 3.3B), suggesting a post-

transcriptional regulatory mechanism to autoregulate cognate mRNA levels. As described previously, many RNA binding proteins bind to and regulate the levels of their cognate mRNA transcripts via cis elements typically located within the 3'UTR (195). The nuclear Pab, ZC3H14, binds polyadenosine RNA with high affinity and is predicted to interact with poly(A) tails added to the 3' end of mRNA transcripts (148). Another nuclear Pab, PABPN1, also has high affinity for polyadenosine RNA and is involved in the stimulation of polyadenylation on mRNA transcripts (29). To test whether ZC3H14 and PABPN1 interact specifically with their cognate mRNAs, we performed RNA-IP analyses with FLAG-tagged ZC3H14 and PABPN1 proteins. Briefly, MCF-7 cells were transfected with plasmids encoding FLAG-ZC3H14, FLAG-PABPN1 or vector alone (control). Transfected cell lysates were prepared as described in Experimental Procedures and subjected to RNA-IP analysis with FLAG antibody-conjugated Protein A beads. As shown in Figure 3.4A, we achieved robust purification of both FLAG-ZC3H14 and -PABPN1 proteins.

To identify RNA transcripts that co-purify with the FLAG-tagged proteins, qRT-PCR analysis was performed with *ZC3H14* and *PABPN1* primers that span the coding region/3'UTR junction and therefore only detect endogenous *ZC3H14* and *PABPN1* transcripts. Primers to detect the *GAPDH* transcript were also used in these analyses. As shown in Figures 3.4 B and C, immunoprecipitation of both FLAG-ZC3H14 and -PABPN1 resulted in significant enrichment of the respective endogenous transcripts. Interestingly, the polyadenylated transcript, *GAPDH*, did not enrich significantly with either FLAG-ZC3H14 or -PABPN1, suggesting that these two nuclear Pabs may achieve

transcript specificity via interactions with another RNA binding protein or through binding to a specific cis element rather than simply to the poly(A) tail.

A previous study in *S. cerevisiae* demonstrated that the ZC3H14 ortholog, Nab2, binds and autoregulates the levels of its own mRNA transcript via an internal encoded stretch of 26 adenosines within the 3'UTR (269). Like Nab2, the human *ZC3H14* 3'UTR contains an internal stretch of 15 adenosines that could confer binding by ZC3H14 (schematized in Figure 3.4D). Interestingly, *PABPN1* also contains an A-rich region within its 3'UTR, located proximal to the end of the coding region (Figure 3.4E). As mentioned previously, ZC3H14 and PABPN1 both possess high affinity for polyadenosine RNA *in vitro* and may therefore interact with their respective transcripts via these templated adenosine-rich regions within their 3'UTRs. In fact, personal communication with a collaborating lab revealed that the two adenosine-rich stretches in the *PABPN1* 3'UTR (Figure 3.4E) are responsible for *PABPN1* autoregulation and pre-mRNA processing, supporting the role for polyadenosine RNA binding proteins in modulating their own mRNA levels via internal polyadenosine stretches. Together, these data suggest a more general role for these templated polyadenosine stretches in Pab-dependent gene expression.

Prevalence of templated stretches of polyadenosine within the transcriptome

As discussed extensively in Chapter 1, the canonical function of Pab proteins is to bind the poly(A) tails of mRNA transcripts and carry out diverse functions that are

essential for proper gene expression (29). However, these non-templated polyadenosine tracts are not the only stretches of polyadenosine found in the transcriptome, as discussed in the previous section. For instance, a handful of studies have described polyadenosine stretches ranging from 9-26 adenosines within mRNA transcripts (346-348), but little work has been done to determine the function of these sequences. Given the length of these internal stretches and the typical Pab footprint of ~11-12 A's (100,116), Pabs may bind to these internal sequences as well as to poly(A) tails. In fact, there is precedence for this mode of regulation. Human PABPC binds to A-rich sequences in the 5'UTR of *PABPC* mRNA and the 3'UTR of *YB-1* mRNA to modulate the translation of these transcripts (147,349-351). Furthermore, binding of *S. cerevisiae* Nab2 to a stretch of 26 adenosines in the 3'UTR of *NAB2* mRNA mediates a negative feedback response in which recruitment of the exosome drives subsequent degradation of the *NAB2* transcript (269). In this study, we observed robust and specific enrichment of endogenous *ZC3H14* and *PABPN1* mRNAs upon immunoprecipitation of FLAG-ZC3H14 and -PABPN1, respectively (Figures 3.4B and C) and predict that these specific interactions are mediated by polyadenosine stretches located within the 3'UTRs of the *ZC3H14* and *PABPN1* transcripts. Together these data suggest that internal polyadenosine sequences could play an important role in regulating gene expression.

To gain insight into the prevalence of internal polyadenosine stretches within the human transcriptome, we analyzed all annotated human transcripts from the UCSC HG19 genome annotation for the presence of polyadenosine stretches. PABPN1 and PABPC require a stretch of 11-12 adenosines for high affinity binding (100,116), so we extracted

stretches containing at least 12 consecutive adenosines, filtered the data for overlapping regions, and mapped the resulting stretches to their locations within transcripts. As a proof of principle, we verified the presence of mRNA transcripts that are known to contain ≥12 nucleotide (nt) adenosine stretches (Dystrophin (348) and Vitamin D Receptor (346)) within our final dataset. Our results indicate that there are 139,334 instances of ≥12 nt adenosine stretches in the human transcriptome, many of which occur in multiple differentially spliced isoforms of the same gene (Figure 3.5A). As expected, the overwhelming majority of adenosine stretches occur in introns (136,655 instances). Interestingly, there are only 2,464 adenosine stretches that occur exclusively in exons (i.e. in the mature transcript) - 1.8% of total instances. Of those, roughly 82% occur exclusively in the UTRs of the gene in which it resides (the majority of which occur in the 3' UTR) (Figure 3.5B), suggesting that the aforementioned examples of regulatory mechanisms that depend upon templated polyadenosine stretches in UTRs could be more prevalent than previously appreciated. Remarkably, less than 0.02% of templated polyadenosine instances occur in the coding region of mRNA transcripts, with the remainder found in non-coding RNAs (Figure 3.5C). These preliminary results reveal that many mRNAs contain internal polyadenosine stretches and therefore have the potential to be bound and modulated by poly(A) binding proteins not only via their non-templated poly(A) tails, but also through these templated internal sequences. The vast enrichment of these stretches in the 3'UTRs of mature transcripts supports the well-establish function of the 3'UTR in post-transcriptional processing (352) and suggests a potential additional point of regulation via 3'UTRs. In the future, it will be interesting to

test the function of these internal polyadenosine sequences as well as investigate whether these sequences are enriched in certain types or classes of RNA transcripts.

DISCUSSION

In this chapter, we describe multiple lines of investigation into the transcriptional (Figure 3.2) and post-transcriptional (Figure 3.3 and 3.4) regulation of *ZC3H14* mRNA and protein levels in human cells. We demonstrate that ZC3H14 steady-state protein levels correlate with Estrogen Receptor status across a number of different breast cancer cell lines while steady-state *ZC3H14* mRNA levels (all splice variants tested) are unchanged across the same cell lines tested. Compilation and analysis of transcriptomic data from the UCSC genome browser suggests that *ZC3H14* is actively transcribed with potential for control by a host of different transcription factors in MCF-7 cells; however, an estrogen time course experiment reveals that *ZC3H14* is not an estrogen-responsive gene. Overexpression experiments with FLAG-tagged ZC3H14 isoforms reveal a pattern of cross regulation between the various splice variants and isoforms of *ZC3H14*. We demonstrate robust and specific interactions between the nuclear Pabs, ZC3H14 and PABPN1, with their cognate mRNAs, suggesting that these two RNA binding proteins, like many others (195), may autoregulate their mRNA transcripts. Finally, we performed a transcriptome-wide analysis to determine the prevalence and location of polyadenosine stretches within the transcriptome. Together, these results suggest that *ZC3H14* mRNA and protein levels in human cells are subject to a number of diverse regulatory pathways, including auto enrichment of its own mRNA transcript.

As shown in Figure 3.1A, we observe that ZC3H14 steady-state protein levels correlate with ER status across the panel of breast cancer cell lines tested (quantified in Figure 3.1B) while the steady-state mRNA levels of *ZC3H14* are consistent between cell lines (Figure 3.2D). This result suggests that ZC3H14 protein levels are regulated through altered translation and/or stability. Consistent with previous work in a human embryonic kidney cell line, HEK293 (154), we observed significantly different steady-state levels of the individual splice variants of *ZC3H14* within each cell type (Figure 3.2D). The steady-state level of *Variant 4* is significantly lower than all other splice variants tested while *Variants 2* and *3* are present at higher levels than *Variant 1* in all cell types. Of note, the only difference in the mRNA transcripts that represent *Variants 1*, *2* and *3* is the inclusion and exclusion of the three small exons found at the center of the message, as these splice variants share the same 5' and 3'UTRs. This data suggests that the short sequences encoding these alternative exons (and the RNA binding proteins that bind them) may be responsible for the observed differences in steady-state level of the individual transcripts as they all appear to be transcribed from the same start site. The observation that *Variant 4* is expressed at much lower levels than the other variants suggests that either the transcriptional activity at that promoter is much lower than *Variants 1-3* (as supported by H3K27Ac and DNase I sensitivity data in Figure 3.2A) or that the stability of this transcript is much lower than the other variants tested, at least in the cell lines examined.

As mentioned previously, understanding the mechanisms that govern the steady-state levels of *ZC3H14* mRNA and protein in a given cell is key to elucidating the role of

ZC3H14 in human cells. We demonstrate here that although ZC3H14 protein correlates with the Estrogen Receptor status of a set of tumor samples, *ZC3H14* is not an estrogen-responsive gene (Figure 3.2B and C). However, a number of ENCODE datasets (overlaid in Figure 3.2A) suggest that a number of different transcription factors are found at (and have the potential to regulate) the *ZC3H14* promoter region. These results suggest that *ZC3H14* is actively transcribed and likely expressed at high levels in multiple cell types, consistent with a number of studies from our lab using an N-terminal ZC3H14 antibody that demonstrate robust ZC3H14 steady-state protein levels in most cell types examined.

In addition to regulation at the level of transcription, *ZC3H14* is likely regulated by multiple post-transcriptional mechanisms. *ZC3H14* has a 1,758 nucleotide 3'UTR with multiple predicted binding sites for miRNAs (353) and RNA binding proteins (354). Interestingly, sequence analysis of the *ZC3H14* 3'UTR reveals a stretch of 15 adenosines located between nucleotides 1,229-1,243. There is precedence for poly(A) binding proteins binding to their own mRNA transcripts via A-rich regions, such as *H. sapiens* PABPC1 binding to an A-rich domain in its 5'UTR (349-351), or *S. cerevisiae* Nab2 binding to a 26-mer of adenosines in its 3'UTR (269). Here, we provide evidence that the two nuclear Pabs, ZC3H14 and PABPN1, interact with their own mRNA transcripts. These studies were performed using RNA immunoprecipitation analyses, which do not allow us to determine the precise sequence element(s) required for binding of either protein to their respective transcripts. Personal communication with a collaborating lab has recently revealed that the two polyadenosine stretches located in the proximal region of the *PABPN1* 3'UTR do, in fact, confer binding by PABPN1 and are likely the

sequence(s) responsible for our observed self-enrichment. Current work in our lab is focused on determining whether the polyadenosine stretch within the *ZC3H14* 3'UTR confers binding by ZC3H14 and if so, whether the binding event has any effect on *ZC3H14* levels.

Our analysis of internal, templated polyadenosine stretches in RNAs (Figure 3.5) reveals clear enrichment of these sequences within the introns and 3′UTRs of mRNAs. The transcripts that contain one (or more) of the 1,972 polyadenosine stretches within their 3'UTR represent a class of transcripts that may be coordinately bound by Pabs to confer regulation in this poly(A) tail-independent manner. Only in a few cases have the function of such templated A stretches been analyzed (346-348), but those studies do confirm the potential for their functional importance. An important question moving forward is whether there is specificity for the binding of individual Pabs for these internal polyadenosine sequences. For instance, are the polyadenosine stretches located within the *PABPN1* 3'UTR bound only by PABPN1 or could these sequences also be bound (competitively and/or cooperatively) by other Pabs, such as ZC3H14 or PABPC? Integrating the presence and function of these polyadenosine sequences into our current model of how Pabs interact with mRNAs will expand our understanding of how Pabs influence gene expression.

Table 3.1. Primer sequences used in this study.

Gene Name	Forward	Reverse
18s rRNA	GAGACTCTGGCATGCTAACTAG	GGACATCTAAGGGCATCACAG
RPLP0	GGGCGACCTGGAAGTCCAACT	CCCATCAGCACCACAGCCTTC
GAPDH	AAGGTCGGAGTCAACGGATTTGG	GATGACAAGCTTCCCGTTCTC
Pan ZC3H14	CTACCATCACCCCATCTCAC	AGGGACAATCTGGTTTAGTACAC
Variant 1	TTATCCCGACTGCAAATCGACCCA	ACTTCCTCAGACAGCTTTGGCTTC
Variant 2	AATCAAGCTGAGATGAGTGAACTGA GTGTGG	GGTGATGGTAGGCACACTC
Variant 3	GCAGATGAGTCAAGCTGAGATGAGT GAACT	GGTGATGGTAGGCACACTC
Variant 4	AGAAACGTTGAGAAAGGAACTCAA CAGAGGC	ATCTCAGCTTGACTCATCTGC
pS2	ATACCATCGACGTCC CTCCA	AAG CGT GTC TGA GGT GTC CG
Endogenous *ZC3H14*	GATGGAATGTCCCTTCTATCATCCA AAACATTGTAG	GACAAGTTCTGTAGAGTATCTTTCAT CAGTACATGA AAACTTCC
Endogenous *PABPN1*	CTACAACAGTCCCGCTCTCGA TTCTAC	CCTCTTTTTTTCCTCTCTCTCCTCCTA ATACACAC

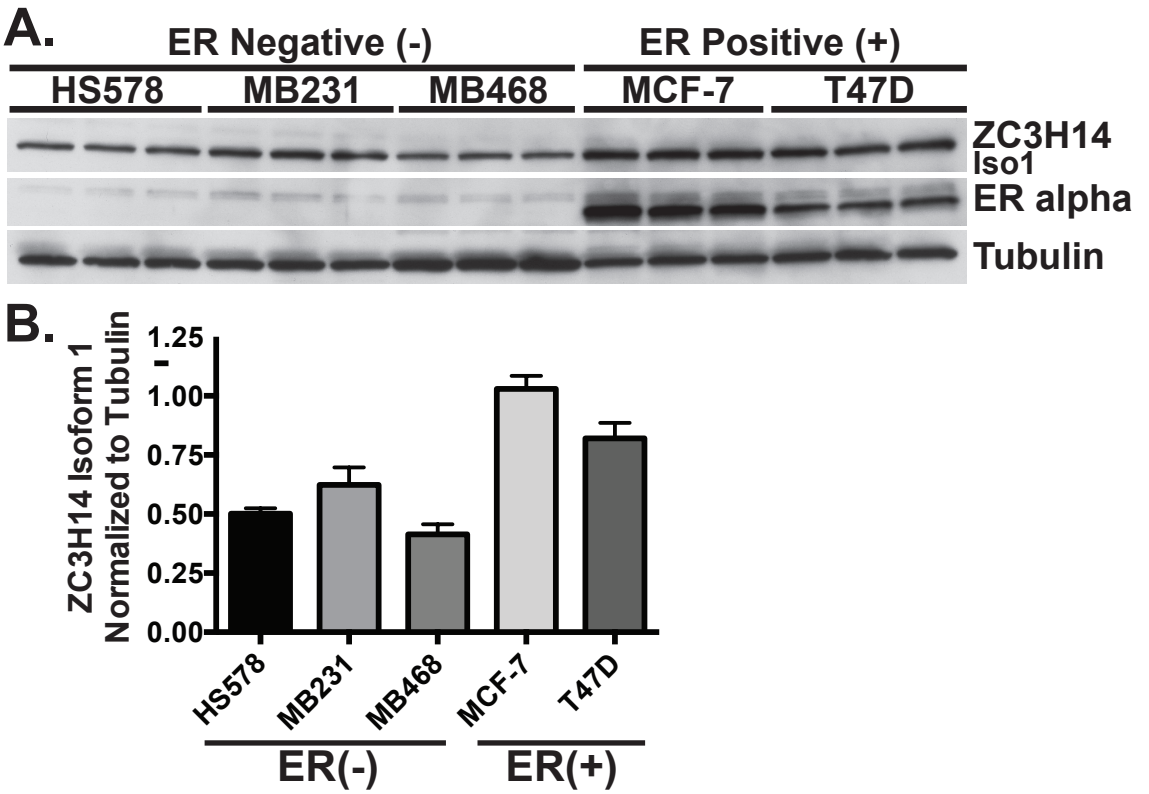

FIGURE 3.1. ZC3H14 steady-state protein levels correlate with Estrogen Receptor (ER) status across a panel of breast cancer cell lines. *A*) Three Estrogen Receptor negative (ER[-]; HS578, MB231 and MB468) and two ER(+) breast cancer cell lines (MCF7 and T47D) were collected in triplicate and subjected to immunoblot analysis with ZC3H14, ER alpha and Tubulin antibodies. *B*) Quantification of ZC3H14 Isoform 1 (Iso1) steady-state levels reveals a correlation between Estrogen Receptor status and ZC3H14 protein levels in these cell lines tested.

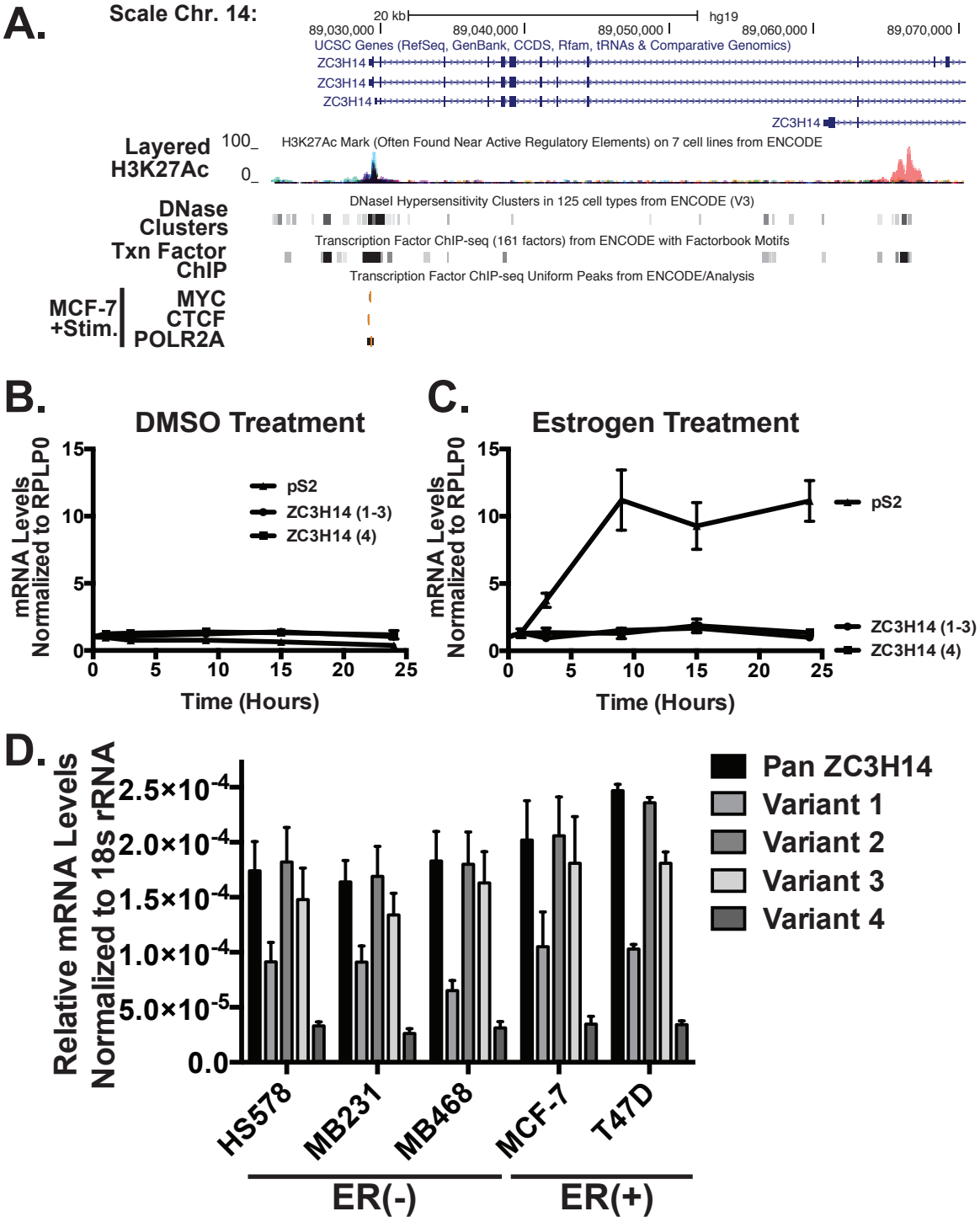

FIGURE 3.2. *ZC3H14* is not transcriptionally activated by Estrogen. *A*) UCSC genome browser view of the 5' region of the ZC3H14 locus, including four confirmed splice variants of ZC3H14. Gene positions are shown at the top, followed by H3K27Ac marks, a sign of active enhancer regions that are commonly located near active regulatory elements, and DNase I hypersensitive clusters, highlighting regions of uncondensed, or exposed chromatin. Transcription factor ChIP-Seq data are shown in the tracks below and reveal confirmed transcription factor binding sites from various human cell lines,

including MCF-7. To determine whether ZC3H14 is transcriptionally activated by Estrogen, MCF-7 cells were hormone starved for 72 hours and then introduced to media containing DMSO (*B*) or 10 nM Estrogen (*C*) and collected at the indicated time points. Total cellular RNA isolated from treated cells was subjected to cDNA generation and subsequent qRT-PCR analysis with primers to detect the known Estrogen-responsive transcript, *pS2*, *ZC3H14 Variants 1-3* or *Variant 4* and *RPLP0*. Treatment with DMSO (*B*) did not result in transcriptional activation of any of the tested transcripts. However, treatment with Estrogen (*C*) resulted in a striking induction of *pS2* transcript levels without impacting *ZC3H14* mRNA levels, suggesting that *ZC3H14* is not an Estrogen-responsive gene. *D*) Total cellular RNA isolated from cells in Figure 3.1A was subjected to cDNA generation and subsequent qRT-PCR analysis with primers to detect *ZC3H14 Variants 1-4* individually or collectively (*Pan ZC3H14*) and *18s rRNA*. Although each variant is expressed at different levels relative to one another across all cell lines tested, the steady-state level of each variant is consistent between cell lines.

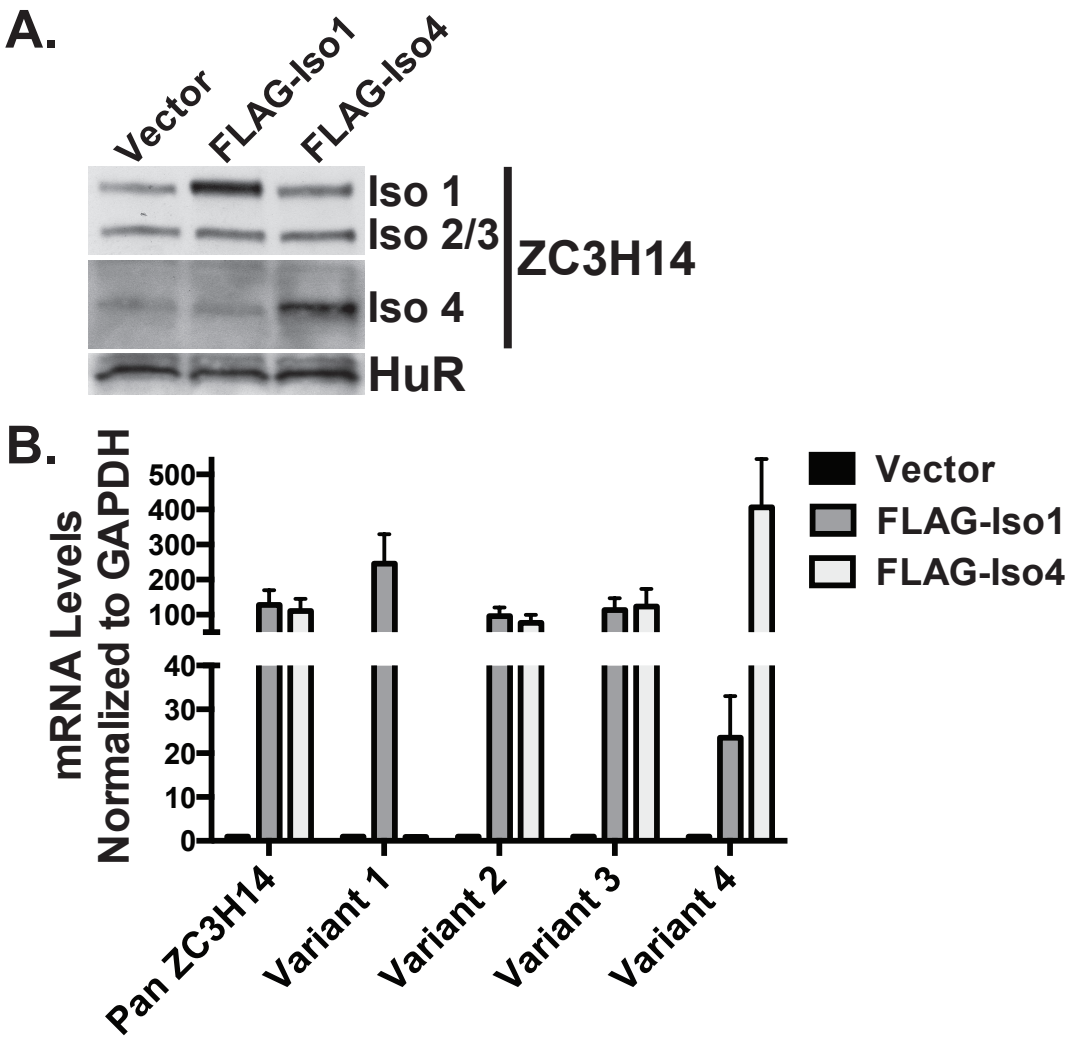

FIGURE 3.3. Overexpression of FLAG-tagged ZC3H14 isoforms 1 and 4 results in selective upregulation of *ZC3H14* splice variants. *A*) MCF-7 cells were transfected with plasmids encoding FLAG-tagged Isoforms 1 and 4 (Iso1 and Iso4, respectively) of ZC3H14 and subjected to immunoblot analysis with ZC3H14 (N-terminal to detect Isoforms 1-3 and Isoform 4-specific) and HuR (loading control) antibodies. We achieve robust expression of FLAG-Iso1 and -Iso4 as evidenced by the ZC3H14 blots. *B*) Total RNA isolated from MCF-7 cells in (*A*) was used for cDNA generation and subsequent qRT-PCR analysis with primers to detect *ZC3H14 Variants 1-4* individually or collectively (*Pan ZC3H14*) and *GAPDH*.

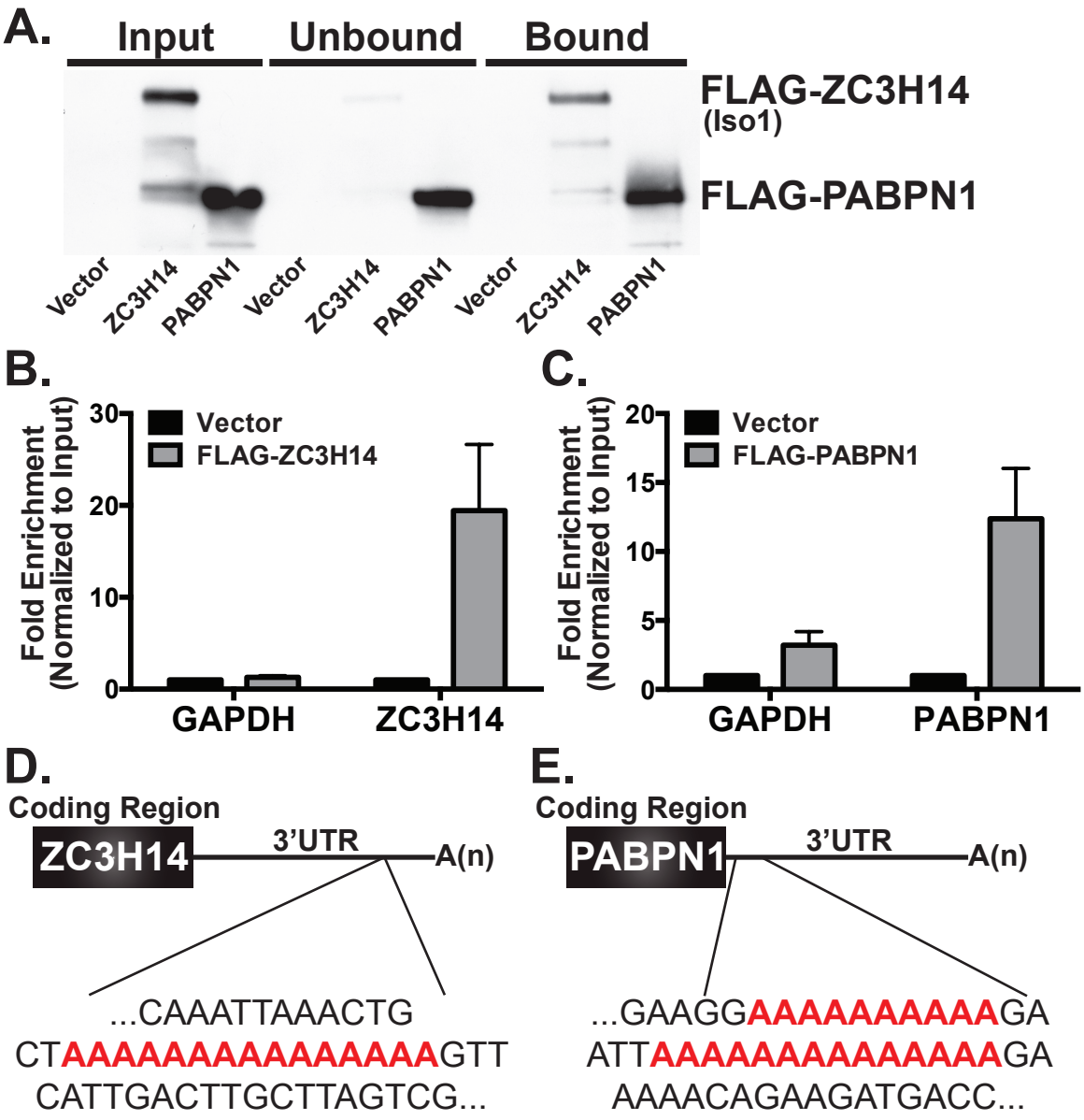

FIGURE 3.4. The nuclear Pabs ZC3H14 and PABPN1 bind their own mRNA transcripts. *A*) HeLa cells were transfected with plasmids encoding FLAG-tagged ZC3H14 Isoform 1 (Iso1), FLAG-PABPN1 or pcDNA3 (Vector control). Cells expressing vector control or FLAG-tagged proteins were subjected to RNA-IP using FLAG antibody-conjugated beads. Immunoblot analysis of IP samples demonstrates specific enrichment of FLAG-ZC3H14 Iso1 and -PABPN1 in the bound fractions. *B*) and *C*) RNA that co-precipitated with FLAG-tagged proteins was subjected to qRT-PCR analyses with *GAPDH*, *ZC3H14* and *PABPN1* primers to detect bound transcripts. *ZC3H14* and *PABPN1* transcripts were significantly enriched upon purification of their respective FLAG-tagged proteins whereas *GAPDH* mRNA did not co-precipitate with either protein. Schematics of the *ZC3H14* (*D*) and *PABPN1* (*E*) transcripts highlight (in red) the striking polyadenosine stretches located within the 3'UTRs of these mRNAs that may represent the cis-elements responsible for the self-enrichment observed in (*B*) and (*C*).

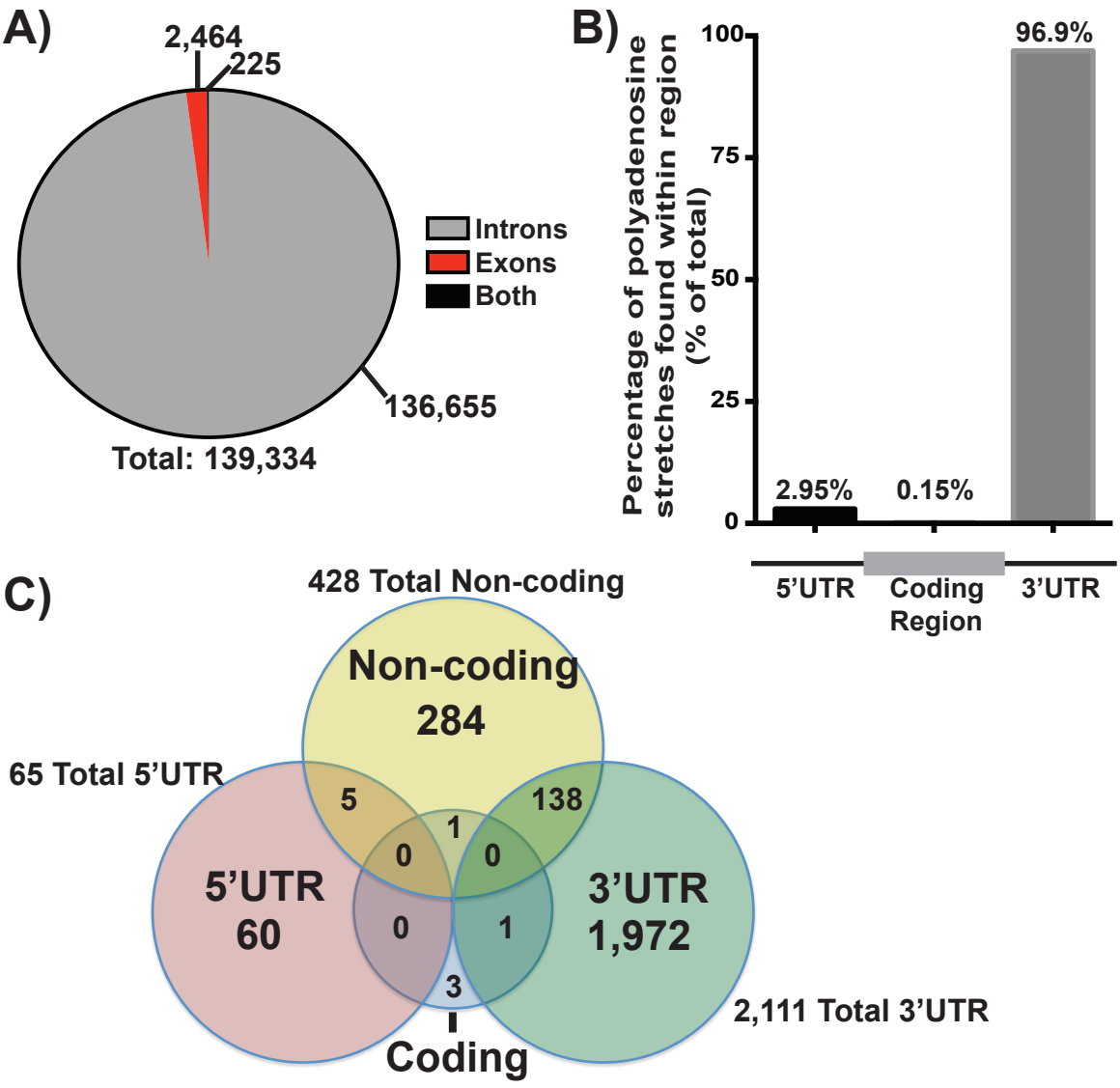

FIGURE 3.5. Prevalence and location of templated, internal polyadenosine stretches within the human transcriptome. *A*) Analysis of the human transcriptome for the frequency and enrichment of internal polyadenosine stretches containing at least 12 consecutive adenosines reveals that the vast majority (136,655 out of 139,334) of these sequences are located in the introns of mRNAs whereas a much smaller fraction are located in exonic regions (2,464 out of 139,334), which includes 5' and 3'UTR regions. A much smaller number of these internal adenosine stretches are found in sequences that can be either introns or exons as a result of alternative splice variants. *B*) Internal polyadenosine stretches found in exonic sequences are almost exclusively located in untranslated regions. Further analysis of the ≥12nt polyadenosine sequences that occur in mature mRNA transcripts reveals that almost all (99.9%) of these instances are located in the UTRs, with an extremely large percentage present in the 3'UTRs (96.9%) of mRNA transcripts. *C*) Non-coding RNAs also include templated stretches of polyadenosine. A number (428) of noncoding RNAs (yellow circle) contain templated polyadenosine sequences, suggesting that Pabs could modulate non-coding RNAs through this

templated binding site. Consistent with a model of 3'UTR regulation, a large number of the internal polyadenosine stretches identified in ncRNAs (138) are found in 3'UTRs (yellow and green overlap).

EXPERIMENTAL PROCEDURES

Cell Culture

MCF-7 cells (Human mammary adenocarcinoma; ATCC HTB-22) and HeLa cells (Human cervical adenocarcinoma; ATCC CCL-2) were obtained from ATCC and maintained in Dulbecco's modified Eagle's medium (DMEM) supplemented with 10% FBS and antibiotics. HS578 (Human mammary carcinoma), MDA-MB231 (Human mammary adenocarcinoma), MDA-MB468 (Human mammary adenocarcinoma) and T47D (Human mammary ductal carcinoma) cells were a generous gift from the Vertino laboratory at the Winship Cancer Institute at Emory University and were maintained in Dulbecco's modified Eagle's medium (DMEM) supplemented with 10% FBS and antibiotics. DNA plasmids were transfected into cultured cells using Lipofectamine2000 (Invitrogen) according to manufacturer's protocol.

Plasmids and Chemicals

FLAG fusion constructs were generated using PCR primers that include the FLAG sequence to create N-terminally FLAG-tagged proteins. PCR products were then purified and subcloned into the pcDNA3.1 vector (Invitrogen). MCF-7 cells were transfected with 1.0 μg FLAG constructs 24 hours after seeding and collected 24 hours later. Primers used throughout the study are shown in Table 3.1.

Immunoblotting

Cells were harvested and washed in 1X PBS and then lysed on ice in RIPA-2 buffer (150 mM NaCl, 1% NP40, 0.5% deoxycholate, 0.1% SDS, 50 mM Tris pH 8.0) containing protease inhibitors (PLAC: 3 μg/ml of pepstatin, leupeptin, aprotinin, and chymostatin and 0.5 mM PMSF). Immunoblotting was performed using standard methods (327). Briefly, 30 μg of total protein lysate per sample was resolved by SDS-PAGE and transferred onto a nitrocellulose membrane. For immunoblotting, a 1:5,000 dilution of rabbit polyclonal ZC3H14 (154) or Tubulin (Sigma; Clone DM1A) antibody, a 1:1,000 dilution of HuR (Santa Cruz; Clone 3A2), FLAG (Santa Cruz; OctA, Rabbit polyclonal), ER alpha (Santa Cruz; HC-20, rabbit polyclonal) or ZC3H14 Isoform 4-specific (Bethyl Laboratories; Rabbit monoclonal, custom) antibody was used followed by 1:3,000 dilutions of HRP-conjugated goat anti-mouse IgG or HRP-conjugated goat anti-rabbit IgG secondary antibodies (Jackson ImmunoResearch).

RNA Isolation

Total RNA was isolated from cells using TRIzol reagent (Invitrogen) in accordance with the manufacturer's instructions. Reverse transcriptase reactions with M-MLV RT (Invitrogen) used 1 μg of RNA for a final concentration of 50 ng/μL cDNA per sample that was used for quantitative RT-PCR.

Quantitative RT-PCR

For qRT-PCR analyses, 1 μg of total RNA was transcribed to cDNA as described above. Relative mRNA levels were measured by quantitative PCR analysis of triplicate samples of 5 ng cDNA with QuantiTect SYBR Green Master Mix using an Applied Biosystems real time machine (ABI). Results were analyzed using the ΔΔCT method (328) and normalized to the *18s rRNA*, *RPLP0*, or *GAPDH* transcript. Statistical significance was determined using a student's t-test or one-way ANOVA. A list of primers used for these analyses is shown in Table 3.1.

Estrogen Time Course

MCF-7 cells were trypsinized and resuspended in phenol red-free DMEM (Invitrogen) containing 3% charcoal-stripped FBS (csFBS; Sigma). After 48 hours in hormone-free media, media containing 10 nM E2 (100 μM stock in DMSO) or 1 μL/mL DMSO (vehicle) was added to the cells. Cells were collected at 0, 1, 3, 9, 15 and 24 hours after drug addition and subjected to RNA isolation and qRT-PCR analysis as described above.

RNA-Immunoprecipitation

To detect FLAG-ZC3H14 or -PABPN1/mRNA interactions, HeLa cells were grown to near confluency in 100-mm plates and transfected with pcDNA3, FLAG-ZC3H14 Iso1, or –PABPN1 plasmids. After 24 hours, cells were rinsed and collected

with ice cold PBS. Lysates were prepared with an equal pellet volume of polysome lysis buffer (PLB; 10 mM HEPES pH 7.0, 100 mM KCl, 5 mM MgCl2, 0.5% NP-40, 1 mM DTT, RNase OUT [Invitrogen], and 1 cOmplete protease inhibitor tablet [Roche]) and stored at -80°C. FLAG-M2 magnetic beads (Sigma) were resuspended in supplemented NT2 buffer (50 mM Tris-HCl, pH 7.4, 150 mM NaCl, 1 mM $MgCl_2$, 0.05% NP-40) supplemented with RNase OUT (Invitrogen) and 1 mM DTT. Thawed and clarified cell lysates were added and the bead-antibody-cell lysate mixture was incubated at 4°C for 4 hours while tumbling end over end. After incubation, beads were magnetized and washed 5 times with cold NT2 buffer. FLAG-ZC3H14 and -PABPN1/mRNA complexes were eluted with excess FLAG peptide (Sigma) and bound RNA was isolated with TRIzol (Invitrogen) and purified according to manufacturer's instructions.

Polyadenosine Motif Discovery and Location Analysis

To obtain sequences for the full human transcriptome, we used the "getfasta" function in the Bedtools program suite (http://bedtools.readthedocs.org/en/latest/index.html) to extract FASTA sequences for all annotated human transcripts from a full human genome FASTA file. Both the genome.fa and transcriptome reference were obtained from the UCSC HG19 genome annotation (http://hgdownload.cse.ucsc.edu/downloads.html). To identify polyadenosine stretches, we used the "fimo" function in the Meme motif discovery suite (http://meme.nbcr.net/meme/) to interrogate the full human transcriptome with a 12-adenosine search motif compatible with the Meme minimal motif format. After filtering

out near-matches and merging overlapping motifs, we used a custom script to cross-reference every identified motif with the HG19 refGene.txt transcript annotation and identified each motif with the following descriptors: exon or intron; and 5' UTR, Coding region, 3' UTR or noncoding transcript. Before quantifying descriptor metadata, we avoided duplication by merging annotated poly-A instances occurring at identical genomic locations but in multiple transcripts into a single annotation. Descriptor numbers were obtained using the command line "grep" functionality on the final merged dataset.

Chapter 4: Post-transcriptional Regulation of *PDCD4* mRNA by the RNA binding proteins HuR and TIA1

This chapter is adapted from the following published work:

Wigington, C.P., Jung, J., Rye, E.A., Belauret, S.L., Philpot, A.M., Feng, Y., Santangelo, P.J. and Corbett, A.H. (2014) *The Journal of Biological Chemistry* E-pub ahead of print. "Post-transcriptional Regulation of Programmed Cell Death 4 (*PDCD4*) mRNA by the RNA Binding Proteins Human Antigen R (HuR) and T-cell Intracellular Antigen 1 (TIA1)."

Imaging analyses were performed by Jeenah Jung in the Santangelo lab at Georgia Tech.

INTRODUCTION

Post-transcriptional processing events are critical to ensure the proper gene expression profile of a cell. These events include the capping, splicing, 3' end processing, export from the nucleus, translation and eventual decay of an mRNA transcript in the cytoplasm (8). A myriad of RNA binding proteins and noncoding RNAs, such as micro RNAs (miRNAs), mediate these post-transcriptional events and are, therefore, key factors in modulating gene expression (330,331). Highlighting the importance of these events, there are a growing number of examples in which the dysregulation of RNA binding proteins or miRNAs and, in turn, the post-transcriptional processing events they mediate are associated with various types of cancer (284-286). The 3' untranslated region (UTR) of an mRNA transcript is the site of binding and regulation for many post-transcriptional factors. The AU-Rich Element Binding Proteins represent one class of RNA binding proteins that mediate their post-transcriptional function by binding to AU- or U-rich RNA elements (AREs) located primarily within the 3′UTRs of target mRNAs. This protein family which includes the mRNA stability factor, Human antigen R (HuR), and the translational repressor, T-cell Intracellular Antigen 1 (TIA1), plays a role in the post-transcriptional regulation of a number of biologically important mRNAs (239,255,355).

HuR is the ubiquitously expressed member of the Embryonic Lethal Abnormal Vision (ELAV) family of RNA binding proteins (203). Two N-terminal RNA Recognition Motifs (RRMs) within HuR mediate recognition of AREs located primarily

within the 3′UTR of target mRNA transcripts (206,249). A third RRM in the C-terminus of HuR has affinity for polyadenosine RNA and is thought to bind to the poly(A) tail of target mRNAs (204,205). A majority of HuR localizes to the nucleus at steady-state but can shuttle out of the nucleus when the cell experiences stress such as oxidative stress (208) or transcriptional inhibition (207). For the majority of HuR target transcripts, association with HuR in the cytoplasm leads to increased stability of the HuR-bound target mRNA, ultimately resulting in an increase in the steady-state protein level (209). In addition to this conventional role of HuR in stabilizing mRNAs, recent work has revealed that HuR can positively regulate the translation of target transcripts without affecting their stability (263,356), or even repress the expression of target transcripts via cooperative interactions with the miRNA machinery (217). Together these studies reveal a complex role for HuR in the post-transcriptional processing of target mRNAs. Further adding to this complexity is the observation that HuR interacts with other AU- or U-rich element RNA binding proteins, both cooperatively (220) and competitively (357), to fine-tune the expression of target transcripts.

TIA1 is an RRM-containing RNA binding protein that modulates the splicing and translation of target mRNAs (192,226). TIA1 contains three tandem RRMs at the N-terminus of the protein followed by a glutamine-rich C-terminal domain (229). RRM2 of TIA1 has specificity for U-rich RNA and mediates high affinity binding to intronic and 3′UTR regions of target mRNAs (230,231). TIA1 is present in both the nucleus and the cytoplasm and can shuttle between the two compartments (232,236). Similar to HuR, TIA1 localization shifts toward the cytoplasm upon transcriptional inhibition (236).

During oxidative stress, TIA1 binding to the 3′UTR of target transcripts promotes the formation and sorting of translationally incompetent preinitiation complexes into stress granules, resulting in translational repression (237).

Recent transcriptome-wide analyses of both HuR and TIA1 binding reveal a large number of candidate mRNA targets that could be bound and regulated by these RNA binding proteins (224,225,231,248,249). These studies suggest HuR binding to approximately 10% of the transcriptome, specifically within the 3′UTRs and introns of these candidate target transcripts. Further analyses of these sequencing studies reveal a robust preference of HuR for U-rich sequences, which challenges the previously held belief that HuR is an exclusively AU-rich RNA binding protein (224,225,248,249). Secondary structural predictions of the candidate HuR binding sites suggest a preference for single-stranded RNA for binding to HuR, specifically within the context of a loop (249,358). A recent TIA1 iCLIP study reveals a high degree of TIA1 binding to U-rich regions found within the 3′UTRs of target transcripts (231). The observation that HuR and TIA1 both bind preferentially to U-rich 3′UTR regions suggest that these two proteins may coordinately regulate a number of target mRNAs.

These transcriptome-wide studies validate many well-characterized HuR targets, including the cell cycle regulators, cyclin A, B1, D1 and E1 (213,359,360), p53 (356,361) and Estrogen Receptor α (ERα) (361) transcripts. Recently, a number of apoptotic factors whose transcripts are bound by HuR have been identified including Prothymosin α (263), Cytochrome C (220), Bcl-2 and Mcl-1 (264). Interestingly, TIA1 also regulates a number

of apoptotic mRNAs including the Tumor Necrosis Factor α mRNA (TNF-α) (191,226). These studies suggest a potential role for HuR and TIA1 in coordinating the apoptotic program (264).

Among the biologically important targets of HuR and TIA1 are several putative cancer-relevant targets. One such transcript identified in transcriptome-wide analyses is the novel tumor suppressor, Programmed Cell Death 4 (*PDCD4*). The PDCD4 protein binds to and inhibits the activity of the eukaryotic translation initiation factor 4A (eIF4A) (362), which is an RNA helicase that is responsible for unwinding the secondary structure in the 5′UTRs of translating mRNAs (363). Reduction of PDCD4 protein levels, which is observed in a number of cancer types (270), results in an increase in protein production and increased tumor promotion (362,364). The finding that PDCD4 is a key regulator of global translational levels suggests that PDCD4 is likely regulated by multiple factors. The oncomiR, *miR-21*, which is overexpressed in almost all cancer types examined (365), is a well-defined regulator of *PDCD4* that functions by binding to the 3′UTR of the *PDCD4* transcript and reducing PDCD4 protein levels (271,272). Furthermore, *PDCD4* expression is regulated at the transcriptional (366,367) and post-translational levels (270,368,369). The recent transcriptome-wide sequencing studies on HuR and TIA1 described above suggest that the *PDCD4* transcript may be a target of these proteins; therefore, an additional mode of regulation could modulate PDCD4 protein levels.

In this study, we extensively characterized the *PDCD4* transcript as a novel target of HuR and TIA1 in a breast cancer cell line, MCF-7 (326). In addition to RNA-

immunoprecipitation (RNA-IP) with HuR and TIA1, we employed RNA-imaging probes deliverable to live cells (370) and proximity ligation assay (PLA) (371,372) to examine the interplay between HuR and TIA1 on the *PDCD4* transcripts with single-interaction sensitivity on a per cell basis. Contrary to previous studies that describe a cooperative relationship between HuR and TIA1 in binding to RNA (220), we observe a competitive interaction between HuR and TIA1 on the *PDCD4* transcript in the cytoplasm. Analysis of the nuclear and cytoplasmic pools of *PDCD4* mRNA reveals a significantly more stable population of PDCD4 mRNA in the cytoplasm compared to the nucleus. Knockdown of HuR and/or TIA1 results in a steady-state decrease of *PDCD4* mRNA and protein levels, supporting a role for these factors in positively regulating *PDCD4* mRNA levels. Together, these data present a novel and dynamic mode of regulation of *PDCD4* mRNA by multiple factors that contribute to fine-tuning the level of PDCD4 protein in breast cancer cells.

RESULTS

PDCD4 mRNA is bound and regulated by HuR in MCF-7 breast cancer cells

Recent transcriptome-wide HuR PAR-CLIP analyses in HeLa and HEK293 cells reveal novel functions and potential targets of the RNA binding protein, HuR (224,225,248,249), including a number of candidate targets with relevance to cancer. One such candidate transcript is *PDCD4*, which encodes a novel tumor suppressor that inhibits neoplastic transformation by interfering with the helicase activity of the

translation initiation factor, eIF4A (362). The *PDCD4* transcript contains multiple predicted AREs (373) within the 3′UTR that overlap with CLIP-Seq tags from independent HuR CLIP studies, suggesting that it is a candidate target of HuR.

To assess whether HuR binds to *PDCD4* mRNA in MCF-7 breast cancer cells, we performed RNA immunoprecipitation (RNA-IP) with endogenous HuR protein. As expected (Figure 4.1A), HuR protein was detected in the bound fraction when purified with HuR antibody but not with IgG control antibody. The input and bound fractions were then analyzed for the presence of bound *PDCD4* transcript using qRT-PCR. As shown in Figure 4.1B, the *PDCD4* transcript was robustly enriched with HuR pulldown. For controls, we also examined a known HuR target, Estrogen Receptor α (361) (*ERα*), as well as *GAPDH*, which is not bound by HuR (358). As expected, the *GAPDH* transcript showed no enrichment with HuR; however, the previously defined HuR target, *ERα* (361), showed enrichment. These results provide evidence that *PDCD4* mRNA is bound by HuR in MCF-7 cells.

The canonical role for HuR in the post-transcriptional regulation of target mRNA transcripts is as a positive regulator of mRNA stability (209), however, recent studies also reveal a role for HuR in modulating mRNA translation (220,263,356) as well as negatively regulating the expression of target transcripts via cooperative interactions with the miRNA machinery (217). To determine whether transient modulation of HuR levels has an impact on *PDCD4* steady-state mRNA or protein levels, we performed siRNA-mediated knockdown of HuR in MCF-7 cells. As shown in Figure 4.1C, immunoblotting

revealed a robust knockdown of HuR with HuR siRNA but not with scramble control siRNA. Probing these same samples with PDCD4 antibody reveals a decrease in PDCD4 protein upon HuR knockdown, but no change in a control protein, Heat Shock Protein 90 (HSP90). Quantification of PDCD4 steady-state protein levels upon HuR knockdown confirmed a significant decrease in PDCD4 protein levels (Figure 4.1C, quantification below representative blot).

To assess whether a change in mRNA transcript levels could underlie the observed decrease in PDCD4 protein levels, we examined RNA isolated from cells transfected with HuR siRNA. qRT-PCR analyses of these samples revealed a significant decrease in *PDCD4* steady-state mRNA levels upon HuR knockdown (Figure 4.1D). Together these results demonstrate that HuR binds to the *PDCD4* transcript in breast cancer cells and plays a role in regulating steady-state *PDCD4* mRNA and protein levels.

HuR RRMs 1 and 2 are required for *PDCD4* binding

The HuR protein contains three RRMs (Figure 4.2A). The two N-terminal RRMs are critical for ARE recognition while the third RRM is thought to recognize polyadenosine sequences (204,205). The crystal structure of RRMs 1 and 2 (residues 18-186) of HuR in complex with an AUUUUUUAUUUU RNA oligomer (PDB # 4ED5) (206) is shown in Figure 4.2A. While RRM1 is the primary ARE recognition domain within HuR, the conformational change that takes place upon RNA binding leads to additional interactions between RRM2 and the target mRNA, ultimately increasing RNA

binding affinity (206). This structure, along with other studies investigating the structural basis of HuR-RNA interactions (374), reveals a number of key residues that are predicted to be important for high affinity RNA binding by HuR (206,374).

To define specific residues within RRM1 and 2 that are critical for HuR binding to target RNA, we focused on three of the residues (asparagine 21 [N21], tyrosine 109 [Y109] and arginine 147 [R147]) shown *in vitro* to be critical for RNA binding (374). We changed each of these residues to alanine in an N-terminally FLAG-tagged HuR expression vector to create a FLAG-HuR binding mutant, which we term FLAG-HuR(BM). To ensure that FLAG-HuR(BM) is expressed at comparable levels to the wild type FLAG-HuR, we transfected MCF-7 cells with the FLAG-HuR and -HuR(BM) constructs and analyzed expression by immunoblotting for HuR (Figure 4.2B). HuR antibody detects both endogenous HuR (lower band) and FLAG-tagged HuR protein (upper band). The steady-state level of FLAG-HuR protein is comparable for HuR and HuR(BM), demonstrating that the amino acid changes within the RRM do not significantly impact the steady-state level of HuR protein. Importantly, the localization of HuR(BM) is also indistinguishable from HuR(WT) as assessed by indirect immunofluorescence (Figure 4.2C).

To test whether the residues altered in HuR(BM) are critical for HuR binding to ARE-containing target mRNA, we expressed FLAG-HuR and -HuR(BM) in MCF-7 cells and subjected these cell lysates to RNA-IP analysis. To ensure specific purification of FLAG-tagged HuR, we performed the RNA-IP with FLAG antibody-conjugated protein

A beads. As shown in Figure 4.2D, we achieved robust purification of both FLAG-HuR and -HuR(BM) with no purification of the untagged, endogenous HuR protein. To identify RNA transcripts that co-purify with the FLAG-tagged HuR proteins, qRT-PCR analysis was performed (Figure 4.2E). As expected, the well-studied HuR target, *ERα* (361), was robustly enriched upon purification of FLAG-HuR. Significantly reduced enrichment of the *ERα* transcript was detected with FLAG-HuR(BM) as compared to WT FLAG-HuR, providing the first evidence that these key residues within HuR RRM1 and RRM2 are important for interaction with HuR target RNA in cells and demonstrating the utility of this mutant for validating ARE-containing HuR target RNAs. As expected, the negative control transcript, *RPLP0*, did not enrich with either FLAG-HuR or -HuR(BM).

We next exploited the HuR(BM) to assess whether *PDCD4* binding depends on HuR RRMs 1 and 2, as established for the ARE-containing *ERα* transcript. We analyzed *PDCD4* mRNA enrichment with both FLAG-HuR and -HuR(BM). Consistent with the results from the endogenous HuR RNA-IP, we observed robust enrichment of the *PDCD4* transcript upon purification of wild type HuR. In contrast, no significant enrichment of *PDCD4* was detected in the HuR binding mutant sample. The loss of enrichment of the *ERα* and *PDCD4* transcripts with FLAG-HuR(BM) demonstrate that *PDCD4* binding to HuR is similar to that of the classical ARE-containing target, *ERα*.

HuR binds to two distinct regions within the *PDCD4* 3′UTR

Previous CLIP-Seq studies examining HuR binding across the transcriptome reveal that HuR binds primarily within the 3′UTRs and introns of mRNAs (224,225,248,249). Additional preliminary data from these CLIP-Seq studies show that the 3′UTR of the PDCD4 transcript contains multiple AU- and U-rich stretches that could be bound by HuR (224,225,248,249). The UCSC Genome Browser defines the *PDCD4* 3′UTR as being 1,918 nt long; however, data from poly(A)-Seq analyses in various human tissues suggest that an evolutionarily conserved upstream polyadenylation site may be used for 3′ end processing of the *PDCD4* transcript, resulting in a 3′UTR of approximately 672 nt. To determine the precise length of the *PDCD4* 3′UTR in MCF-7 cells, we performed 3′ RACE analysis using primers specific to the *PDCD4* 3′UTR. The *GAPDH* 3′UTR was used as a control. To define the size of the *PDCD4* 3′UTR in two other human cancer cell lines, we also performed 3′ RACE analyses using cDNA from HeLa (cervical adenocarcinoma; ATCC CCL-2) and MDA-MB-231 (mammary adenocarcinoma; ATCC HTB-26) cells. As shown in Figure 4.3A and verified by sequence analysis, the 3′UTR of *PDCD4* is 672 nucleotides in all cell types analyzed. These results focus our analysis of post-transcriptional regulation of *PDCD4* on the 672 nt 3′UTR present in MCF-7 cells.

To determine whether HuR binds to the 3′UTR of *PDCD4*, we generated a biotinylated RNA probe that corresponds to the 672 nt region of the *PDCD4* 3′UTR. For controls, we employed the *c-Myc* 3′UTR, which is a well-defined target of HuR (203) and the *GAPDH* 3′UTR, which is not a HuR target (Figure 4.3B). The biotinylated probes were incubated with MCF-7 cell lysates, precipitated with neutravidin-coated beads, and

then subjected to immunoblot analysis with HuR antibody to detect HuR bound to the probes. As shown in Figure 4.3C, HuR protein was readily detected in the input fractions, verifying the presence of HuR protein in these cell lysates. We detected robust HuR binding to the full-length *PDCD4* 3′UTR probe, suggesting that HuR binds the 3′UTR of *PDCD4*. As expected, we detected HuR protein bound to the *c-Myc* 3′UTR probe but not samples without a probe or with the negative control *GAPDH* 3'UTR probe. We also tested biotinylated probes that correspond to the 5'UTR and coding region of the *PDCD4* transcript in this assay. Consistent with preliminary data that suggests binding of HuR to the *PDCD4* 3'UTR specifically, we did not detect co-precipitation of HuR upon pulldown with the *PDCD4* 5'UTR and coding region probes (data not shown). These results confirm that HuR binds to the 3′UTR of *PDCD4* mRNA.

To define specific regions of the *PDCD4* 3′UTR that confer HuR binding, we generated a set of biotinylated probes that correspond to the first 290 and final 382 nucleotides of the *PDCD4* 3′UTR (5′290 and Δ290 probes, respectively; Figure 4.3B). As shown in Figure 4.3C, we detected robust HuR binding to the 5′290 probe. We did not, however, detect binding of HuR to the Δ290 probe, suggesting that HuR binds specifically to the 5′290 nucleotides of the *PDCD4* 3′UTR. Interestingly, the 5′290 nucleotides of the *PDCD4* 3′UTR contain multiple AU- and U-rich stretches that could be bound by HuR (373). To determine whether HuR binds to one or more of these stretches, we generated additional biotinylated probes that correspond to 100 or 90 nucleotide regions of the *PDCD4* 5′290 3′UTR region (Figure 4.3B; Probes A, B and C). We detected robust binding of HuR to the first two 100 nucleotide regions of the *PDCD4*

3′UTR, but not to the third 90 nucleotides (Figure 4.3C). These results show two distinct HuR binding sites within the first 200 nucleotides of the *PDCD4* 3′UTR.

RNA imaging probes can be used to visualize *PDCD4* mRNA in live cells

Recent studies demonstrate the ability to accurately visualize RNA granules and RNA-protein interactions at a single molecule level in live cells (370,371,375). To detect HuR-*PDCD4* interactions in MCF-7 cells, we designed four imaging probes that target four different sequences in the *PDCD4* 3′UTR, avoiding the defined HuR binding sites (HuR BS) (Figure 4.4A). To determine probe specificity, we delivered each probe, labeled with Cy3b fluorophores, along with the other three probes labeled with Dylight 650 fluorophores. For example, in order to examine the specificity of probe 1, probe 1 was labeled with Cy3b while probes 2, 3, and 4 were labeled with Dylight 650 (Figure 4.4B). Therefore, colocalization of probe 1 with the other three probes would suggest specificity of probe 1 in targeting the *PDCD4* 3′UTR.

For each probe, three images were obtained for analysis and colocalization was quantified by Mander's coefficient. The mean Mander's coefficients for probes 1-3 were greater than 0.8 and were not statistically different from one another ($p>0.9$), suggesting good colocalization. Probes 1-3 overlapped well with the other probes, as shown in the intensity profile of the representative mRNA punctae (Figure 4.4B). However, the mean Mander's coefficient for probe 4 was 0.6 and was significantly less than the other three probes ($p<0.009$). Generally, probe 4 did not overlap well with the other probes as shown

in the intensity profile (Figure 4.4B). Where the probe signal was bright, the signal of the other probes was dim or vice versa. Thus, probe 4 was deemed non-specific and was not used for further analysis and probes 1-3 were employed in all experiments. These results suggest that probes 1-3 specifically recognize the *PDCD4* 3′UTR and allow us to visualize *PDCD4* RNA granules in MCF-7 cells.

Proximity ligation assay can detect HuR-*PDCD4* mRNA interactions

To visualize HuR protein-*PDCD4* mRNA interactions in MCF-7 cells, we performed proximity ligation assay (PLA) between HuR and the FLAG peptides on the *PDCD4* RNA probes. As schematized in Figure 4.4C, primary antibodies of different species bind to HuR and the FLAG tag (mouse and rabbit, respectively), which can then be detected by species-specific PLA probes with oligonucleotides. The oligonucleotides attached to the PLA probe form a circularized DNA strand by enzymatic ligation, one of which can serve as a primer for rolling circle amplification. This amplification ultimately results in a coiled single-stranded DNA, or the PLA product, which is complementary to the circular DNA strand. The PLA product is then detected by hybridizing complementary fluorophore-labeled oligonucleotides (Figure 4.4C) (371,372).

Due to the cell permeabilization and probe delivery conditions, this PLA assay specifically detects cytoplasmic protein-RNA interactions. Previous work demonstrates that the steady-state localization of HuR in MCF-7 cells is primarily nuclear with a small amount located in the cytoplasm due to nucleocytoplasmic shuttling of HuR (359). To

increase the cytoplasmic pool of HuR for analysis in the PLA assays, cells were treated with the transcriptional inhibitor, Actinomycin D (ActD), which increases the cytoplasmic localization of HuR (212). To confirm the steady-state nuclear localization of HuR in these cells as well as the cytoplasmic enrichment of HuR upon ActD treatment, we performed nucleocytoplasmic fractionation of MCF-7 cells subjected to a 90 minute treatment with vehicle control (PBS) or ActD. As shown in Figure 4.4D, fractionation of vehicle treated cells confirms that the majority of HuR protein is localized to the nucleus (compare lanes 1 and 3). Treatment with ActD results in an increase in the amount of HuR detected in the cytoplasm (Figure 4.4D, compare lanes 2 and 4). Thus treatment of MCF-7 cells with ActD increases the cytoplasmic pool of HuR.

As shown in Figure 4.4E, we observe endogenous HuR-*PDCD4* interactions by PLA in untransfected and untreated cells (top row; quantified in Figure 4.4G), which supports the HuR-*PDCD4* binding data obtained from both RNA-IP (Figures 4.1 and 2) and biotin pulldown analyses (Figure 4.3). As expected, we observed no PLA signal in cells incubated with negative control probes lacking FLAG tags (NA; Figure 4.4E). To validate the interaction of HuR with the *PDCD4* transcript, we also modulated both HuR levels and localization and assessed the impact on PLA signal. These experiments were carried out either in cells expressing endogenous HuR or where total levels of HuR were increased by expression of HuR-GFP. To assess changes in the frequency of HuR-*PDCD4* mRNA interactions, we counted the number of HuR-*PDCD4* PLA punctae and normalized to the amount of mRNA in each cell, which was quantified by measuring the volume of probe signal for each cell. The probe volume was the same in both

untransfected and HuR-GFP transfected cells with ($p=0.16$) and without ($p=0.26$) ActD (Figure 4.4F). This analysis confirms that the probe delivery and binding as well as the amount of RNA granules are not significantly affected by transfection. As expected for treatment with a transcriptional inhibitor, incubation of cells with ActD reduced the total volume of PDCD4 mRNA by approximately 40% ($p<0.001$; quantified in Figure 4.4F).

Treatment with ActD resulted in significantly more HuR-*PDCD4* PLA punctae than untreated cells due to increased cytoplasmic HuR in both untransfected ($p<0.02$) and HuR-GFP transfected cells ($p<0.001$; quantified in Figure 4.4G). As experiments employed a low amount of HuR-GFP plasmid (0.8 μg) for transfection, HuR-GFP-transfected cells not treated with ActD showed only a slight increase in PLA frequency compared to the untransfected samples ($p=0.046$). As demonstrated above, addition of ActD caused HuR to localize to the cytoplasm and resulted in a greater increase in HuR-*PDCD4* interactions in the HuR-GFP transfected cells than in untransfected cells ($p<0.001$). These results demonstrate individual HuR-*PDCD4* interactions in MCF-7 cells and further validate the interaction between HuR and the *PDCD4* transcript.

Cytoplasmic *PDCD4* mRNA is regulated differently than nuclear *PDCD4* mRNA

As mentioned above, canonically, HuR binding to target mRNAs results in increased transcript stability (209). In fact, many HuR target mRNAs are inherently labile and responsive to cellular stimuli (158,376). As shown in Figure 4.1C and D, knockdown of HuR in MCF-7 cells results in decreased steady-state *PDCD4* mRNA and protein

levels, suggesting that HuR could positively regulate the stability of the *PDCD4* transcript. To determine the half-life of the *PDCD4* transcript in MCF-7 cells, we treated cells with the potent transcriptional inhibitor, ActD (156), and collected cells at 30 minutes, 2, 4, 6 and 8 hours after drug addition. We performed qRT-PCR analysis with *PDCD4* primers to determine the percent mRNA remaining over time following ActD treatment (Figure 4.5A). For controls, we also analyzed the *c-Myc* transcript, which has a short half-life (376) as well as the very stable *RPLP0* transcript (377). As shown in Figure 4.5A, the *PDCD4* transcript showed significant decay over the course of the experiment, with a calculated half-life of ~6.1 hours, which is less than the average mRNA half-life of ~9 hours (378). These results suggest that the *PDCD4* transcript is labile. As expected, the *c-Myc* transcript levels decreased dramatically after ActD treatment with a calculated half-life of ~1.6 hours, which is comparable to previously determined *c-Myc* mRNA half-life values (376). The *RPLP0* transcript decayed a very small amount over the time course examined as expected for a highly stable transcript.

Immunoblot analysis of protein samples isolated across the ActD time course reveals a sharp decrease in PDCD4 steady-state protein levels upon ActD treatment (Figure 4.5B, lanes 6-10), but not vehicle control-treated cells (lanes 1-5). The observed decrease in PDCD4 protein levels is consistent with previous work that demonstrates activation (by phosphorylation of serine 70) of S6K1, the kinase responsible for phosphorylation and subsequent degradation of PDCD4 (368), upon treatment with Actinomycin D (379). As expected, the steady-state levels of Tubulin and HuR are unchanged across the time course of ActD treatment.

The observation that HuR interacts with *PDCD4* mRNA in the cytoplasm (Figure 4.4E) as well as the fact that cytoplasmic HuR protein levels increase upon ActD treatment (Figure 4.4D) led us to question whether there may be differential regulation of the nuclear and cytoplasmic pools of *PDCD4* mRNA. To isolate nuclear and cytoplasmic fractions from MCF-7 cells treated with ActD (or vehicle control), we performed cellular fractionation as described in Experimental Procedures and collected nuclear and cytoplasmic fractions at 30 minutes, 3, 6 and 8 hours after drug treatment. Immunoblot analysis of fractionated cells reveals robust and clean fractionation of nuclear and cytoplasmic compartments as evidenced by distinct partitioning of steady-state nuclear (HuR) and cytoplasmic proteins (HSP90). As shown in Figure 4.5C, we observe cytoplasmic localization of PDCD4, consistent with its role in translational regulation (362,363). As expected, HSP90 levels remain unchanged in control and ActD-treated cells. Consistent with the results obtained from total cellular protein levels upon ActD treatment (Figure 4.5B), we observe a decrease in PDCD4 protein levels upon ActD treatment in the cytoplasmic fractions.

As previously shown (Figure 4.4D), the steady-state level of HuR protein increases in the cytoplasm upon ActD treatment with no change in the vehicle control-treated cells (Figure 4.5C). Immunoblot analysis of another RNA binding protein that shuttles between the nucleus and cytoplasm and shifts in localization upon ActD treatment (236), TIA1, reveals a sharp decrease in steady-state nuclear protein levels with a concomitant increase in cytoplasmic levels. Interestingly, in these cells, the shift to

cytoplasmic localization for TIA1 may occur faster than HuR as evidenced by increased cytoplasmic levels of TIA1 at 30 minutes of ActD exposure (as compared to vehicle control-treated cells at 30 minutes).

To identify any differences in mRNA decay profiles between nuclear and cytoplasmic pools of mRNA, we performed qRT-PCR analysis of RNA isolated from each compartment with primers to detect *β-actin*, *c-Myc* and *PDCD4* transcripts (Figure 4.5D-F). The highly stable *β-actin* transcript (380) and the extremely labile *c-Myc* transcript (376), both previously defined targets of HuR (203,205,217,254), display similar decay profiles between the nuclear and cytoplasmic compartments (Figures 4.5D and E, respectively). The *PDCD4* transcript, however, displays a striking difference in mRNA decay between the nucleus and cytoplasm. As shown in Figure 4.5F, the cytoplasmic pool of *PDCD4* mRNA is significantly more stable than the nuclear pool, coincident with changes in the localization of RNA binding proteins (Figure 4.5C) that may regulate this critically important transcript. These results suggest that *PDCD4* mRNA may be regulated in a unique manner than other HuR target mRNAs.

The U-rich element RNA binding protein, TIA1, binds to *PDCD4* mRNA in MCF-7 cells

The observation that the cytoplasmic pool of *PDCD4* mRNA is significantly more stable than nuclear *PDCD4* mRNA (Figure 4.5F) coupled with the shift in localization that occurs for many RNA binding proteins, including two U-rich element binding

proteins, HuR and TIA1 (Figure 4.5C), led us to hypothesize that other factors may bind to and modulate the *PDCD4* transcript via the 3'UTR. One well-studied mode of regulation of the *PDCD4* transcript occurs via an interaction between *miR-21* and the *PDCD4* 3'UTR, which negatively regulates cellular PDCD4 levels (271,272). Recent advances in sequencing technology have allowed for extensive characterization of candidate mRNA targets of many RNA binding proteins. As shown in Figure 4.6A, alignment of iCLIP-Seq tags from a recent transcriptome-wide TIA1 iCLIP study in HeLa cells (231) reveals two predicted TIA1 binding sites that overlap with the 3′UTR regions bound by HuR (Figure 4.3C). These observations suggest that HuR and TIA1 could bind to similar or overlapping regions in the *PDCD4* 3′UTR. Interestingly, previous work has defined a cooperative relationship between HuR and TIA1 in regulating the translation of specific target RNAs (220) and therefore provides precedence for interactions and/or competition between these two RNA binding proteins on target mRNAs.

To assess whether TIA1 binds to *PDCD4* mRNA in MCF-7 cells, we performed RNA-IP with endogenous TIA1 protein. As shown in Figure 4.6B, TIA1 protein was detected in the bound fraction when purified with TIA1 antibody but not with IgG control antibody. The input and bound fractions were then analyzed for *PDCD4* transcript using qRT-PCR. As shown in Figure 4.6C, the *PDCD4* transcript was robustly enriched with TIA1. For controls, we also examined two known TIA1 targets, Cytochrome c (*CYCS*) (220) and Prothymosin α (*PTMA*) (263), as well as *GAPDH*, which is not bound by TIA1. As expected, the *GAPDH* transcript showed no enrichment with TIA1, however,

the previously defined TIA1 targets, *CYCS* and *PTMA*, demonstrated significant enrichment. These results confirm that *PDCD4* mRNA is bound by TIA1 in MCF-7 cells.

To further validate the interaction between TIA1 and *PDCD4* mRNA, we performed PLA between TIA1 and the FLAG-tagged probes designed for the *PDCD4* 3'UTR (see Figure 4.4A) with and without TIA1-GFP transfection (Figure 4.6D). As shown in Figure 4.6E, we observed no significant difference in the amount of mRNA probes under any of the experimental conditions employed ($p=0.855$), suggesting that probe delivery and binding was not affected by TIA1-GFP transfection. TIA1-*PDCD4* mRNA interactions were observed by PLA with endogenous TIA1 and, as expected, a significant increase in TIA1-*PDCD4* interactions was observed by PLA upon increasing TIA1 levels via transfection of TIA1-GFP ($p<0.001$), which demonstrates specific interaction between TIA1 and *PDCD4* mRNA in these cells (Figure 4.6F).

Given that the probes bind in this region and that we are able to detect TIA1 interactions readily via PLA, it is likely that TIA1 binds within the first ~200 nt of the 3'UTR, in a similar region to where we map HuR binding (Figure 4.3C). These results suggest that TIA1 represents another factor that binds to the *PDCD4* transcript and could play a role in regulating PDCD4 steady-state levels.

Knockdown of HuR and/or TIA1 decreases steady-state *PDCD4* mRNA and protein levels

Both binding and PLA studies reveal interactions between HuR and TIA1 with the *PDCD4* transcript. As shown in Figure 4.1C and D, we observe a significant decrease in steady-state *PDCD4* mRNA and protein levels upon knockdown of HuR in MCF-7 cells. To determine whether TIA1 also has an effect on PDCD4 steady-state levels, we transiently transfected MCF-7 cells with siRNA targeting TIA1. We also transfected a population of cells with HuR and TIA1 siRNA together to determine whether reduction of both factors had any additional effect on PDCD4 steady-state levels. As shown in Figure 4.7A, we achieve robust knockdown of HuR and TIA1 (alone and in tandem) in these cells. Upon knockdown of HuR and/or TIA1, PDCD4 steady-state protein levels are reduced ~30-40% (quantification below the representative blot). As expected, a control protein, HSP90, displays no difference in steady-state levels across all treatment groups. qRT-PCR analysis of RNA isolated from HuR and TIA1 knockdown samples with primers to *PDCD4* and *RPLP0* revealed a significant reduction of *PDCD4* steady-state mRNA levels (Figure 4.7B), consistent with the trend observed at the protein level (Figure 4.7A).

As discussed previously, *miR-21* is a well-studied regulator of *PDCD4* levels in MCF-7 cells (272). Recent work has described a role for HuR in modulating miRNA loading onto target transcripts (193,217) as well a potential role for HuR in miRNA biogenesis (224,225,381). To determine whether HuR and/or TIA1 knockdown impacts steady-state *miR-21* levels in these cells, we performed qRT-PCR analysis with primers to detect *miR-21* as well as a control small ncRNA, *RNU48* (382). As shown in Figure 4.7C, knockdown of HuR and/or TIA1 did not alter steady-state *miR-21* levels; however,

this finding does not exclude the possibility that HuR and/or TIA1 could modulate the loading of *miR-21* onto the *PDCD4* transcript.

The best-characterized role of TIA1 in post-transcriptional processing is that of a negative regulator of translation (191). Although we observe a decrease in both the steady-state mRNA and protein level of *PDCD4* upon TIA1 knockdown, we questioned whether TIA1 or HuR could also modulate translation of the *PDCD4* transcript. To assess the translational profile of *PDCD4* mRNA upon knockdown of TIA1 and/or HuR, we performed polysome profiling on MCF-7 cytoplasmic lysates via sucrose gradient fractionation. Cytoplasmic lysates were either untreated (N.T.) or treated with EDTA (+EDTA) to ensure the identity of the polysomes. Analysis was also performed for cells treated with scramble control siRNA or siRNA targeting HuR, TIA1 or both. Total RNA isolated from each fraction was used for cDNA generation and subsequent qRT-PCR analysis with *PDCD4* and *GAPDH* primers. The percent distribution of *PDCD4* mRNA in each fraction was determined and plotted as shown in Figure 4.7D. Untreated MCF-7 cells display a *PDCD4* polysome profile characteristic of an actively translated mRNA, such as *GAPDH* (218), as indicated by a sharp peak in Fraction 8, which corresponds with the polysomes (assessed by A_{254} absorbance, data not shown). As expected, treatment of cytoplasmic lysates with EDTA disrupted polysomes and resulted in a striking leftward shift on the profile (Figure 4.7D).

As expected, polysome profiling of the actively translated mRNA, *GAPDH*, upon HuR and/or TIA knockdown reveals no difference in the translational profile of this

message (Figure 4.7E). As shown in Figure 4.7F, analysis of *PDCD4* translation across the same treatment groups also reveals no significant difference in *PDCD4* translational profile in these cells. Together these data support a role for HuR and TIA1 in positively regulating *PDCD4* mRNA levels.

HuR and TIA1 compete for binding to *PDCD4* mRNA

We have demonstrated by various methods that both HuR and TIA1 bind the *PDCD4* transcript in MCF-7 cells. We also show that knockdown of HuR and/or TIA1 results in a steady-state decrease in *PDCD4* mRNA and protein levels. However, we also observe a very interesting and seemingly dynamic mode of regulation of the *PDCD4* transcript, specifically in the cytoplasm. To assess whether HuR and TIA1 cooperate or compete for binding to the *PDCD4* transcript in the cytoplasm, we modulated the levels of TIA1 or HuR in MCF-7 cells and analyzed HuR-*PDCD4* interactions using PLA (Figure 4.8A-C). No difference in the probe volume was observed between the treatment groups ($p=0.12$; data not shown), demonstrating that probe delivery and binding as well as the level of *PDCD4* mRNA were not affected by transfection. As expected, upon reduction of HuR, HuR-*PDCD4* interactions decreased significantly ($p<0.001$; quantified in Figure 4.8C). A similar decrease in HuR-*PDCD4* interactions was observed upon overexpression of TIA1 through transfection of TIA1-GFP ($p<0.001$). In contrast, knockdown of TIA1 resulted in increased HuR-*PDCD4* interactions comparable to HuR-GFP transfected cells ($p=0.76$). These results suggest that increasing TIA1 may prevent HuR from binding to the *PDCD4* 3′UTR, while decreasing TIA1 facilitates HuR-*PDCD4*

interactions (Figure 4.8A-C), which suggests a competitive relationship between HuR and TIA1 for binding to the *PDCD4* 3′UTR.

To determine whether changing HuR levels affects TIA1-*PDCD4* interactions, we modulated HuR by siRNA or HuR-GFP transfection and assessed TIA1-*PDCD4* PLA values. Again, we found no difference in the probe volume between different transfection groups ($p=0.21$; data not shown), indicating that probe delivery and binding as well as the level of *PDCD4* mRNA were not affected by transfection. As expected, knockdown and overexpression of TIA1 resulted in decreased and increased, respectively, TIA1-*PDCD4* PLA interactions (Figure 4.8D, F). Consistent with our model where HuR and TIA1 compete for binding to *PDCD4*, upon reduction of HuR, we observed an increase in TIA1 binding to *PDCD4* mRNA ($p<0.001$; Figure 4.8D, F). In contrast, overexpression of HuR did not have a significant effect on TIA1 binding to *PDCD4* ($p=0.21$), but the level of HuR overexpression was quite modest (Figure 4.8D-F). These results suggest that the *PDCD4* transcript is competitively bound by HuR and TIA1 (schematized in Figure 4.8G) and therefore may be regulated in a different manner than a previously described target mRNA that is cooperatively regulated by HuR and TIA1 (220).

DISCUSSION

In this study, we identified the *PDCD4* mRNA transcript as a novel target of the RNA binding proteins, HuR and TIA1. Our results show that HuR binds to the *PDCD4* transcript via at least two distinct binding sites within the 3′UTR that overlap with TIA1

binding sites identified by CLIP-Seq (231). We demonstrate binding of TIA1 to the *PDCD4* transcript and also show that modulation of TIA1 levels regulates HuR-*PDCD4* interactions in MCF-7 cells, suggesting a competitive interaction between HuR and TIA1 on the *PDCD4* transcript in the cytoplasm, specifically via the *PDCD4* 3'UTR. Nucleocytoplasmic fractionation reveals a significantly more stable pool of *PDCD4* mRNA in the cytoplasm compared with the nucleus, suggesting that these pools of *PDCD4* mRNA are regulated in a distinct manner. Knockdown of HuR and/or TIA1 results in significant reduction of *PDCD4* mRNA, supporting a role for these factors in positively regulating *PDCD4* mRNA levels. This work as well as recent studies implicating HuR and TIA1 as dynamic and coordinate regulators of target mRNA expression (195,220) suggests a novel mode of regulation of *PDCD4* by HuR and TIA1 and yields mechanistic insight into the post-transcriptional regulation of U-rich-containing mRNAs, such as *PDCD4*.

The PDCD4 protein is an inhibitor of the eIF4A helicase, which unwinds secondary structural elements located within the 5′UTR of mRNA transcripts to facilitate translation (362). PDCD4 expression is upregulated after the initiation of programmed cell death (or apoptosis) (383) and a reduction in PDCD4 protein levels leads to neoplastic transformation (384). Because of the critical role for PDCD4 as a global regulator of protein synthesis and as a tumor suppressor, *PDCD4* expression is regulated at multiple levels (270). *PDCD4* is regulated at the transcriptional level by the transcription factor, v-Myb (385) as well as by epigenetic regulation through DNA methylation (386). With regard to post-transcriptional regulation of *PDCD4*, the only

study beyond the extensive analysis of *miR-21* (271,272), examined the regulation of the *PDCD4* transcript by the splicing factor, SRSF3 (387). SRSF3 binds to the 5′UTR of the *PDCD4* transcript and modulates splicing and translational efficiency (387). The work presented here, which provides evidence for two additional RNA binding proteins that bind to and regulate the *PDCD4* transcript, expands our understanding of the post-transcriptional regulation of *PDCD4*.

Our results show that HuR binds to two independent regions within the first 200 nt of the *PDCD4* 3′UTR. The *PDCD4* 3′UTR is considerably AU- or U-rich (68% and 37%, respectively) and contains two striking U-rich stretches within the 5′290 nt region of the 3′UTR. Indeed, these two U-rich regions are found within the first 200 nt of the 3′UTR and are consistent with the mapped HuR binding sites (Figure 4.3). Preliminary secondary structure prediction analyses of the 672 nt 3′UTR of *PDCD4* predict two single-stranded U-rich motifs within the first 200 nt, suggesting that these are the motifs bound by HuR (388). The predicted binding sites of TIA1 on the *PDCD4* 3′UTR (231) overlap with the HuR binding sites and, due to the U-rich preference of TIA1, likely represent U-rich regions that are competitively bound by HuR and TIA1.

Previous studies demonstrate that competition between HuR and TIA1 for binding to 5′ splice sites regulates alternative splicing in numerous cell types (223,250,251). However, there is no precedent for competition between HuR and TIA1 that influences mRNA stability and/or translation. Employing RNA imaging probes and PLA, we detected and quantified individual interactions between native *PDCD4* mRNA and either

endogenous HuR or TIA1 in single cells *in situ*. These PLA studies (Figure 4.8) provide evidence that HuR and TIA1 compete for binding to the *PDCD4* 3′UTR. Overexpression of TIA1 reduced interactions between HuR and *PDCD4*, while knockdown of TIA1 increased HuR-*PDCD4* interactions (Figure 4.8). Similarly, knockdown of HuR increased TIA1 interactions with *PDCD4* (Figure 4.8). This competition between HuR and TIA1 could provide a way for cells to fine-tune the levels of PDCD4 to modulate programmed cell death.

While the data presented in this study suggest a model where HuR and TIA1 compete for binding to overlapping *cis*-acting sequences, other RNAs are regulated through a mechanism where these RNA binding proteins cooperate with one another. For example, post-transcriptional regulation of the *cytochrome c* gene, which encodes a key regulator of apoptosis (252), occurs through HuR and TIA1 binding to non-overlapping binding sites in the AU-rich regions within the 3′UTR (220). This study reported that HuR binding promotes the translation the *cytochrome c* mRNA without affecting mRNA levels while TIA1 binding inhibits translation (220). In contrast to the competition between HuR and TIA1 that we detect (Figure 4.8) on *PDCD4*, the study of the *cytochrome c* transcript reported that HuR and TIA1 bind cooperatively to the *cytochrome c* 3′UTR such that increasing TIA1 levels increased HuR binding; however, increasing HuR levels had no detectable effect on TIA1 binding (220). The caveat of this study, as the authors noted, is that the analysis of *cytochrome c* employed recombinant, exogenous proteins. In direct binding assays that employed RNA electrophoretic mobility shift assays, the authors did not detect simultaneous binding of HuR and TIA1 (220).

These results indicate that coordinate regulation by RNA binding proteins needs to be individually defined for each transcript. In this study, we provide evidence for overlapping binding sites for HuR and TIA1 on the *PDCD4* 3'UTR, which supports a model (Figure 4.8G) where these two factors would compete for binding and subsequent regulation of the transcript.

Although the steady-state localization of HuR and TIA1 in MCF-7 cells is predominantly nuclear (Figure 4.5C), both of these proteins shuttle in and out of the nucleus (207,208,232,236). Previous studies demonstrate that HuR and TIA1 accumulate in the cytoplasm in response to various cues, including transcriptional inhibition (207,236), creating two pools of protein that have the potential for distinct regulation of target transcripts. Consistent with this idea, nucleocytoplasmic fractionation of MCF-7 cells treated with ActD reveal a very stable pool of *PDCD4* mRNA in the cytoplasm (Figure 4.5F). Analysis of two other HuR target mRNAs (*c-Myc* and *β-actin*) (203,205,217,254), however, revealed similar decay profiles between the nucleus and cytoplasm (Figure 4.5D and E), suggesting that the *PDCD4* transcript is regulated in a specific manner. The observed stability of the *PDCD4* transcript in the cytoplasm could be indicative of a stress response due to ActD treatment. In fact, ActD treatment results in a distinct increase in cytoplasmic localization of both HuR and TIA1 (Figure 4.5C), consistent with other sources of cellular stress that result in shifts in the localization of RNA binding proteins (158). We hypothesize that the enhanced stability of the *PDCD4* transcript in the cytoplasm relative to the nucleus may be a result of the increased levels of HuR and TIA1, both of which play a role in positively regulating *PDCD4* mRNA

levels (Figure 4.7B). However, we cannot rule out that stress could trigger other changes in these cells that could influence the regulation of PDCD4.

There is precedent for post-translational modification of PDCD4 in response to various cellular cues, including methylation of PDCD4 at an N-terminal arginine residue that accelerates tumor growth (369) and promotes tumor cell viability during nutrient deprivation (389). PDCD4 is also phosphorylated at serine 67 upon activation of Akt or S6K1, which leads to significantly decreased PDCD4 protein levels via increased proteasomal degradation (368,390). We observe a rapid decrease in PDCD4 protein levels upon treatment with ActD (Figures 4.5B and C), consistent with increased activation of S6K1 (379), the kinase responsible for phosphorylation of PDCD4 at serine 67 (368). Alternatively, treatment with ActD could alter the translational profile of *PDCD4*, perhaps due to an increase in the cytoplasmic pool of the documented translational repressor, TIA1 (Figure 4.5C) (191). Although PDCD4 protein levels are rapidly degraded in these cells, we observe an underlying stable pool of PDCD4 mRNA, specifically in the cytoplasm (Figure 4.5A and F). We hypothesize that this stable population of *PDCD4* mRNA represents a pool of transcript that is readily available for translation upon extracellular cues and/or alleviation of cellular stress. This reserve would allow cells to fine-tune the expression of PDCD4 protein in response to various cellular environments. The observation that reduction of HuR and/or TIA1 results in reduced *PDCD4* mRNA and protein levels (Figure 4.7) suggests that HuR and TIA1 play a role in positively regulating steady-state *PDCD4* mRNA levels and may therefore assist in modulating the dynamic cytoplasmic pool of *PDCD4* mRNA.

Analysis of RNA regulons and the cooperation and/or competition of multiple RNA binding proteins on target mRNAs suggests a complex and dynamic post-transcriptional regulatory program (331). The observation that RNA binding proteins such as HuR interface with the miRNA machinery (216) adds additional complexity to the regulation of target mRNAs. In fact, recent studies demonstrate a competitive relationship between HuR and miRNA machinery at both the individual transcript (41,381,391-393) and transcriptome-wide (224,225) levels. The transcriptome-wide PAR-CLIP analyses that examined interplay between HuR and miRNAs suggested that transcripts with non-overlapping HuR/miRNA binding sites (such as *PDCD4*) are more likely regulated by the miRNA than by HuR (224,225). Our results demonstrate that modulation of HuR and TIA1 impacts the steady-state mRNA and protein levels of *PDCD4* and suggests a model where HuR modulates the stability of *PDCD4*. The mechanism by which HuR modulates stability is not well understood; however, recent studies demonstrate that direct competition between HuR and miRNAs can influence stability (41). Alternatively, HuR binding could influence the secondary structure of the 3'UTR to modulate miRNA binding/accessibility (216). This type of coordination is challenging to study and is therefore less understood than direct competition.

As mentioned previously, the *PDCD4* 3'UTR is a well-studied target of the oncomiR, *miR-21* (271,272), which is overexpressed in many cancer types (365) and targets the *PDCD4* transcript via a well-studied seed region within the 3′UTR (271). The *miR-21* seed region lies within the 290 nt region of the *PDCD4* 3′UTR that was identified

in a HuR iCLIP study (249). However, the *miR-21* seed region does not overlap with the HuR binding sites identified here (Figure 4.3) and is instead located more distal to the coding region (miRNA seed region designated by red asterisk in Figure 4.3B). If *miR-21* is involved in HuR-mediated regulation of *PDCD4* stability, the location of the *miR-21* binding site is more consistent with a model where HuR impacts the local RNA structure to modulate miRNA binding than direct competition.

In addition to possible modulation of *miR-21* binding, growing evidence shows that HuR binds to and regulates the processing of primary miRNA (pri-miR) transcripts (224,225,381). A recent study demonstrated HuR binding to and destabilizing *miR-7* (224), suggesting that this may represent another mode of regulation by HuR in post-transcriptional processing. Interestingly, another study identified HuR binding to the *pri-miR-21* transcript (225), which could indicate direct regulation of the *miR-21* transcript by HuR. We did not observe an effect on steady-state *miR-21* levels upon knockdown of HuR (Figure 4.7C); however, this result does not preclude the possibility that HuR may be involved in the loading of *miR-21* on to the *PDCD4* transcript. Further study is required to understand how direct interactions and feedback mechanisms between *miR-21*, as well as other miRNAs predicted to bind the *PDCD4* 3′UTR, and RNA binding proteins, such as HuR and TIA1, function coordinately to control post-transcriptional regulation of biologically important transcripts such as *PDCD4*.

An important question moving forward is how HuR and TIA1 regulate *PDCD4* mRNA and protein levels in various cellular contexts. Previous studies demonstrate that

both HuR and TIA1 can modulate the post-transcriptional processing of target transcripts in diverse ways in response to stress (158). For instance, HuR and TIA1 contribute to decreased translation of the *Cytochrome c* transcript, specifically in the context of ER stress (220). Additionally, exposure of HeLa cells to UV light results in a dramatic association between HuR and the apoptosome inhibitor, Prothymosin α mRNA, resulting in increased translation (263). These previous studies as well as others (158) support a model where HuR and TIA1 can have alternative modes of regulation on target transcripts in response to stress. Further study is required to elucidate whether HuR and TIA1 differentially modulate PDCD4 levels in various stress conditions, specifically in the context of the tumor microenvironment.

Table 4.1. Primer sequences used in this study.

Gene Name	Forward	Reverse
18s rRNA	GAGACTCTGGCATGCTAACTAG	GGACATCTAAGGGCATCACAG
RPLP0	GGGCGACCTGGAAGTCCAACT	CCCATCAGCACCACAGCCTTC
GAPDH	AAGGTCGGAGTCAACGGATTTGG	GATGACAAGCTTCCCGTTCTC
β-actin	GGACTTCGAGCAAGAGATGG	AGCACTGTGTTGGCGTACAG
c-Myc	TTCGGGTAGTGGAAAACCAGCAGC	CCGAGTCGTAGTCGAGGTCATAG TTCC
PDCD4	GACTACCAAAGAAAGGTGGTGCAG GAGG	CATAAACACAGTTCTCCTGGTCA TCATCATAGTTAGGAT
ER Alpha	TGAACCGTCCGCAGCTCAAGATC	GTCTGACCGTAGACCTGCGC GTTG
Prothymosin-α	CACCCAACCCAAACCATGAGAATT TGC	CATGGTCACACCACAAGTAAAGT CAGAAGTAG
Cytochrome C	GTTCAACTTTTCACAAAGATGGTG AGTGCC	CCTTTAAGAGGCAAATGAACATG AACACAAAACAC
HuR N21A	GACTGCAGGGGTGACATCGGGAGA ACGGCTTTGATCGTCAACTACCTCC CTCAGAACATG	CATGTTCTGAGGGAGGTAGTTGA CGATCAAAGCCGTTCTCCC GATGTCACCCCTGCAGTC
HuR Y109A	GTGATCAAAGACGCCAACTTGGCC ATCAGCGGGCTCCCGCGG	CCGCGGGAGCCCGCTGATGGCCA AGTTGGCGTCTTTGATCAC
R147A	GTCCTCGTGGATCAGACTACAGGT TTGTCCGCAGGGGTTGCGTTTATCC GGTTTGACAAA	TTTGTCAAACCGGATAAACGCAA CCCCTGCGGACAAACCTGTAGTC TGATCCACGAGGAC
3'RACE Clamp		GACGAGCTCGGATCCTGCAGTTT TTTTTTTTTTTTTTVN
Outer 3'RACE Primer		GACGAGCTCGGATCCTGCAGTTT TTT
***GAPDH* 3'RACE Primer**	CAACAGGGTGGTGGACCTCATG	
***PDCD4* 3'RACE Primer**	GAGGTCGTCTTAAACCAGAGAGCT ACTGA	

Table 4.2. Probes used to detect *PDCD4* mRNA.

Target	Ligand	Location within transcript (from start of CR)
PDCD4 3′UTR 1	5′-biotin-TXTTTT**AAGGAGXGGCAGXCAGACAXCAAU**-3′	1706-1729
PDCD4 3′UTR 2	5′-biotin-TXTTTT**AAXAAAGCUUUGUAXAAACCAGXGA**-3′	1761-1785
PDCD4 3′UTR 3	5′-biotin-TXTTTT**GUXCCAGCCACCXUUUACUXAACUG**-3′	1959-1983
PDCD4 3′UTR 4	5′-biotin-TXTTTT**ACXCCCAAXAAAGAAUCAAUACXG**-3′	2057-2080
Boldface: 2′-O-Methyl RNA; X: dT-C6-NH_2; all others are DNA; underline: binding region		

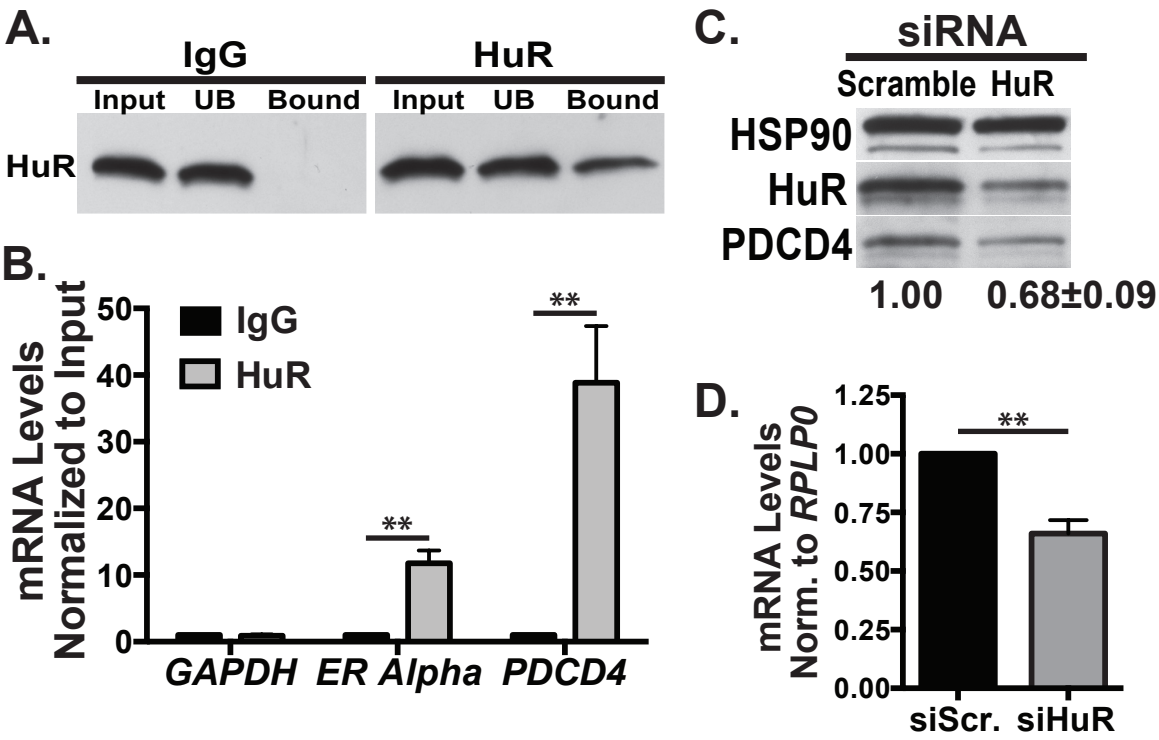

FIGURE 4.1. HuR binds to the *PDCD4* transcript and modulates steady-state *PDCD4* mRNA and protein levels in MCF-7 cells. Endogenous HuR protein was immunoprecipitated from MCF-7 cells using either HuR antibody-coated protein A beads or isotype control Mouse IgG-coated beads. *A*) Proteins from the Input, unbound (UB) and Bound fractions were resolved on an SDS-PAGE gel and subjected to immunoblotting with HuR antibody. HuR was detected in the HuR bound fraction but not the IgG bound fraction. *B*) RNA isolated from the HuR RNA-IP was subjected to qRT-PCR analyses with *GAPDH*, *ER Alpha* and *PDCD4* primers. mRNA levels in HuR bound fractions were normalized to input levels and then compared by fold-enrichment over IgG control. Significant enrichment of *ERα* and *PDCD4* transcripts was observed with HuR IP. *C*) MCF-7 cells transiently transfected with Scramble or HuR siRNA (siScr. and siHuR, respectively) were subjected to immunoblot analysis with HSP90, HuR, or PDCD4 antibody. Steady-state PDCD4 protein levels were normalized to HSP90 loading control and siScramble set to 1.00. A decrease in PDCD4 steady-state protein levels upon HuR knockdown is quantified below the representative blot. *D*) qRT-PCR analysis of total RNA isolated from siRNA-treated cells with *PDCD4* and *RPLP0* primers demonstrates a significant decrease in *PDCD4* steady-state mRNA levels upon HuR knockdown. Values represent the mean ± SEM for n=3 independent experiments. ** represents $p \leq 0.01$.

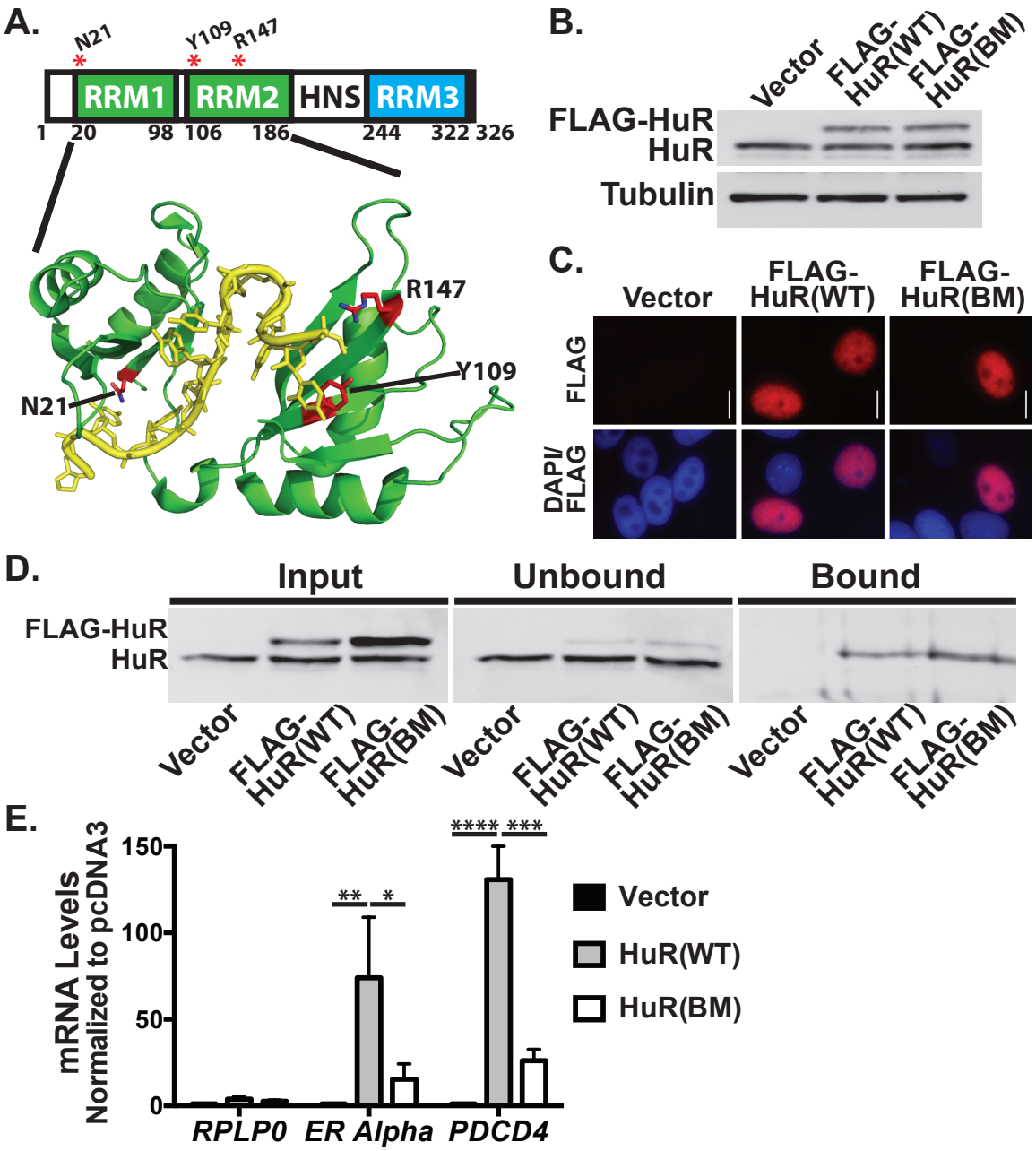

FIGURE 4.2. Key residues in HuR RRMs 1 and 2 are required for binding to ARE-containing target mRNAs, including *PDCD4*. *A*) The HuR protein contains three RRMs (RRM1, RRM2 and RRM3) and a HuR Nucleocytoplasmic Shuttling sequence (HNS), which mediates bidirectional transport of HuR between the nucleus and cytoplasm (16). The two N-terminal RRMs (green) are responsible for ARE recognition while the C-terminal RRM (blue) is thought to bind to the poly(A) tail of mRNA transcripts. Shown below the linearized map of HuR is a recently solved co-crystal structure (PDB # 4ED5) of HuR RRMs 1 and 2 (green) in complex with an AUUUUUUAUUUU RNA oligomer (yellow). Residues shown to be important for RNA recognition in in vitro binding studies are highlighted in red (N21, Y109 and R147). A putative HuR RNA binding mutant (BM) was generated by changing these residues to alanine in a FLAG-

tagged HuR expression construct. *B*) MCF-7 cells were transfected with vector control, FLAG-HuR(WT) or -HuR(BM) plasmids and subjected to immunoblotting with HuR and Tubulin antibodies. FLAG-HuR proteins were detected only in FLAG-transfected cells and levels of BM are comparable to WT. *C*) Transfected MCF-7 cells were analyzed by indirect immunofluorescence with FLAG antibody to detect FLAG-HuR(WT) or (BM). Colocalization with DAPI reveals steady-state nuclear localization of both FLAG-HuR proteins (WT and BM). Scale bar, 10 μm. *D*) Cells expressing vector control or FLAG-HuR proteins were subjected to RNA-IP using FLAG antibody-conjugated beads. Immunoblot analysis of IP samples demonstrates specific enrichment of FLAG-HuR proteins in bound fractions. *E*) RNA that co-precipitated with FLAG-HuR proteins was subjected to qRT-PCR analyses with *RPLP0*, *ER Alpha* and *PDCD4* primers to detect bound transcripts. *ER Alpha* and *PDCD4* transcripts were significant enriched upon wildtype HuR purification; however, a significant decrease in enrichment was observed upon purification of HuR binding mutant. mRNA levels in FLAG-HuR-bound fractions were normalized to input levels and then compared by fold-enrichment over vector control samples. Values represent the mean ± SEM for n=3. *, **, *** and **** represents $p \leq 0.05$, $p \leq 0.01$, $p \leq 0.001$ and $p \leq 0.0001$, respectively.

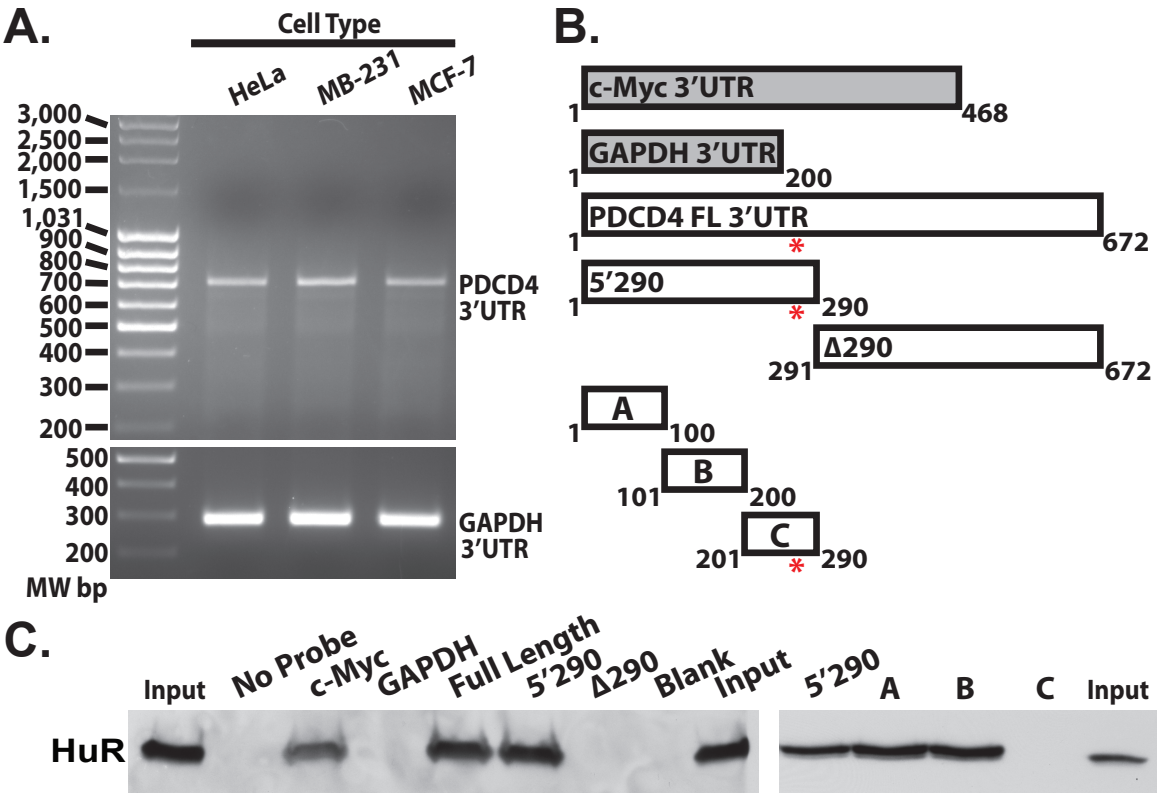

FIGURE 4.3. HuR binds to sites within the *PDCD4* 3′UTR. *A*) Total RNA isolated from HeLa, MB-231 and MCF-7 cells was subjected to 3′RACE analysis using *PDCD4* and *GAPDH* 3′UTR-specific primers as described in Materials and Methods. PCR products were resolved on a 2% agarose gel and represent the 3′UTR plus the length of the primers used for amplification. The *PDCD4* 3′UTR is 672 nt and was verified by sequencing. The *GAPDH* 3′UTR is shown as a control. Molecular weight markers in base pairs (MW bp) are shown to the left of the gel. *B*) Biotinylated probes corresponding to the 3′UTRs of the *c-Myc*, *GAPDH* and *PDCD4* transcripts were generated and used for biotin pulldown experiments in MCF-7 cells. The red asterisk denotes the well-defined *miR-21* seed region (46) in the *PDCD4* 3'UTR. The *PDCD4* 3'UTR was also dissected to generate various biotin probes that represent different regions of the transcript. *C*) Proteins that co-precipitated with the avidin-bound biotinylated probes, as shown in (*B*), were subjected to immunoblotting with HuR antibody. HuR protein co-precipitates with a probe corresponding to the *c-Myc* 3′UTR as well as the first two 100 nt regions of the *PDCD4* 3′UTR. Images are representative of n=3 independent experiments.

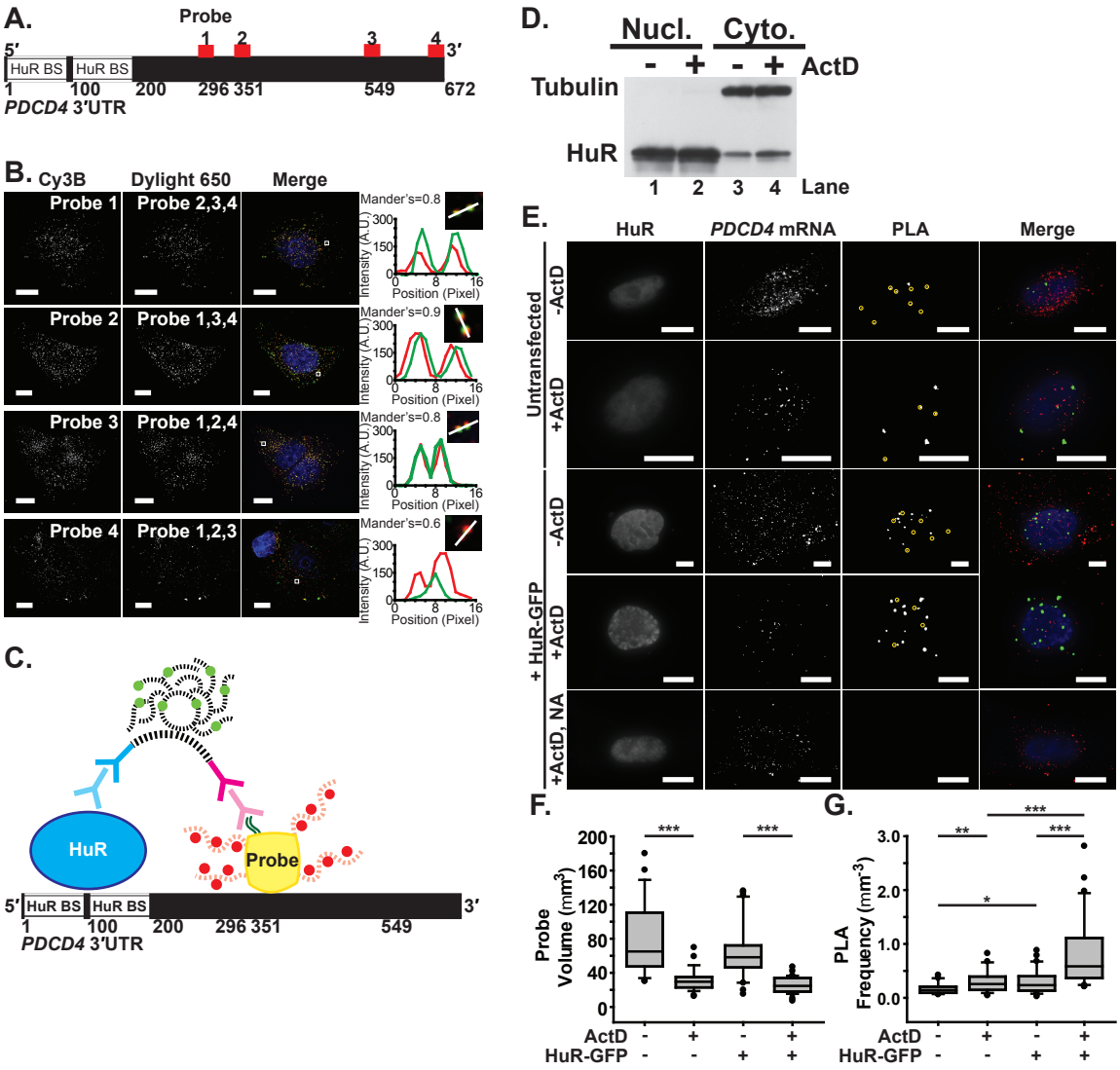

FIGURE 4.4. Visualization of HuR-*PDCD4* interactions in situ using FLAG-tagged probes. *A*) The 672 nt *PDCD4* 3′UTR contains two HuR binding sites (HuR BS) within the first 200 nt. Four mRNA probes (1, 2, 3 and 4) were designed to target distinct positions within the *PDCD4* 3′UTR (shown in red). *B*) Each of four *PDCD4* 3′UTR probes labeled with Cy3B fluorophores was delivered to MCF-7 cells along with the other three probes labeled with Dylight 650 fluorophores. Merge images of Cy3B-labeled probe (red), Dylight 650-labeled probe (green), and DAPI-stained nuclei (blue) are also shown. All image planes are represented. Magnified, merge images of overlapping probes in the boxed region are shown with profile plot of the fluorescence intensity of Cy3B (red) and Dylight 650 (green) along an intersection of the probes (white line). Scale bar, 10 μm. The mean Mander's coefficient of Cy3B and Dylight 650 probe colocalization is shown. *C*) A schematic of the proximity ligation assay (PLA), which measures the interaction between HuR and probes specific to the *PDCD4* 3′UTR is shown. As described in Experimental Procedures, PLA was performed between HuR and FLAG-tagged (dark green lines) probes with four Cy3b-labeled (red) oligonucleotides (red dash lines) and a neutravidin core (yellow) in nucleotides 296-549 of the *PDCD4*

3′UTR. Anti-HuR mouse primary antibody (light blue) and anti-mouse PLA probe (dark blue) bind to HuR, while anti-FLAG rabbit primary antibody (light magenta) and anti-rabbit PLA probe (dark magenta) bind to FLAG. Once they are in proximity, the oligonucleotides (black dash lines) attached to the PLA probe come together via ligation to form a template for DNA polymerase, which resulted in a coiled DNA product that can be labeled with Cy5-equivalent fluorophore (light green) bound complementary DNA strands (black dash lines). *D*) MCF-7 cells treated with vehicle control or Actinomycin D (ActD) for 90 minutes were subjected to subcellular fractionation (as described in Experimental Procedures) and subsequent immunoblotting with HuR and Tubulin antibody. A distinct enrichment of HuR is observed in the cytoplasm upon ActD treatment. *E*) HuR, *PDCD4* mRNA and PLA between HuR and *PDCD4* mRNA were imaged in untransfected and HuR-GFP transfected MCF-7 cells exposed to (+ActD) or unexposed to (-ActD) actinomycin D. MCF-7 cells transfected with HuR-GFP and exposed to ActD received *PDCD4* mRNA probes with neutravidin lacking the FLAG tag (NA) and were used as a negative control. PLA punctae that are less than 2μm in diameter have been marked with yellow circles. Merge images of HuR (blue), *PDCD4* mRNA (red) and PLA between HuR and *PDCD4* mRNA (green) are shown. All image planes are represented. Scale bar, 10 μm. *F*) Probe volume (μm3) measured for each untransfected and HuR-GFP transfected cell exposed or unexposed to ActD (Untransfected: n=46 cells; Untransfected, +ActD: n=125; HuR-GFP transfected: n=51; HuR-GFP transfected, +ActD: n=62). *G*) PLA frequency normalized to the probe volume (μm-3) for each cell. * represents $p \geq 0.025$, $p < 0.05$; ** represents $p > 0.001$, $p < 0.025$; *** represents $p < 0.001$ (one-way ANOVA with Dunn's method).

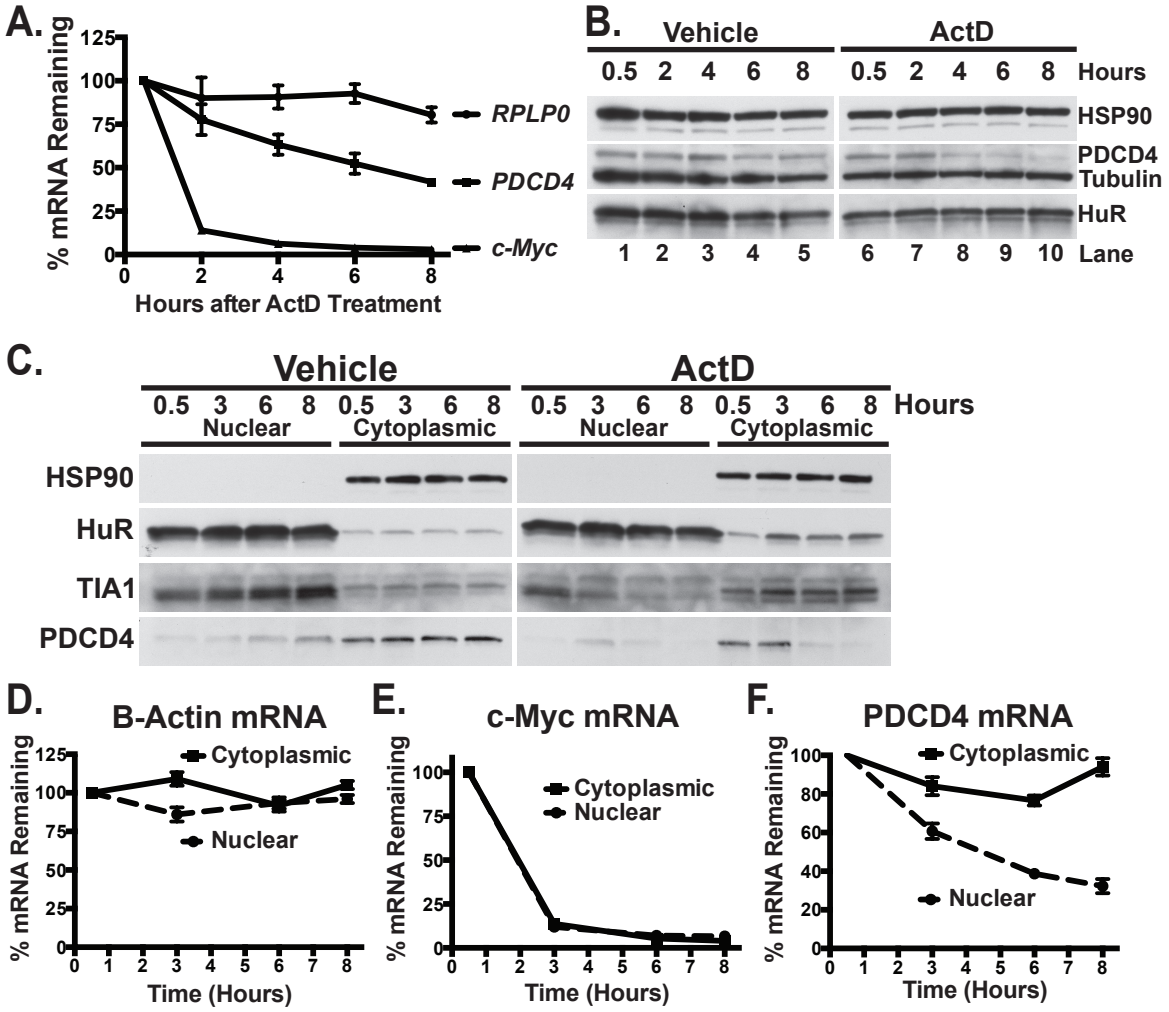

FIGURE 4.5. The cytoplasmic pool of *PDCD4* mRNA is highly stable compared to the nuclear pool. *A*) MCF-7 cells were treated with ActD and collected at the indicated time points after drug addition. Total RNA isolated from ActD-treated cells was subjected to qRT-PCR analysis with *RPLP0*, *PDCD4* and *c-Myc* primers. mRNA levels are represented as % of amount present at 30 minutes of ActD exposure. The half-life of the *c-Myc* and *PDCD4* transcripts was calculated to be 1.6 and 6.1 hours, respectively. *B*) Immunoblot analysis of total protein isolated from the samples in (*A*) to detect PDCD4, HSP90, Tubulin and HuR reveal a sharp decrease in PDCD4 protein upon treatment with ActD, but not vehicle control. *C*) MCF-7 cells treated with vehicle control or ActD over the indicated time course were subjected to subcellular fractionation followed by immunoblotting with HSP90, HuR, TIA1, or PDCD4 antibody. Immunoblots reveal an accumulation of both HuR and TIA1 in the cytoplasm across the ActD time course, but no accumulation is observed during vehicle control treatment, as expected. PDCD4 is predominantly cytoplasmic in these cells and the cytoplasmic pool of PDCD4 demonstrates the robust decrease after ~3 hours of ActD treatment. RNA isolated from nuclear and cytoplasmic fractions from (*C*) were subjected to qRT-PCR analysis with *β-actin* (*D*), *c-Myc* (*E*) and *PDCD4* (*F*) primers. The decay profiles of *β-actin* and *c-Myc* mRNA are similar between the nuclear and cytoplasmic compartments (*D* and *E*), however the cytoplasmic pool of

PDCD4 mRNA displays a significantly increased decay profile compared to the nuclear pool of *PDCD4* mRNA (*F*). Ct values were normalized to *18s rRNA* and decay profiles are represented as % of amount at 30 minutes of ActD exposure. Data points represent the mean ± SEM for n=3 independent experiments. * represents $p<0.05$. Images are representative of n=3 independent experiments.

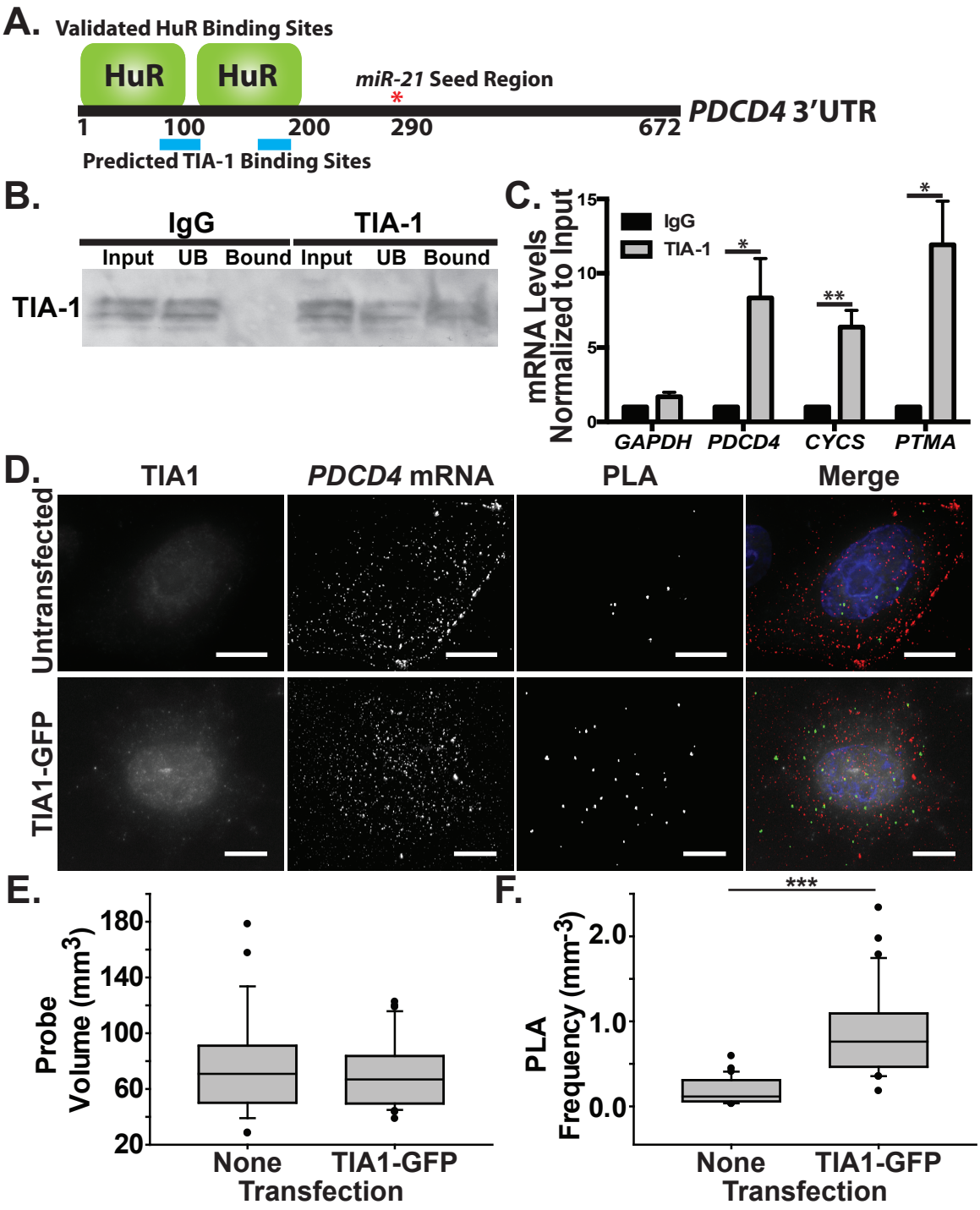

FIGURE 4.6. The RNA binding protein, TIA1, interacts with *PDCD4* mRNA. *A*) A recent TIA1 iCLIP study reveals two predicted TIA1 binding sites (shown here in blue) within the first 200 nt of the *PDCD4* 3′UTR (27) that overlap with the validated HuR binding sites (green) defined here. The red asterisk denotes the well-defined *miR-21* seed region. *B*) Endogenous TIA1 protein was immunoprecipitated from MCF-7 cells using TIA1 antibody-coated protein A beads alongside isotype control Goat IgG-coated beads.

Proteins from the Input, unbound (UB) and Bound fractions were subjected to immunoblotting with TIA1 antibody. TIA1 was detected in the TIA1-bound fraction but not the control IgG bound fraction. TIA1 is alternatively spliced to generate two distinct protein products that correspond to the two bands detected. *C*) qRT-PCR analysis of RNA isolated from the TIA1 RNA-IP using *PDCD4*, *CYCS* and *PTMA* primers reveals clear enrichment of these transcripts upon TIA1 pulldown. A control mRNA, *GAPDH*, did not co-precipitate with TIA1. Values represent the mean ± SEM for n=3 independent experiments. * and ** represent $p \leq 0.05$ and $p \leq 0.01$, respectively. *D*) PLAs performed with TIA1 antibody and *PDCD4* 3′UTR probes 1-3 reveal interactions between TIA1 and the *PDCD4* 3′UTR. Merge images of nuclei (blue), TIA1 (white), *PDCD4* mRNA (red) and PLA between TIA1 and *PDCD4* mRNA (green) are shown. All image planes are represented. Scale bar, 10 μm. *E*) Probe volume (μm3) measured for each untransfected (n=11 cells) and TIA1-GFP transfected (n=15) cell. *F*) The PLA frequency normalized to the probe volume (μm-3) for each cell. *** represents $p<0.001$ (Mann-Whitney rank sum test).

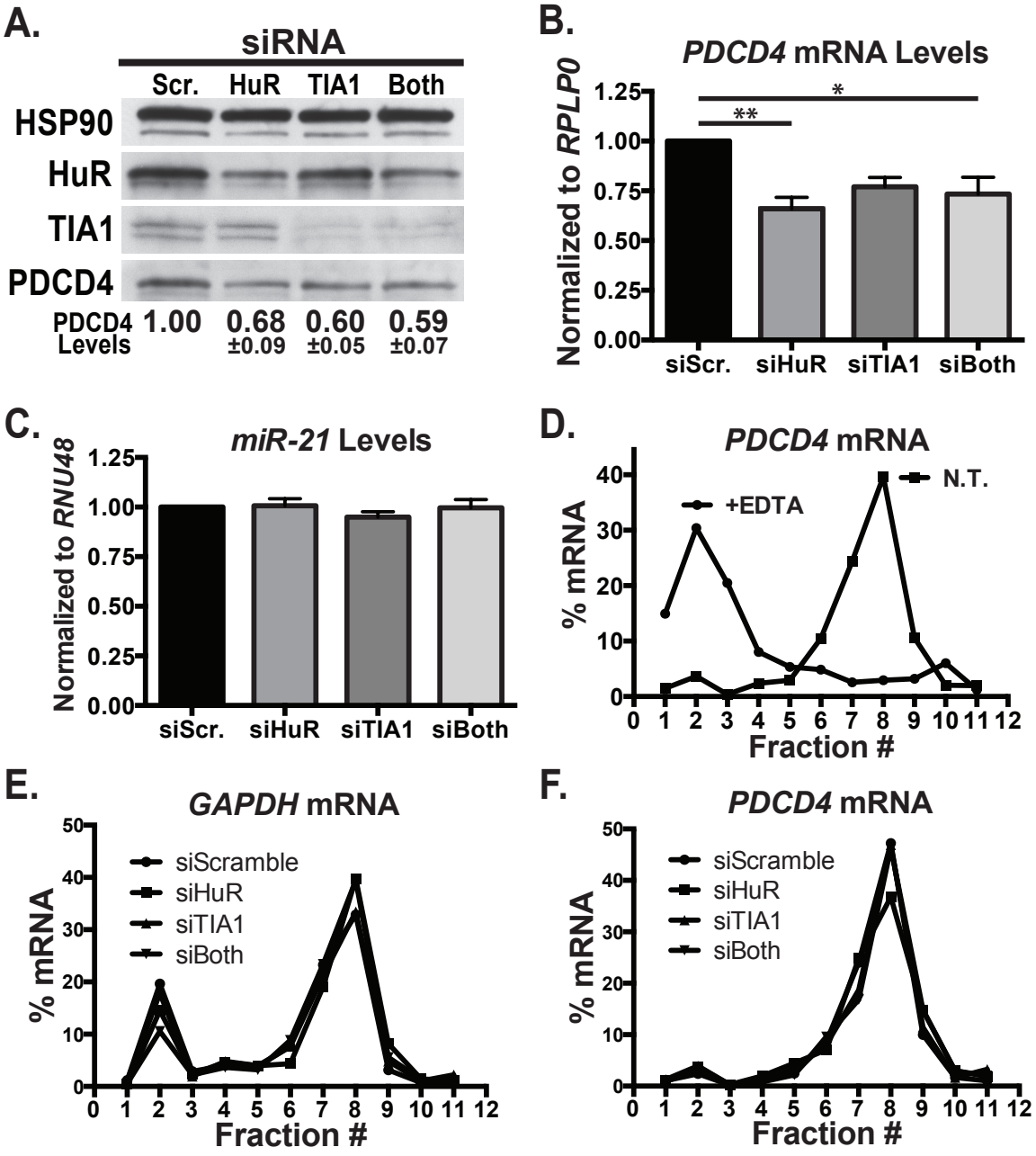

FIGURE 4.7. Knockdown of HuR and TIA1 lead to decreased *PDCD4* steady-state mRNA and protein levels. *A*) MCF-7 cells transiently transfected with Scramble, HuR and/or TIA1 siRNA (siScr., siHuR, siTIA1 and siBoth) were subjected to immunoblot analysis with HSP90, HuR, TIA1 or PDCD4 antibody. Steady-state PDCD4 protein levels were normalized to HSP90 loading control and siScramble set to 1.00. Decreased PDCD4 steady-state protein levels upon HuR and/or TIA1 knockdown is quantified below the representative blot. *B*) qRT-PCR analysis of total RNA isolated from siRNA-treated cells with *PDCD4* and *RPLP0* primers demonstrates a significant decrease in *PDCD4* steady-state mRNA levels upon HuR and/or TIA1 knockdown. *C*) qRT-PCR analysis of steady-state *miR-21* and *RNU48* (loading control) levels upon knockdown of

HuR and/or TIA1 reveals no significant difference in *miR-21* levels across all treatment groups. *D*) Polysome profiling was performed on MCF-7 cells as described in Experimental Methods. Cytoplasmic lysates from MCF-7 cells were treated with EDTA (to disrupt polyribosomes) or left untreated (No Treatment, N.T.) and subjected to polysome fractionation. Untreated MCF-7 cells demonstrate active translation of *PDCD4* mRNA (as represented by a sharp peak in fraction 8) while EDTA-treated cell lysates display a collapse of the polyribosomes on the *PDCD4* transcript, as expected. Polysome profiling was performed on MCF-7 cell lysates transfected with scramble control, HuR and/or TIA1 siRNA. Analysis of the *GAPDH* (*E*) and *PDCD4* (*F*) transcripts reveals that *PDCD4* mRNA is actively translated in MCF-7 cells, similar to *GAPDH*, and that knockdown of HuR and/or TIA1 has no effect on the translation of the *PDCD4* transcript under these conditions. Polysome profiles are representative of two technical qRT-PCR replicates of a single fractionation experiment. Values represent the mean ± SEM for n=3 independent experiments. * and ** represents $p \leq 0.05$ and $p \leq 0.01$, respectively.

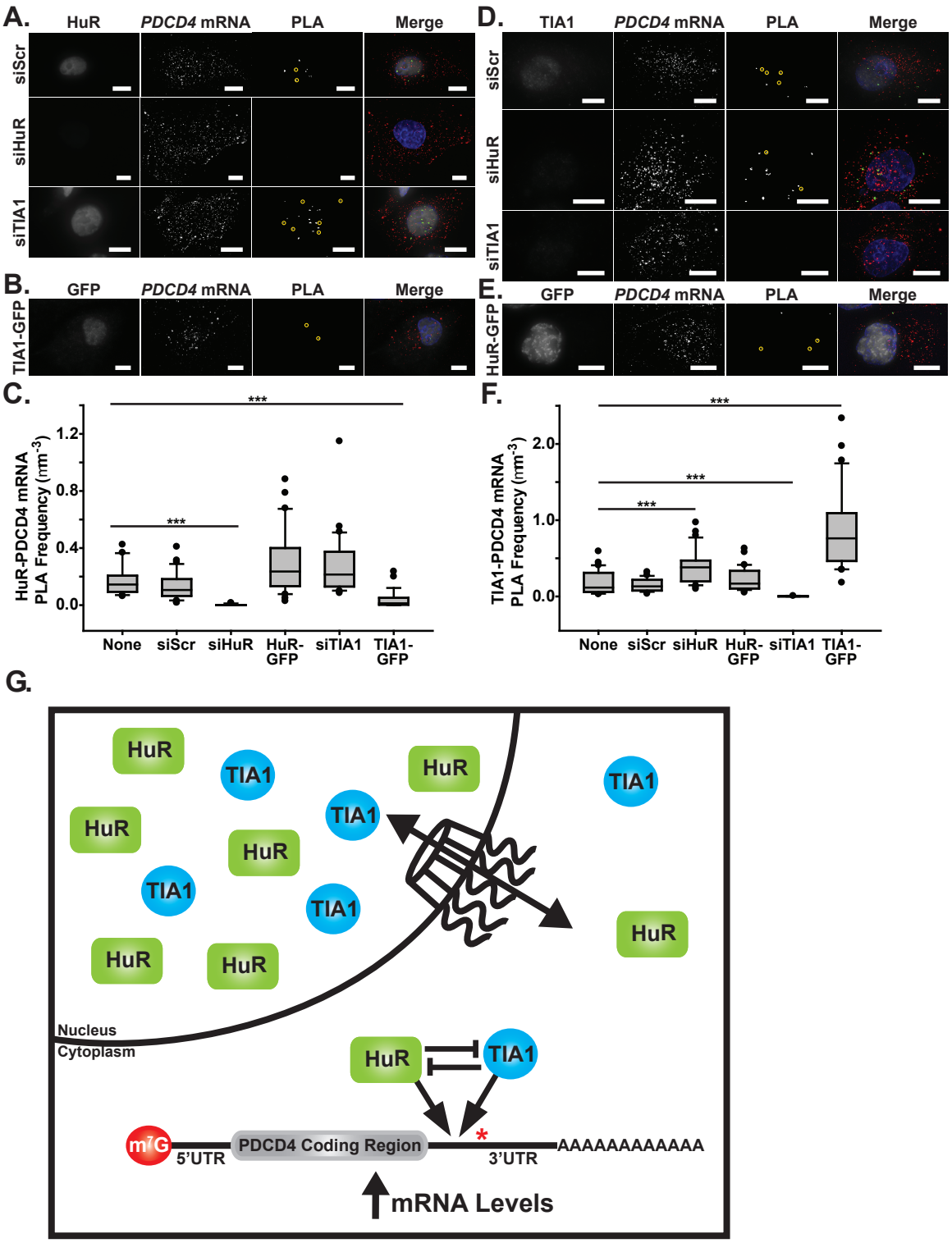
A.
HuR
PDCD4 mRNA
PLA
Merge
siScr
siHuR
siTIA1
B.
GFP
PDCD4 mRNA
PLA
Merge
TIA1-GFP
C.
HuR-PDCD4 mRNA PLA Frequency (mm-3)
1.2
0.8
0.4
0.0
***
***
None
siScr
siHuR
HuR-GFP
siTIA1
TIA1-GFP
D.
TIA1
PDCD4 mRNA
PLA
Merge
siScr
siHuR
siTIA1
E.
GFP
PDCD4 mRNA
PLA
Merge
HuR-GFP
F.
TIA1-PDCD4 mRNA PLA Frequency (mm-3)
2.0
1.0
0.0
***
***
***
None
siScr
siHuR
HuR-GFP
siTIA1
TIA1-GFP
G.
HuR
TIA1
Nucleus
Cytoplasm
m7G
5'UTR
PDCD4 Coding Region
3'UTR
AAAAAAAAAAAA
mRNA Levels

FIGURE 4.8. HuR and TIA1 compete for binding to the *PDCD4* 3′UTR. *A*) Visualization of HuR protein, *PDCD4* mRNA and interaction between HuR and *PDCD4* mRNA (PLA) in control cells transfected with scrambled siRNA (siScr), or siRNA directed against either HuR (siHuR) or TIA1 (siTIA1). Merged images of HuR (white), *PDCD4* mRNA (red), PLA (green) and nuclei (blue) are also shown. PLA punctae that are less than 2μm in diameter have been marked with yellow circles. All image planes are represented. Scale bar, 10 μm. *B*) Visualization of GFP, *PDCD4* mRNA and interaction between HuR and *PDCD4* mRNA in TIA1-GFP transfected cells. Merged images of GFP (white), *PDCD4* mRNA (red), PLA (green) and nuclei (blue) are also shown. PLA punctae that are less than 2μm in diameter have been marked with yellow circles. All image planes are represented. Scale bar, 10 μm. *C*) HuR-*PDCD4* mRNA PLA frequency normalized to probe volume (μm-3) for untransfected (n=46 cells), siScramble (n=81), siHuR (n=25), HuR-GFP (n=51), siTIA1 (n=97), and TIA1-GFP (n=69) cells. *** represents $p<0.001$ (one-way ANOVA with Dunn's method). *D*) Visualization of TIA1 protein, *PDCD4* mRNA and PLA interaction between TIA1 and *PDCD4* mRNA in siScramble (siScr), siHuR and siTIA1 transfected cells. Merged images of TIA1 (white), *PDCD4* mRNA (red), PLA (green) and nuclei (blue) are also shown. PLA punctae that are less than 2μm in diameter have been marked with yellow circles. All image planes are represented. Scale bar, 10 μm. *E*) Visualization of GFP, *PDCD4* mRNA and PLA interaction between TIA1 and *PDCD4* mRNA in HuR-GFP transfected cells. Merged images of HuR (white), *PDCD4* mRNA (red), PLA (green) and nuclei (blue) are shown. PLA punctae that are less than 2μm in diameter have been marked with yellow circles. All image planes are represented. Scale bar, 10 μm. *F*) TIA1-*PDCD4* mRNA PLA frequency normalized to probe volume (μm-3) for untransfected (n=55 cells), siScramble (n=49), siHuR (n=66), HuR-GFP (n=46), siTIA1 (n=44), and TIA1-GFP (n=76) cells. *** represents $p<0.001$ (one-way ANOVA with Dunn's method). *G*) Model for the post-transcriptional regulation of *PDCD4* mRNA in the cytoplasm. In MCF-7 cells, the steady-state localization of both HuR (green rectangle) and TIA1 (blue circle) is predominantly nuclear with a small pool that shuttles in and out of the cytoplasm (black bi-directional arrow). We observe a competitive mode of binding between HuR and TIA1 on the *PDCD4* 3'UTR in the cytoplasm, in close proximity to a well-defined *miR-21* binding site (red asterisk).

EXPERIMENTAL PROCEDURES

Cell Culture

MCF-7 cells (ATCC HTB-22; Estrogen Receptor positive [ER+] breast cancer cell line (326)) were obtained from ATCC and maintained in Dulbecco's modified Eagle's medium (DMEM) supplemented with 10% FBS and antibiotics. DNA plasmids and siRNA (Invitrogen) were transfected into cultured cells using Lipofectamine2000 (Invitrogen) or Neon Electroporation System (Invitrogen) according to manufacturer's protocol. Cells were plated on No 1.5 glass coverslips (Ted Pella) one day prior to transfection for imaging.

Plasmids and Chemicals

A FLAG fusion construct for HuR was generated using PCR primers that include the FLAG sequence, creating an N-terminally FLAG tagged protein. The PCR product was then subcloned into the pcDNA3.1 vector (Invitrogen). The HuR RNA binding mutant (HuR[BM]; N21A, Y109A, R147A) was generated by site-directed mutagenesis using the Quikchange Kit (Stratagene). Primers used throughout the study are shown in Table 1. MCF-7 cells were transfected with 0.8 μg HuR-GFP or 0.8 μg TIA1-GFP plasmid (gifts from Dr. Myriam Gorospe, NIH/NIA). mRNA-targeted probes were delivered 36 hours after plasmid transfection. A set of three pre-designed Stealth siRNAs (Assay ID numbers s4608, s4609 and s4610; Invitrogen) or 200 nM On-TARGET

SMARTPool HuR siRNA (Thermo Scientific Dharmacon) was employed for knockdown of HuR. A set of three pre-designed Stealth siRNAs (Assay ID numbers S14131, S14132 and S14133; Invitrogen) was employed for knockdown of TIA1. For control, 200 nM On-TARGETplus Non-targeting siRNA #1 (Thermo Scientific Dharmacon) was used. mRNA-targeted probes were delivered 48 hours after siRNA transfection.

Immunoblotting

MCF-7 cells were harvested and washed in 1X PBS and then lysed on ice in RIPA-2 buffer (150 mM NaCl, 1% NP40, 0.5% deoxycholate, 0.1% SDS, 50 mM Tris pH 8.0) containing protease inhibitors (PLAC: 3 μg/ml of pepstatin, leupeptin, aprotinin, and chymostatin and 0.5 mM PMSF). Immunoblotting was performed using standard methods (327). Briefly, 30 μg of total protein lysate per sample was resolved by SDS-PAGE and transferred onto a nitrocellulose membrane. For immunoblotting, a 1:1,000 dilution of HuR or TIA1 antibody (Santa Cruz; Clones 3A2 and c-20, respectively), a 1:2,000 dilution of HSP90 (Santa Cruz; Clone F-8) or PARP antibody (BD Pharmingen; Clone 4C10-5), a 1:4,000 dilution of PDCD4 antibody (Rockland; Rabbit polyclonal), or a 1:5,000 dilution of α-tubulin antibody (Sigma; Clone DM1A) was used followed by 1:3,000 dilutions of HRP-conjugated goat anti-mouse IgG, HRP-conjugated goat anti-rabbit IgG, or HRP-conjugated mouse anti-goat IgG secondary antibodies (Jackson ImmunoResearch).

RNA Isolation

Total RNA was isolated from MCF-7 cells using TRIzol reagent (Invitrogen) in accordance with the manufacturer's instructions. Reverse transcriptase reactions with M-MLV RT (Invitrogen) used 1 μg of RNA for a final concentration of 50 ng/μL cDNA per sample that was used for quantitative RT-PCR.

Isolation and enrichment of miRNAs from MCF-7 cells was performed using a miRNeasy Mini Kit (Qiagen). For reverse transcription, 10 ng of isolated RNA was used with the TaqMan miRNA RT kit (Invitrogen; *miR-21* and *RNU48* assays) according to manufacturer's instructions.

Quantitative RT-PCR

For qRT-PCR analyses, 1 μg of total RNA was transcribed to cDNA as described above. Relative mRNA levels were measured by quantitative PCR analysis of triplicate samples of 5 ng cDNA with QuantiTect SYBR Green Master Mix using an Applied Biosystems real time machine (ABI). Results were analyzed using the ΔΔCT method (328) and normalized to the *18s rRNA* or *RPLP0* transcript. Statistical significance was determined using One-way ANOVA. A list of primers used for these analyses is shown in Table 1.

miR-21 and *RNU48* levels were detected using TaqMan primers for each transcript and the TaqMan Universal PCR Master Mix, no UNG (Invitrogen). Results

were analyzed using the ΔΔCT method (328) and normalized to the *RNU48* transcript. Statistical significance was determined using One-Way ANOVA.

RNA-Immunoprecipitation

RNA-IPs to assay endogenous HuR/*PDCD4* mRNA interactions were performed using standard methods (394). Briefly, MCF-7 cells were grown to confluency in 100-mm dishes and rinsed twice with ice cold PBS. Lysates were prepared with an equal pellet volume of polysome lysis buffer (PLB; 10 mM HEPES pH 7.0, 100 mM KCl, 5 mM MgCl2, 0.5% NP-40, 1 mM DTT, RNase OUT [Invitrogen], and 1 cOmplete protease inhibitor tablet [Roche]) and stored at -80°C. Protein A sepharose beads (Santa Cruz) were incubated at 4°C overnight with either mouse IgG or HuR antibody (Santa Cruz). Beads coated in antibody were resuspended in NT2 buffer (50 mM Tris-HCl, pH 7.4, 150 mM NaCl, 1 mM $MgCl_2$, 0.05% NP-40) supplemented with RNase OUT (Invitrogen) and 1 mM DTT. Thawed and clarified cell lysates were added and the bead-antibody-cell lysate mixture was incubated at 4°C for 2 hours while tumbling end over end. After incubation, beads were spun down and washed 5 times with cold NT2 buffer. The bound RNA was isolated with TRIzol (Invitrogen) and purified according to manufacturer's instructions.

To detect FLAG-HuR/*PDCD4* mRNA interactions, MCF-7 cells were grown to near confluency in 100-mm plates and transfected with pcDNA3, FLAG-HuR, or -HuR(BM) plasmids. After 48 hours, cell lysates were prepared and frozen as described

above. FLAG-M2 magnetic beads (Sigma) were resuspended in supplemented NT2 buffer described above. Thawed and clarified cell lysates were added to beads and incubated at 4°C for 2 hours while tumbling end over end. After incubation, beads were magnetized and washed 5 times with cold NT2 buffer. FLAG-HuR/RNA complexes were eluted with excess FLAG peptide (Sigma) and bound RNA was isolated with TRIzol (Invitrogen) and purified according to manufacturer's instructions.

Immunofluorescence

Prior to visualization by indirect immunofluorescence, MCF-7 cells were fixed with 1-2% formaldehyde (EM Science) for 10 min, permeabilized with 0.1%Triton X-100 for 5 min, and incubated with Hoechst or DAPI (Invitrogen) to mark the position of the nucleus. To localize endogenous HuR, FLAG-HuR, or HuR-GFP by immunofluorescence, cells were probed with mouse monoclonal anti-HuR (1:1,000; 3A2, Santa Cruz) or mouse monoclonal anti-FLAG (1:1,000; M2, Sigma), or goat polyclonal anti-GFP (1:500; ab5450, Abcam) antibody followed by staining with Texas Red or Fluorescein-conjugated secondary antibodies (Jackson ImmunoResearch). For immunostaining endogenous TIA1 or TIA1-GFP, cells were probed with polyclonal rabbit anti-TIA1 (1:500; AV40981, Sigma) or anti-GFP (1:500; ab5450, Abcam) antibody followed by staining with Cy3 or Fluorescein-conjugated secondary antibody (Jackson ImmunoResearch). Images were obtained using an Olympus IX81 microscope with a 0.3 numerical aperture (NA) 100× Zeiss Plan-Neofluor objective or an Axiovert 200 M microscope (Zeiss) with a 1.4 NA 63× Plan-Apochromat objective unless

otherwise stated. Images were captured using a Hamamatsu digital camera with Slidebook software (version 1.63) or Volocity acquisition software (PerkinElmer) and globally processed for brightness and contrast using Adobe Photoshop.

3′ Rapid Amplification of cDNA Ends (RACE)

To determine the precise length of the *PDCD4* 3′UTR in human cell lines, we isolated RNA from HeLa (ATCC CCL-2), MDA-MB-231 (ATCC HTB-26) and MCF-7 (ATCC HTB-22) cells using TRIzol reagent (Invitrogen) in accordance with the manufacturer's instructions. Reverse transcriptase reactions were carried out as follows: 1 μg of RNA was combined with 1 μL of dNTPs (10 mM), 1 μL of the 3′RACE adaptor (See Table 1; 10 mM) and DEPC-treated water for a total volume of 13 μL. Samples were incubated at 65^{o}C for 5 minutes and then transferred to ice. To the RNA mixture-3′RACE adaptor mixture, 4 μL 5X First-Strand buffer (Invitrogen), 1 μL 0.1 M DTT and 1 μL RNaseOUT (40 U/μL; Invitrogen) were added. Samples were incubated at 42^{o}C for 2 minutes before adding 1 uL SuperScript III RT (200 U/μL; Invitrogen), briefly vortexing, and returning to 42^{o}C for 50 minutes. Following first strand synthesis, samples were heated to 70^{o}C for 15 minutes to denature the RT enzyme. For each PCR reaction, 40 ng of cDNA was used along with the outer 3′RACE primer and a gene-specific inner primer (see Table 1) with the AmpliTaq Gold 360 Master Mix (Invitrogen), according to manufacturer's instructions. PCR products were resolved on a 2% agarose gel and confirmed by TOPO cloning (Invitrogen) and sequencing.

Biotin Pulldown

To assess direct binding of HuR to the *PDCD4* transcript, DNA sequences corresponding to the 3′UTRs of *c-Myc* and *GAPDH* as well as various regions of the *PDCD4* 3′UTR (full length, 5′290, Δ290, 1-100, 101-200, and 201-290) were amplified by PCR and inserted into pGEM T-easy vectors (Promega) and linearized by digestion with *SpeI* (New England Biolabs). Biotinylated RNA probes were generated by *in vitro* transcription using the T7 Maxiscript kit (Ambion) with Biotin-11-cytidine-5′-triphosphate (biotin-11-CTP; Roche). Biotinylated CTP and normal CTP were used at a ratio of 1:4 to ensure adequate transcription yield and sufficient labeling. Nonincorporated nucleotides were removed with a G-25 column (GE Healthcare Bio-Sciences) followed by ethanol precipitation. RNA concentration was determined by A260 absorption and the quality was examined by denatured RNA electrophoresis. MCF-7 cells were lysed in IP buffer (50 mM Tris-HCl, pH 7.5, 150 mM NaCl, 5 mM $MgCl_2$, 0.5 mM DTT, 1% NP-40 supplemented with cOmplete protease inhibitor tablets [Roche] and RNase OUT [Invitrogen]), spun at 13,000 RPM for 20 minutes at 4°C, and ~200 μg of purified cell lysate were rotated end-over-end with 400 ng of biotinylated RNA probe for 20 minutes at room temperature. To precipitate biotinylated RNA probes from MCF-7 cell lysates, NeutrAvidin beads (Thermo Scientific) pre-blocked with BSA (Roche) were added and rotated end-over-end for 30 minutes at 4°C. After precipitation, the beads were washed 5 times in IP buffer and then subjected to elution by boiling in reducing sample buffer (RSB). Bound proteins were analyzed by immunoblotting to detect HuR.

Nucleocytoplasmic Fractionation

To isolate distinct pools of RNA and protein from nuclear and cytoplasmic fractions, cells were collected on ice, spun down, and resuspended in ice-cold fractionation buffer (10 mM Tris-HCl, pH 7.4, 10 mM NaCl, 3 mM $MgCl_2$, 0.5% (v/v) NP-40) supplemented with 1 mini cOmplete protease inhibitor tablet (Roche; 1 tablet/10 mL of buffer) for 10 minutes on ice. Cell lysates were spun down and the supernatant, or cytoplasmic fraction was separated from the nuclear pellet. RNA was isolated from each fraction with TRIzol reagent (Invitrogen) and protein samples were prepared with RIPA-2 buffer (as described above).

mRNA Stability

To measure mRNA stability in MCF-7 cells, 5 μg/ml actinomycin D (Sigma) was added to the growth medium to inhibit transcription and cells were harvested 30 minutes, 2, 4, 6 and 8 hours later (fractionated cells were collected at 30 minutes, 3, 6 and 8 hours after ActD addition). Nuclear and cytoplasmic RNA was isolated from cells (described above) and analyzed by qRT-PCR. Half-lives were determined by normalization to *18s* rRNA and to the 30 minute time point.

Probe Synthesis

Probes were synthesized as previously described (370,371). Briefly, FLAG-hyNic (Solulink) was added to 4FB-modified (Solulink) neutravidin (Thermo Scientific Pierce) according to the manufacturer's protocol. For each probe, 2′-O-methyl RNA-DNA oligonucleotide chimeras complementary to the target sequence were designed with a 5′-biotin and dT-C6-NH2 internal modifications (Biosearch Technologies). Cy3B NHS ester fluorophores (GE Healthcare) or Dylight 650 NHS Ester fluorophores (Thermo Scientific Pierce) were conjugated to the oligonucleotide amino groups using the manufacturer's protocol. Free dye was removed using 30 kDa Amicon spin columns (EMD Millipore). The purified, labeled oligonucleotides were tetramerized by incubation for 1 hour at room temperature with untagged or FLAG-tagged neutravidin. Free ligands were removed using 30 kDa Amicon spin columns (EMD Millipore). Three probes each targeting different sequences in the 3′ UTR of *PDCD4* mRNA (Table 2) were assembled separately prior to delivery and combined during delivery. To deliver total 60nM probes targeting *PDCD4* mRNA, 20 nM of each probe was combined.

Probe Delivery

For probe delivery, cells were washed in Dulbecco's phosphate buffered saline (DPBS) without Ca^{2+} and Mg^{2+} (Lonza) and subsequently, incubated with 0.15 U/mL activated streptolysin O (Sigma) in OptiMEM (Invitrogen) containing 60 nM *PDCD4* mRNA probes for 10 min at 37°C. Delivery media were replaced with growth media for 15 min to restore membrane integrity before actinomycin D treatment or fixation. For

actinomycin D treatment, cells were incubated for 90 min at 37°C with 5 μg/mL actinomycin D (Sigma) in growth media and fixed at the end of the exposure.

Proximity Ligation Assay

The Proximity Ligation Assay (PLA) was performed as previously described (371). Cells were fixed with 1% paraformaldehyde (Electron Microscopy Science) in PBS for 10 min, permeabilized with 0.2% Triton X-100 (Sigma) for 5 min, and blocked for 1 h with a blocking solution. The blocking solution consisted of 0.5% Tween-20 (CalBioChem), 0.1% Triton X-100, 0.1% gelatin (Aurion), 2% donkey serum (Sigma), and 1% bovine serum albumin (BSA) (EMD) in PBS. Cells were washed with PBS, incubated in two primary antibodies, one against the FLAG-tagged neutravidin and one against the protein of interest. For anti-FLAG antibodies, either rabbit polyclonal (1:2000; F7425, Sigma) or mouse monoclonal (1:2000; M2, Sigma) anti-FLAG antibody was used. Mouse monoclonal anti-HuR (1:750; 3A2, Santa Cruz) was used to detect HuR, and rabbit polyclonal anti-TIA1 (1:1500; AV40981, Sigma) was used to detect TIA1. After washing with Duolink wash solution (Olink Bioscience), the cells were incubated with species-corresponding oligonucleotide-labeled PLA probes (Olink Bioscience) diluted in 0.05% Tween-20 in PBS and washed with Duolink wash solution. The ligation and rolling circle amplification reaction (Olink Bioscience) were performed as instructed in the manufacturer's protocol. The cells were then immunostained and DAPI-stained (Invitrogen) and mounted on slides using Prolong (Invitrogen).

PLA Fluorescence Imaging

All the images were collected using an Axiovert 200 M microscope (Zeiss) with a 63×, NA 1.4 Plan-Apochromat objective and an ORCA-ER AG camera (Hamamatsu). The images were acquired using the Volocity acquisition software (PerkinElmer). Image stacks were recorded at 200 nm intervals to sample volumes for iterative deconvolution using Volocity's deconvolution algorithms. Probe and PLA signal quantification and Mander's coefficients were computed in Volocity and imported into Excel (Microsoft) and Sigma Plot (Systat) for further analysis and plotting. Images presented have been linearly contrast enhanced for clarity. All calculations were performed directly on raw, deconvolved widefield data.

Image Quantification

The RNA volume and PLA frequency normalized to the RNA volume were measured using Volocity (PerkinElmer). Each cell was identified by the probe signal or immunofluorescence and analyzed individually. The Mander's coefficient calculation for probe colocalization was performed using Volocity. We analyzed three representative images. In Sigma Plot, all pairwise multiple comparison procedure was performed with Tukey method to compare the Mander's coefficients for each probe. The RNA volume was determined based on standard deviation intensity of the probe. The PLA signal initially was identified as objects by their standard deviation intensity then separated into individual punctae using the 'separate touching objects' tool. The punctae were further

filtered based on size and maximum intensity. For each experiment, we analyzed at least ten images of each coverslip and three repeated experiments. In Sigma Plot, when comparing more than two groups, all pairwise multiple comparison procedure was performed with Dunn's method to compare the RNA volume and PLA frequency. When comparing two groups, Mann-Whitney rank sum test was used.

Polysome Profiling

To analyze the translation of *PDCD4* and *GAPDH* (control) mRNAs across various treatment groups, linear sucrose gradient fractionation of MCF-7 cell cytoplasmic extracts was performed as previously described (395,396). Briefly, cells were incubated for 15 minutes with 100 μg/mL cyclohexamide (VWR) to arrest translation prior to isolation. MCF-7 cells were lysed in polysome-preserving buffer (20 mM Tris-HCl, pH 7.5, 100 mM KCl, 5 mM $MgCl_2$, 0.15% Triton-X 100 [Sigma], 100 μg/mL cyclohexamide, 200 U RNase Inhibitor [Promega], and protease inhibitors [Roche]) or polysome-disrupting buffer (identical to polysome-preserving buffer except it lacks $MgCl_2$ and contains 20 mM EDTA) and then centrifuged at 13,000 RPM for 30 minutes at 4°C to remove cellular debris. The clarified lysates (0.8 mL) were loaded onto 15-45% (w/v) linear sucrose gradients containing 100 mM KCl, 20 mM Tris-HCl (pH 7.5), and 5 mM $MgCl_2$ (polysome-disrupted lysates were loaded onto the same gradient lacking $MgCl_2$ and containing 1 mM EDTA), and subjected to centrifugation in a Beckman SW41 rotor at 33,000 RPM for 90 minutes at 4°C.

Each gradient was fractionated into eleven 1 mL fractions by bottom displacement using a gradient fractionator (Isco) with the ribosomal profile monitored at OD_{254}. Total RNA from each fraction was isolated using standard phenol-chloroform extraction. Resulting RNA pellets were resuspended in 15 µL RNase-free water and used for cDNA generation and subsequent qRT-PCR analysis using primers specific to *PDCD4* and *GAPDH* transcripts. The % mRNA present in each fraction was calculated using the $2^{\wedge\text{-Ct}}$ method.

Chapter 5: Discussion

A portion of this chapter is adapted from the following published work:

Wigington, C.P., Williams, K.R., Meers, M.P., Bassell, G.J., and Corbett, A.H. (2014) *Wiley Interdisciplinary Reviews RNA* **5**, 601-622. "Poly(A) RNA Binding Proteins and Polyadenosine RNA: New Members and Novel Functions."

Overview

In this dissertation, I characterize the recognition and post-transcriptional processing of two select mRNAs, which are bound and regulated by RNA binding proteins that are dysregulated in human disease. The work presented here suggests that the proteins encoded by these transcripts perform critical cellular functions and that, when dysregulated, may represent the underlying molecular pathogenesis of disease. Our studies provide insight into how these transcripts are recognized as well as the post-transcriptional consequence of being bound by the respective RNA binding protein.

Previous studies demonstrate that the novel polyadenosine RNA binding protein, ZC3H14, plays a critical role in neurons (150,268). I show that knockdown of ZC3H14 in human cells results in improper processing and subsequent reduction of *ATP5G1* mRNA (Chapter 2), which encodes a key ATP synthase subunit. Consistent with loss of ATP synthase activity, we observe a robust decrease in cellular ATP levels and altered mitochondrial morphology upon knockdown of ZC3H14 (Chapter 2), suggesting that ZC3H14 plays a role in maintaining proper energy levels in neurons. I go on to explore the regulation of *ZC3H14* in human cells (Chapter 3), including autoregulation of the *ZC3H14* transcript, likely via a conserved polyadenosine stretch within the 3'UTR. These findings are consistent with many other RNA binding proteins that bind their cognate mRNAs (195) and provide an autoregulatory feedback loop for maintaining tight control of cellular ZC3H14 levels (Chapter 3). Finally, I present an additional mode of regulation of the *PDCD4* transcript (Chapter 4), which encodes a novel tumor suppressor that is downregulated in a number of cancer types. The described regulation occurs via a competitive binding event between HuR and TIA1 on the *PDCD4* 3'UTR and is

important for maintaining *PDCD4* stability in the cytoplasm (Chapter 4). We hypothesize that this pool of stable *PDCD4* mRNA in the cytoplasm represents a reserve that cells can access in times of cellular stress and/or transformation. Together, these studies underscore the importance of post-transcriptional processing events and the factors that mediate them in maintaining proper gene expression.

ZC3H14: Implications for mRNA processing and the brain

Objectives and challenges

One of the primary objectives in my dissertation research was to elucidate the role of ZC3H14 in RNA processing events that take place in human cells. As described in the Introduction, there are a number of studies on ZC3H14 orthologs in model organisms that point to ZC3H14 playing a diverse role in post-transcriptional processing events. Therefore, determining which, if any, of these events are conserved in human cells is a critical objective. To approach this question, I selected a transcript that was robustly and specifically affected upon knockdown of ZC3H14 in human cells, as identified by a genome-wide microarray approach. Using this transcript as a "molecular ruler," I was able to perform various experiments to query the role of ZC3H14 in modulating this transcript. Our results (outlined in Chapter 2) suggest that ZC3H14 interacts preferentially with pre-mRNA transcripts and somehow coordinates processing events necessary to generate the mature forms of these messages (Figure 5.1). These results are consistent with previous work from our lab (161) as well as work from a collaborating

lab (170) suggesting that Nab2 functions at the level of the un-spliced pre-mRNA and plays a role in ensuring proper production of export-competent mRNPs.

One of the challenges in investigating post-transcriptional processing events, particularly those that take place in the nucleus, is the tight coupling of these events to one another. For instance, disruption of mRNA export could lead us to observe upstream processing effects, such as extended poly(A) tails or increased mRNA surveillance by the RNA exosome. Studies performed in *S. cerevisiae* have demonstrated roles for Nab2 in poly(A) tail length regulation (163), mRNA surveillance (269), mRNA export (159,162) and transcript stability (291). However, recent studies suggest that perhaps Nab2 is a regulator of these processes, ensuring the execution of these events and thus allowing for the selective export of properly processed mRNAs to the cytoplasm (160,161). An important objective moving forward will be delineating these tightly coupled processes in order to identify the specific role(s) of ZC3H14 in mRNA processing events.

One limitation to the studies performed in *S. cerevisiae* stems from the presence of only one (characterized) nuclear poly(A) binding protein. Fission yeast (*S. pombe*) and higher eukaryotes express at least two nuclear poly(A) binding proteins. The well-studied PABPN1 protein is present in mammalian cells and has an extensively characterized role in 3' end processing and polyadenylation as well as control of poly(A) tail length (29), although, many of the studies characterizing PABPN1 function were performed in *in vitro* systems with purified, recombinant proteins (96). Where ZC3H14 fits into the picture of Pab-dependent mRNA processing in the nucleus is unclear. Our work suggests that ZC3H14 binds preferentially to pre-mRNAs and could therefore be present as transcripts are being processed and then either removed upon completion of processing or

during the course of mRNA export, which is consistent with studies of *S. cerevisiae* Nab2 (31). Integrating the roles of multiple Pabs in human cells is discussed in more detail in the following section.

Another level of complexity provided by studies in mammalian cells is the presence of multiple splice variants of *ZC3H14* (154). The N-terminal antibody that we use for the bulk of our studies recognizes the nuclear isoforms of ZC3H14 (154), which are most similar to Nab2/dNab2, from which we derive the majority of our preliminary studies. However, the presence of a cytoplasmic isoform of ZC3H14 that contains a divergent N-terminus but has the C-terminal CCCH zinc fingers suggests that this isoform should be able to interact with polyadenosine RNA with similar affinity as the longer, nuclear isoforms (148,154), but likely plays a unique role in mRNA regulation in the cytoplasm. Current work on this cytoplasmic isoform is focused on whether it has a role in mRNA trafficking and/or local translation in neurons. As described in the introduction, we observe an accumulation of ZC3H14 nuclear isoforms in the cytoplasm upon treatment with the transcriptional inhibitor, ActD (data not shown). These preliminary results suggest that the nuclear isoforms of ZC3H14, like many other nuclear RNA binding proteins (158), relocalize to the cytoplasm during cellular stress. These observations, coupled with the presence of a cytoplasmic isoform of ZC3H14, present a potentially complex network of regulation for these proteins. Identification of binding partners for ZC3H14 within the nuclear and cytoplasmic compartments will shed light into the distinct roles for ZC3H14 within each compartment as well as where and how these distinct isoforms interface with one another.

Implications for the brain

Our work describing a role for ZC3H14 in the post-transcriptional processing of *ATP5G1* mRNA (Chapter 2) was performed primarily in a commonly used breast cancer cell line, MCF-7. However, we do observe a more general effect on *ATP5G1* steady-state mRNA levels upon knockdown of ZC3H14 in multiple cell lines, including a human medulloblastoma cell line, which suggests a conserved role for ZC3H14 in regulating *ATP5G1* levels in neurons. We observe a robust effect on mitochondrial morphology upon ZC3H14 knockdown, consistent with previous work on cells with reduced levels of ATP5G1 (301,306). Our study, along with many others, demonstrates that proper mitochondrial morphology is critical for proper cellular function, particularly in neurons (267,317,319,320). These findings are particularly interesting in light of the observation that patients with loss-of-function mutations in *ZC3H14* have a certain form of nonsyndromic autosomal recessive intellectual disability (150). Studies in *Drosophila* reveal a conserved role for ZC3H14/dNab2 in proper neuronal function, as evidenced by *dNab2* null flies with defects in learning and memory as well as axonal path finding (150,268,290). Therefore, elucidating the critical role of ZC3H14 in neurons is our primary objective moving forward.

The observation that the *ATP5G1* transcript is trafficked to axons in neurons (306) suggests that proper maintenance of the stability of this transcript is critical. Trafficked mRNAs, specifically those in neurons, are translationally repressed by sequestration of the 5' cap structure, which in turn aids in the prevention of degradation by mRNA decay machinery (397). Recent studies in budding yeast demonstrated that approximately half of the nuclear-encoded mRNAs that encode mitochondrial proteins are asymmetrically

localized to the region surrounding the mitochondria (398,399), suggesting coordination between post-transcriptional factors and the mitochondrial protein import machinery (reviewed in (400)). Preliminary data from our lab suggests that the nuclear isoforms of ZC3H14 display punctate cytoplasmic localization in primary hippocampal neurons (unpublished observations), suggesting that the neuronal isoforms of ZC3H14 may have roles in the cytoplasm. Furthermore, *S. cerevisiae* Nab2 shuttles in and out of the nucleus (159), so, like Nab2, ZC3H14 may also shuttle and accompany mRNPs to their proper location in the cytoplasm. ZC3H14 could play a role in delivering target mRNAs to axonal synapses, specifically to the highly active population of mitochondria located at the synapse. Interestingly, upon knockdown of ZC3H14, we observe a slight reduction in *ATP5G1* mRNA stability (data not shown). The siRNAs that we employ for ZC3H14 knockdown target the region of *ZC3H14* that corresponds to the C-terminal zinc fingers and therefore targets all known splice variants. Whether the loss of the cytoplasmic isoform of ZC3H14 is responsible for this reduction in mRNA stability is yet to be determined. A future direction is to identify binding partners of ZC3H14 in neuronal cells to determine whether ZC3H14 is involved in the trafficking, stability and/or local translation of target transcripts, such as *ATP5G1*, in neurons.

As mentioned earlier, a previous study demonstrated that the *ATP5G1* 3'UTR is targeted by *miR-338* in rat neuronal cells (316). The binding to and regulation of *ATP5G1* by *miR-338* results in decreased ATP5G1 protein and increased axonal ROS as well as an axonal growth defect (316), which is consistent with defects observed in rat neurons treated with *ATP5G1* siRNA (306). The *miR-338* targeting sequence is conserved in the human *ATP5G1* 3'UTR (miRBase; Figure 5.1) and therefore may be a functionally

relevant target of *miR-338* in human neuronal cells as well as in rats. Whether or not ZC3H14 has a role in miRNA processing and/or targeting is yet to be determined. There is, however, clear evidence that miRNA machinery is intimately involved with the poly(A) tail via interactions between PABPC1 and Glycine-Tryptophan protein of 182 kDa (GW182) (43). This interaction promotes rapid deadenylation and subsequent degradation of target transcripts (43,401). The recent study demonstrating that ZC3H14 has a conserved role in poly(A) tail length regulation in mammalian neurons (168) clearly supports a role for ZC3H14 in post-transcriptional processing via the poly(A) tail and could fit into this regulation by miRNAs.

To date, there are multiple studies that point toward a critical role for ZC3H14 in the brain (150,151,268). However, how the loss of this ubiquitously expressed protein results in a tissue-specific disease remains unclear. As described in the Introduction, there are multiple models for how loss of ZC3H14 could specifically impact cells in the brain. One of these models focuses on the disruption of functions and/or requirements that are unique to neuronal cells. Properly functioning mitochondria are clearly important in all cell types, but particularly in the cells of the brain, which are responsible for the consumption of 25% and 20% of our daily glucose and oxygen consumption, respectively (317,318). Neurons rely almost exclusively on ATP production via oxidative phosphorylation (319) and are unable to switch to glycolysis when oxidative phosphorylation becomes limited (320). Of note, disruption of normal mitochondrial function and dynamics is observed in many neurological diseases, including dominant optic atrophy, Charcot-Marie-Tooth type 2A, Parkinson's disease, Alzheimer's disease, and Huntington's disease (267). Therefore, we hypothesize that regulation of *ATP5G1* by

ZC3H14 is likely to have effects on mitochondria that could be detrimental to neurons and may represent at least one aspect of the molecular pathogenesis underlying the intellectual disability observed in these patients.

Integrating the roles of multiple Pabs in human cells

As described here, our understanding of the functions and members of the Pab protein family has increased in recent years. The studies discussed in this dissertation highlight the diversity found within the Pab family, as represented not only by the diverse roles of Pabs in modulating gene expression, but also by novel Pab family members that bind to RNA via unconventional polyadenosine RNA binding modules. The function of Pab proteins likely depends on the cellular context, specific regulatory elements, and the complement of RNA binding proteins present. Highlighting the importance of context for Pab protein function are the tissue-specific diseases that result from mutation of *PABPN1* and *ZC3H14*. Both PABPN1 and ZC3H14 play important roles in RNA processing, which are likely critical in numerous cell types, so why defects in PABPN1 cause muscle-specific pathology and loss of ZC3H14 causes defects specifically in brain function is not at all obvious. Clearly to understand these tissue-specific diseases, studies will not only need to assess contributions of these proteins within the biological context of the affected tissues but also to define the complete molecular functions of the Pabs that underlie these contributions. Indeed, there are likely additional roles that have yet to be discovered for members of the Pab protein family raising several key questions for contemplation.

The first question is how the diverse functions of the multiple Pab proteins are coordinated throughout the intimately linked steps of post-transcriptional processing. Given that all Pab proteins bind to polyadenosine RNA, they should all technically compete for the same target sequences, including poly(A) tails added to nearly all mRNAs. Presumably there is remodeling and/or replacement of the complement of Pabs associated with a poly(A) RNA as that RNA moves through processing within the nucleus to ultimately fulfill its cytoplasmic destiny. The question of whether all polyadenylated RNAs are bound at some point in their life by the full complement of Pabs or whether Pabs show preferential binding to specific transcripts or subsets of transcripts will also need to be addressed to understand how overall Pab family function is coordinated. Very little is known about how Pab proteins are exchanged for one another at different stages of poly(A) RNA biogenesis and/or function.

One possible mode of Pab regulation is association with protein binding partners. For example, PABPC is regulated by binding to a number of PAb-Interacting Proteins (PAIPs), including LARP4. Given this precedent, there are likely additional partners that interact with and regulate other Pab family members. Such interactions could contribute to selectivity for certain transcripts in cases where these Pab binding partners themselves are sequence-specific RNA binding proteins. Clearly, further studies are needed to define molecular interactions with both target RNAs and protein partners to fully understand how members of the Pab family of proteins cooperate to regulate gene expression.

A second important and related question is whether all adenosine sequences are functionally equivalent. For instance, the non-templated poly(A) tails present at the 3' end of mRNAs represent just one type of polyadenosine found in the human

transcriptome. Our analysis of internal, templated polyadenosine stretches in RNAs reveals clear enrichment of these sequences within the introns and 3'UTRs of mRNAs. These sequences could be bound by Pabs to confer regulation. Only in a few cases have the function of such templated A stretches been analyzed but those studies do confirm the potential for their functional importance. With regard to the question of whether all polyadenosine stretches are equivalent, recent work reveals that methylation of adenosine residues (m^6A) on circadian clock transcripts contributes to their processing efficiency and plays a role in maintaining proper circadian rhythm (402). The observation that post-transcriptional modification of adenosine residues modulates mRNA processing raises the possibility that adenosine residues on poly(A) tails or within internal polyadenosine stretches could be methylated to create distinct motifs that could be differentially recognized by Pab proteins. Future analyses should explore whether modification of adenine within Pab target sequences influences Pab recognition and/or regulation.

In summary, the family of Pab proteins is expanding in both number and diversity of function. In fact, there are likely additional Pab family members that we have yet to define as such or to discover. While insight into the molecular roles of the individual Pab proteins is growing, developing a comprehensive model for how the functions of this protein family are coordinated to modulate gene expression remains the goal for the future.

Implications for HuR and TIA1 in breast cancer: PDCD4 is a relevant target

As described throughout the Introduction and Chapter 4, HuR has a well-studied role in breast cancer (259,403) and although TIA1 has a less characterized association

with cancer, it clearly regulates the splicing and translation of many cancer-relevant mRNAs (226). Recent studies that demonstrate the complex and coordinate relationship between HuR and TIA1 on target mRNAs (195,220,223,250,251) suggest that these two proteins may coordinate and/or compete on many common targets to fine-tune the expression of the respective protein products. Many target mRNAs of HuR and TIA1 encode factors important for the execution of the apoptotic program (226,264), suggesting a role for HuR and TIA1 in apoptosis. We hypothesize that the regulation of the Programmed Cell Death 4 (*PDCD4*) mRNA by HuR and TIA1 in breast cancer cells (outlined in Chapter 4) presents an additional example of the importance of these two RNA binding proteins in coordinating the apoptotic program.

The PDCD4 protein is an inhibitor of the eIF4A helicase, which is responsible for unwinding secondary structural elements located within the 5′UTR of mRNA transcripts to facilitate translation (362). PDCD4 expression is upregulated after the initiation of apoptosis (383) and reduction of PDCD4 protein levels leads to neoplastic transformation (384). Because of the critical role for PDCD4 as a global regulator of protein synthesis and as a tumor suppressor, *PDCD4* expression is regulated at multiple levels (270). In addition to transcriptional and post-translational regulation of *PDCD4*, previous studies demonstrate that *PDCD4* is regulated at the post-transcriptional level by *miR-21* and the splicing factor, SRSF3 (272,387). Our study demonstrating regulation by HuR and TIA1 on the *PDCD4* 3'UTR provides an additional mode of post-transcriptional regulation on this tightly regulated transcript (Figure 5.2).

The role of PDCD4 in breast cancer is well studied (272,404-407). Comparison of normal breast tissue to neoplastic breast tissue reveals altered cellular localization and

decreased PDCD4 protein levels in neoplastic breast tissue. Decreased PDCD4 protein levels in breast tissue also significantly correlates with node positivity and worse overall survival (408). A recent study demonstrates that decreased PDCD4 protein levels correlates with poor prognosis, specifically in hormone receptor-positive breast cancer and points to a role for PDCD4 as a potential prognostic marker or therapeutic target (409).

We observe multiple pathways that converge to modulate PDCD4 protein levels. Increased activation of the PI3K-Akt pathway, which is commonly observed in cancer (410,411), leads to phosphorylation of PDCD4 (368) and rapid degradation of PDCD4, thus preventing its inhibition of eIF4A (368,412). As shown in Chapter 4, treatment of MCF-7 cells with ActD, which has been shown to activate PI3K signaling (379), results in a rapid decrease in steady-state PDCD4 protein levels, likely due to phosphorylation and degradation. However, underneath this highly labile pool of PDCD4 protein is an extremely stable reserve of *PDCD4* mRNA. We hypothesize that this pool, which appears to be positively regulated by HuR and TIA1, represents a population of *PDCD4* mRNA that is ready to be rapidly translated upon cellular stimuli. In the future, it will be important to not only identify any and all factors that play a role in modulating the *PDCD4* transcript, but also to determine whether these interactions and or/the mode of regulation changes under conditions of cellular stress, such as the case in the tumor microenvironment.

Future directions

ZC3H14

With regard to the study of ZC3H14 function in mammalian cells, the primary objective moving forward is to identify the specific role of ZC3H14 in mRNA processing. The work presented in Chapter 2 provides us with one important example of a transcript that is regulated by ZC3H14; however, whether ZC3H14 regulates all target mRNAs in the same manner is unclear. Preliminary data from RNA-seq experiments performed on neuronal tissue from our (newly generated) *ZC3H14* knockout mouse supports a transcript-specific effect of ZC3H14, consistent with the results of my microarray analysis. However, current work is focused on analyzing this data for insights into specific effects on mRNA processing as well as the identification of affected target mRNAs.

Understanding how ZC3H14 achieves specificity on the *ATP5G1* transcript (in binding and function) is also an important question moving forward. Current work in our lab is focused on identifying binding partners of ZC3H14 in mammalian cells, specifically the identification of factors that display compartment-specific interactions with ZC3H14. The identification of factors that interact with ZC3H14 should not only yield insight into the ability of ZC3H14 to achieve transcript specificity, but also into the role it plays in mRNA processing events.

Because so many of our studies moving forward will be performed in the *ZC3H14* knockout mouse, it will be interesting to see if the interaction between ZC3H14 and *ATP5G1* is conserved in murine cells. The *ATP5G1* transcript is highly conserved

between mouse and human, suggesting that any sequence elements required for this interaction are likely present. It will also be interesting to investigate the mitochondrial morphology in the neurons of these mice. Perhaps the specific interaction between ZC3H14 and *ATP5G1* is itself not conserved, but a tight control on mitochondrial function and neuronal signaling could underlie the neuronal defects observed in *ZC3H14* patients.

HuR and TIA1

Our work characterizing the interactions between HuR and TIA1 on the *PDCD4* transcript provides evidence for an additional point of regulation on this critically important transcript. As described in Chapter 4, *PDCD4* is a novel tumor suppressor that is downregulated in a number of different cancer types, including breast cancer. Understanding the spectrum of RNA binding proteins (and ncRNAs) that modulate the post-transcriptional regulation of *PDCD4* is a very important objective moving forward. However, another interesting objective surrounds the idea of alternative functions for these two factors (HuR and TIA1) in altered cellular states. As described in the Introduction and throughout Chapter 4, HuR and TIA1 both display altered localization upon transcriptional inhibition and oxidative stress. Additionally, a number of recent studies have demonstrated that HuR and TIA1 display altered and/or enhanced function on target transcripts depending on the cellular context (158,220,263). For instance, treatment of HeLa cells with UV light, which induces apoptosis, results in a preferential association between HuR and the Prothymosin α transcript in translating polysomes, leading to increased translation (263). As described earlier, we observe a robust reduction

of PDCD4 protein levels in cells undergoing stress, such as transcriptional inhibition. Whether HuR and TIA1 (as well as any other post-transcriptional factors) employ enhanced and/or altered function on the *PDCD4* transcript during these times of cellular stress is an important step moving forward (Figure 5.2).

Another important objective for analysis of *PDCD4* is determining whether HuR and/or TIA1 have any role in the loading of *miR-21* onto its well-defined site in the *PDCD4* 3'UTR. Our work in Chapter 4 demonstrates that knockdown of HuR and/or TIA1 does not affect the steady-state level of *miR-21*; however, recent information gleaned from the transcriptome-wide CLIP-seq analyses with HuR suggests that HuR has a role in miRNA regulation (224,225) and may therefore assist in the maturation or targeting of miRNAs. Finally, we demonstrate that the U-rich regions on the 3'UTR of *PDCD4* confer binding by HuR and TIA1; however, there are a number of other AU- and U-rich RNA binding proteins that could also interact with these elements. Determining the spectrum of post-transcriptional factors that bind to the PDCD4 transcript and their role in maintaining tight expression of this critical cellular factor is an exciting next step for this project.

Final conclusions

The studies presented here highlight the importance of post-transcriptional processing events in maintaining precise control of gene expression. As described throughout this dissertation, the dysregulation or loss of many RNA binding proteins results in various types of human disease, including intellectual disability and cancer. Understanding the function of newly discovered RNA binding proteins as well as novel

targets for canonical RNA binding proteins is critical to understand their role in disease. Additionally, elucidating the spectrum of RNAs that are bound by specific RNA binding proteins is critical to unveil targets that may play a role in the molecular pathogenesis of disease. Our work in Chapter 2 has identified the *ATP5G1* transcript as a target of the novel polyadenosine RNA binding protein, ZC3H14. The interaction between ZC3H14 and *ATP5G1* is critical to ensure proper cellular energy levels and normal mitochondrial morphology. The high energy requirements of neuronal cells suggests that the loss of ZC3H14, as observed in patients with intellectual disability, may render these cells susceptible to altered function. The work in Chapter 4 focuses on the interaction between two well-studied U-rich RNA binding proteins, HuR and TIA1, and the *PDCD4* transcript. We demonstrate that these two proteins participate in a competitive mode of interaction on the *PDCD4* 3'UTR that is important for maintaining PDCD4 levels in breast cancer cells. Together, these studies provide support for these disease-relevant targets as potential mediators of the molecular pathogenesis of disease.

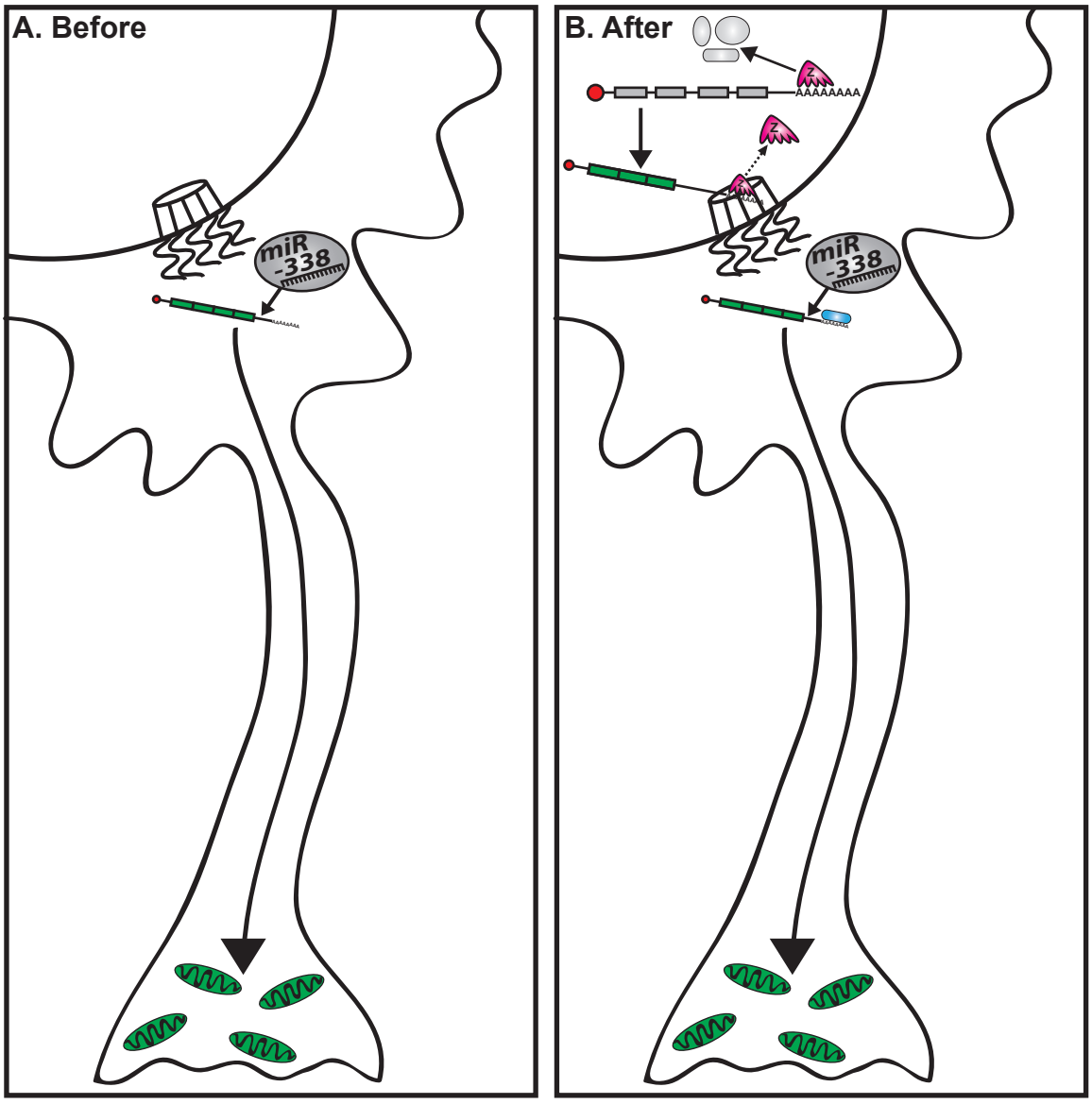

Figure 5.1. Proper *ATP5G1* regulation is critical for neuronal cell function. *A*) Previous studies demonstrate that in rat neurons, the *ATP5G1* 3'UTR is a target of *miR-338* and is trafficked to axonal synapses and locally translated there. Precise regulation of *ATP5G1* in rat neurons promotes axonal outgrowth and proper mitochondrial (green ovals) function. *B*) My work (detailed in Chapter 2) demonstrates that the novel poly(A) binding protein, ZC3H14 (pink, five-fingered shape), promotes and coordinates pre-mRNA processing events (processing factors represented by light grey shapes) critical for the production and export of mature *ATP5G1* mRNA. Loss of ZC3H14 results in improper pre-mRNA processing/export of *ATP5G1*, decreased cellular ATP levels and subsequent mitochondrial fragmentation. Understanding the factors and/or sequences that confer specificity on the *ATP5G1* transcript is a primary objective moving forward.

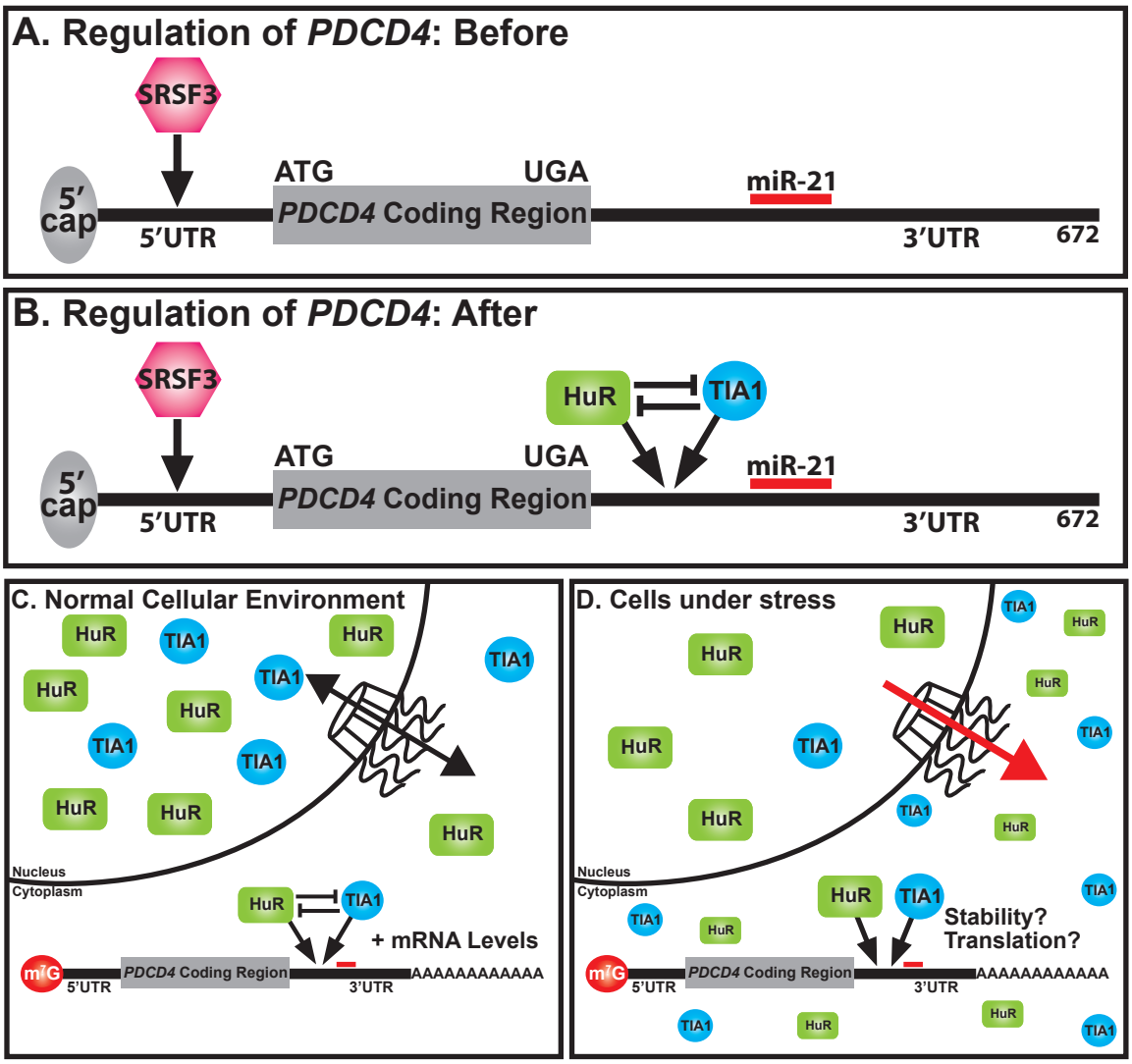

Figure 5.2 *PDCD4* is regulated by multiple post-transcriptional mechanisms. A) Previous studies have extensively characterized the *PDCD4* 3'UTR transcript as a target of the onco*miR-21* (red line). A more recent study demonstrated that the splicing factor SRSF3 (pink hexagon) also modulates *PDCD4* by repressing translation via an interaction with the 5'UTR. *B*) Our work (detailed in Chapter 4) reveals overlapping binding sites for the RNA binding proteins HuR and TIA1 (green rectangle and blue circle, respectively) within a U-rich region of the *PDCD4* 3'UTR, proximal to the well-defined *miR-21* binding site. Our work demonstrates that the overlapping binding sites for these two U-rich binding proteins result in a competitive mode of interaction for the *PDCD4* transcript. *C*) The steady-state localization of HuR and TIA1 is primarily nuclear, although both proteins shuttle in and out of the nucleus (bidirectional arrow). In an unstressed, normal cellular environment, HuR and TIA1 compete for binding to the *PDCD4* 3'UTR, an interaction that promotes the stability of the *PDCD4* transcript. *D*) In a stressful cellular environment, HuR and TIA1 undergo a shift in localization toward the cytoplasm (red arrow). Whether the interactions and functions of HuR and/or TIA1 are altered in these conditions is an important question moving forward.

REFERENCES

1. Evans, R. M., and Mangelsdorf, D. J. (2014) Nuclear Receptors, RXR, and the Big Bang. *Cell* **157**, 255-266
2. Whitmarsh, A. J., and Davis, R. J. (2000) Regulation of transcription factor function by phosphorylation. *Cellular and molecular life sciences : CMLS* **57**, 1172-1183
3. Menssen, A., and Hermeking, H. (2002) Characterization of the c-MYC-regulated transcriptome by SAGE: identification and analysis of c-MYC target genes. *Proceedings of the National Academy of Sciences of the United States of America* **99**, 6274-6279
4. Vervoorts, J., Luscher-Firzlaff, J., and Luscher, B. (2006) The ins and outs of MYC regulation by posttranslational mechanisms. *The Journal of biological chemistry* **281**, 34725-34729
5. Habib, T., Park, H., Tsang, M., de Alboran, I. M., Nicks, A., Wilson, L., Knoepfler, P. S., Andrews, S., Rawlings, D. J., Eisenman, R. N., and Iritani, B. M. (2007) Myc stimulates B lymphocyte differentiation and amplifies calcium signaling. *The Journal of cell biology* **179**, 717-731
6. Bannister, A. J., and Kouzarides, T. (2011) Regulation of chromatin by histone modifications. *Cell research* **21**, 381-395
7. Robertson, K. D. (2002) DNA methylation and chromatin - unraveling the tangled web. *Oncogene* **21**, 5361-5379
8. Moore, M. J. (2005) From birth to death: the complex lives of eukaryotic mRNAs. *Science* **309**, 1514-1518
9. Kornberg, R. D. (1999) Eukaryotic transcriptional control. *Trends in cell biology* **9**, M46-49
10. Phatnani, H. P., and Greenleaf, A. L. (2006) Phosphorylation and functions of the RNA polymerase II CTD. *Genes & development* **20**, 2922-2936
11. Bentley, D. L. (2014) Coupling mRNA processing with transcription in time and space. *Nature reviews. Genetics* **15**, 163-175
12. Rottman, F., Shatkin, A. J., and Perry, R. P. (1974) Sequences containing methylated nucleotides at the 5' termini of messenger RNAs: possible implications for processing. *Cell* **3**, 197-199
13. Izaurralde, E., Lewis, J., McGuigan, C., Jankowska, M., Darzynkiewicz, E., and Mattaj, I. W. (1994) A nuclear cap binding protein complex involved in pre-mRNA splicing. *Cell* **78**, 657-668
14. Cheng, H., Dufu, K., Lee, C. S., Hsu, J. L., Dias, A., and Reed, R. (2006) Human mRNA export machinery recruited to the 5' end of mRNA. *Cell* **127**, 1389-1400
15. Flaherty, S. M., Fortes, P., Izaurralde, E., Mattaj, I. W., and Gilmartin, G. M. (1997) Participation of the nuclear cap binding complex in pre-mRNA 3' processing. *Proceedings of the National Academy of Sciences of the United States of America* **94**, 11893-11898
16. Topisirovic, I., Svitkin, Y. V., Sonenberg, N., and Shatkin, A. J. (2011) Cap and cap-binding proteins in the control of gene expression. *Wiley interdisciplinary reviews. RNA* **2**, 277-298

17. Zheng, C. L., Fu, X. D., and Gribskov, M. (2005) Characteristics and regulatory elements defining constitutive splicing and different modes of alternative splicing in human and mouse. *Rna* **11**, 1777-1787
18. Brett, D., Pospisil, H., Valcarcel, J., Reich, J., and Bork, P. (2002) Alternative splicing and genome complexity. *Nature genetics* **30**, 29-30
19. Black, D. L. (2003) Mechanisms of alternative pre-messenger RNA splicing. *Annual review of biochemistry* **72**, 291-336
20. Le Hir, H., Gatfield, D., Izaurralde, E., and Moore, M. J. (2001) The exon-exon junction complex provides a binding platform for factors involved in mRNA export and nonsense-mediated mRNA decay. *The EMBO journal* **20**, 4987-4997
21. Le Hir, H., Moore, M. J., and Maquat, L. E. (2000) Pre-mRNA splicing alters mRNP composition: evidence for stable association of proteins at exon-exon junctions. *Genes & development* **14**, 1098-1108
22. McCracken, S., Fong, N., Yankulov, K., Ballantyne, S., Pan, G., Greenblatt, J., Patterson, S. D., Wickens, M., and Bentley, D. L. (1997) The C-terminal domain of RNA polymerase II couples mRNA processing to transcription. *Nature* **385**, 357-361
23. Meinhart, A., and Cramer, P. (2004) Recognition of RNA polymerase II carboxy-terminal domain by 3'-RNA-processing factors. *Nature* **430**, 223-226
24. Kuhn, U., Gundel, M., Knoth, A., Kerwitz, Y., Rudel, S., and Wahle, E. (2009) Poly(A) tail length is controlled by the nuclear poly(A)-binding protein regulating the interaction between poly(A) polymerase and the cleavage and polyadenylation specificity factor. *The Journal of biological chemistry* **284**, 22803-22814
25. Marzluff, W. F., Wagner, E. J., and Duronio, R. J. (2008) Metabolism and regulation of canonical histone mRNAs: life without a poly(A) tail. *Nature reviews. Genetics* **9**, 843-854
26. Wahle, E., and Ruegsegger, U. (1999) 3'-End processing of pre-mRNA in eukaryotes. *FEMS microbiology reviews* **23**, 277-295
27. Chang, H., Lim, J., Ha, M., and Kim, V. N. (2014) TAIL-seq: genome-wide determination of poly(A) tail length and 3' end modifications. *Molecular cell* **53**, 1044-1052
28. Subtelny, A. O., Eichhorn, S. W., Chen, G. R., Sive, H., and Bartel, D. P. (2014) Poly(A)-tail profiling reveals an embryonic switch in translational control. *Nature* **508**, 66-71
29. Wigington, C. P., Williams, K. R., Meers, M. P., Bassell, G. J., and Corbett, A. H. (2014) Poly(A) RNA-binding proteins and polyadenosine RNA: new members and novel functions. *Wiley interdisciplinary reviews. RNA* **5**, 601-622
30. Korner, C. G., and Wahle, E. (1997) Poly(A) tail shortening by a mammalian poly(A)-specific 3'-exoribonuclease. *The Journal of biological chemistry* **272**, 10448-10456
31. Kelly, S. M., and Corbett, A. H. (2009) Messenger RNA export from the nucleus: a series of molecular wardrobe changes. *Traffic* **10**, 1199-1208
32. Natalizio, B. J., and Wente, S. R. (2013) Postage for the messenger: designating routes for nuclear mRNA export. *Trends in cell biology* **23**, 365-373

33. Isken, O., and Maquat, L. E. (2007) Quality control of eukaryotic mRNA: safeguarding cells from abnormal mRNA function. *Genes & development* **21**, 1833-1856
34. Lykke-Andersen, J. (2001) mRNA quality control: Marking the message for life or death. *Current biology : CB* **11**, R88-91
35. Maquat, L. E., Hwang, J., Sato, H., and Tang, Y. (2010) CBP80-promoted mRNP rearrangements during the pioneer round of translation, nonsense-mediated mRNA decay, and thereafter. *Cold Spring Harbor symposia on quantitative biology* **75**, 127-134
36. Eliscovich, C., Buxbaum, A. R., Katz, Z. B., and Singer, R. H. (2013) mRNA on the move: the road to its biological destiny. *The Journal of biological chemistry* **288**, 20361-20368
37. Xing, L., and Bassell, G. J. (2013) mRNA localization: an orchestration of assembly, traffic and synthesis. *Traffic* **14**, 2-14
38. Sinnamon, J. R., and Czaplinski, K. (2011) mRNA trafficking and local translation: the Yin and Yang of regulating mRNA localization in neurons. *Acta biochimica et biophysica Sinica* **43**, 663-670
39. Hutten, S., Sharangdhar, T., and Kiebler, M. (2014) Unmasking the messenger. *RNA biology* **11**, 992-997
40. Balagopal, V., and Parker, R. (2009) Polysomes, P bodies and stress granules: states and fates of eukaryotic mRNAs. *Current opinion in cell biology* **21**, 403-408
41. Bhattacharyya, S. N., Habermacher, R., Martine, U., Closs, E. I., and Filipowicz, W. (2006) Relief of microRNA-mediated translational repression in human cells subjected to stress. *Cell* **125**, 1111-1124
42. Brengues, M., Teixeira, D., and Parker, R. (2005) Movement of eukaryotic mRNAs between polysomes and cytoplasmic processing bodies. *Science* **310**, 486-489
43. Wu, X., and Brewer, G. (2012) The regulation of mRNA stability in mammalian cells: 2.0. *Gene* **500**, 10-21
44. Shyu, A. B., Greenberg, M. E., and Belasco, J. G. (1989) The c-fos transcript is targeted for rapid decay by two distinct mRNA degradation pathways. *Genes & development* **3**, 60-72
45. Parker, R., and Song, H. (2004) The enzymes and control of eukaryotic mRNA turnover. *Nature structural & molecular biology* **11**, 121-127
46. Komarnitsky, P., Cho, E. J., and Buratowski, S. (2000) Different phosphorylated forms of RNA polymerase II and associated mRNA processing factors during transcription. *Genes & development* **14**, 2452-2460
47. David, C. J., Boyne, A. R., Millhouse, S. R., and Manley, J. L. (2011) The RNA polymerase II C-terminal domain promotes splicing activation through recruitment of a U2AF65-Prp19 complex. *Genes & development* **25**, 972-983
48. Egloff, S., O'Reilly, D., Chapman, R. D., Taylor, A., Tanzhaus, K., Pitts, L., Eick, D., and Murphy, S. (2007) Serine-7 of the RNA polymerase II CTD is specifically required for snRNA gene expression. *Science* **318**, 1777-1779

49. Gu, B., Eick, D., and Bensaude, O. (2013) CTD serine-2 plays a critical role in splicing and termination factor recruitment to RNA polymerase II in vivo. *Nucleic acids research* **41**, 1591-1603
50. Ho, C. K., and Shuman, S. (1999) Distinct roles for CTD Ser-2 and Ser-5 phosphorylation in the recruitment and allosteric activation of mammalian mRNA capping enzyme. *Molecular cell* **3**, 405-411
51. Gerstberger, S., Hafner, M., and Tuschl, T. (2014) A census of human RNA-binding proteins. *Nature reviews. Genetics* **15**, 829-845
52. Maris, C., Dominguez, C., and Allain, F. H. (2005) The RNA recognition motif, a plastic RNA-binding platform to regulate post-transcriptional gene expression. *The FEBS journal* **272**, 2118-2131
53. Bartel, D. P. (2009) MicroRNAs: target recognition and regulatory functions. *Cell* **136**, 215-233
54. Shukla, G. C., Singh, J., and Barik, S. (2011) MicroRNAs: Processing, Maturation, Target Recognition and Regulatory Functions. *Molecular and cellular pharmacology* **3**, 83-92
55. Boyerinas, B., Park, S. M., Hau, A., Murmann, A. E., and Peter, M. E. (2010) The role of let-7 in cell differentiation and cancer. *Endocrine-related cancer* **17**, F19-36
56. McKeown, M. (1993) The role of small nuclear RNAs in RNA splicing. *Current opinion in cell biology* **5**, 448-454
57. Valadkhan, S. (2005) snRNAs as the catalysts of pre-mRNA splicing. *Current opinion in chemical biology* **9**, 603-608
58. Bratkovic, T., and Rogelj, B. (2014) The many faces of small nucleolar RNAs. *Biochimica et biophysica acta* **1839**, 438-443
59. Decatur, W. A., and Fournier, M. J. (2003) RNA-guided nucleotide modification of ribosomal and other RNAs. *The Journal of biological chemistry* **278**, 695-698
60. De Benedetti, A., and Graff, J. R. (2004) eIF-4E expression and its role in malignancies and metastases. *Oncogene* **23**, 3189-3199
61. Lazaris-Karatzas, A., Montine, K. S., and Sonenberg, N. (1990) Malignant transformation by a eukaryotic initiation factor subunit that binds to mRNA 5' cap. *Nature* **345**, 544-547
62. Li, B. D., Liu, L., Dawson, M., and De Benedetti, A. (1997) Overexpression of eukaryotic initiation factor 4E (eIF4E) in breast carcinoma. *Cancer* **79**, 2385-2390
63. Kolb, S. J., and Kissel, J. T. (2011) Spinal muscular atrophy: a timely review. *Archives of neurology* **68**, 979-984
64. Fallini, C., Bassell, G. J., and Rossoll, W. (2012) Spinal muscular atrophy: the role of SMN in axonal mRNA regulation. *Brain research* **1462**, 81-92
65. Coady, T. H., and Lorson, C. L. (2011) SMN in spinal muscular atrophy and snRNP biogenesis. *Wiley interdisciplinary reviews. RNA* **2**, 546-564
66. Proudfoot, N. J. (2011) Ending the message: poly(A) signals then and now. *Genes & development* **25**, 1770-1782
67. Adesnik, M., Salditt, M., Thomas, W., and Darnell, J. E. (1972) Evidence that all messenger RNA molecules (except histone messenger RNA) contain Poly (A) sequences and that the Poly(A) has a nuclear function. *Journal of molecular biology* **71**, 21-30

68. Birnboim, H. C., Mitchel, R. E., and Straus, N. A. (1973) Analysis of long pyrimidine polynucleotides in HeLa cell nuclear DNA: absence of polydeoxythymidylate. *Proceedings of the National Academy of Sciences of the United States of America* **70**, 2189-2192
69. Edmonds, M., Vaughan, M. H., Jr., and Nakazato, H. (1971) Polyadenylic acid sequences in the heterogeneous nuclear RNA and rapidly-labeled polyribosomal RNA of HeLa cells: possible evidence for a precursor relationship. *Proceedings of the National Academy of Sciences of the United States of America* **68**, 1336-1340
70. Lim, L., and Canellakis, E. S. (1970) Adenine-rich polymer associated with rabbit reticulocyte messenger RNA. *Nature* **227**, 710-712
71. Mendecki, J., Lee, S. Y., and Brawerman, G. (1972) Characteristics of the polyadenylic acid segment associated with messenger ribonucleic acid in mouse sarcoma 180 ascites cells. *Biochemistry* **11**, 792-798
72. Proudfoot, N. J., and Brownlee, G. G. (1976) 3' non-coding region sequences in eukaryotic messenger RNA. *Nature* **263**, 211-214
73. Tian, B., Hu, J., Zhang, H., and Lutz, C. S. (2005) A large-scale analysis of mRNA polyadenylation of human and mouse genes. *Nucleic acids research* **33**, 201-212
74. Wickens, M., and Stephenson, P. (1984) Role of the conserved AAUAAA sequence: four AAUAAA point mutants prevent messenger RNA 3' end formation. *Science* **226**, 1045-1051
75. Zhao, J., Hyman, L., and Moore, C. (1999) Formation of mRNA 3' ends in eukaryotes: mechanism, regulation, and interrelationships with other steps in mRNA synthesis. *Microbiology and molecular biology reviews : MMBR* **63**, 405-445
76. Fitzgerald, M., and Shenk, T. (1981) The sequence 5'-AAUAAA-3'forms parts of the recognition site for polyadenylation of late SV40 mRNAs. *Cell* **24**, 251-260
77. Proudfoot, N. J., and Longley, J. I. (1976) The 3' terminal sequences of human alpha and beta globin messenger RNAs: comparison with rabbit globin messenger RNA. *Cell* **9**, 733-746
78. Mandel, C. R., Bai, Y., and Tong, L. (2008) Protein factors in pre-mRNA 3'-end processing. *Cellular and molecular life sciences : CMLS* **65**, 1099-1122
79. Murthy, K. G., and Manley, J. L. (1995) The 160-kD subunit of human cleavage-polyadenylation specificity factor coordinates pre-mRNA 3'-end formation. *Genes & development* **9**, 2672-2683
80. Mandel, C. R., Kaneko, S., Zhang, H., Gebauer, D., Vethantham, V., Manley, J. L., and Tong, L. (2006) Polyadenylation factor CPSF-73 is the pre-mRNA 3'-end-processing endonuclease. *Nature* **444**, 953-956
81. Chou, Z. F., Chen, F., and Wilusz, J. (1994) Sequence and position requirements for uridylate-rich downstream elements of polyadenylation signals. *Nucleic acids research* **22**, 2525-2531
82. McLauchlan, J., Gaffney, D., Whitton, J. L., and Clements, J. B. (1985) The consensus sequence YGTGTTYY located downstream from the AATAAA signal is required for efficient formation of mRNA 3' termini. *Nucleic acids research* **13**, 1347-1368

83. Millevoi, S., and Vagner, S. (2010) Molecular mechanisms of eukaryotic pre-mRNA 3' end processing regulation. *Nucleic acids research* **38**, 2757-2774
84. Higgs, D. R., Goodbourn, S. E., Lamb, J., Clegg, J. B., Weatherall, D. J., and Proudfoot, N. J. (1983) Alpha-thalassaemia caused by a polyadenylation signal mutation. *Nature* **306**, 398-400
85. Orkin, S. H., Cheng, T. C., Antonarakis, S. E., and Kazazian, H. H., Jr. (1985) Thalassemia due to a mutation in the cleavage-polyadenylation signal of the human beta-globin gene. *The EMBO journal* **4**, 453-456
86. Gick, O., Kramer, A., Keller, W., and Birnstiel, M. L. (1986) Generation of histone mRNA 3' ends by endonucleolytic cleavage of the pre-mRNA in a snRNP-dependent in vitro reaction. *The EMBO journal* **5**, 1319-1326
87. Proudfoot, N. (2004) New perspectives on connecting messenger RNA 3' end formation to transcription. *Current opinion in cell biology* **16**, 272-278
88. Hirose, Y., and Manley, J. L. (1998) RNA polymerase II is an essential mRNA polyadenylation factor. *Nature* **395**, 93-96
89. Ryan, K., Murthy, K. G., Kaneko, S., and Manley, J. L. (2002) Requirements of the RNA polymerase II C-terminal domain for reconstituting pre-mRNA 3' cleavage. *Molecular and cellular biology* **22**, 1684-1692
90. Edwalds-Gilbert, G., Veraldi, K. L., and Milcarek, C. (1997) Alternative poly(A) site selection in complex transcription units: means to an end? *Nucleic acids research* **25**, 2547-2561
91. Lutz, C. S., and Moreira, A. (2011) Alternative mRNA polyadenylation in eukaryotes: an effective regulator of gene expression. *Wiley interdisciplinary reviews. RNA* **2**, 22-31
92. Sandberg, R., Neilson, J. R., Sarma, A., Sharp, P. A., and Burge, C. B. (2008) Proliferating cells express mRNAs with shortened 3' untranslated regions and fewer microRNA target sites. *Science* **320**, 1643-1647
93. Mayr, C., and Bartel, D. P. (2009) Widespread shortening of 3'UTRs by alternative cleavage and polyadenylation activates oncogenes in cancer cells. *Cell* **138**, 673-684
94. Szostak, E., and Gebauer, F. (2013) Translational control by 3'-UTR-binding proteins. *Briefings in functional genomics* **12**, 58-65
95. Goss, D. J., and Kleiman, F. E. (2013) Poly(A) binding proteins: are they all created equal? *Wiley interdisciplinary reviews. RNA* **4**, 167-179
96. Banerjee, A., Apponi, L. H., Pavlath, G. K., and Corbett, A. H. (2013) PABPN1: molecular function and muscle disease. *The FEBS journal* **280**, 4230-4250
97. Mangus, D. A., Evans, M. C., and Jacobson, A. (2003) Poly(A)-binding proteins: multifunctional scaffolds for the post-transcriptional control of gene expression. *Genome biology* **4**, 223
98. Kuhn, U., Nemeth, A., Meyer, S., and Wahle, E. (2003) The RNA binding domains of the nuclear poly(A)-binding protein. *The Journal of biological chemistry* **278**, 16916-16925
99. Nemeth, A., Krause, S., Blank, D., Jenny, A., Jeno, P., Lustig, A., and Wahle, E. (1995) Isolation of genomic and cDNA clones encoding bovine poly(A) binding protein II. *Nucleic acids research* **23**, 4034-4041

100. Meyer, S., Urbanke, C., and Wahle, E. (2002) Equilibrium studies on the association of the nuclear poly(A) binding protein with poly(A) of different lengths. *Biochemistry* **41**, 6082-6089
101. Smith, J. J., Rucknagel, K. P., Schierhorn, A., Tang, J., Nemeth, A., Linder, M., Herschman, H. R., and Wahle, E. (1999) Unusual sites of arginine methylation in Poly(A)-binding protein II and in vitro methylation by protein arginine methyltransferases PRMT1 and PRMT3. *The Journal of biological chemistry* **274**, 13229-13234
102. Fronz, K., Guttinger, S., Burkert, K., Kuhn, U., Stohr, N., Schierhorn, A., and Wahle, E. (2011) Arginine methylation of the nuclear poly(a) binding protein weakens the interaction with its nuclear import receptor, transportin. *The Journal of biological chemistry* **286**, 32986-32994
103. Wahle, E., and Moritz, B. (2013) Methylation of the nuclear poly(A)-binding protein by type I protein arginine methyltransferases - how and why. *Biological chemistry* **394**, 1029-1043
104. Wahle, E. (1991) A novel poly(A)-binding protein acts as a specificity factor in the second phase of messenger RNA polyadenylation. *Cell* **66**, 759-768
105. Kerwitz, Y., Kuhn, U., Lilie, H., Knoth, A., Scheuermann, T., Friedrich, H., Schwarz, E., and Wahle, E. (2003) Stimulation of poly(A) polymerase through a direct interaction with the nuclear poly(A) binding protein allosterically regulated by RNA. *The EMBO journal* **22**, 3705-3714
106. Chan, S., Choi, E. A., and Shi, Y. (2011) Pre-mRNA 3'-end processing complex assembly and function. *Wiley interdisciplinary reviews. RNA* **2**, 321-335
107. Keller, R. W., Kuhn, U., Aragon, M., Bornikova, L., Wahle, E., and Bear, D. G. (2000) The nuclear poly(A) binding protein, PABP2, forms an oligomeric particle covering the length of the poly(A) tail. *Journal of molecular biology* **297**, 569-583
108. Calado, A., Tome, F. M., Brais, B., Rouleau, G. A., Kuhn, U., Wahle, E., and Carmo-Fonseca, M. (2000) Nuclear inclusions in oculopharyngeal muscular dystrophy consist of poly(A) binding protein 2 aggregates which sequester poly(A) RNA. *Human molecular genetics* **9**, 2321-2328
109. Chen, Z., Li, Y., and Krug, R. M. (1999) Influenza A virus NS1 protein targets poly(A)-binding protein II of the cellular 3'-end processing machinery. *The EMBO journal* **18**, 2273-2283
110. Apponi, L. H., Leung, S. W., Williams, K. R., Valentini, S. R., Corbett, A. H., and Pavlath, G. K. (2010) Loss of nuclear poly(A)-binding protein 1 causes defects in myogenesis and mRNA biogenesis. *Human molecular genetics* **19**, 1058-1065
111. Eckner, R., Ellmeier, W., and Birnstiel, M. L. (1991) Mature mRNA 3' end formation stimulates RNA export from the nucleus. *The EMBO journal* **10**, 3513-3522
112. Huang, Y., and Carmichael, G. G. (1996) Role of polyadenylation in nucleocytoplasmic transport of mRNA. *Molecular and cellular biology* **16**, 1534-1542
113. Poon, L. L., Fodor, E., and Brownlee, G. G. (2000) Polyuridylated mRNA synthesized by a recombinant influenza virus is defective in nuclear export. *Journal of virology* **74**, 418-427

114. Dower, K., Kuperwasser, N., Merrikh, H., and Rosbash, M. (2004) A synthetic A tail rescues yeast nuclear accumulation of a ribozyme-terminated transcript. *Rna* **10**, 1888-1899
115. Kuhn, U., and Wahle, E. (2004) Structure and function of poly(A) binding proteins. *Biochimica et biophysica acta* **1678**, 67-84
116. Sachs, A. B., Davis, R. W., and Kornberg, R. D. (1987) A single domain of yeast poly(A)-binding protein is necessary and sufficient for RNA binding and cell viability. *Molecular and cellular biology* **7**, 3268-3276
117. Kuhn, U., and Pieler, T. (1996) Xenopus poly(A) binding protein: functional domains in RNA binding and protein-protein interaction. *Journal of molecular biology* **256**, 20-30
118. Baer, B. W., and Kornberg, R. D. (1983) The protein responsible for the repeating structure of cytoplasmic poly(A)-ribonucleoprotein. *The Journal of cell biology* **96**, 717-721
119. Tarun, S. Z., Jr., Wells, S. E., Deardorff, J. A., and Sachs, A. B. (1997) Translation initiation factor eIF4G mediates in vitro poly(A) tail-dependent translation. *Proceedings of the National Academy of Sciences of the United States of America* **94**, 9046-9051
120. Hoshino, S., Imai, M., Kobayashi, T., Uchida, N., and Katada, T. (1999) The eukaryotic polypeptide chain releasing factor (eRF3/GSPT) carrying the translation termination signal to the 3'-Poly(A) tail of mRNA. Direct association of erf3/GSPT with polyadenylate-binding protein. *The Journal of biological chemistry* **274**, 16677-16680
121. Lin, J., Fabian, M., Sonenberg, N., and Meller, A. (2012) Nanopore detachment kinetics of poly(A) binding proteins from RNA molecules reveals the critical role of C-terminus interactions. *Biophysical journal* **102**, 1427-1434
122. Gray, N. K., Coller, J. M., Dickson, K. S., and Wickens, M. (2000) Multiple portions of poly(A)-binding protein stimulate translation in vivo. *The EMBO journal* **19**, 4723-4733
123. Khaleghpour, K., Kahvejian, A., De Crescenzo, G., Roy, G., Svitkin, Y. V., Imataka, H., O'Connor-McCourt, M., and Sonenberg, N. (2001) Dual interactions of the translational repressor Paip2 with poly(A) binding protein. *Molecular and cellular biology* **21**, 5200-5213
124. Braun, J. E., Huntzinger, E., and Izaurralde, E. (2013) The role of GW182 proteins in miRNA-mediated gene silencing. *Advances in experimental medicine and biology* **768**, 147-163
125. Kahvejian, A., Roy, G., and Sonenberg, N. (2001) The mRNA closed-loop model: the function of PABP and PABP-interacting proteins in mRNA translation. *Cold Spring Harbor symposia on quantitative biology* **66**, 293-300
126. Tarun, S. Z., Jr., and Sachs, A. B. (1995) A common function for mRNA 5' and 3' ends in translation initiation in yeast. *Genes & development* **9**, 2997-3007
127. Tarun, S. Z., Jr., and Sachs, A. B. (1996) Association of the yeast poly(A) tail binding protein with translation initiation factor eIF-4G. *The EMBO journal* **15**, 7168-7177
128. Wells, S. E., Hillner, P. E., Vale, R. D., and Sachs, A. B. (1998) Circularization of mRNA by eukaryotic translation initiation factors. *Molecular cell* **2**, 135-140

129. Kahvejian, A., Svitkin, Y. V., Sukarieh, R., M'Boutchou, M. N., and Sonenberg, N. (2005) Mammalian poly(A)-binding protein is a eukaryotic translation initiation factor, which acts via multiple mechanisms. *Genes & development* **19**, 104-113
130. Munroe, D., and Jacobson, A. (1990) mRNA poly(A) tail, a 3' enhancer of translational initiation. *Molecular and cellular biology* **10**, 3441-3455
131. Searfoss, A., Dever, T. E., and Wickner, R. (2001) Linking the 3' poly(A) tail to the subunit joining step of translation initiation: relations of Pab1p, eukaryotic translation initiation factor 5b (Fun12p), and Ski2p-Slh1p. *Molecular and cellular biology* **21**, 4900-4908
132. Uchida, N., Hoshino, S., Imataka, H., Sonenberg, N., and Katada, T. (2002) A novel role of the mammalian GSPT/eRF3 associating with poly(A)-binding protein in Cap/Poly(A)-dependent translation. *The Journal of biological chemistry* **277**, 50286-50292
133. Tucker, M., Staples, R. R., Valencia-Sanchez, M. A., Muhlrad, D., and Parker, R. (2002) Ccr4p is the catalytic subunit of a Ccr4p/Pop2p/Notp mRNA deadenylase complex in Saccharomyces cerevisiae. *The EMBO journal* **21**, 1427-1436
134. Wang, Z., Day, N., Trifillis, P., and Kiledjian, M. (1999) An mRNA stability complex functions with poly(A)-binding protein to stabilize mRNA in vitro. *Molecular and cellular biology* **19**, 4552-4560
135. Wang, Z., and Kiledjian, M. (2000) The poly(A)-binding protein and an mRNA stability protein jointly regulate an endoribonuclease activity. *Molecular and cellular biology* **20**, 6334-6341
136. Grosset, C., Chen, C. Y., Xu, N., Sonenberg, N., Jacquemin-Sablon, H., and Shyu, A. B. (2000) A mechanism for translationally coupled mRNA turnover: interaction between the poly(A) tail and a c-fos RNA coding determinant via a protein complex. *Cell* **103**, 29-40
137. de Klerk, E., Venema, A., Anvar, S. Y., Goeman, J. J., Hu, O., Trollet, C., Dickson, G., den Dunnen, J. T., van der Maarel, S. M., Raz, V., and t Hoen, P. A. (2012) Poly(A) binding protein nuclear 1 levels affect alternative polyadenylation. *Nucleic acids research* **40**, 9089-9101
138. Jenal, M., Elkon, R., Loayza-Puch, F., van Haaften, G., Kuhn, U., Menzies, F. M., Oude Vrielink, J. A., Bos, A. J., Drost, J., Rooijers, K., Rubinsztein, D. C., and Agami, R. (2012) The poly(A)-binding protein nuclear 1 suppresses alternative cleavage and polyadenylation sites. *Cell* **149**, 538-553
139. Beaulieu, Y. B., Kleinman, C. L., Landry-Voyer, A. M., Majewski, J., and Bachand, F. (2012) Polyadenylation-dependent control of long noncoding RNA expression by the poly(A)-binding protein nuclear 1. *PLoS genetics* **8**, e1003078
140. Bresson, S. M., and Conrad, N. K. (2013) The human nuclear poly(a)-binding protein promotes RNA hyperadenylation and decay. *PLoS genetics* **9**, e1003893
141. Sato, H., and Maquat, L. E. (2009) Remodeling of the pioneer translation initiation complex involves translation and the karyopherin importin beta. *Genes & development* **23**, 2537-2550
142. Amrani, N., Ganesan, R., Kervestin, S., Mangus, D. A., Ghosh, S., and Jacobson, A. (2004) A faux 3'-UTR promotes aberrant termination and triggers nonsense-mediated mRNA decay. *Nature* **432**, 112-118

143. Dai, L., Taylor, M. S., O'Donnell, K. A., and Boeke, J. D. (2012) Poly(A) binding protein C1 is essential for efficient L1 retrotransposition and affects L1 RNP formation. *Molecular and cellular biology* **32**, 4323-4336
144. Muddashetty, R., Khanam, T., Kondrashov, A., Bundman, M., Iacoangeli, A., Kremerskothen, J., Duning, K., Barnekow, A., Huttenhofer, A., Tiedge, H., and Brosius, J. (2002) Poly(A)-binding protein is associated with neuronal BC1 and BC200 ribonucleoprotein particles. *Journal of molecular biology* **321**, 433-445
145. Vazquez-Pianzola, P., Urlaub, H., and Suter, B. (2011) Pabp binds to the osk 3'UTR and specifically contributes to osk mRNA stability and oocyte accumulation. *Developmental biology* **357**, 404-418
146. Mohr, E., Prakash, N., Vieluf, K., Fuhrmann, C., Buck, F., and Richter, D. (2001) Vasopressin mRNA localization in nerve cells: characterization of cis-acting elements and trans-acting factors. *Proceedings of the National Academy of Sciences of the United States of America* **98**, 7072-7079
147. Skabkina, O. V., Skabkin, M. A., Popova, N. V., Lyabin, D. N., Penalva, L. O., and Ovchinnikov, L. P. (2003) Poly(A)-binding protein positively affects YB-1 mRNA translation through specific interaction with YB-1 mRNA. *The Journal of biological chemistry* **278**, 18191-18198
148. Kelly, S. M., Pabit, S. A., Kitchen, C. M., Guo, P., Marfatia, K. A., Murphy, T. J., Corbett, A. H., and Berland, K. M. (2007) Recognition of polyadenosine RNA by zinc finger proteins. *Proceedings of the National Academy of Sciences of the United States of America* **104**, 12306-12311
149. Anderson, J. T., Wilson, S. M., Datar, K. V., and Swanson, M. S. (1993) NAB2: a yeast nuclear polyadenylated RNA-binding protein essential for cell viability. *Molecular and cellular biology* **13**, 2730-2741
150. Pak, C., Garshasbi, M., Kahrizi, K., Gross, C., Apponi, L. H., Noto, J. J., Kelly, S. M., Leung, S. W., Tzschach, A., Behjati, F., Abedini, S. S., Mohseni, M., Jensen, L. R., Hu, H., Huang, B., Stahley, S. N., Liu, G., Williams, K. R., Burdick, S., Feng, Y., Sanyal, S., Bassell, G. J., Ropers, H. H., Najmabadi, H., Corbett, A. H., Moberg, K. H., and Kuss, A. W. (2011) Mutation of the conserved polyadenosine RNA binding protein, ZC3H14/dNab2, impairs neural function in Drosophila and humans. *Proceedings of the National Academy of Sciences of the United States of America* **108**, 12390-12395
151. Guthrie, C. R., Schellenberg, G. D., and Kraemer, B. C. (2009) SUT-2 potentiates tau-induced neurotoxicity in Caenorhabditis elegans. *Human molecular genetics* **18**, 1825-1838
152. Guthrie, C. R., Greenup, L., Leverenz, J. B., and Kraemer, B. C. (2011) MSUT2 is a determinant of susceptibility to tau neurotoxicity. *Human molecular genetics* **20**, 1989-1999
153. Fasken, M. B., Stewart, M., and Corbett, A. H. (2008) Functional significance of the interaction between the mRNA-binding protein, Nab2, and the nuclear pore-associated protein, Mlp1, in mRNA export. *The Journal of biological chemistry* **283**, 27130-27143
154. Leung, S. W., Apponi, L. H., Cornejo, O. E., Kitchen, C. M., Valentini, S. R., Pavlath, G. K., Dunham, C. M., and Corbett, A. H. (2009) Splice variants of the

human ZC3H14 gene generate multiple isoforms of a zinc finger polyadenosine RNA binding protein. *Gene* **439**, 71-78
155. Lamond, A. I., and Spector, D. L. (2003) Nuclear speckles: a model for nuclear organelles. *Nature reviews. Molecular cell biology* **4**, 605-612
156. Hurwitz, J., Furth, J. J., Malamy, M., and Alexander, M. (1962) The role of deoxyribonucleic acid in ribonucleic acid synthesis. III. The inhibition of the enzymatic synthesis of ribonucleic acid and deoxyribonucleic acid by actinomycin D and proflavin. *Proceedings of the National Academy of Sciences of the United States of America* **48**, 1222-1230
157. Spector, D. L., Schrier, W. H., and Busch, H. (1983) Immunoelectron microscopic localization of snRNPs. *Biology of the cell / under the auspices of the European Cell Biology Organization* **49**, 1-10
158. von Roretz, C., Di Marco, S., Mazroui, R., and Gallouzi, I. E. (2011) Turnover of AU-rich-containing mRNAs during stress: a matter of survival. *Wiley interdisciplinary reviews. RNA* **2**, 336-347
159. Green, D. M., Marfatia, K. A., Crafton, E. B., Zhang, X., Cheng, X., and Corbett, A. H. (2002) Nab2p is required for poly(A) RNA export in Saccharomyces cerevisiae and is regulated by arginine methylation via Hmt1p. *The Journal of biological chemistry* **277**, 7752-7760
160. Tuck, A. C., and Tollervey, D. (2013) A transcriptome-wide atlas of RNP composition reveals diverse classes of mRNAs and lncRNAs. *Cell* **154**, 996-1009
161. Sharon Soucek, Y. Z., Deepti L. Bellur, Megan Bergkessel, Christine Guthrie, Jonathan P. Staley, Anita H. Corbett. (2014) A Role for the Polyadenosine RNA Binding Protein, Nab2, in Splicing and RNA Surveillance. *Molecular biology of the cell* **In resubmission.**
162. Marfatia, K. A., Crafton, E. B., Green, D. M., and Corbett, A. H. (2003) Domain analysis of the Saccharomyces cerevisiae heterogeneous nuclear ribonucleoprotein, Nab2p. Dissecting the requirements for Nab2p-facilitated poly(A) RNA export. *The Journal of biological chemistry* **278**, 6731-6740
163. Soucek, S., Corbett, A. H., and Fasken, M. B. (2012) The long and the short of it: the role of the zinc finger polyadenosine RNA binding protein, Nab2, in control of poly(A) tail length. *Biochimica et biophysica acta* **1819**, 546-554
164. Brockmann, C., Soucek, S., Kuhlmann, S. I., Mills-Lujan, K., Kelly, S. M., Yang, J. C., Iglesias, N., Stutz, F., Corbett, A. H., Neuhaus, D., and Stewart, M. (2012) Structural basis for polyadenosine-RNA binding by Nab2 Zn fingers and its function in mRNA nuclear export. *Structure* **20**, 1007-1018
165. Kuhlmann, S. I., Valkov, E., and Stewart, M. (2013) Structural basis for the molecular recognition of polyadenosine RNA by Nab2 Zn fingers. *Nucleic acids research*
166. Viphakone, N., Voisinet-Hakil, F., and Minvielle-Sebastia, L. (2008) Molecular dissection of mRNA poly(A) tail length control in yeast. *Nucleic acids research* **36**, 2418-2433
167. Kelly, S. M., Leung, S. W., Apponi, L. H., Bramley, A. M., Tran, E. J., Chekanova, J. A., Wente, S. R., and Corbett, A. H. (2010) Recognition of polyadenosine RNA by the zinc finger domain of nuclear poly(A) RNA-binding

protein 2 (Nab2) is required for correct mRNA 3'-end formation. *The Journal of biological chemistry* **285**, 26022-26032

168. Kelly, S. M. L., S. W.; Pak, C.; Banerjee, A.; Moberg, K. H.; Corbett, A. H. (2014) A Conserved Role for the Zinc Finger Polyadenosine RNA Binding Protein, ZC3H14, in Control of Poly(A) Tail Length. *Rna* **In Submission**
169. Rankin, C. A., and Gamblin, T. C. (2008) Assessing the toxicity of tau aggregation. *Journal of Alzheimer's disease : JAD* **14**, 411-416
170. Grenier St-Sauveur, V., Soucek, S., Corbett, A. H., and Bachand, F. (2013) Poly(A) tail-mediated gene regulation by opposing roles of Nab2 and Pab2 nuclear poly(A)-binding proteins in pre-mRNA decay. *Molecular and cellular biology* **33**, 4718-4731
171. Lenzken, S. C., Achsel, T., Carri, M. T., and Barabino, S. M. (2014) Neuronal RNA-binding proteins in health and disease. *Wiley interdisciplinary reviews. RNA* **5**, 565-576
172. Miura, P., Shenker, S., Andreu-Agullo, C., Westholm, J. O., and Lai, E. C. (2013) Widespread and extensive lengthening of 3' UTRs in the mammalian brain. *Genome research* **23**, 812-825
173. Wang, L., and Yi, R. (2014) 3'UTRs take a long shot in the brain. *BioEssays : news and reviews in molecular, cellular and developmental biology* **36**, 39-45
174. Mouse Genome Sequencing, C., Waterston, R. H., Lindblad-Toh, K., Birney, E., Rogers, J., Abril, J. F., Agarwal, P., Agarwala, R., Ainscough, R., Alexandersson, M., An, P., Antonarakis, S. E., Attwood, J., Baertsch, R., Bailey, J., Barlow, K., Beck, S., Berry, E., Birren, B., Bloom, T., Bork, P., Botcherby, M., Bray, N., Brent, M. R., Brown, D. G., Brown, S. D., Bult, C., Burton, J., Butler, J., Campbell, R. D., Carninci, P., Cawley, S., Chiaromonte, F., Chinwalla, A. T., Church, D. M., Clamp, M., Clee, C., Collins, F. S., Cook, L. L., Copley, R. R., Coulson, A., Couronne, O., Cuff, J., Curwen, V., Cutts, T., Daly, M., David, R., Davies, J., Delehaunty, K. D., Deri, J., Dermitzakis, E. T., Dewey, C., Dickens, N. J., Diekhans, M., Dodge, S., Dubchak, I., Dunn, D. M., Eddy, S. R., Elnitski, L., Emes, R. D., Eswara, P., Eyras, E., Felsenfeld, A., Fewell, G. A., Flicek, P., Foley, K., Frankel, W. N., Fulton, L. A., Fulton, R. S., Furey, T. S., Gage, D., Gibbs, R. A., Glusman, G., Gnerre, S., Goldman, N., Goodstadt, L., Grafham, D., Graves, T. A., Green, E. D., Gregory, S., Guigo, R., Guyer, M., Hardison, R. C., Haussler, D., Hayashizaki, Y., Hillier, L. W., Hinrichs, A., Hlavina, W., Holzer, T., Hsu, F., Hua, A., Hubbard, T., Hunt, A., Jackson, I., Jaffe, D. B., Johnson, L. S., Jones, M., Jones, T. A., Joy, A., Kamal, M., Karlsson, E. K., Karolchik, D., Kasprzyk, A., Kawai, J., Keibler, E., Kells, C., Kent, W. J., Kirby, A., Kolbe, D. L., Korf, I., Kucherlapati, R. S., Kulbokas, E. J., Kulp, D., Landers, T., Leger, J. P., Leonard, S., Letunic, I., Levine, R., Li, J., Li, M., Lloyd, C., Lucas, S., Ma, B., Maglott, D. R., Mardis, E. R., Matthews, L., Mauceli, E., Mayer, J. H., McCarthy, M., McCombie, W. R., McLaren, S., McLay, K., McPherson, J. D., Meldrim, J., Meredith, B., Mesirov, J. P., Miller, W., Miner, T. L., Mongin, E., Montgomery, K. T., Morgan, M., Mott, R., Mullikin, J. C., Muzny, D. M., Nash, W. E., Nelson, J. O., Nhan, M. N., Nicol, R., Ning, Z., Nusbaum, C., O'Connor, M. J., Okazaki, Y., Oliver, K., Overton-Larty, E., Pachter, L., Parra, G., Pepin, K. H., Peterson, J., Pevzner, P., Plumb, R., Pohl, C. S., Poliakov, A., Ponce, T. C., Ponting, C. P.,

Potter, S., Quail, M., Reymond, A., Roe, B. A., Roskin, K. M., Rubin, E. M., Rust, A. G., Santos, R., Sapojnikov, V., Schultz, B., Schultz, J., Schwartz, M. S., Schwartz, S., Scott, C., Seaman, S., Searle, S., Sharpe, T., Sheridan, A., Shownkeen, R., Sims, S., Singer, J. B., Slater, G., Smit, A., Smith, D. R., Spencer, B., Stabenau, A., Stange-Thomann, N., Sugnet, C., Suyama, M., Tesler, G., Thompson, J., Torrents, D., Trevaskis, E., Tromp, J., Ucla, C., Ureta-Vidal, A., Vinson, J. P., Von Niederhausern, A. C., Wade, C. M., Wall, M., Weber, R. J., Weiss, R. B., Wendl, M. C., West, A. P., Wetterstrand, K., Wheeler, R., Whelan, S., Wierzbowski, J., Willey, D., Williams, S., Wilson, R. K., Winter, E., Worley, K. C., Wyman, D., Yang, S., Yang, S. P., Zdobnov, E. M., Zody, M. C., and Lander, E. S. (2002) Initial sequencing and comparative analysis of the mouse genome. *Nature* **420**, 520-562

175. Eom, T., Antar, L. N., Singer, R. H., and Bassell, G. J. (2003) Localization of a beta-actin messenger ribonucleoprotein complex with zipcode-binding protein modulates the density of dendritic filopodia and filopodial synapses. *The Journal of neuroscience : the official journal of the Society for Neuroscience* **23**, 10433-10444
176. Jambhekar, A., and Derisi, J. L. (2007) Cis-acting determinants of asymmetric, cytoplasmic RNA transport. *Rna* **13**, 625-642
177. Richter, J. D. (2007) CPEB: a life in translation. *Trends in biochemical sciences* **32**, 279-285
178. Barreau, C., Paillard, L., and Osborne, H. B. (2005) AU-rich elements and associated factors: are there unifying principles? *Nucleic acids research* **33**, 7138-7150
179. Chi, S. W., Zang, J. B., Mele, A., and Darnell, R. B. (2009) Argonaute HITS-CLIP decodes microRNA-mRNA interaction maps. *Nature* **460**, 479-486
180. Ho, J. J., and Marsden, P. A. (2014) Competition and collaboration between RNA-binding proteins and microRNAs. *Wiley interdisciplinary reviews. RNA* **5**, 69-86
181. Boutet, S. C., Cheung, T. H., Quach, N. L., Liu, L., Prescott, S. L., Edalati, A., Iori, K., and Rando, T. A. (2012) Alternative polyadenylation mediates microRNA regulation of muscle stem cell function. *Cell stem cell* **10**, 327-336
182. Ji, Z., and Tian, B. (2009) Reprogramming of 3' untranslated regions of mRNAs by alternative polyadenylation in generation of pluripotent stem cells from different cell types. *PloS one* **4**, e8419
183. Zammit, P. S., Relaix, F., Nagata, Y., Ruiz, A. P., Collins, C. A., Partridge, T. A., and Beauchamp, J. R. (2006) Pax7 and myogenic progression in skeletal muscle satellite cells. *Journal of cell science* **119**, 1824-1832
184. Kim, H. K., Lee, Y. S., Sivaprasad, U., Malhotra, A., and Dutta, A. (2006) Muscle-specific microRNA miR-206 promotes muscle differentiation. *The Journal of cell biology* **174**, 677-687
185. Wang, L., Dowell, R. D., and Yi, R. (2013) Genome-wide maps of polyadenylation reveal dynamic mRNA 3'-end formation in mammalian cell lineages. *Rna* **19**, 413-425
186. Caput, D., Beutler, B., Hartog, K., Thayer, R., Brown-Shimer, S., and Cerami, A. (1986) Identification of a common nucleotide sequence in the 3'-untranslated

region of mRNA molecules specifying inflammatory mediators. *Proceedings of the National Academy of Sciences of the United States of America* **83**, 1670-1674
187. Milde-Langosch, K. (2005) The Fos family of transcription factors and their role in tumourigenesis. *European journal of cancer* **41**, 2449-2461
188. Treisman, R. (1985) Transient accumulation of c-fos RNA following serum stimulation requires a conserved 5' element and c-fos 3' sequences. *Cell* **42**, 889-902
189. Shaw, G., and Kamen, R. (1986) A conserved AU sequence from the 3' untranslated region of GM-CSF mRNA mediates selective mRNA degradation. *Cell* **46**, 659-667
190. Lee, W. M., Lin, C., and Curran, T. (1988) Activation of the transforming potential of the human fos proto-oncogene requires message stabilization and results in increased amounts of partially modified fos protein. *Molecular and cellular biology* **8**, 5521-5527
191. Piecyk, M., Wax, S., Beck, A. R., Kedersha, N., Gupta, M., Maritim, B., Chen, S., Gueydan, C., Kruys, V., Streuli, M., and Anderson, P. (2000) TIA-1 is a translational silencer that selectively regulates the expression of TNF-alpha. *The EMBO journal* **19**, 4154-4163
192. Del Gatto-Konczak, F., Bourgeois, C. F., Le Guiner, C., Kister, L., Gesnel, M. C., Stevenin, J., and Breathnach, R. (2000) The RNA-binding protein TIA-1 is a novel mammalian splicing regulator acting through intron sequences adjacent to a 5' splice site. *Molecular and cellular biology* **20**, 6287-6299
193. Simone, L. E., and Keene, J. D. (2013) Mechanisms coordinating ELAV/Hu mRNA regulons. *Current opinion in genetics & development* **23**, 35-43
194. Halees, A. S., El-Badrawi, R., and Khabar, K. S. (2008) ARED Organism: expansion of ARED reveals AU-rich element cluster variations between human and mouse. *Nucleic acids research* **36**, D137-140
195. Pullmann, R., Jr., Kim, H. H., Abdelmohsen, K., Lal, A., Martindale, J. L., Yang, X., and Gorospe, M. (2007) Analysis of turnover and translation regulatory RNA-binding protein expression through binding to cognate mRNAs. *Molecular and cellular biology* **27**, 6265-6278
196. Szabo, A., Dalmau, J., Manley, G., Rosenfeld, M., Wong, E., Henson, J., Posner, J. B., and Furneaux, H. M. (1991) HuD, a paraneoplastic encephalomyelitis antigen, contains RNA-binding domains and is homologous to Elav and Sex-lethal. *Cell* **67**, 325-333
197. Robinow, S., Campos, A. R., Yao, K. M., and White, K. (1988) The elav gene product of Drosophila, required in neurons, has three RNP consensus motifs. *Science* **242**, 1570-1572
198. Hinman, M. N., and Lou, H. (2008) Diverse molecular functions of Hu proteins. *Cellular and molecular life sciences : CMLS* **65**, 3168-3181
199. King, P. H., Levine, T. D., Fremeau, R. T., Jr., and Keene, J. D. (1994) Mammalian homologs of Drosophila ELAV localized to a neuronal subset can bind in vitro to the 3' UTR of mRNA encoding the Id transcriptional repressor. *The Journal of neuroscience : the official journal of the Society for Neuroscience* **14**, 1943-1952

200. Levine, T. D., Gao, F., King, P. H., Andrews, L. G., and Keene, J. D. (1993) Hel-N1: an autoimmune RNA-binding protein with specificity for 3' uridylate-rich untranslated regions of growth factor mRNAs. *Molecular and cellular biology* **13**, 3494-3504
201. Liu, J., Dalmau, J., Szabo, A., Rosenfeld, M., Huber, J., and Furneaux, H. (1995) Paraneoplastic encephalomyelitis antigens bind to the AU-rich elements of mRNA. *Neurology* **45**, 544-550
202. Ince-Dunn, G., Okano, H. J., Jensen, K. B., Park, W. Y., Zhong, R., Ule, J., Mele, A., Fak, J. J., Yang, C., Zhang, C., Yoo, J., Herre, M., Okano, H., Noebels, J. L., and Darnell, R. B. (2012) Neuronal Elav-like (Hu) proteins regulate RNA splicing and abundance to control glutamate levels and neuronal excitability. *Neuron* **75**, 1067-1080
203. Ma, W. J., Cheng, S., Campbell, C., Wright, A., and Furneaux, H. (1996) Cloning and characterization of HuR, a ubiquitously expressed Elav-like protein. *The Journal of biological chemistry* **271**, 8144-8151
204. Abe, R., Sakashita, E., Yamamoto, K., and Sakamoto, H. (1996) Two different RNA binding activities for the AU-rich element and the poly(A) sequence of the mouse neuronal protein mHuC. *Nucleic acids research* **24**, 4895-4901
205. Ma, W. J., Chung, S., and Furneaux, H. (1997) The Elav-like proteins bind to AU-rich elements and to the poly(A) tail of mRNA. *Nucleic acids research* **25**, 3564-3569
206. Wang, H., Zeng, F., Liu, Q., Liu, H., Liu, Z., Niu, L., Teng, M., and Li, X. (2013) The structure of the ARE-binding domains of Hu antigen R (HuR) undergoes conformational changes during RNA binding. *Acta crystallographica. Section D, Biological crystallography* **69**, 373-380
207. Fan, X. C., and Steitz, J. A. (1998) HNS, a nuclear-cytoplasmic shuttling sequence in HuR. *Proceedings of the National Academy of Sciences of the United States of America* **95**, 15293-15298
208. Doller, A., Pfeilschifter, J., and Eberhardt, W. (2008) Signalling pathways regulating nucleo-cytoplasmic shuttling of the mRNA-binding protein HuR. *Cellular signalling* **20**, 2165-2173
209. Brennan, C. M., and Steitz, J. A. (2001) HuR and mRNA stability. *Cellular and molecular life sciences : CMLS* **58**, 266-277
210. Chen, C. Y., Xu, N., and Shyu, A. B. (2002) Highly selective actions of HuR in antagonizing AU-rich element-mediated mRNA destabilization. *Molecular and cellular biology* **22**, 7268-7278
211. Fan, X. C., and Steitz, J. A. (1998) Overexpression of HuR, a nuclear-cytoplasmic shuttling protein, increases the in vivo stability of ARE-containing mRNAs. *The EMBO journal* **17**, 3448-3460
212. Peng, S. S., Chen, C. Y., Xu, N., and Shyu, A. B. (1998) RNA stabilization by the AU-rich element binding protein, HuR, an ELAV protein. *The EMBO journal* **17**, 3461-3470
213. Lal, A., Mazan-Mamczarz, K., Kawai, T., Yang, X., Martindale, J. L., and Gorospe, M. (2004) Concurrent versus individual binding of HuR and AUF1 to common labile target mRNAs. *The EMBO journal* **23**, 3092-3102

214. Dean, J. L., Wait, R., Mahtani, K. R., Sully, G., Clark, A. R., and Saklatvala, J. (2001) The 3' untranslated region of tumor necrosis factor alpha mRNA is a target of the mRNA-stabilizing factor HuR. *Molecular and cellular biology* **21**, 721-730
215. Sengupta, S., Jang, B. C., Wu, M. T., Paik, J. H., Furneaux, H., and Hla, T. (2003) The RNA-binding protein HuR regulates the expression of cyclooxygenase-2. *The Journal of biological chemistry* **278**, 25227-25233
216. Srikantan, S., Tominaga, K., and Gorospe, M. (2012) Functional interplay between RNA-binding protein HuR and microRNAs. *Current protein & peptide science* **13**, 372-379
217. Kim, H. H., Kuwano, Y., Srikantan, S., Lee, E. K., Martindale, J. L., and Gorospe, M. (2009) HuR recruits let-7/RISC to repress c-Myc expression. *Genes & development* **23**, 1743-1748
218. Abdelmohsen, K., Panda, A. C., Kang, M. J., Guo, R., Kim, J., Grammatikakis, I., Yoon, J. H., Dudekula, D. B., Noh, J. H., Yang, X., Martindale, J. L., and Gorospe, M. (2014) 7SL RNA represses p53 translation by competing with HuR. *Nucleic acids research* **42**, 10099-10111
219. Galban, S., Kuwano, Y., Pullmann, R., Jr., Martindale, J. L., Kim, H. H., Lal, A., Abdelmohsen, K., Yang, X., Dang, Y., Liu, J. O., Lewis, S. M., Holcik, M., and Gorospe, M. (2008) RNA-binding proteins HuR and PTB promote the translation of hypoxia-inducible factor 1alpha. *Molecular and cellular biology* **28**, 93-107
220. Kawai, T., Lal, A., Yang, X., Galban, S., Mazan-Mamczarz, K., and Gorospe, M. (2006) Translational control of cytochrome c by RNA-binding proteins TIA-1 and HuR. *Molecular and cellular biology* **26**, 3295-3307
221. Al-Ahmadi, W., Al-Ghamdi, M., Al-Haj, L., Al-Saif, M., and Khabar, K. S. (2009) Alternative polyadenylation variants of the RNA binding protein, HuR: abundance, role of AU-rich elements and auto-Regulation. *Nucleic acids research* **37**, 3612-3624
222. Dai, W., Zhang, G., and Makeyev, E. V. (2012) RNA-binding protein HuR autoregulates its expression by promoting alternative polyadenylation site usage. *Nucleic acids research* **40**, 787-800
223. Izquierdo, J. M. (2008) Hu antigen R (HuR) functions as an alternative pre-mRNA splicing regulator of Fas apoptosis-promoting receptor on exon definition. *The Journal of biological chemistry* **283**, 19077-19084
224. Lebedeva, S., Jens, M., Theil, K., Schwanhausser, B., Selbach, M., Landthaler, M., and Rajewsky, N. (2011) Transcriptome-wide analysis of regulatory interactions of the RNA-binding protein HuR. *Molecular cell* **43**, 340-352
225. Mukherjee, N., Corcoran, D. L., Nusbaum, J. D., Reid, D. W., Georgiev, S., Hafner, M., Ascano, M., Jr., Tuschl, T., Ohler, U., and Keene, J. D. (2011) Integrative regulatory mapping indicates that the RNA-binding protein HuR couples pre-mRNA processing and mRNA stability. *Molecular cell* **43**, 327-339
226. Forch, P., and Valcarcel, J. (2001) Molecular mechanisms of gene expression regulation by the apoptosis-promoting protein TIA-1. *Apoptosis : an international journal on programmed cell death* **6**, 463-468
227. Tian, Q., Streuli, M., Saito, H., Schlossman, S. F., and Anderson, P. (1991) A polyadenylate binding protein localized to the granules of cytolytic lymphocytes induces DNA fragmentation in target cells. *Cell* **67**, 629-639

228. Groscurth, P. (1989) Cytotoxic effector cells of the immune system. *Anatomy and embryology* **180**, 109-119
229. Kawakami, A., Tian, Q., Duan, X., Streuli, M., Schlossman, S. F., and Anderson, P. (1992) Identification and functional characterization of a TIA-1-related nucleolysin. *Proceedings of the National Academy of Sciences of the United States of America* **89**, 8681-8685
230. Dember, L. M., Kim, N. D., Liu, K. Q., and Anderson, P. (1996) Individual RNA recognition motifs of TIA-1 and TIAR have different RNA binding specificities. *The Journal of biological chemistry* **271**, 2783-2788
231. Wang, Z., Kayikci, M., Briese, M., Zarnack, K., Luscombe, N. M., Rot, G., Zupan, B., Curk, T., and Ule, J. (2010) iCLIP predicts the dual splicing effects of TIA-RNA interactions. *PLoS biology* **8**, e1000530
232. Kedersha, N., Cho, M. R., Li, W., Yacono, P. W., Chen, S., Gilks, N., Golan, D. E., and Anderson, P. (2000) Dynamic shuttling of TIA-1 accompanies the recruitment of mRNA to mammalian stress granules. *The Journal of cell biology* **151**, 1257-1268
233. Kedersha, N. L., Gupta, M., Li, W., Miller, I., and Anderson, P. (1999) RNA-binding proteins TIA-1 and TIAR link the phosphorylation of eIF-2 alpha to the assembly of mammalian stress granules. *The Journal of cell biology* **147**, 1431-1442
234. Gilks, N., Kedersha, N., Ayodele, M., Shen, L., Stoecklin, G., Dember, L. M., and Anderson, P. (2004) Stress granule assembly is mediated by prion-like aggregation of TIA-1. *Molecular biology of the cell* **15**, 5383-5398
235. Forch, P., Puig, O., Martinez, C., Seraphin, B., and Valcarcel, J. (2002) The splicing regulator TIA-1 interacts with U1-C to promote U1 snRNP recruitment to 5' splice sites. *The EMBO journal* **21**, 6882-6892
236. Zhang, T., Delestienne, N., Huez, G., Kruys, V., and Gueydan, C. (2005) Identification of the sequence determinants mediating the nucleo-cytoplasmic shuttling of TIAR and TIA-1 RNA-binding proteins. *Journal of cell science* **118**, 5453-5463
237. Anderson, P., and Kedersha, N. (2002) Visibly stressed: the role of eIF2, TIA-1, and stress granules in protein translation. *Cell stress & chaperones* **7**, 213-221
238. Wigington, C. P., Jung, J., Rye, E. A., Belauret, S. L., Philpot, A. M., Feng, Y., Santangelo, P. J., and Corbett, A. H. (2014) Post-transcriptional Regulation of Programmed Cell Death 4 (PDCD4) mRNA by the RNA Binding Proteins Human Antigen R (HuR) and T-cell Intracellular Antigen 1 (TIA1). *The Journal of biological chemistry*
239. Dixon, D. A., Balch, G. C., Kedersha, N., Anderson, P., Zimmerman, G. A., Beauchamp, R. D., and Prescott, S. M. (2003) Regulation of cyclooxygenase-2 expression by the translational silencer TIA-1. *The Journal of experimental medicine* **198**, 475-481
240. Yu, Q., Cok, S. J., Zeng, C., and Morrison, A. R. (2003) Translational repression of human matrix metalloproteinases-13 by an alternatively spliced form of T-cell-restricted intracellular antigen-related protein (TIAR). *The Journal of biological chemistry* **278**, 1579-1584

241. Kandasamy, K., Joseph, K., Subramaniam, K., Raymond, J. R., and Tholanikunnel, B. G. (2005) Translational control of beta2-adrenergic receptor mRNA by T-cell-restricted intracellular antigen-related protein. *The Journal of biological chemistry* **280**, 1931-1943
242. Anderson, P., and Kedersha, N. (2006) RNA granules. *The Journal of cell biology* **172**, 803-808
243. Forch, P., Puig, O., Kedersha, N., Martinez, C., Granneman, S., Seraphin, B., Anderson, P., and Valcarcel, J. (2000) The apoptosis-promoting factor TIA-1 is a regulator of alternative pre-mRNA splicing. *Molecular cell* **6**, 1089-1098
244. Ruby, S. W., and Abelson, J. (1988) An early hierarchic role of U1 small nuclear ribonucleoprotein in spliceosome assembly. *Science* **242**, 1028-1035
245. Seraphin, B., and Rosbash, M. (1989) Identification of functional U1 snRNA-pre-mRNA complexes committed to spliceosome assembly and splicing. *Cell* **59**, 349-358
246. Barron, V. A., and Lou, H. (2012) Alternative splicing of the neurofibromatosis type I pre-mRNA. *Bioscience reports* **32**, 131-138
247. Krammer, P. H. (2000) CD95's deadly mission in the immune system. *Nature* **407**, 789-795
248. Kishore, S., Jaskiewicz, L., Burger, L., Hausser, J., Khorshid, M., and Zavolan, M. (2011) A quantitative analysis of CLIP methods for identifying binding sites of RNA-binding proteins. *Nature methods* **8**, 559-564
249. Uren, P. J., Burns, S. C., Ruan, J., Singh, K. K., Smith, A. D., and Penalva, L. O. (2011) Genomic analyses of the RNA-binding protein Hu antigen R (HuR) identify a complex network of target genes and novel characteristics of its binding sites. *The Journal of biological chemistry* **286**, 37063-37066
250. Zhu, H., Hasman, R. A., Barron, V. A., Luo, G., and Lou, H. (2006) A nuclear function of Hu proteins as neuron-specific alternative RNA processing regulators. *Molecular biology of the cell* **17**, 5105-5114
251. Zhu, H., Hinman, M. N., Hasman, R. A., Mehta, P., and Lou, H. (2008) Regulation of neuron-specific alternative splicing of neurofibromatosis type 1 pre-mRNA. *Molecular and cellular biology* **28**, 1240-1251
252. Kulikov, A. V., Shilov, E. S., Mufazalov, I. A., Gogvadze, V., Nedospasov, S. A., and Zhivotovsky, B. (2012) Cytochrome c: the Achilles' heel in apoptosis. *Cellular and molecular life sciences : CMLS* **69**, 1787-1797
253. Carrascoso, I., Sanchez-Jimenez, C., and Izquierdo, J. M. (2014) Long-term reduction of T-cell intracellular antigens leads to increased beta-actin expression. *Molecular cancer* **13**, 90
254. Dormoy-Raclet, V., Menard, I., Clair, E., Kurban, G., Mazroui, R., Di Marco, S., von Roretz, C., Pause, A., and Gallouzi, I. E. (2007) The RNA-binding protein HuR promotes cell migration and cell invasion by stabilizing the beta-actin mRNA in a U-rich-element-dependent manner. *Molecular and cellular biology* **27**, 5365-5380
255. Abdelmohsen, K., and Gorospe, M. (2010) Posttranscriptional regulation of cancer traits by HuR. *Wiley interdisciplinary reviews. RNA* **1**, 214-229
256. Hanahan, D., and Weinberg, R. A. (2000) The hallmarks of cancer. *Cell* **100**, 57-70

257. Denkert, C., Koch, I., von Keyserlingk, N., Noske, A., Niesporek, S., Dietel, M., and Weichert, W. (2006) Expression of the ELAV-like protein HuR in human colon cancer: association with tumor stage and cyclooxygenase-2. *Modern pathology : an official journal of the United States and Canadian Academy of Pathology, Inc* **19**, 1261-1269
258. Erkinheimo, T. L., Lassus, H., Sivula, A., Sengupta, S., Furneaux, H., Hla, T., Haglund, C., Butzow, R., and Ristimaki, A. (2003) Cytoplasmic HuR expression correlates with poor outcome and with cyclooxygenase 2 expression in serous ovarian carcinoma. *Cancer research* **63**, 7591-7594
259. Heinonen, M., Bono, P., Narko, K., Chang, S. H., Lundin, J., Joensuu, H., Furneaux, H., Hla, T., Haglund, C., and Ristimaki, A. (2005) Cytoplasmic HuR expression is a prognostic factor in invasive ductal breast carcinoma. *Cancer research* **65**, 2157-2161
260. Hug, H. (1997) Fas-mediated apoptosis in tumor formation and defense. *Biological chemistry* **378**, 1405-1412
261. Cascino, I., Fiucci, G., Papoff, G., and Ruberti, G. (1995) Three functional soluble forms of the human apoptosis-inducing Fas molecule are produced by alternative splicing. *Journal of immunology* **154**, 2706-2713
262. Cheng, J., Zhou, T., Liu, C., Shapiro, J. P., Brauer, M. J., Kiefer, M. C., Barr, P. J., and Mountz, J. D. (1994) Protection from Fas-mediated apoptosis by a soluble form of the Fas molecule. *Science* **263**, 1759-1762
263. Lal, A., Kawai, T., Yang, X., Mazan-Mamczarz, K., and Gorospe, M. (2005) Antiapoptotic function of RNA-binding protein HuR effected through prothymosin alpha. *The EMBO journal* **24**, 1852-1862
264. Abdelmohsen, K., Lal, A., Kim, H. H., and Gorospe, M. (2007) Posttranscriptional orchestration of an anti-apoptotic program by HuR. *Cell cycle* **6**, 1288-1292
265. Houstek, J., Andersson, U., Tvrdik, P., Nedergaard, J., and Cannon, B. (1995) The expression of subunit c correlates with and thus may limit the biosynthesis of the mitochondrial F0F1-ATPase in brown adipose tissue. *The Journal of biological chemistry* **270**, 7689-7694
266. Kramarova, T. V., Shabalina, I. G., Andersson, U., Westerberg, R., Carlberg, I., Houstek, J., Nedergaard, J., and Cannon, B. (2008) Mitochondrial ATP synthase levels in brown adipose tissue are governed by the c-Fo subunit P1 isoform. *FASEB journal : official publication of the Federation of American Societies for Experimental Biology* **22**, 55-63
267. Chen, H., and Chan, D. C. (2009) Mitochondrial dynamics--fusion, fission, movement, and mitophagy--in neurodegenerative diseases. *Human molecular genetics* **18**, R169-176
268. Kelly, S. M., Leung, S. W., Pak, C., Banerjee, A., Moberg, K. H., and Corbett, A. H. (2014) A conserved role for the zinc finger polyadenosine RNA binding protein, ZC3H14, in control of poly(A) tail length. *Rna* **20**, 681-688
269. Roth, K. M., Wolf, M. K., Rossi, M., and Butler, J. S. (2005) The nuclear exosome contributes to autogenous control of NAB2 mRNA levels. *Molecular and cellular biology* **25**, 1577-1585

270. Lankat-Buttgereit, B., and Goke, R. (2009) The tumour suppressor Pdcd4: recent advances in the elucidation of function and regulation. *Biology of the cell / under the auspices of the European Cell Biology Organization* **101**, 309-317
271. Asangani, I. A., Rasheed, S. A., Nikolova, D. A., Leupold, J. H., Colburn, N. H., Post, S., and Allgayer, H. (2008) MicroRNA-21 (miR-21) post-transcriptionally downregulates tumor suppressor Pdcd4 and stimulates invasion, intravasation and metastasis in colorectal cancer. *Oncogene* **27**, 2128-2136
272. Frankel, L. B., Christoffersen, N. R., Jacobsen, A., Lindow, M., Krogh, A., and Lund, A. H. (2008) Programmed cell death 4 (PDCD4) is an important functional target of the microRNA miR-21 in breast cancer cells. *The Journal of biological chemistry* **283**, 1026-1033
273. Lankat-Buttgereit, B., and Goke, R. (2003) Programmed cell death protein 4 (pdcd4): a novel target for antineoplastic therapy? *Biology of the cell / under the auspices of the European Cell Biology Organization* **95**, 515-519
274. Jin, P., and Warren, S. T. (2000) Understanding the molecular basis of fragile X syndrome. *Human molecular genetics* **9**, 901-908
275. Miller, J. W., Urbinati, C. R., Teng-Umnuay, P., Stenberg, M. G., Byrne, B. J., Thornton, C. A., and Swanson, M. S. (2000) Recruitment of human muscleblind proteins to (CUG)(n) expansions associated with myotonic dystrophy. *The EMBO journal* **19**, 4439-4448
276. Karni, R., de Stanchina, E., Lowe, S. W., Sinha, R., Mu, D., and Krainer, A. R. (2007) The gene encoding the splicing factor SF2/ASF is a proto-oncogene. *Nature structural & molecular biology* **14**, 185-193
277. Bielli, P., Busa, R., Paronetto, M. P., and Sette, C. (2011) The RNA-binding protein Sam68 is a multifunctional player in human cancer. *Endocrine-related cancer* **18**, R91-R102
278. Zong, F. Y., Fu, X., Wei, W. J., Luo, Y. G., Heiner, M., Cao, L. J., Fang, Z., Fang, R., Lu, D., Ji, H., and Hui, J. (2014) The RNA-binding protein QKI suppresses cancer-associated aberrant splicing. *PLoS genetics* **10**, e1004289
279. Dean, M., Park, M., and Vande Woude, G. F. (1987) Characterization of the rearranged tpr-met oncogene breakpoint. *Molecular and cellular biology* **7**, 921-924
280. Kang, S., and Hong, S. (2009) Molecular pathogenesis of spinocerebellar ataxia type 1 disease. *Molecules and cells* **27**, 621-627
281. Hackman, P., Sarparanta, J., Lehtinen, S., Vihola, A., Evila, A., Jonson, P. H., Luque, H., Kere, J., Screen, M., Chinnery, P. F., Ahlberg, G., Edstrom, L., and Udd, B. (2013) Welander distal myopathy is caused by a mutation in the RNA-binding protein TIA1. *Annals of neurology* **73**, 500-509
282. Phillips, T. (2008) Regulation of Transcription and Gene Expression in Eukaryotes. *Nature Education* **1**, 199
283. Glisovic, T., Bachorik, J. L., Yong, J., and Dreyfuss, G. (2008) RNA-binding proteins and post-transcriptional gene regulation. *FEBS letters* **582**, 1977-1986
284. Blackinton, J. G., and Keene, J. D. (2014) Post-transcriptional RNA regulons affecting cell cycle and proliferation. *Seminars in cell & developmental biology*

285. Chan, Y. A., Hieter, P., and Stirling, P. C. (2014) Mechanisms of genome instability induced by RNA-processing defects. *Trends in genetics : TIG* **30**, 245-253
286. Lukong, K. E., Chang, K. W., Khandjian, E. W., and Richard, S. (2008) RNA-binding proteins in human genetic disease. *Trends in genetics : TIG* **24**, 416-425
287. Liu-Yesucevitz, L., Bassell, G. J., Gitler, A. D., Hart, A. C., Klann, E., Richter, J. D., Warren, S. T., and Wolozin, B. (2011) Local RNA translation at the synapse and in disease. *The Journal of neuroscience : the official journal of the Society for Neuroscience* **31**, 16086-16093
288. Romano, M., and Buratti, E. (2013) Targeting RNA binding proteins involved in neurodegeneration. *Journal of biomolecular screening* **18**, 967-983
289. Wilson, A. C., Dugger, B. N., Dickson, D. W., and Wang, D. S. (2011) TDP-43 in aging and Alzheimer's disease - a review. *International journal of clinical and experimental pathology* **4**, 147-155
290. Kelly, S., Pak, C., Garshasbi, M., Kuss, A., Corbett, A. H., and Moberg, K. (2012) New kid on the ID block: neural functions of the Nab2/ZC3H14 class of Cys(3)His tandem zinc-finger polyadenosine RNA binding proteins. *RNA biology* **9**, 555-562
291. Apponi, L. H., Kelly, S. M., Harreman, M. T., Lehner, A. N., Corbett, A. H., and Valentini, S. R. (2007) An interaction between two RNA binding proteins, Nab2 and Pub1, links mRNA processing/export and mRNA stability. *Molecular and cellular biology* **27**, 6569-6579
292. Dyer, M. R., and Walker, J. E. (1993) Sequences of members of the human gene family for the c subunit of mitochondrial ATP synthase. *The Biochemical journal* **293 (Pt 1)**, 51-64
293. Jonckheere, A. I., Smeitink, J. A., and Rodenburg, R. J. (2012) Mitochondrial ATP synthase: architecture, function and pathology. *Journal of inherited metabolic disease* **35**, 211-225
294. Abouantoun, T. J., and MacDonald, T. J. (2009) Imatinib blocks migration and invasion of medulloblastoma cells by concurrently inhibiting activation of platelet-derived growth factor receptor and transactivation of epidermal growth factor receptor. *Molecular cancer therapeutics* **8**, 1137-1147
295. Guppy, M., Leedman, P., Zu, X., and Russell, V. (2002) Contribution by different fuels and metabolic pathways to the total ATP turnover of proliferating MCF-7 breast cancer cells. *The Biochemical journal* **364**, 309-315
296. Reitzer, L. J., Wice, B. M., and Kennell, D. (1979) Evidence that glutamine, not sugar, is the major energy source for cultured HeLa cells. *The Journal of biological chemistry* **254**, 2669-2676
297. Watt, I. N., Montgomery, M. G., Runswick, M. J., Leslie, A. G., and Walker, J. E. (2010) Bioenergetic cost of making an adenosine triphosphate molecule in animal mitochondria. *Proceedings of the National Academy of Sciences of the United States of America* **107**, 16823-16827
298. Dyer, M. R., Gay, N. J., and Walker, J. E. (1989) DNA sequences of a bovine gene and of two related pseudogenes for the proteolipid subunit of mitochondrial ATP synthase. *The Biochemical journal* **260**, 249-258

299. Yan, W. L., Lerner, T. J., Haines, J. L., and Gusella, J. F. (1994) Sequence analysis and mapping of a novel human mitochondrial ATP synthase subunit 9 cDNA (ATP5G3). *Genomics* **24**, 375-377
300. Sangawa, H., Himeda, T., Shibata, H., and Higuti, T. (1997) Gene expression of subunit c(P1), subunit c(P2), and oligomycin sensitivity-conferring protein may play a key role in biogenesis of H+-ATP synthase in various rat tissues. *The Journal of biological chemistry* **272**, 6034-6037
301. Vives-Bauza, C., Magrane, J., Andreu, A. L., and Manfredi, G. (2010) Novel role of ATPase subunit C targeting peptides beyond mitochondrial protein import. *Molecular biology of the cell* **21**, 131-139
302. De Grassi, A., Lanave, C., and Saccone, C. (2006) Evolution of ATP synthase subunit c and cytochrome c gene families in selected Metazoan classes. *Gene* **371**, 224-233
303. Gay, N. J., and Walker, J. E. (1985) Two genes encoding the bovine mitochondrial ATP synthase proteolipid specify precursors with different import sequences and are expressed in a tissue-specific manner. *The EMBO journal* **4**, 3519-3524
304. Chance, B., Williams, G. R., and Hollunger, G. (1963) Inhibition of electron and energy transfer in mitochondria. I. Effects of Amytal, thiopental, rotenone, progesterone, and methylene glycol. *The Journal of biological chemistry* **238**, 418-431
305. Duborjal, H., Beugnot, R., Mousson de Camaret, B., and Issartel, J. P. (2002) Large functional range of steady-state levels of nuclear and mitochondrial transcripts coding for the subunits of the human mitochondrial OXPHOS system. *Genome research* **12**, 1901-1909
306. Natera-Naranjo, O., Kar, A. N., Aschrafi, A., Gervasi, N. M., Macgibeny, M. A., Gioio, A. E., and Kaplan, B. B. (2012) Local translation of ATP synthase subunit 9 mRNA alters ATP levels and the production of ROS in the axon. *Molecular and cellular neurosciences* **49**, 263-270
307. Karbowski, M., and Youle, R. J. (2003) Dynamics of mitochondrial morphology in healthy cells and during apoptosis. *Cell death and differentiation* **10**, 870-880
308. Yaffe, M. P. (1999) The machinery of mitochondrial inheritance and behavior. *Science* **283**, 1493-1497
309. Kaput, J., Brandriss, M. C., and Prussak-Wieckowska, T. (1989) In vitro import of cytochrome c peroxidase into the intermembrane space: release of the processed form by intact mitochondria. *The Journal of cell biology* **109**, 101-112
310. Singh, B., Patel, H. V., Ridley, R. G., Freeman, K. B., and Gupta, R. S. (1990) Mitochondrial import of the human chaperonin (HSP60) protein. *Biochemical and biophysical research communications* **169**, 391-396
311. Suen, D. F., Norris, K. L., and Youle, R. J. (2008) Mitochondrial dynamics and apoptosis. *Genes & development* **22**, 1577-1590
312. Kaufmann, S. H., Desnoyers, S., Ottaviano, Y., Davidson, N. E., and Poirier, G. G. (1993) Specific proteolytic cleavage of poly(ADP-ribose) polymerase: an early marker of chemotherapy-induced apoptosis. *Cancer research* **53**, 3976-3985

313. Belmokhtar, C. A., Hillion, J., and Segal-Bendirdjian, E. (2001) Staurosporine induces apoptosis through both caspase-dependent and caspase-independent mechanisms. *Oncogene* **20**, 3354-3362
314. Yang, J., Liu, X., Bhalla, K., Kim, C. N., Ibrado, A. M., Cai, J., Peng, T. I., Jones, D. P., and Wang, X. (1997) Prevention of apoptosis by Bcl-2: release of cytochrome c from mitochondria blocked. *Science* **275**, 1129-1132
315. Andersson, U., Houstek, J., and Cannon, B. (1997) ATP synthase subunit c expression: physiological regulation of the P1 and P2 genes. *The Biochemical journal* **323 (Pt 2)**, 379-385
316. Aschrafi, A., Kar, A. N., Natera-Naranjo, O., Macgibeny, M. A., Gioio, A. E., and Kaplan, B. B. (2012) MicroRNA-338 regulates the axonal expression of multiple nuclear-encoded mitochondrial mRNAs encoding subunits of the oxidative phosphorylation machinery. *Cellular and molecular life sciences : CMLS*
317. Kann, O., and Kovacs, R. (2007) Mitochondria and neuronal activity. *American journal of physiology. Cell physiology* **292**, C641-657
318. Silver, I., and Erecinska, M. (1998) Oxygen and ion concentrations in normoxic and hypoxic brain cells. *Advances in experimental medicine and biology* **454**, 7-16
319. Ames, A., 3rd. (2000) CNS energy metabolism as related to function. *Brain research. Brain research reviews* **34**, 42-68
320. Knott, A. B., Perkins, G., Schwarzenbacher, R., and Bossy-Wetzel, E. (2008) Mitochondrial fragmentation in neurodegeneration. *Nature reviews. Neuroscience* **9**, 505-518
321. Koopman, W. J., Visch, H. J., Verkaart, S., van den Heuvel, L. W., Smeitink, J. A., and Willems, P. H. (2005) Mitochondrial network complexity and pathological decrease in complex I activity are tightly correlated in isolated human complex I deficiency. *American journal of physiology. Cell physiology* **289**, C881-890
322. Kwong, J. Q., Henning, M. S., Starkov, A. A., and Manfredi, G. (2007) The mitochondrial respiratory chain is a modulator of apoptosis. *The Journal of cell biology* **179**, 1163-1177
323. Sauvanet, C., Duvezin-Caubet, S., di Rago, J. P., and Rojo, M. (2010) Energetic requirements and bioenergetic modulation of mitochondrial morphology and dynamics. *Seminars in cell & developmental biology* **21**, 558-565
324. Chan, D. C. (2012) Fusion and fission: interlinked processes critical for mitochondrial health. *Annual review of genetics* **46**, 265-287
325. Youle, R. J., and van der Bliek, A. M. (2012) Mitochondrial fission, fusion, and stress. *Science* **337**, 1062-1065
326. Soule, H. D., Vazguez, J., Long, A., Albert, S., and Brennan, M. (1973) A human cell line from a pleural effusion derived from a breast carcinoma. *Journal of the National Cancer Institute* **51**, 1409-1416
327. Towbin, H., Staehelin, T., and Gordon, J. (1979) Electrophoretic transfer of proteins from polyacrylamide gels to nitrocellulose sheets: procedure and some applications. *Proceedings of the National Academy of Sciences of the United States of America* **76**, 4350-4354

328. Livak, K. J., and Schmittgen, T. D. (2001) Analysis of relative gene expression data using real-time quantitative PCR and the 2(-Delta Delta C(T)) Method. *Methods* **25**, 402-408
329. Yang, N. C., Ho, W. M., Chen, Y. H., and Hu, M. L. (2002) A convenient one-step extraction of cellular ATP using boiling water for the luciferin-luciferase assay of ATP. *Analytical biochemistry* **306**, 323-327
330. Cech, T. R., and Steitz, J. A. (2014) The noncoding RNA revolution-trashing old rules to forge new ones. *Cell* **157**, 77-94
331. Keene, J. D. (2007) RNA regulons: coordination of post-transcriptional events. *Nature reviews. Genetics* **8**, 533-543
332. Rhodes, D. R., Yu, J., Shanker, K., Deshpande, N., Varambally, R., Ghosh, D., Barrette, T., Pandey, A., and Chinnaiyan, A. M. (2004) ONCOMINE: a cancer microarray database and integrated data-mining platform. *Neoplasia* **6**, 1-6
333. Hammond, M. E., Hayes, D. F., Wolff, A. C., Mangu, P. B., and Temin, S. (2010) American society of clinical oncology/college of american pathologists guideline recommendations for immunohistochemical testing of estrogen and progesterone receptors in breast cancer. *Journal of oncology practice / American Society of Clinical Oncology* **6**, 195-197
334. Lee, M., Lee, C. S., and Tan, P. H. (2013) Hormone receptor expression in breast cancer: postanalytical issues. *Journal of clinical pathology* **66**, 478-484
335. Bourdeau, V., Deschenes, J., Metivier, R., Nagai, Y., Nguyen, D., Bretschneider, N., Gannon, F., White, J. H., and Mader, S. (2004) Genome-wide identification of high-affinity estrogen response elements in human and mouse. *Molecular endocrinology* **18**, 1411-1427
336. Klinge, C. M. (2000) Estrogen receptor interaction with co-activators and co-repressors. *Steroids* **65**, 227-251
337. O'Lone, R., Frith, M. C., Karlsson, E. K., and Hansen, U. (2004) Genomic targets of nuclear estrogen receptors. *Molecular endocrinology* **18**, 1859-1875
338. Kimura, H. (2013) Histone modifications for human epigenome analysis. *Journal of human genetics* **58**, 439-445
339. Thurman, R. E., Rynes, E., Humbert, R., Vierstra, J., Maurano, M. T., Haugen, E., Sheffield, N. C., Stergachis, A. B., Wang, H., Vernot, B., Garg, K., John, S., Sandstrom, R., Bates, D., Boatman, L., Canfield, T. K., Diegel, M., Dunn, D., Ebersol, A. K., Frum, T., Giste, E., Johnson, A. K., Johnson, E. M., Kutyavin, T., Lajoie, B., Lee, B. K., Lee, K., London, D., Lotakis, D., Neph, S., Neri, F., Nguyen, E. D., Qu, H., Reynolds, A. P., Roach, V., Safi, A., Sanchez, M. E., Sanyal, A., Shafer, A., Simon, J. M., Song, L., Vong, S., Weaver, M., Yan, Y., Zhang, Z., Zhang, Z., Lenhard, B., Tewari, M., Dorschner, M. O., Hansen, R. S., Navas, P. A., Stamatoyannopoulos, G., Iyer, V. R., Lieb, J. D., Sunyaev, S. R., Akey, J. M., Sabo, P. J., Kaul, R., Furey, T. S., Dekker, J., Crawford, G. E., and Stamatoyannopoulos, J. A. (2012) The accessible chromatin landscape of the human genome. *Nature* **489**, 75-82
340. Consortium, E. P. (2012) An integrated encyclopedia of DNA elements in the human genome. *Nature* **489**, 57-74
341. Luscher, B., and Vervoorts, J. (2012) Regulation of gene transcription by the oncoprotein MYC. *Gene* **494**, 145-160

342. Zeller, K. I., Zhao, X., Lee, C. W., Chiu, K. P., Yao, F., Yustein, J. T., Ooi, H. S., Orlov, Y. L., Shahab, A., Yong, H. C., Fu, Y., Weng, Z., Kuznetsov, V. A., Sung, W. K., Ruan, Y., Dang, C. V., and Wei, C. L. (2006) Global mapping of c-Myc binding sites and target gene networks in human B cells. *Proceedings of the National Academy of Sciences of the United States of America* **103**, 17834-17839
343. Bretones, G., Delgado, M. D., and Leon, J. (2014) Myc and cell cycle control. *Biochimica et biophysica acta*
344. Wang, C., Mayer, J. A., Mazumdar, A., Fertuck, K., Kim, H., Brown, M., and Brown, P. H. (2011) Estrogen induces c-myc gene expression via an upstream enhancer activated by the estrogen receptor and the AP-1 transcription factor. *Molecular endocrinology* **25**, 1527-1538
345. Brown, A. M., Jeltsch, J. M., Roberts, M., and Chambon, P. (1984) Activation of pS2 gene transcription is a primary response to estrogen in the human breast cancer cell line MCF-7. *Proceedings of the National Academy of Sciences of the United States of America* **81**, 6344-6348
346. Grundberg, E., Brandstrom, H., Ribom, E. L., Ljunggren, O., Kindmark, A., and Mallmin, H. (2003) A poly adenosine repeat in the human vitamin D receptor gene is associated with bone mineral density in young Swedish women. *Calcified tissue international* **73**, 455-462
347. Leeb, T., Kriegesmann, B., Baumgartner, B. G., Klett, C., Yerle, M., Hameister, H., and Brenig, B. (1997) Molecular cloning of the porcine beta-1,2-N-acetylglucosaminyltransferase II gene and assignment to chromosome 1q23-q27. *Biochimica et biophysica acta* **1336**, 361-366
348. Tuffery, S., Moine, P., Demaille, J., and Claustres, M. (1995) Identification of variable length polyadenosine tract at the dystrophin locus. *Human genetics* **95**, 590-592
349. Bag, J., and Wu, J. (1996) Translational control of poly(A)-binding protein expression. *European journal of biochemistry / FEBS* **237**, 143-152
350. de Melo Neto, O. P., Standart, N., and Martins de Sa, C. (1995) Autoregulation of poly(A)-binding protein synthesis in vitro. *Nucleic acids research* **23**, 2198-2205
351. Hornstein, E., Harel, H., Levy, G., and Meyuhas, O. (1999) Overexpression of poly(A)-binding protein down-regulates the translation or the abundance of its own mRNA. *FEBS letters* **457**, 209-213
352. Matoulkova, E., Michalova, E., Vojtesek, B., and Hrstka, R. (2012) The role of the 3' untranslated region in post-transcriptional regulation of protein expression in mammalian cells. *RNA biology* **9**, 563-576
353. Kozomara, A., and Griffiths-Jones, S. (2014) miRBase: annotating high confidence microRNAs using deep sequencing data. *Nucleic acids research* **42**, D68-73
354. Blin, K., Dieterich, C., Wurmus, R., Rajewsky, N., Landthaler, M., and Akalin, A. (2014) DoRiNA 2.0-upgrading the doRiNA database of RNA interactions in post-transcriptional regulation. *Nucleic acids research*
355. Subramaniam, K., Ooi, L. L., and Hui, K. M. (2010) Transcriptional down-regulation of IGFBP-3 in human hepatocellular carcinoma cells is mediated by the binding of TIA-1 to its AT-rich element in the 3'-untranslated region. *Cancer letters* **297**, 259-268

356. Mazan-Mamczarz, K., Galban, S., Lopez de Silanes, I., Martindale, J. L., Atasoy, U., Keene, J. D., and Gorospe, M. (2003) RNA-binding protein HuR enhances p53 translation in response to ultraviolet light irradiation. *Proceedings of the National Academy of Sciences of the United States of America* **100**, 8354-8359
357. Yu, T. X., Rao, J. N., Zou, T., Liu, L., Xiao, L., Ouyang, M., Cao, S., Gorospe, M., and Wang, J. Y. (2013) Competitive binding of CUGBP1 and HuR to occludin mRNA controls its translation and modulates epithelial barrier function. *Molecular biology of the cell* **24**, 85-99
358. Lopez de Silanes, I., Zhan, M., Lal, A., Yang, X., and Gorospe, M. (2004) Identification of a target RNA motif for RNA-binding protein HuR. *Proceedings of the National Academy of Sciences of the United States of America* **101**, 2987-2992
359. Guo, X., and Hartley, R. S. (2006) HuR contributes to cyclin E1 deregulation in MCF-7 breast cancer cells. *Cancer research* **66**, 7948-7956
360. Wang, W., Caldwell, M. C., Lin, S., Furneaux, H., and Gorospe, M. (2000) HuR regulates cyclin A and cyclin B1 mRNA stability during cell proliferation. *The EMBO journal* **19**, 2340-2350
361. Pryzbylkowski, P., Obajimi, O., and Keen, J. C. (2008) Trichostatin A and 5 Aza-2' deoxycytidine decrease estrogen receptor mRNA stability in ER positive MCF7 cells through modulation of HuR. *Breast cancer research and treatment* **111**, 15-25
362. Yang, H. S., Jansen, A. P., Komar, A. A., Zheng, X., Merrick, W. C., Costes, S., Lockett, S. J., Sonenberg, N., and Colburn, N. H. (2003) The transformation suppressor Pdcd4 is a novel eukaryotic translation initiation factor 4A binding protein that inhibits translation. *Molecular and cellular biology* **23**, 26-37
363. Rogers, G. W., Jr., Richter, N. J., and Merrick, W. C. (1999) Biochemical and kinetic characterization of the RNA helicase activity of eukaryotic initiation factor 4A. *The Journal of biological chemistry* **274**, 12236-12244
364. Cmarik, J. L., Min, H., Hegamyer, G., Zhan, S., Kulesz-Martin, M., Yoshinaga, H., Matsuhashi, S., and Colburn, N. H. (1999) Differentially expressed protein Pdcd4 inhibits tumor promoter-induced neoplastic transformation. *Proceedings of the National Academy of Sciences of the United States of America* **96**, 14037-14042
365. Pan, X., Wang, Z. X., and Wang, R. (2010) MicroRNA-21: a novel therapeutic target in human cancer. *Cancer biology & therapy* **10**, 1224-1232
366. Leupold, J. H., Asangani, I. A., Mudduluru, G., and Allgayer, H. (2012) Promoter cloning and characterization of the human programmed cell death protein 4 (pdcd4) gene: evidence for ZBP-89 and Sp-binding motifs as essential Pdcd4 regulators. *Bioscience reports* **32**, 281-297
367. Vikhreva, P. N., Shepelev, M. V., and Korobko, I. V. (2014) mTOR-dependent transcriptional repression of Pdcd4 tumor suppressor in lung cancer cells. *Biochimica et biophysica acta* **1839**, 43-49
368. Dorrello, N. V., Peschiaroli, A., Guardavaccaro, D., Colburn, N. H., Sherman, N. E., and Pagano, M. (2006) S6K1- and betaTRCP-mediated degradation of PDCD4 promotes protein translation and cell growth. *Science* **314**, 467-471

369. Powers, M. A., Fay, M. M., Factor, R. E., Welm, A. L., and Ullman, K. S. (2011) Protein arginine methyltransferase 5 accelerates tumor growth by arginine methylation of the tumor suppressor programmed cell death 4. *Cancer research* **71**, 5579-5587
370. Santangelo, P. J., Lifland, A. W., Curt, P., Sasaki, Y., Bassell, G. J., Lindquist, M. E., and Crowe, J. E., Jr. (2009) Single molecule-sensitive probes for imaging RNA in live cells. *Nature methods* **6**, 347-349
371. Jung, J., Lifland, A. W., Zurla, C., Alonas, E. J., and Santangelo, P. J. (2013) Quantifying RNA-protein interactions in situ using modified-MTRIPs and proximity ligation. *Nucleic acids research* **41**, e12
372. Soderberg, O., Gullberg, M., Jarvius, M., Ridderstrale, K., Leuchowius, K. J., Jarvius, J., Wester, K., Hydbring, P., Bahram, F., Larsson, L. G., and Landegren, U. (2006) Direct observation of individual endogenous protein complexes in situ by proximity ligation. *Nature methods* **3**, 995-1000
373. Gruber, A. R., Fallmann, J., Kratochvill, F., Kovarik, P., and Hofacker, I. L. (2011) AREsite: a database for the comprehensive investigation of AU-rich elements. *Nucleic acids research* **39**, D66-69
374. Wang, H., Li, H., Shi, H., Liu, Y., Liu, H., Zhao, H., Niu, L., Teng, M., and Li, X. (2011) Preliminary crystallographic analysis of the RNA-binding domain of HuR and its poly(U)-binding properties. *Acta crystallographica. Section F, Structural biology and crystallization communications* **67**, 546-550
375. Santangelo, P. J., Alonas, E., Jung, J., Lifland, A. W., and Zurla, C. (2012) Probes for intracellular RNA imaging in live cells. *Methods in enzymology* **505**, 383-399
376. Dani, C., Blanchard, J. M., Piechaczyk, M., El Sabouty, S., Marty, L., and Jeanteur, P. (1984) Extreme instability of myc mRNA in normal and transformed human cells. *Proceedings of the National Academy of Sciences of the United States of America* **81**, 7046-7050
377. Tani, H., Mizutani, R., Salam, K. A., Tano, K., Ijiri, K., Wakamatsu, A., Isogai, T., Suzuki, Y., and Akimitsu, N. (2012) Genome-wide determination of RNA stability reveals hundreds of short-lived noncoding transcripts in mammals. *Genome research* **22**, 947-956
378. Schwanhausser, B., Busse, D., Li, N., Dittmar, G., Schuchhardt, J., Wolf, J., Chen, W., and Selbach, M. (2011) Global quantification of mammalian gene expression control. *Nature* **473**, 337-342
379. Loreni, F., Thomas, G., and Amaldi, F. (2000) Transcription inhibitors stimulate translation of 5' TOP mRNAs through activation of S6 kinase and the mTOR/FRAP signalling pathway. *European journal of biochemistry / FEBS* **267**, 6594-6601
380. Yang, E., van Nimwegen, E., Zavolan, M., Rajewsky, N., Schroeder, M., Magnasco, M., and Darnell, J. E., Jr. (2003) Decay rates of human mRNAs: correlation with functional characteristics and sequence attributes. *Genome research* **13**, 1863-1872
381. Young, L. E., Moore, A. E., Sokol, L., Meisner-Kober, N., and Dixon, D. A. (2012) The mRNA stability factor HuR inhibits microRNA-16 targeting of COX-2. *Molecular cancer research : MCR* **10**, 167-180

382. Davoren, P. A., McNeill, R. E., Lowery, A. J., Kerin, M. J., and Miller, N. (2008) Identification of suitable endogenous control genes for microRNA gene expression analysis in human breast cancer. *BMC molecular biology* **9**, 76
383. Shibahara, K., Asano, M., Ishida, Y., Aoki, T., Koike, T., and Honjo, T. (1995) Isolation of a novel mouse gene MA-3 that is induced upon programmed cell death. *Gene* **166**, 297-301
384. Yang, H. S., Jansen, A. P., Nair, R., Shibahara, K., Verma, A. K., Cmarik, J. L., and Colburn, N. H. (2001) A novel transformation suppressor, Pdcd4, inhibits AP-1 transactivation but not NF-kappaB or ODC transactivation. *Oncogene* **20**, 669-676
385. Schlichter, U., Burk, O., Worpenberg, S., and Klempnauer, K. H. (2001) The chicken Pdcd4 gene is regulated by v-Myb. *Oncogene* **20**, 231-239
386. Fan, H., Zhao, Z., Quan, Y., Xu, J., Zhang, J., and Xie, W. (2007) DNA methyltransferase 1 knockdown induces silenced CDH1 gene reexpression by demethylation of methylated CpG in hepatocellular carcinoma cell line SMMC-7721. *European journal of gastroenterology & hepatology* **19**, 952-961
387. Kim, J., Park, R. Y., Chen, J. K., Kim, J., Jeong, S., and Ohn, T. (2014) Splicing factor SRSF3 represses the translation of programmed cell death 4 mRNA by associating with the 5'-UTR region. *Cell death and differentiation* **21**, 481-490
388. Zuker, M. (2003) Mfold web server for nucleic acid folding and hybridization prediction. *Nucleic acids research* **31**, 3406-3415
389. Fay, M. M., Clegg, J. M., Uchida, K. A., Powers, M. A., and Ullman, K. S. (2014) Enhanced Arginine Methylation of Programmed Cell Death 4 Protein during Nutrient Deprivation Promotes Tumor Cell Viability. *The Journal of biological chemistry* **289**, 17541-17552
390. Schmid, T., Jansen, A. P., Baker, A. R., Hegamyer, G., Hagan, J. P., and Colburn, N. H. (2008) Translation inhibitor Pdcd4 is targeted for degradation during tumor promotion. *Cancer research* **68**, 1254-1260
391. Epis, M. R., Barker, A., Giles, K. M., Beveridge, D. J., and Leedman, P. J. (2011) The RNA-binding protein HuR opposes the repression of ERBB-2 gene expression by microRNA miR-331-3p in prostate cancer cells. *The Journal of biological chemistry* **286**, 41442-41454
392. Srikantan, S., Abdelmohsen, K., Lee, E. K., Tominaga, K., Subaran, S. S., Kuwano, Y., Kulshrestha, R., Panchakshari, R., Kim, H. H., Yang, X., Martindale, J. L., Marasa, B. S., Kim, M. M., Wersto, R. P., Indig, F. E., Chowdhury, D., and Gorospe, M. (2011) Translational control of TOP2A influences doxorubicin efficacy. *Molecular and cellular biology* **31**, 3790-3801
393. Tominaga, K., Srikantan, S., Lee, E. K., Subaran, S. S., Martindale, J. L., Abdelmohsen, K., and Gorospe, M. (2011) Competitive regulation of nucleolin expression by HuR and miR-494. *Molecular and cellular biology* **31**, 4219-4231
394. Jain, R., Devine, T., George, A. D., Chittur, S. V., Baroni, T. E., Penalva, L. O., and Tenenbaum, S. A. (2011) RIP-Chip analysis: RNA-Binding Protein Immunoprecipitation-Microarray (Chip) Profiling. *Methods in molecular biology* **703**, 247-263
395. Feng, Y., Absher, D., Eberhart, D. E., Brown, V., Malter, H. E., and Warren, S. T. (1997) FMRP associates with polyribosomes as an mRNP, and the I304N

mutation of severe fragile X syndrome abolishes this association. *Molecular cell* **1**, 109-118
396. Irier, H. A., Shaw, R., Lau, A., Feng, Y., and Dingledine, R. (2009) Translational regulation of GluR2 mRNAs in rat hippocampus by alternative 3' untranslated regions. *Journal of neurochemistry* **109**, 584-594
397. Walters, R., and Parker, R. (2014) Quality control: Is there quality control of localized mRNAs? *The Journal of cell biology* **204**, 863-868
398. Marc, P., Margeot, A., Devaux, F., Blugeon, C., Corral-Debrinski, M., and Jacq, C. (2002) Genome-wide analysis of mRNAs targeted to yeast mitochondria. *EMBO reports* **3**, 159-164
399. Saint-Georges, Y., Garcia, M., Delaveau, T., Jourdren, L., Le Crom, S., Lemoine, S., Tanty, V., Devaux, F., and Jacq, C. (2008) Yeast mitochondrial biogenesis: a role for the PUF RNA-binding protein Puf3p in mRNA localization. *PloS one* **3**, e2293
400. Devaux, F., Lelandais, G., Garcia, M., Goussard, S., and Jacq, C. (2010) Posttranscriptional control of mitochondrial biogenesis: spatio-temporal regulation of the protein import process. *FEBS letters* **584**, 4273-4279
401. Wu, L., Fan, J., and Belasco, J. G. (2006) MicroRNAs direct rapid deadenylation of mRNA. *Proceedings of the National Academy of Sciences of the United States of America* **103**, 4034-4039
402. Fustin, J. M., Doi, M., Yamaguchi, Y., Hida, H., Nishimura, S., Yoshida, M., Isagawa, T., Morioka, M. S., Kakeya, H., Manabe, I., and Okamura, H. (2013) RNA-methylation-dependent RNA processing controls the speed of the circadian clock. *Cell* **155**, 793-806
403. Yuan, Z., Sanders, A. J., Ye, L., and Jiang, W. G. (2010) HuR, a key post-transcriptional regulator, and its implication in progression of breast cancer. *Histology and histopathology* **25**, 1331-1340
404. Nieves-Alicea, R., Colburn, N. H., Simeone, A. M., and Tari, A. M. (2009) Programmed cell death 4 inhibits breast cancer cell invasion by increasing tissue inhibitor of metalloproteinases-2 expression. *Breast cancer research and treatment* **114**, 203-209
405. Wickramasinghe, N. S., Manavalan, T. T., Dougherty, S. M., Riggs, K. A., Li, Y., and Klinge, C. M. (2009) Estradiol downregulates miR-21 expression and increases miR-21 target gene expression in MCF-7 breast cancer cells. *Nucleic acids research* **37**, 2584-2595
406. Gonzalez-Villasana, V., Nieves-Alicea, R., McMurtry, V., Gutierrez-Puente, Y., and Tari, A. M. (2012) Programmed cell death 4 inhibits leptin-induced breast cancer cell invasion. *Oncology reports* **27**, 861-866
407. Santhanam, A. N., Baker, A. R., Hegamyer, G., Kirschmann, D. A., and Colburn, N. H. (2010) Pdcd4 repression of lysyl oxidase inhibits hypoxia-induced breast cancer cell invasion. *Oncogene* **29**, 3921-3932
408. Wen, Y. H., Shi, X., Chiriboga, L., Matsahashi, S., Yee, H., and Afonja, O. (2007) Alterations in the expression of PDCD4 in ductal carcinoma of the breast. *Oncology reports* **18**, 1387-1393
409. Meric-Bernstam, F., Chen, H., Akcakanat, A., Do, K. A., Lluch, A., Hennessy, B. T., Hortobagyi, G. N., Mills, G. B., and Gonzalez-Angulo, A. M. (2012)

Aberrations in translational regulation are associated with poor prognosis in hormone receptor-positive breast cancer. *Breast cancer research : BCR* **14**, R138

410. Engelman, J. A. (2009) Targeting PI3K signalling in cancer: opportunities, challenges and limitations. *Nature reviews. Cancer* **9**, 550-562
411. Silvera, D., Formenti, S. C., and Schneider, R. J. (2010) Translational control in cancer. *Nature reviews. Cancer* **10**, 254-266
412. Holz, M. K., Ballif, B. A., Gygi, S. P., and Blenis, J. (2005) mTOR and S6K1 mediate assembly of the translation preinitiation complex through dynamic protein interchange and ordered phosphorylation events. *Cell* **123**, 569-580